UNIVERSITY OF OKLAHOMA

GRADUATE COLLEGE

SYNTHESIS OF, AND APPLICATION OF THE COMPENSATED ARRHENIUS FORMULATION TO, ORGANIC CARBONATES AND OLIGOETHERS

A DISSERTATION

SUBMITTED TO THE GRADUATE FACULTY

in partial fulfillment of the requirements for the

Degree of

DOCTOR OF PHILOSOPHY

By

MOHD FARID ISMAIL
Norman, Oklahoma
2013

SYNTHESIS OF, AND APPLICATION OF THE COMPENSATED ARRHENIUS FORMULATION TO, ORGANIC CARBONATES AND OLIGOETHERS

A DISSERTATION APPROVED FOR THE
DEPARTMENT OF CHEMISTRY AND BIOCHEMISTRY

BY

_____
Dr. Daniel Glatzhofer, Chair

_____
Dr. Roger Frech

_____
Dr. Robert Cichewicz

_____
Dr. Wai Tak Yip

_____
Dr. Lloyd Bumm

Acknowledgements

I would like to thank the members of my graduate committee, Dr. Glatzhofer, Dr. Frech, Dr. Cichewicz, Dr. Yip, and Dr. Bumm for all the help, suggestions, and opportunity. I want to thank Dr. Glatzhofer for all the encouragement, knowledge, and wisdom provided throughout these years. I want to thank Dr. Frech for giving me the opportunity to be involved in the interesting world of transport phenomena.

I would like to thank all members of Dr. Glatzhofer's lab who have helped me and taught me about research and life in general. To Dr. Matt Petrowsky and Dr. Allison Fleshman, a big thanks for introducing me to CAF and for all the help and discussions. This dissertation would not have been possible without your help.

I want to thank Dr. Striolo and Dr. Ralph Wheeler for all knowledge that was taught to me, and to the Department of Chemistry and Biochemistry at the University of Oklahoma for the opportunity to grow.

Table of Contents

Acknowledgements iv

List of Tables viii

List of Figures xiii

Abstract xxi

Chapter 1 : Introduction To Mass Transport 1

1.1 What is Mass Transport? 1

1.2 What is Diffusion? 2

1.3 The theory of self-diffusion 3

1.4 What is Ionic Conductivity? 7

1.5 Theory of Ionic Conductivity 8

1.6 The Compensated Arrhenius Equation (CAE) 11

1.7 Theory of dielectric constant 12

1.8 Techniques used 18

1.9 Purpose of Work and Summary of Chapters 19

Chapter 2 : The Compensated Arrhenius Equation 23

2.1 Introduction 23

2.1.1 General Concept 23

2.2 Scaling Procedure Detail Example for Conductivity Data 27

2.3 The Effect of Fitting Parameters on the E_a 33

2.4 Considerations for Choosing Reference Temperature, T_r. 43

2.5 The Exponential Pre-factor and the Master Curve 47

Chapter 3 : Synthesis and Application of the Compensated Arrhenius Formulation to Acyclic Carbonates 49
3.1 Introduction 49
3.1.1 Project Goals 52
3.2 Results and Discussions 53
3.2.1 Synthesis of Acyclic Carbonates 53
3.2.2 Application of the CAF to the Acyclic Carbonates 62
3.2.2.1 Dielectric Constant and Diffusion of Acyclic Carbonates 62
3.3 Conclusion 70
3.4 Detailed Synthesis, Sample Preparations, and Measurements 71
3.4.1 Detail Synthesis 71
Chapter 4 : Synthesis and Application of the Compensated Arrhenius Formulation (CAF) to Cyclic Carbonates 74
4.1 Introduction 74
4.1.1 Project Goals 75
4.2 Results and Discussions 76
4.2.1 Synthetic Development 76
4.2.1.1 Synthesis of Cyclic Carbonates 76
4.2.1.2 Synthesis of 1,2-diols 84
4.2.2 Dielectric Constant and Self-Diffusion of Pure Cyclic Carbonates 85
4.2.3 Dielectric Constant and Conductivity of LiTf and TbaTf in Cyclic Carbonates 95
4.3 Conclusions 106

4.4 Detail Synthesis, Sample Preparations, and Measurements 106
4.4.1 Detail Synthesis 106
4.4.2 Sample Preparations 109
4.4.3 Measurements 110
Chapter 5 : Synthesis and Application of Compensated Arrhenius Formulation (CAF) to Oligomers of Poly(ethylene Oxide) 113
5.1 Introduction 113
5.1.1 Project Goals 115
5.2 Results and Discussion 116
5.2.1 Synthesis of Poly(ethylene oxide) Oligomers 116
5.2.2 Dielectric Constant and Diffusion of Pure Oligoethers 123
5.2.3 Dielectric Constant and Conductivity of 0.1 molal LiTf in Glyme Derivatives 137
5.3 Conclusions 154
5.4 Detailed Synthesis of Glyme Series 161
Chapter 6: Conclusion 166
6.1 Overall conclusion 166
6.2 Future Directions 167
References 169

List of Tables

Table 1-1 Dielectric constant of selected organic solvents at 20°C[63] 20

Table 2-1 Dielectric constant and conductivity data for 0.0055M TbaTf in the nitrile solvent family. Data are taken from published literature values[53]. ε_s = dielectric constant, σ = conductivity. 28

Table 2-2 The E_a for the nitrile derivatives at reference temperature, T_r from 5°C to 85°C. 33

Table 2-3 The E_a for the conductivity of 0.0055M TbaTf in nitrile analogs. The curve fit employed is the exponential form, y = A exp[Bx] 37

Table 2-4 The E_a for the conductivity of 0.0055M TbaTf in nitrile analogs. The curve fit employed is the exponential form, y = yo + A exp[Bx]. 37

Table 2-5 The E_a for the conductivity of 0.0055M TbaTf in nitrile analogs. The curve fit employed is the polynomial of second order, $y = Ax^2 + Bx + C$. 38

Table 2-6 The E_a for the diffusion of the nitrile analogs. The curve fit employed is the exponential form, y = A exp[Bx]. 39

Table 2-7 The E_a for the diffusion of the nitrile analogs. The curve fit employed is the exponential form, y = yo + A exp[Bx]. 40

Table 2-8 The E_a for the diffusion of the nitrile analogs. The curve fit employed is the exponential form, $y = Ax^2 + Bx + C$. 40

Table 2-9 The E_a for the conductivity of 0.0055M TbaTf in 2-ketone analogs. The curve fit employed is the exponential form, y = A exp[Bx] 41

Table 2-10 The E_a for the conductivity of 0.0055M TbaTf in 2-ketone analogs. The curve fit employed is the exponential form, y = yo + A exp[Bx]. 41

Table 2-11 The E_a for the conductivity of 0.0055M TbaTf in 2-ketone analogs. The curve fit employed is the polynomial of second order, $y = Ax^2 + Bx + C$. 42

Table 2-12 The E_a for the diffusion of the 2-ketone analogs. The curve fit employed is the exponential form, $y = A \exp[Bx]$ 42

Table 2-13 The E_a for the diffusion of the 2-ketone analogs. The curve fit employed is the exponential form, $y = yo + A \exp[Bx]$. 42

Table 2-14 The E_a for the diffusion of the 2-ketone analogs. The curve fit employed is the exponential form, $y = Ax^2 + Bx + C$. 43

Table 3-1 Optimization of the reaction condition for the synthesis of asymmetric acyclic carbonates. 61

Table 3-2 The dielectric constant and diffusion coefficient for acyclic carbonate solvents. ε_s = dielectric consant, D = self-diffusion coefficient. 63

Table 3-3 The R^2-values for different mathematical model to fit the reference temperature curve. 67

Table 3-4 The E_a values for the diffusion of pure acyclic carbonate at reference temperature 5^{o}C to 85^{o}C. 67

Table 4-1 Optimization of the reaction condition for the synthesis of cyclic carbonates. 83

Table 4-2 Alumina screening for purification with column. 84

Table 4-3 The dielectric constant and self-diffusion coefficient data for cyclic carbonates investigated. ε_s = dielectric constant, D = self-diffusion coefficient. 86

Table 4-4 Density of pure cyclic carbonates used in the calculation of the dipole density 89

Table 4-5 The calculated vs. experimental dielectric constant for pure cyclic carbonates (Exp=experimental, Calc=calculated). 90

Table 4-6 The R^2-values for different mathematical model to fit the reference temperature curve. 92

Table 4-7 The E_a values for the diffusion of pure cyclic carbonate at reference temperature 5^{o}C to 85^{o}C. 92

Table 4-8 Comparison of activation energy for various aprotic solvents. 94

Table 4-9 Dielectric constant and conductivity values for 0.3 molal LiTf in cyclic carbonates. ε_s = dielectric constant, σ = conductivity. 95

Table 4-10 Dielectric constant and conductivity values for 0.3 molal TbaTf in cyclic carbonates. ε_s = dielectric constant, σ = conductivity. 95

Table 4-11 R^2-values for 0.3 molal LiTf in cyclic carbonate solution. 100

Table 4-12 R^2-values for 0.3 molal TbaTf in cyclic carbonate solution. 101

Table 4-13 The energy of activation, E_a for 0.3 molal LiTf in cyclic carbonate solutions. 102

Table 4-14 The energy of activation, E_a for 0.3 molal TbaTf in cyclic carbonate solutions. 103

Table 5-1 Optimum conditions for the reaction to form the intermediate alkoxide.... 121

Table 5-2 The optimum conditions for the synthesis of the glyme series. 123

Table 5-3 Dielectric constant and self-diffusion coefficient for monoglyme analogs, diglyme analogs, and triglyme analogs. ε_s = dielectric constant, D = self-diffusion coefficient. 124

Table 5-4 R^2-values for various fitting model applied to pure monoglyme reference curves. 131

Table 5-5 R^2-values for various fitting model applied to pure diglyme reference curves. 131

Table 5-6 R^2-values for various fitting model applied to pure triglyme reference curves. 132

Table 5-7 The E_a values for the diffusion of pure monoglyme family at reference temperature 5°C to 85°C. 132

Table 5-8 The E_a values for the diffusion of pure diglyme family at reference temperature 5°C to 85°C. 132

Table 5-9 The E_a values for the diffusion of pure triglyme family at reference temperature 5°C to 85°C. 133

Table 5-10 The activation energy for pure glyme family. 135

Table 5-11 Dielectric constant and ionic conductivity for 0.1 molal LiTf in monoglyme family, diglyme family, and triglyme family. ε_s = dielectric constant, σ = ionic conductivity. 139

Table 5-12 R^2-values of the reference curves for 0.1 molal LiTf in monoglyme solutions. 145

Table 5-13 R^2-values of the reference curves for 0.1 molal LiTf in diglyme solutions. 146

Table 5-14 R^2-values of the reference curves for 0.1 molal LiTf in triglyme solutions. 146

Table 5-15 The E_a values for 0.1 molal LiTf in monoglyme solutions at various reference temperature. 150

Table 5-16 The E_a values for 0.1 molal LiTf in diglyme solutions at various reference temperature. 151

Table 5-17 The E_a values for 0.1 molal LiTf in triglyme solutions at various reference temperature. 151

Table 5-18 Activation energy for ionic conductivity. 151

List of Figures

Figure 1-1 Schematic of Diffusion Process [http://en.wikipedia.org/wiki/File:Diffusion.svg] 2

Figure 1-2 Schematic of a rough process of lithium ion transport in a battery [http://www.sigmaaldrich.com/technical-documents/articles/material-matters/u-s-department-of0.html] 8

Figure 1-3 Description of dielectric constant. In essence, the addition of the dielectric material between the two conducting plates lowers the force felt by the charges on each plate. [http://www.universetoday.com/83378/dielectric-constant/] 13

Figure 1-4 Polarization of the dielectric materials by the applied external electric field. The schematic is a rough representation. In reality, the direction of each molecule is not perfectly aligned with the direction of the external electric field. 15

Figure 2-1 The simple Arrhenius plot (top) and the CAF plot (bottom) for conductivity of 0.1 molal LiTf in triglyme. 24

Figure 2-2 Plot of conductivity versus dielectric constant as the molecular volume is varied at constant temperature (top curve) and as the temperature is varied (bottom curve) for 1-hexanol. (σ=conductivity, ε=dielectric constant) Adapted from Petrowsky[40] 26

Figure 2-3 : Plot of dielectric constants vs. conductivity. The reference curves (75^{o}C and 85^{o}C shown) are shown, as well as the variable temperature plot for each nitrile analog. 29

Figure 2-4 Scheme for creating plots for the E_a at each reference temperature. σ_{hex} is the conductivity for each analog (heptanenitrile, octanenitrile, ..., dodecanenitrile),

while the σ_r is the conductivity at each reference temperature (T_r=5°C, 15°C, …, 85°C). 31

Figure 2-5 The plot of $\ln(\sigma/\sigma_r)$ vs. (1/T) for reference temperature, T_r= 5°C to 85°C. . 32

Figure 2-6 Curve fitting for each reference temperature Tr for the nitrile solvent family. Only the mathematical function for T_r = 15°C and T_r=85°C are shown. The fitting functional form used is polynomial of order 2. 34

Figure 2-7 Using the polynomial curve fitting of order 2 to obtain the conductivity $\sigma_r(T_r,\varepsilon_s)$ for reference temperature T_r=55°C. The dielectric constant at each temperature T is measured. Using the dielectric constant value and the equation for the curve fitting, the $\sigma_r(T_r,\varepsilon_s)$ is obtained for each T..... 35

Figure 2-8 An example of curve fitting the nitrile conductivity data with polynomial of the fourth order. While the R^2-values are all equal to 1, the curves fitted do not represent a general relationship between conductivity and dielectric constant..... 36

Figure 2-9 The range of the dielectric constant of the reference temperature curve at 15°C overlaps the heptanenitrile, octanenitrile, and nonanenitrile fully, but not decanenitrile and dodecanenitrile. 45

Figure 2-10 Plot of $\ln[\sigma_{hex}(T,\varepsilon_s)/\sigma_r(T_r,\varepsilon_s)]$ versus 1/T for decanenitrile at T_r=15°C..... 46

Figure 2-11 Plot of $\ln[\sigma_{hex}(T,\varepsilon_s)/\sigma_r(T_r,\varepsilon_s)]$ versus 1/T for decanenitrile at T_r=25°C..... 46

Figure 2-12 The master curve for the conductivity of 0.0055M TbaTf in the nitrile solvent..... 48

Figure 3-1 Molecular structure of 2-ketones and acetate. 51

Figure 3-2 An example of an acyclic carbonate. 52

Figure 3-3 The methyl alkyl species used in the experiment. 53

Figure 3-4 Examples of reactions to form acyclic carbonates. Catalysts and side products (if any) are not shown. 54

Figure 3-5 The mixture of products in the reactions to form acyclic carbonates are the symmetrical dialkyl carbonates. 56

Figure 3-6 Trans-esterification reaction scheme for acyclic carbonates. 57

Figure 3-7 Reactions with starting reagent containing alkoxy group. Here, the methyl group on the starting acetate is the leaving group. 58

Figure 3-8 The methyl haloformates. The halogens are known to be good leaving group, whereas the methoxy is poor leaving group. 58

Figure 3-9 Reaction scheme for making the desired methyl hexyl-, methyl octyl-, methyl decyl-, and methyl dodecyl carbonates. 59

Figure 3-10 Plot of dielectric constant versus temperature for acyclic carbonate. Hex=methyl hexyl carbonate, Oct=methyl octyl carbonate, Dec=methyl decyl carbonate, Dodec=methyl dodecyl carbonate. 64

Figure 3-11 Plot of diffusion coefficient versus temperature for acyclic carbonate. Hex=methyl hexyl carbonate, Oct=methyl octyl carbonate, Dec=methyl decyl carbonate, Dodec=methyl dodecyl carbonate. 65

Figure 3-12 Reference curve for acyclic carbonate self-diffusion coefficient (D) and dielectric constant data. 66

Figure 3-13 Plot of ln (D/D_r) vs (1/T) for selected acyclic carbonate analogs. 69

Figure 3-14 The master curve for acyclic carbonate series. 70

Figure 4-1 Two cyclic carbonate compounds typically used in batteries, ethylene carbonate and propylene carbonate. 74

Figure 4-2 Plot of molar conductivity versus dielectric constant for 0.0055M TbaTf solutions at 25°C. Adapted from Petrowsky[40]. 75
Figure 4-3 The formation of acyclic carbonates from previous work (see chapter 3). . 78
Figure 4-4 Pyridine acts as a base that deprotonates the hydroxyl hydrogen. 78
Figure 4-5 Pyridine acts as a nucleophile that attacks the carbonyl carbon and forms the carbonyl-pyridinium complex. 78
Figure 4-6 The first reaction to synthesize cyclic carbonate. 79
Figure 4-7 The final synthetic scheme for the synthesis of cyclic carbonates from the respective 1,2-diols. 80
Figure 4-8 The bis-carbonate side products formed. 81
Figure 4-9 Synthetic scheme for the synthesis of 1,2-undecane diol. 84
Figure 4-10 Plot of dielectric constant versus temperature for pure cyclic carbonates. 86
Figure 4-11 Plot of self-diffusion of cyclic carbonates under varying temperature..... 87
Figure 4-12 The reference curve for the self-diffusion coefficient (D) and dielectric constant of cyclic carbonates. 91
Figure 4-13 Master curve from Pure Cyclic Carbonate Diffusion Data. 93
Figure 4-14 Plot of dielectric constant versus temperature for 0.3 molal LiTf-cyclic carbonates solution. 96
Figure 4-15 Plot of dielectric constant versus temperature for 0.3 molal TbaTf-cyclic carbonates solution. 97
Figure 4-16 Plot of conductivity versus temperature for 0.3 molal LiTf-cyclic carbonates solution. 97

Figure 4-17 Plot of conductivity versus temperature for 0.3 molal TbaTf-cyclic carbonates solution. 98

Figure 4-18 The reference curve of conductivity versus dielectric constant for 0.3 molal LiTf in cyclic carbonates. σ = conductivity. 99

Figure 4-19 The reference curve of conductivity versus dielectric constant for 0.3 molal TbaTf in cyclic carbonates. σ = conductivity. 100

Figure 4-20 Simple Arrhenius (top) and Compensated Arrhenius (bottom) plot of conductivity against inverse temperature. The simple Arrhenius plot contains a more curved data compared to the Compensated Arrhenius plot. 102

Figure 4-21 Master curve from LiTf Conductivity Data. 105

Figure 4-22 Master curve from TbaTf Conductivity Data. 105

Figure 5-1 Poly(ethylene oxide). 114

Figure 5-2 From top to bottom: monoglyme, diglyme, triglyme. 116

Figure 5-3 From top to bottom: monoglyme-, diglyme-, and triglyme-derivatives. ... 117

Figure 5-4 Reaction scheme for ring opening polymerization of poly(ethylene oxide). 117

Figure 5-5 Applying the ring opening reaction of epoxide to the synthesis of alkyl monoglyme. 118

Figure 5-6 Commercially available ethylene glycol monomethyl ether derivatives... 118

Figure 5-7 An example of the S_N2 reaction. 119

Figure 5-8 Reaction of a hydroxyl group with alkali metal to produce an alkoxide metal species as well as liberate hydrogen gas. 120

Figure 5-9 The reaction scheme for making alkyl glyme series. 120

Figure 5-10 The scheme for S_N2 and E2 reaction. 122

Figure 5-11 Plot of dielectric constant for all the glyme series versus temperature (MG=monoglyme, DG=diglyme, TG=triglyme). 125

Figure 5-12 Plot of self-diffusion coefficient, D versus temperature, T for all analogs of monoglyme, diglyme, triglyme (MG=monoglyme, DG=diglyme, TG=triglyme)..... 126

Figure 5-13 Dielectric constant versus temperature for hexyl glyme series (MG=monoglyme, DG=diglyme, TG=triglyme). 127

Figure 5-14 Diffusion coefficient versus temperature for hexyl glyme series (MG=monoglyme, DG=diglyme, TG=triglyme). 128

Figure 5-15 Reference curve for pure monoglyme self-diffusion coefficient data and dielectric constant data. 128

Figure 5-16 Reference curves for pure diglyme from self-duffusion coefficient and dielectric constant data. 129

Figure 5-17 Reference curves for pure triglyme from self-duffusion coefficient and dielectric constant data. 130

Figure 5-18 Master curve for the pure monoglyme..... 135

Figure 5-19 Master curve for the diglyme series..... 136

Figure 5-20 Master curve for the triglyme series. 136

Figure 5-21 Combine master curve for all glyme series. MG=monoglyme, DG=diglyme, TG= triglyme..... 137

Figure 5-22 Dielectric constant of 0.1 molal LiTf solution in the gylme series versus temperature (MG=monoglyme, DG=diglyme, TG=triglyme). 140

Figure 5-23 Dielectric constant versus temperature for hexyl monoglyme, hexyl diglyme, hexyl triglyme. 140
Figure 5-24 Ionic conductivity of 0.1 molal LiTf solution in the gylme series versus temperature (MG=monoglyme, DG=diglyme, TG=triglyme). 142
Figure 5-25 Ionic conductivity versus temperature for hexyl monoglyme, hexyl diglyme, hexyl triglyme. 142
Figure 5-26 Reference curve for 0.1 molal LiTf in monoglyme solvents. 143
Figure 5-27 Reference curve for 0.1 molal LiTf in diglyme solvents. 144
Figure 5-28 Reference curve for 0.1 molal LiTf in triglyme solvents. 144
Figure 5-29 Erroneous $\ln(\sigma/\sigma_r)$ vs (1/T) for 0.1 molal LiTf in diglyme electrolytes using second order polynomial curve fitting. Plots shown for selected T_r's. 147
Figure 5-30 Erroneous $\ln(\sigma/\sigma_r)$ versus (1/T) for 0.1 molal LiTf in triglyme electrolytes using second order polynomial curve fitting. Plots shown for selected T_r's. 148
Figure 5-31 Plots of $\ln(\sigma/\sigma_r)$ vs (1/T) using simple exponential curve fitting model for 0.1 molal LiTf in hexyl diglyme electrolyte for selected T_r's. 149
Figure 5-32 A plot of $\ln(\sigma)$ versus (1/T) for 0.1 molal LiTf in hexyl diglyme electrolyte. The simple Arrhenius plot produces non-linear curve. Because of this, a single E_a cannot be obtained since at different temperature, the slope is different. 149
Figure 5-33 Master curve for the 0.1 molal LiTf in monoglyme series. 152
Figure 5-34 Master curve for the 0.1 molal LiTf in diglyme series. 153
Figure 5-35 Master curve for the 0.1 molal LiTf in triglyme series. 153
Figure 5-36 Master curve for 0.1 molal LiTf in glyme series. (MG=monoglyme, DG=diglyme, TG=triglyme). 154

Figure 5-37 Plot of dielectric constant versus oligomer repeat units for pure glyme oligomers at 25°C. 155

Figure 5-38 Plot of diffusion versus number of oligomer repeat units for pure glyme oligomers at 25°C. 156

Figure 5-39 Plot of E_a versus oligomer repeat units for pure glyme series at 25°C.... 157

Figure 5-40 Plot of dielectric constant versus number of repeat unit for 0.1 molal LiTf in glyme oligomers at 25°C. 158

Figure 5-41 Plot of ionic conductivity versus oligomer repeat units for 0.1 molal LiTf in glyme oligomers at 25°C. 159

Figure 5-42 Plot of activation energy versus oligomer repeat unit for 0.1 molal LiTf in glymes at 25°C. 160

Abstract

It has been proposed and shown that transport properties like self-diffusion and ionic conductivity in organic liquids are dependent on the dielectric constants and the activation energies in these liquids. The formal method that relates the self-diffusion and ionic conductivity to the dielectric constants and activation energies in these liquids is called the Compensated Arrhenius Formalism (CAF). Various systems have shown to be in compliance with the CAF.

The CAF has been applied to liquids of varying dielectric constant values. In order to extend the library of the solvent applicable for analysis by the CAF and to understand the limitation of the CAF, two organic liquids, one with very low dielectric constant, acyclic carbonates, and the other with very high dielectric constant, cyclic carbonates are synthesized and analyzed using the CAF. The CAF is also tested for analysis of transport properties in polymers.

This thesis involves the synthesis of acyclic carbonates, cyclic carbonates, and oligomers of poly(ethylene oxide), and the application of the CAF to these organic liquids and oligomers in order to try and understand the limitations of the CAF. The application of the CAF to these liquids and oligomers also can help in trying to understand the transport properties in these liquids and in polymers.

The synthesis of asymmetric acyclic carbonates was accomplished using a convenient method where an unwanted secondary reaction was avoided by precipitation of a side product during the reaction. The cyclic carbonate derivatives were synthesized via the cyclization reaction of methyl chloroformate and 1,2-diols. The synthesis of

poly(ethylene oxide) oligomers was achieved using simple S_N2 reactions with alkyl bromide.

The transport properties of acyclic carbonates and the cyclic carbonates can also be described by the CAF. Acyclic carbonates have low dielectric constants, but similar energy of activation for self-diffusion as other higher dielectric constant organic liquids like 2-ketones, nitriles, and acetates. The low dielectric constant values of acyclic carbonates prevent salts from dissolving in acyclic carbonates. Thus the conductivity in acyclic carbonates could not be measured.

The cyclic carbonates have high dielectric constants. The energy of activation for self-diffusion of cyclic carbonate is higher compared to other aprotic organic liquids previously investigated. The energy of activation for ionic conductivity is also found to be high for cyclic carbonates compared to other polar aprotic liquids like 2-ketones and nitriles. The energy of activation is very high such that even though the dielectric constant in cyclic carbonates is higher than the dielectric constants in 2-ketones and nitriles, the conductivity is lower in cyclic carbonates.

It was found that the CAF can be applied to oligomers of poly(ethylene oxide). However, the results suggest that to apply the CAF to oligomers and predict transport properties in polymers, the oligomers repeat units have to be high compared to the alkyl chain length tethered to the oligomers.

Chapter 1 : Introduction To Mass Transport

1.1 What is Mass Transport?

Mass transport refers to the mobility of charged or neutral species in liquid or solid media. Two types of mass transport that are considered to be the most important are diffusion and ionic conductivity. These two types of mass transport occur in many natural aspects of people's lives that include blood flow, corrosion, water flow, ion transport in batteries, and pretty much anything that involves flow. Controlling drug flow in blood allows for better drug delivery and has the potential to save and to improve the quality of lives. Designing better electrolytes allows for better ion conduction that could lead to improved batteries, fuel cells, and drug delivery systems.

Another example is in polymers - a type of material that is used in cars, household items, even human bodies, and arguably the most integrated material to human lives. Many polymer properties are related to their viscosity, which describes the flow of the polymeric molecules. Because of this, the mass transport of polymeric materials is important in understanding polymer properties. Other complex fluids like glue and ketchup, where their properties are controlled by the flow of their individual component molecules, are also affected by mass transport.

In addition to these phenomena, other processes like ion transport in electrolytes, ionic liquids, and heat transfer in liquid media are also affected by mass transport. Understanding the factors that affect mass transport in these processes provides the potential to save millions of dollars, as well as advancing the technological aspect of human lives. From the examples mentioned, it is obvious that the world is

affected by mass transport. It is important that the principles behind transport phenomena are known.

1.2 What is Diffusion?

Diffusion is a phenomenon that describes the flow of molecules in some media because of concentration gradients that exist in the media. In general, diffusion in liquids can be divided into two categories. Gradient driven diffusion occurs when a species diffuses in a medium from a high concentration region to a lower concentration region. The second category is when a species diffuses in a medium without any concentration gradient. This type of diffusion is in general called intra-diffusion. Intra-diffusion itself is usually divided into several categories. The intra-diffusion of a pure liquid is called self-diffusion, while the intra-diffusion of species one in species two or in a mixture of multicomponent species is called tracer-self-diffusion[1, 2]. An example of self-diffusion is the flow of liquid hexane molecules in a beaker, under equilibrium, at room temperature and pressure. Another example of tracer-self-diffusion is the motion of lithium ions, with or without counter anions, in liquid water or in liquid tetrahydrofuran.

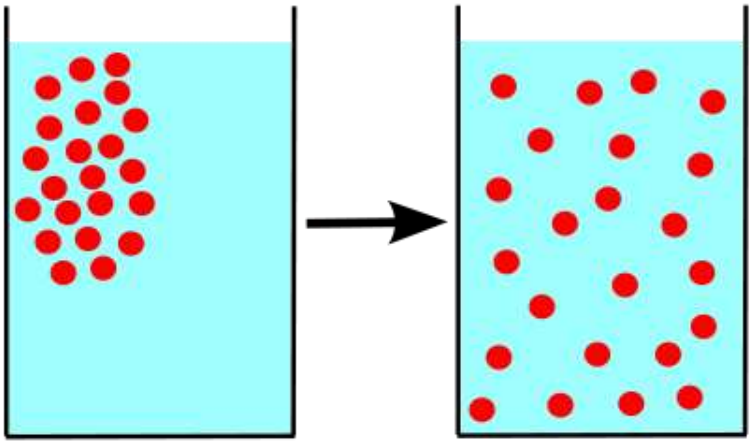

Figure 1-1 Schematic of Diffusion Process
[http://en.wikipedia.org/wiki/File:Diffusion.svg]

1.3 The theory of self-diffusion

Self-diffusion is described by Fick's (first) law of diffusion. Mathematically, it is described by the following equation[3]:

$$J = -D\left(\frac{dc_i}{dx}\right) \qquad (1\text{-}1)$$

where *J* describes the amount of the mass that flows per unit area per unit time (flux of the diffusing species), *D* is the diffusion coefficient in units of length squared per unit time, and the term in the parentheses is the concentration gradient in units of molecules per unit volume per unit length (here it is described for a concentration gradient in one dimension along the x-axis). Essentially, the flux is driven by a force in the form of the concentration gradient. While this equation is easy to understand in cases where the concentration gradient is obvious, for example the initial state of a solution when a solid is dissolved in a bulk solvent or when a dye is added to a solvent, for self-diffusion and tracer-diffusion where the distribution of the diffusing species are homogenous in the solution, the concentration gradient here is not obvious and is not well understood.

From equation 1-1, it is clear that the amount of mass that flows will be higher if the concentration gradient of the diffusing species is increased, or if the value of the diffusion coefficient, *D*, is increased. Since the transient concentration gradient is not well understood, there is no way to control the concentration gradient for self-diffusion and tracer-diffusion. On the other hand, the diffusion coefficient, *D* is thought to be dependent on a number of factors, including the medium containing the diffusing species. Thus, to understand the self- and tracer-diffusion and be able to manipulate *D*, it is desirable to understand the relation between *D* and the structure of the molecule

making up both the media and the diffusing species. In addition to this, the mechanism of the diffusion process has to be uncovered.

A few theories have been developed to describe the relation between the self-diffusion coefficient, *D* and the bulk properties of the media, as well as the structure of the diffusing molecule. For liquids, two theories are prominent. The hydrodynamic theory relates the diffusion coefficient to the inverse of the solvent viscosity and the radius of the diffusing species. Essentially,

$$D \propto \frac{1}{\eta\, r} \tag{1-2}$$

One specific example is the Einstein-Smoluchowski equation, where the diffusion coefficient is related to the friction coefficient

$$D = \frac{k_B\, T}{\xi} \tag{1-3}$$

Here, ξ is the friction coefficient of species 1, k_B is the Boltzmann constant, while *T* is temperature. The friction coefficient itself is described by Stoke's law for spherical particles to be

$$\xi = 6\,\pi\,\eta\,r \tag{1-3a}$$

where η is the solvent viscosity, and *r* is the diffusing particle radius.

This equation is related to the bulk viscosity by combining equations (3) and (3a) into the well-known Stokes-Einstein[4] equation

$$D = \frac{k_B\, T}{6\,\pi\,\eta\,r} \tag{1-4}$$

The unique feature of these equations is the inclusion of radius of the diffusing species, thus relating the diffusion coefficient to the size of the diffusing particles. This is equation is the closest relation that is able to relate the diffusion coefficient to some

form of molecular structure of the diffusing species. In addition, the equation relates the diffusion coefficient to a property of the bulk media, the viscosity.

However, the hydrodynamic theory is really a macroscopic theory. The relation to the microscopic view is only through application of statistical mechanics, but it contains some flaws. An example of a flaw in the theory is an assumption made about the diffusing species[5, 6]. It is always assumed to be a single molecule of the diffusing species. In fact, it has been shown by molecular dynamics simulation experiments[7, 8] that the diffusing species might not be a single molecule; instead it may be an aggregate of molecules including molecules that made up the medium. This is particularly true for the diffusion of charge species in liquid electrolyte solutions[7-9].

Furthermore, there have been cases where the diffusion of ions with a bigger radius is faster than ions with smaller radius[10]. This is an obvious violation of equation (1-4) above.

On top of that, there is no known relation between the viscosity and the structure of the molecules of the media. Thus, there is no guidance on modifying the structure of the molecules making up the media. Finally, while the hydrodynamic theory does suggest that the diffusing species moves through the media, the actual mechanism is still not known. A lot of the remaining studies[5, 6, 11-25] on hydrodynamic theory focus on correcting these errors through empirical parameters, thus providing no guidance on the structure-property relationship as well as the mechanism of the diffusion.

Besides the hydrodynamic theory, the kinetic and free volume theory[26] relates the diffusion coefficient to the activation energy. This results in an Arrhenius-like equation,

$$D = A(\eta)\, e^{(-\frac{E_a}{k_B T})} \qquad (1\text{-}5)$$

In this equation, A is the exponential pre-factor with a unit similar to D, and E_a is the activation energy. A lot of effort has been put to determine the value of A and E_a. Most of the results of the investigations focus on the idea that A depends on the viscosity of the solution, similar to the hydrodynamic theory discussed above. Through a similarity with kinetic theory suggested by Eyring, E_a is thought to be the energy required to get the diffusing species to overcome the activation barrier needed for diffusion. This is further expanded into free volume theory, where the position of the molecule before and after the jump is separated by a transition state[26]. Thus, the E_a is also considered as the energy to form a free volume for the diffusing species to jump into. The appearance of temperature provides another degree of freedom to the system that can be manipulated to validate the equation. The kinetic and free volume theories also provide a few possible mechanisms at the microscopic level that involve formation of free volume[27, 28] for the diffusing species to move into, as well as quasi-lattice activated jump theory[29-33].

However, many studies have provided data that are inconsistent with the assumptions in these theories. One problem was shown in a few investigations[34, 35] where data fitted using these equations relating D to viscosity do not fit well outside a very small window. Thus, it is obvious that these equations do not provide a complete picture of the factors affecting D. On top of that, a few simple analyses using statistical mechanics and available thermodynamic data suggest that the assumption that E_a is related to a transition state is inconsistent with the values of the activation energies[36, 37] obtained at room temperature and the population of the species in the activation states. In short, the molecular picture of factors affecting E_a is still murky. As a consequence,

the relationship between the structures of the molecules involved and the value of E_a is still a mystery.

In summary, while both the hydrodynamic theory, as well as the kinetic and free volume theories, relate the diffusion coefficient *D* to the viscosity as well as the radius of the diffusing species, available experimental data do not fit even the macroscopic relation well. It is important to understand these phenomena at the microscopic level for improvements to be made. The value of the diffusion coefficient *D* is related to both the properties of diffusing species, as well as the properties of the molecules that make up the medium. The only way to improve *D* is then to understand the relation between these properties and the molecular structures of the species involved.

1.4 What is Ionic Conductivity?

Ionic conductivity refers to the transport of charged species driven by the potential difference between two electrodes (Figure 1-2). Besides the obvious use in batteries, it has also been shown that ion transport in other parts of living bodies also involves ionic conductivity[38, 39].

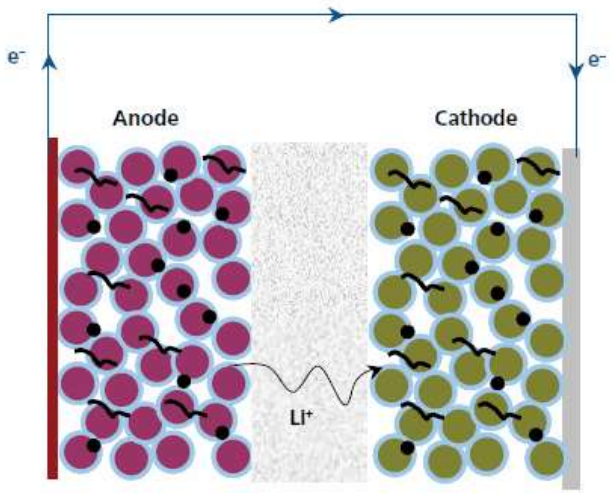

Figure 1-2 Schematic of a rough process of lithium ion transport in a battery [http://www.sigmaaldrich.com/technical-documents/articles/material-matters/u-s-department-of0.html]

1.5 Theory of Ionic Conductivity

Like diffusion, ionic conductivity has been studied for over a hundred years. However, the principles governing the process are still unknown. Studies of ionic conductivity can be divided into macroscopic investigations and microscopic investigations. In order to understand ionic conductivity processes, a microscopic picture of the process needs to be developed.

The most general equation relating ionic parameters to conductivity, σ is given by equation 1-6:

$$\sigma = \sum_i q_i c_i \mu_i \qquad (1\text{-}6)$$

Here, σ is total conductivity, q is the charge value of the species i, c is the concentration of ionic species i, and μ is the mobility, or the speed of the individual charge carrier. This relation provides no connection between ionic conductivity and solvent properties. As such it does not help in designing better electrolyte molecules.

Besides this relation, specific laws are formulated for specific cases that attempt to provide more insight into ionic conductivity phenomena. Concentration dependences of ionic conductivity are divided into strong electrolyte and weak electrolyte cases. For a weak electrolyte case, the ionic conductivity is dependent on the degree of association between the cation and the anion species in the electrolyte. Thus the ionic conductivity in a weak electrolyte is complicated. Walden's rule attempts to ascribe ionic conductivity to the properties of the ions and the media. Walden's rule (equation 1-7) states that the ionic conductivity, Λ is controlled by the media viscosity, η and the size of the ionic species, *r*. The *c* in equation 1-7 is an arbitrary constant determined empirically.

$$\Lambda = \frac{c}{\eta r} \qquad (1\text{-}7)$$

Walden's rule is related to the Stokes-Einstein equation described in section 1.3.

While Walden's rule attempts to include the properties of the media, the inclusion of viscosity, as mentioned in section 1.3, has limited use in understanding the structure-property relationship of the molecules making up the media. In particular, the relation between the viscosity of the medium to the structure of its constituting species is not well understood.

In addition, the inclusion of the ion size in the equation has been shown to be inaccurate[40]. Various studies have shown that bigger ions can results in higher ionic conductivity values. As mentioned in section 1.3, molecular dynamics studies[7, 41-43] have suggested that the ions form complexes with the species of the medium, making the actual size of the diffusing species unrelated to the size of the ions.

For the strong electrolyte case, the ions are assumed to fully dissociate. For ionic conductivity in strong electrolytes, Kohlrauch[44] studied various aqueous electrolyte systems and determined that the concentration dependence conductivity can be written as

$$\Lambda = \Lambda^o - K\sqrt{c} \qquad (1\text{-}8)$$

Here, Λ is the molar conductivity, Λ^o is the molar conductivity at infinite dilution, K is a constant specific to the electrolyte system, and c is the concentration salt in the solution.

In theory, Kohlrausch's law describes ionic conductivity from the point of view of the ions involved. The dissociation of any particular ionic compound, which controls the number of charge carriers, is controlled by the media that the ions are in. Thus, the relation (1-8) developed by Kohlrausch does not help in designing better medium for ionic conductivity; the factors affecting the mobility of the ions is not available from Kohlrausch's relation (1-8).

The temperature dependence of ionic conductivity is usually described by the William-Landel-Ferry (WLF)[45] or the Vogel-Tamman-Fulcher (VTF)[46-48] empirical relationships. The WLF equation is described as

$$\log\frac{\sigma(T)}{\sigma(T_s)} = \frac{C_1(T-T_s)}{C_2+(T-T_s)} \qquad (1\text{-}9)$$

Here, σ is the conductivity, T and T_s are the temperature and the reference temperature respectively, and C_1 and C_2 are constants that are determined empirically for specific solvent materials.

The VTF relation is described as

$$\sigma = \frac{\sigma_o}{T^{1/2}}\, e^{\frac{-B}{(T-T_o)}} \qquad (1\text{-}10)$$

Here, σ is the conductivity, T is the temperature, while σ_o, T_o and B are constants specific to the solvent material.

Both of these widely used empirical relations are in essence different forms of the more general Arrhenius equation:

$$\sigma = A\, e^{\frac{-E_a}{RT}} \tag{1-11}$$

Here, σ is conductivity, A is the exponential pre-factor, E_a is the activation energy, R is the gas constant, and T is the temperature in Kelvin. Similar to diffusion, the exponential pre-factor A is determined empirically, although some assumption that relates A to viscosity is also made. The problem with the simple Arrhenius equation is similar to the case of diffusion, in that the assumption that the exponential pre-factor depends on the viscosity proves to be inaccurate, and that the even if the assumption is true, the viscosity provides no understanding of the structure of the molecules needed to increase or decrease ionic conductivity.

1.6 The Compensated Arrhenius Equation (CAE)

In 2008, Frech and coworkers[49-54] showed that the exponential pre-factor in equation (1-5) and (1-11) above is better described by the static dielectric constant, ε_s. They modified equation 1-5 and 1-11 into

$$D(T) = D_o(\varepsilon_s(T))\, e^{\left(-\frac{E_a}{k_B T}\right)} \tag{1-12}$$

$$\sigma(T) = \sigma_o(\varepsilon_s(T))\, e^{\left(-\frac{E_a}{k_B T}\right)} \tag{1-13}$$

In equations (1-12) and (1-13), D_o is the diffusion exponential pre-factor, and σ_o is the conductivity exponential pre-factor. In these equations, both the diffusion and conductivity exponential pre-factor are dependent on the dielectric constants. In their work, they have shown that a single energy of activation is obtained for each of the

diffusion coefficient and ionic conductivity data is obtained using what they described as the Compensated Arrhenius Formulation, CAF[35, 40].

What is more important however, is the fact that by showing that the diffusion coefficient and ionic conductivity are dependent on static dielectric constant, there are no more viscosity dependent terms as in the Arrhenius equation. Unlike viscosity, the microscopic view of the static (and the frequency dependent) dielectric constant is more established from the works of many including Debye, Onsager, and Kirkwood. They have shown that the static dielectric constant is related to the dipole moment of the species involved and the volume occupied by the dipole moment. This allows for connection between diffusion coefficient, *D* as well as ionic conductivity and the structures of the diffusing molecules. A short review of these works is presented in section 1.7. The details of the CAF are described in Chapter 2.

1.7 Theory of dielectric constant

A dielectric constant is a property of bulk materials. It describes the relative screening of the forces acting between two charges in the bulk molecules, compared to when the charges are in a vacuum (Figure 1-3). A dielectric constant is usually measured using dielectric spectroscopy (described in more detail below); as such, the description of dielectric constant involves the response of a material under the influence of external electric field. Dielectric constants can be divided into two parts, the static dielectric constant, and the time-dependent (frequency dependent) dielectric constant. Both of these have been extensively studied experimentally and theoretically.

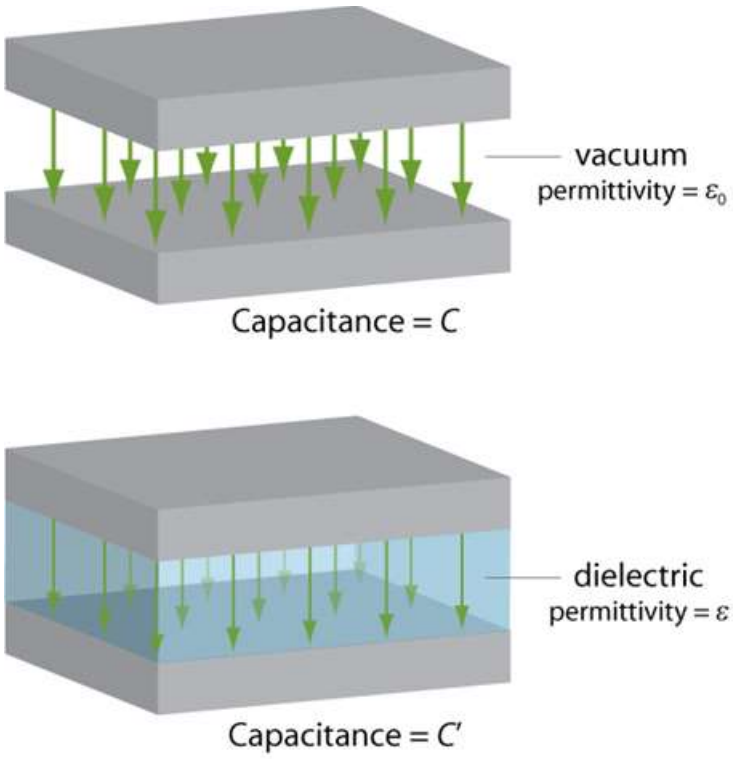

Figure 1-3 Description of dielectric constant. In essence, the addition of the dielectric material between the two conducting plates lowers the force felt by the charges on each plate. [http://www.universetoday.com/83378/dielectric-constant/]

As mentioned above, the dielectric properties of a material are measured as the screening force between two charges, with the screening force appearing in the form of the "charges" that arise from polarization of electrons, atoms, and permanent moments in the dielectric materials. Thus, polarization can be divided into two different types. The electronic polarization is the polarization that results from the shift of electrons in the molecules as the external electric field is applied. The atomic polarization is the polarization that occurs from the shift of an atom as the external field is applied to the molecules. Both of these types of polarization are of the intra-molecular polarization type. They occur within a single molecule, for all molecules in the system. Since it is an internal polarization, this type of polarization is not affected by thermodynamic

properties like temperature and pressure. Both of these types of polarization are also called translational polarization.

A second type of polarization is the configuration polarization, or molecular polarization. This polarization appears as a result of the change in orientation of the molecules with permanent dipoles as the molecules are subjected to an external electric field. This type of polarization is related to the whole system, and is an inter-molecular polarization. The more the molecules align themselves under the influence of the external electric field, the higher the polarization will be. This type of polarization is affected by temperature and density, as well as the chemical composition of the system. This type of polarization is also known as rotational polarization (Figure 1-4).

Static dielectric constants are proportional to these polarizations in the dielectric material. The polarization itself is related to the dipole density. However, a more accurate description of polarization is the moment density, where instead of the dipole moment of a single molecule per unit volume, the moment is the total vector from the addition of the dipole moment vector of all the molecules in the volume. Thus the dielectric constant is proportional to the moment density of the dielectric material.

Since polarization is proportional to the moment density, it is thus proportional to the moment and volume. A consequence of this is that the moment of dielectric materials can also be divided into two parts. Just like polarization, the first part is the translational moment, which is the moment that arises from the electrons and atoms in a molecule.

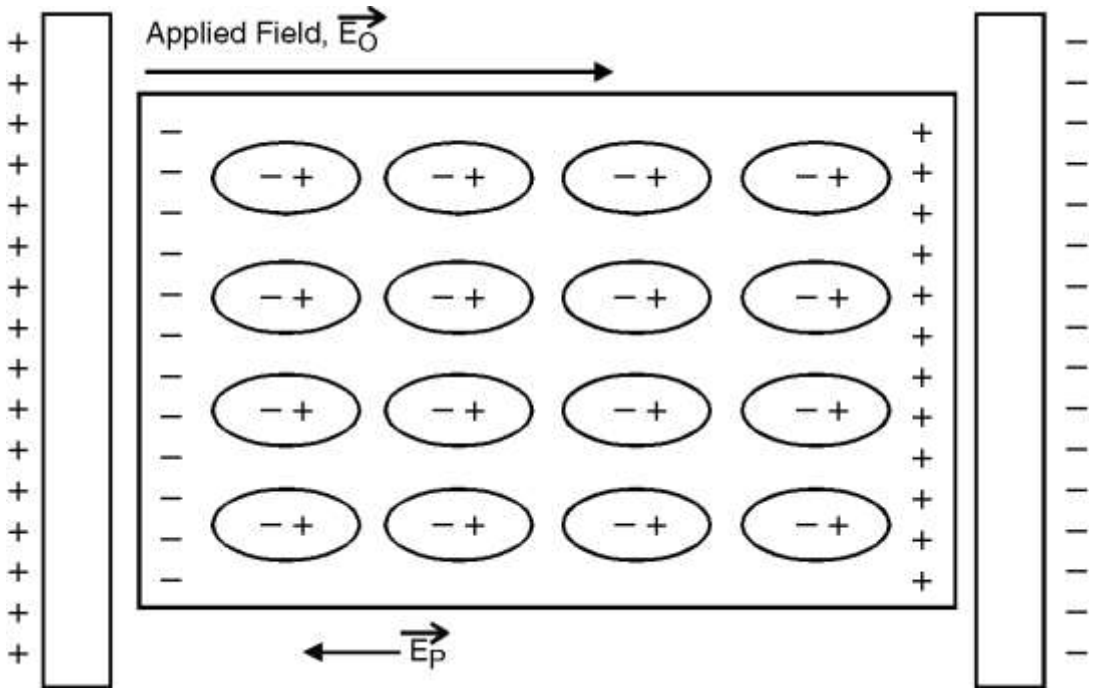

Figure 1-4 Polarization of the dielectric materials by the applied external electric field. The schematic is a rough representation. In reality, the direction of each molecule is not perfectly aligned with the direction of the external electric field. [http://www.winnerscience.com/electromagnetic-field-theory/polarization-or-dielectric-polarization/attachment/figure-polarization-2/]

The second type of moment, called the rotational moment, is applicable for cases where there is a permanent dipole moment. In the rotational moment, the value of the moment depends on the degree of alignment of all the molecules in the dielectric material. The rotational moment is affected by temperature, density, and the composition of the dielectric material.

For static dielectric constants, three pertinent equations are widely used to relate dielectric constant to dipole moment and volume:

Debye equation: $$\frac{\varepsilon-1}{\varepsilon+2} = \frac{4}{3}\,\pi\, N\,(\,\alpha + \frac{\mu^2}{3\,k\,T}\,)$$

Onsager equation: $$\frac{(\varepsilon-\varepsilon_\infty)(\,2\varepsilon+\varepsilon_\infty\,)}{\varepsilon\,(\varepsilon_\infty+2)^2} = \frac{4\,\pi\,N\mu^2}{9\,k\,T}$$

Kirkwood-Frohlich equation: $\frac{(\varepsilon - \varepsilon_\infty)(2\varepsilon + \varepsilon_\infty)}{\varepsilon(\varepsilon_\infty + 2)^2} = g\frac{4\pi N \mu^2}{9kT}$

In these equations, ε is the static dielectric constant, ε_∞ is the dielectric constant at infinite frequency, N is the number density, α is the polarizability of the dielectric material, k is Boltzmann constant, T is the temperature, and μ is the permanent dipole moment of the molecule. In the Kirkwood-Frochlich equation, g is the association factor, where a value of 1 describes no association, and any association between the molecules will result in a g value above 1.

From these equations, it is obvious that the static dielectric constant is proportional to the square of the dipole moment, μ, and inversely proportional to the temperature, T. It is also inversely proportional to the occupied volume of the bulk solvent through the number density N. Thus, the higher the temperature of volume, the lower the dielectric constant will become.

These equations have their own applicability and flaws. The Debye equation was the first to be formulated by Peter Debye to be applicable to almost all molecules. However the values of dipole moment calculated using the Debye equation are shown to be in disagreement with the values of dipole moment for highly polar liquids[55]. The Onsager equation is essentially an improved Debye equation, but with a correction to the values from the contribution of the electronic polarization. Because of this, it is applicable even with pure polar liquids. In this work, the Onsager equation is used to relate the dielectric constant to molecular dipole moment. The Kirkwood equation is formulated using statistical mechanics. It includes a constant, called the g-factor that describes the degree of association between the molecules.

All of these equations describe the dielectric constant, a macroscopic property, to dipole moment and molecular volume – both are microscopic properties. This provides guidance in interpreting the relationship between molecular structure and dielectric constant.

From the various relations between dielectric constant and polarization and moment density, and the subsequent dipole moment, a few guidelines on creating dielectric media with specific dielectric constant values can be formulated. To attain high dielectric constants, the moment density has to be high. The moment density is a function of two properties, the moment itself and the volume. The volume is related to the mass density of the dielectric media.

Since there are two types of moment, the moments are controlled by a few factors. The intra-moment, the moment related to the displacement of electrons or atoms in the molecule. These values are relatively small, and as such are not considered an effective way of controlling the moment. The rotational moment is related to the permanent dipole moment of a molecule. The more aligned the molecules, the higher the moment. However, the factors controlling the alignment are not clear. However the contribution of the permanent dipole is usually the dominant factor. Thus, usually the dielectric constant of a dielectric material is controlled by customizing the shape of the molecules in the dielectric material such that the dipole moment of an individual molecule is high.

Besides the static dielectric constant, a time-dependent field creates the notion of dielectric relaxation. This relaxation is the lag in the response of the polarization to the changing external electric field. This lag in response can be attributed to the lag in the

fluctuation of the moment and of the volume. Murphy and Morgan have shown that the lag in moment from the displacement of electrons is on the order of femtoseconds, while that of the displacement of atoms is in the order of picoseconds to tenths of femtoseconds[56]. For orientation polarization, the time order for the phenomenon to occur varies from tenths of pico seconds to minutes, depending on the internal friction of the molecules in the dielectric material.

Kauzmann has postulated that dielectric relaxation can be treated similarly to a chemical rate process[57]. In this work, Kauzmann showed the mathematical solution for relaxation in both the static as well as time-dependent dielectric constant. Thus, the frequency dependence of the dielectric constant is known. The interesting part of Kauzmann's work is the similarity in what he proposes compared to what Frech and coworkers later propose[58]. Both equations involve activation parameters, E_a, as well as exponential pre-factors.

1.8 Techniques used

Self-diffusion coefficients, and dielectric constant data were measured for several solvents and electrolytes. Experimentally, the self-diffusion coefficients were measured using the pulsed-field gradient (PFG) method described below. The static dielectric constant data were measured using impedance spectroscopy.

PFG

Diffusion coefficients are measured using the Nuclear Magnetic Resonance (NMR) Pulsed-Field Gradient (PFG) method[59, 60]. In this method, the nuclei of interest are hit with two pulsed-fields, the second which would invert the orientation of the magnetic vector. The rate of the diffusion will determine the orientation of the inverted

vector. The higher the diffusion rate, the less aligned the inverted vector is. This will lower the signal intensity produced. The plot of the signal intensity versus the gradient strength produces a linear relationship. The slope of this relationship is the diffusion coefficient.

Impedance Analysis

Static dielectric constants were measured using impedance analysis. In impedance analysis, the capacitance of two conducting plates is measured at different frequencies. The capacitance is measured as the ratio between the frequency dependent voltage to the frequency dependent current. The inverse value of the impedance, the admittance, is divided by the current to get the capacitance, *C*. The dielectric constant is then calculated from the equation $\varepsilon_s = \alpha \, x \, C \, x \, C_o$, where α is the constant that accounts for the stray capacitance, and C_o is the atmospheric capacitance.

It should be noted that much of the work presented here was of a collaborative nature between Glatzhofer's group and Frech's group. As such, care will be taken in the following chapters to specify when PFG and Impedance measurements were carried out by Dr. Matt Petrowsky.

1.9 Purpose of Work and Summary of Chapters

The CAF has been applied to a lot of solvent families like 1-alcohols[49], 2-ketones[61], acetates[62], nitriles[53], and thiols[53]. To investigate the utility of the CAF as an instrument to uncover transport properties, it is important that the solvent library that the CAF is applicable to is extended further. As mentioned in section 1.6, the CAF assumes that the pre-factor in the Arrhenius equation is dependent on the dielectric constant. Thus, the dielectric constant of the solvents is important. Table 1-1 shows the

dielectric constant value of the simplest molecule for each of the solvent families investigated previously. From this table, it can be inferred that the CAF is applicable to solvents with dielectric constant values between 4 and 36.

Solvent	Dielectric Constant, ε_s
Methanol	32.6
Acetone	20.7
Methyl acetate	6.7
Acetonitrile	38.8
Ethanethiol	8

Table 1-1 Dielectric constant of selected organic solvents at 20°C[63].

To extend the library of solvents applicable to the CAF, this work will attempt to study two solvents. One solvent is at the lower end of the dielectric constant range, while the other is at the higher end of the dielectric constant range. The organic carbonates are two electrolyte materials used in an actual batteries[64]. Acyclic carbonates like dimethyl carbonates have low dielectric constant of 3.107 at 25°C[64], while cyclic carbonates like propylene carbonates have high dielectric constant of over 64.9 at 25°C[64]. Since the dielectric constant values of these two families of organic carbonates are lower than 6.7 (methyl acetate) and higher than 38.8 (acetonitrile), they are suitable for testing the limits of the CAF. Furthermore, if they are applicable for analysis with the CAF, the transport properties in these organic electrolyte materials will be better understood which can in turn help understand ionic conductivity in these batteries.

Besides these small organic solvents, polymers are also important materials that are not well understood. Properties of polymers are known to depend on their rheological behavior[65]. To understand the rheological behavior of polymers, the transport properties of the individual polymer molecule have to be understood.

Viscosity has also been used to describe the rheological behavior of polymers. Just like for liquids, viscosity provides no insight into the structure-property relationship of polymers. Furthermore, polymers are essentially slow moving liquids in their amorphous phase[65]. Thus, polymers in theory can be analyzed with the CAF. This work will attempt to determine the applicability of the CAF to polymers by applying the CAF to poly(ethylene oxide).

The rest of the chapters are arranged as follows:

Chapter 2 describes the details of the Compensated Arrhenius Formulation (CAF) method. An example is shown for the charge transport in the family of nitrile solvents using the data from literature[53]. The trends for various properties like dielectric constant, ionic conductivity, self-diffusion, and the energy of activation are examined and discussed.

Chapter 3 describes the synthesis and application of the CAF to acyclic carbonates. Acyclic carbonates – for example dimethyl carbonate and diethyl carbonate – are used as additives in battery electrolytes[64]. The acyclic carbonates were synthesized via substitution reaction of acyl chloride derivatives with 1-alcohols. A convenient method that allows for easy separation of the synthesized products was discovered. The low dielectric constant of the acyclic carbonates prevents the collection of data for ionic conductivity in acyclic carbonates. The self-diffusion data shows that the E_a for diffusion is similar to other solvents studied previously[51, 53, 61, 62].

Chapter 4 describes the synthesis and application of the CAF to cyclic carbonates – which are widely used as electrolytes in battery applications. The cyclic carbonates used in these experiment are not commercially available and were synthesized in house

using a cyclization reaction of 1,2-diols with acyl chloride derivatives. It has been shown that propylene carbonate, which has a high dielectric constant, has lower ionic conductivity compared to nitriles or ketones, both of which have lower dielectric constants. It was shown that the reason for the lower ionic conductivity in cyclic carbonate solvents is because of the higher E_a for ionic conductivity in this solvent family.

Chapter 5 describes the synthesis and application of the CAF to oligoethers, model compounds of poly(ethylene oxide), a polymer that has been investigated extensively as a solid polymer electrolyte. The ethylene oxide oligomers used in the studies were also not commercially available and thus were synthesized in house using substitution reactions of alkoxy ethers with alkyl halides. The unexpected results in the ionic conductivity trend are predicted by the CAF, showing the success of the CAF.

Chapter 6 concludes the results of the projects, and describes future studies that can be performed to increase the understanding of mass transport.

Chapter 2 : The Compensated Arrhenius Equation

2.1 Introduction

2.1.1 General Concept

As discussed in Chapter 1, the CAF is an improvement to the simple Arrhenius equation by including the temperature dependence term in the exponential pre-factor[49]. The main success of the CAF is evident in two aspects. The first is the fact that the simple Arrhenius equation produces different E_a values at different temperature ranges for the same system under investigation, while the CAF produces a single E_a. This is depicted in Figure 2-1 where the bottom curve shows a better linear fit to the conductivity values with an R^2-value of 0.9987, whereas the top simple Arrhenius curve produces a linear fit with a lower R^2-value of 0.9753. This shows that the simple Arrhenius curve is not really linear. More extreme cases have been observed where the simple Arrhenius plot produces curved plots instead of a linear plots[66, 67]. Since the E_a in the simple Arrhenius plot of ln(σ) versus (1/T) is the slope, a non-linear curve does not have one slope. Thus, for a simple Arrhenius plot, there is not one E_a defined for a particular system. Instead, the E_a changes as the temperature is changed. In addition, the temperature dependence of the dielectric constant in the CAF provides insight into the structure-property relationship between transport phenomena and the solvent molecules.

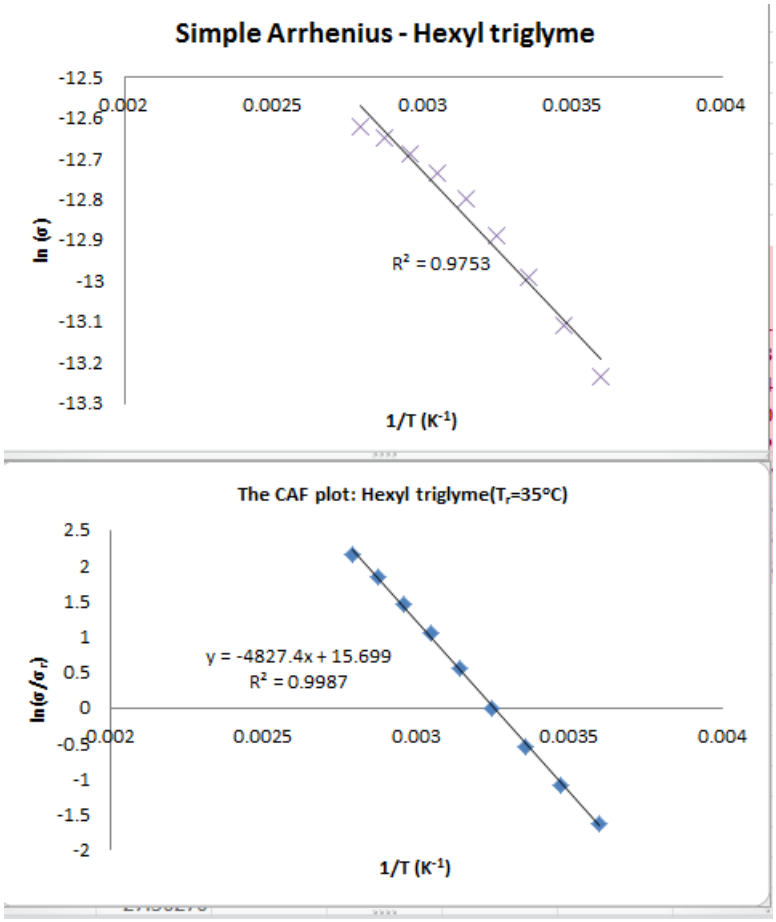

Figure 2-1 The simple Arrhenius plot (top) and the CAF plot (bottom) for conductivity of 0.1 molal LiTf in triglyme.

As formulated by Petrowsky, Frech, and coworkers[49], in general, the CAF works as follows. The diffusion and conductivity equation in the CAF is described as:

$$D(T) = D_o(\varepsilon_s(T))\, e^{\left(-\frac{E_a}{k_B T}\right)} \tag{1-12}$$

$$\sigma(T) = \sigma_o(\varepsilon_s(T))\, e^{\left(-\frac{E_a}{k_B T}\right)} \tag{1-13}$$

In these equations, D is the self-diffusion coefficient, D_o and σ_o are the exponential pre-factors, T is temperature, ε_s is the static dielectric constant, E_a is the activation energy, k_B is the Boltzmann constant, and σ is the conductivity. Unlike the simple Arrhenius equation, the pre-factor contains a temperature term. Furthermore, the solvent property

affected by temperature in the pre-factor is assumed to only be dependent on the dielectric constant of the solvent.

Recall from Chapter 1 that besides temperature, dielectric constant is also affected by the dipole density. This is shown by the dependence of the dielectric constant to the dipole density, *N*. The dipole density can be altered by altering the individual solvent's molecular volume. Thus, the dielectric constant of the solvent can be varied either by varying the individual volume of the molecule or by varying the temperature. This is depicted in Figure 2-2 for the case of conductivity, which shows a plot of conductivity, σ versus static dielectric constant, ε_s. In Figure 2-2, the σ_r is the conductivity value at each reference temperature (the subscript "*r*" means reference), T_r is the reference temperature, ε is the static dielectric constant, ε_x refers to a specific dielectric constant (where x=1,2,3,…), σ_{hex} is the conductivity of 1-hexanol at a specific temperature, and *T* is the temperature (where T_1, T_2, T_3, … refers to specific temperature). Some of these variables are discussed in more detail in section 2.2.

In Figure 2-2, the top curve reflects the variation in molecular volume. The molecular volume is varied by varying the length of the alkyl chain attached to the functional group of interest. Thus the top curve is a plot of dielectric constant and conductivity values for 1-ethanol, 1-propanol, 1-butanol, 1-hexanol, and 1-octanol at one (reference) temperature T_r. The bottom curve is obtained by varying the temperature of 1-hexanol.

Since the pre-factor is assumed to be dependent on the dielectric constant only, the pre-factor can be cancelled out by choosing a point on the plot in Figure 2-2 where the dielectric constant value is the same for both curves.

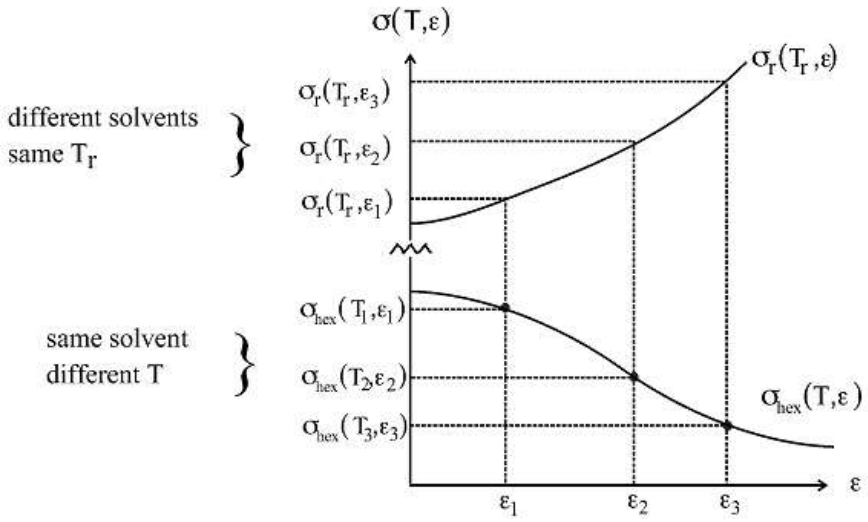

Figure 2-2 Plot of conductivity versus dielectric constant as the molecular volume is varied at constant temperature (top curve) and as the temperature is varied (bottom curve) for 1-hexanol. (σ=conductivity, ε=dielectric constant) Adapted from Petrowsky[40].

If a point is selected from the dielectric constant axis, say ε_2, this will result in two values of known conductivity, $\sigma_r(T_r,\varepsilon_2)$ and $\sigma_{hex}(T_2,\varepsilon_2)$, and one value of known temperature, T_r. It is possible then to write:

$$\sigma_r(T_r,\varepsilon_2) = \sigma_o(\varepsilon_2(T_r))e^{\frac{-Ea}{RT_r}} \quad (2\text{-}1)$$

$$\sigma_{hex}(T_2,\varepsilon_2) = \sigma_o(\varepsilon_2(T_2))e^{\frac{-Ea}{RT}} \quad (2\text{-}2)$$

Dividing equation (2-2) by equation (2-1) then allows the pre-factor $\sigma_o(\varepsilon_2)$ to cancel:

$$\frac{\sigma_{hex}(T_2,\varepsilon_2)}{\sigma_r(T_r,\varepsilon_2)} = \frac{e^{\frac{-Ea}{RT}}}{e^{\frac{-Ea}{RT_r}}} \quad (2\text{-}3)$$

Taking the natural log of equation (2-3) results in:

$$ln\left(\frac{\sigma_{hex}(T_2,\varepsilon_2)}{\sigma_r(T_r,\varepsilon_2)}\right) = ln\left(\frac{e^{\frac{-Ea}{RT}}}{e^{\frac{-Ea}{RT_r}}}\right) \quad (2\text{-}4)$$

$$ln\left(\frac{\sigma_{hex}(T_2,\varepsilon_2)}{\sigma_r(T_r,\varepsilon_2)}\right) = -\frac{Ea}{RT} + \frac{Ea}{RT_r} \quad (2\text{-}5)$$

Plotting the value ln $\left(\frac{\sigma_{hex}(T_2,\varepsilon_2)}{\sigma_r(T_r,\varepsilon_2)}\right)$ vs $\frac{1}{T}$ will give a linear plot, where the slope is equals to $-\frac{Ea}{R}$ and the y-intercept is equals to $+\frac{Ea}{RT_r}$. Thus, two E_a values can be obtained. In section 2.2 below, it will be shown that the E_a obtained from the slope and the y-intercept is very close to each other. The reported E_a is the average of these two E_a values, as well as the E_a values from different reference temperature, T_r, and the E_a values from different solvent analogs of the same solvent family. A more detailed CAF procedure is described below with an example of its application to the nitrile solvent family.

2.2 Scaling Procedure Detail Example for Conductivity Data

As an example, the scaling procedure is described here for the conductivity of 0.0055M Tba-Tf in the nitrile solvent family. The conductivity and dielectric constant data at 5 to 85 ^{o}C for the example is obtained from published values on nitriles[53]. The data are presented in table 2.1 below. This scaling procedure described here was invented by Petrowsky and has been described in the literature by Petrowsky, Frech and coworkers[34, 35, 40, 49].

Heptanenitrile			Octanenitrile			Nonanenitrile		
T (^{o}C)	ε_s	σ (S/cm)	T (^{o}C)	ε_s	σ (S/cm)	T (^{o}C)	ε_s	σ (S/cm)
5	17.2	7.78×10^{-5}	5	15.5	4.42×10^{-5}	5	14.1	2.93×10^{-5}
15	16.6	9.10×10^{-5}	15	15.0	5.29×10^{-5}	15	13.7	3.59×10^{-5}
25	16.1	1.04×10^{-4}	25	14.5	6.24×10^{-5}	25	13.2	4.34×10^{-5}
35	15.5	1.20×10^{-4}	35	14.0	7.31×10^{-5}	35	12.8	5.15×10^{-5}
45	15.0	1.37×10^{-4}	45	13.5	8.49×10^{-5}	45	12.3	6.03×10^{-5}
55	14.4	1.54×10^{-4}	55	13.0	9.69×10^{-5}	55	11.9	6.93×10^{-5}
65	13.9	1.72×10^{-4}	65	12.5	1.09×10^{-4}	65	11.5	7.84×10^{-5}
75	13.5	1.89×10^{-4}	75	12.1	1.21×10^{-4}	75	11.1	8.75×10^{-5}
85	13.0	2.06×10^{-4}	85	11.7	1.34×10^{-4}	85	10.7	9.70×10^{-5}

Decanenitrile			Dodecanenitrile		
T (^{o}C)	ε_s	σ (S/cm)	T (^{o}C)	ε_s	σ (S/cm)
5	12.7	1.54×10^{-5}	5		
15	12.3	1.92×10^{-5}	15	10.7	7.18×10^{-6}
25	12.0	2.36×10^{-5}	25	10.4	9.14×10^{-6}
35	11.6	2.86×10^{-5}	35	10.1	1.14×10^{-5}
45	11.2	3.41×10^{-5}	45	9.75	1.41×10^{-5}
55	10.8	4.01×10^{-5}	55	9.43	1.69×10^{-5}
65	10.5	4.61×10^{-5}	65	9.12	1.99×10^{-5}
75	10.2	5.20×10^{-5}	75	8.89	2.30×10^{-5}
85	9.86	5.80×10^{-5}	85	8.62	2.61×10^{-5}

Table 2-1 Dielectric constant and conductivity data for 0.0055M TbaTf in the nitrile solvent family. Data are taken from published literature values[53]. ε_s = dielectric constant, σ = conductivity.

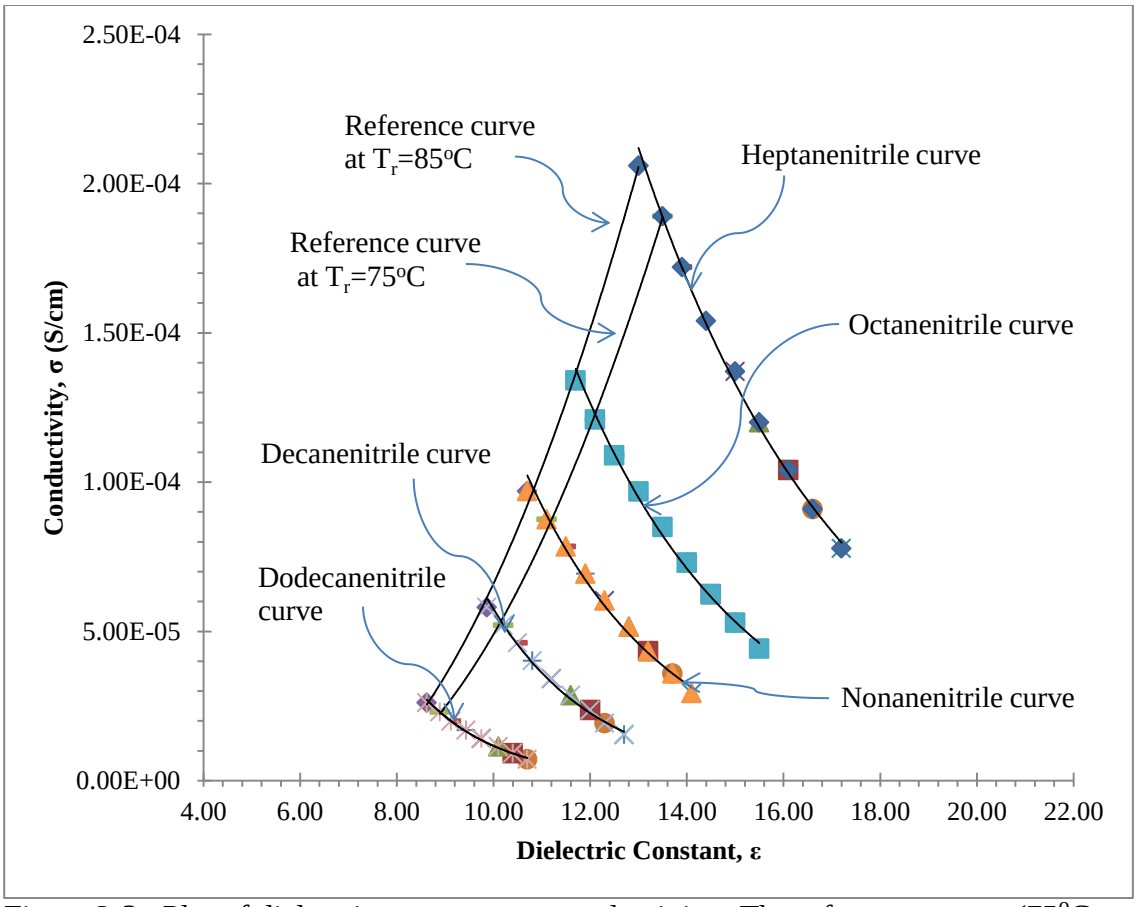

Figure 2-3 : Plot of dielectric constants vs. conductivity. The reference curves (75°C and 85°C shown) are shown, as well as the variable temperature plot for each nitrile analog.

From the data, a plot of conductivity against dielectric constant as temperature is varied, for each solvents: heptanenitrile, octanenitrile, nonanenitrile, decanenitrile, and dodecanenitrile, is generated. On the same plot, the data for the dielectric constant against conductivity as the alkyl chain length is varied, is plotted. Note that these two data are the same data. But the step is essential so that the curve fitting can be applied to these data. This second plot is performed for all temperature values. Each of these second curves generated is a reference curve at T_r. For example, the plot of the dielectric constant and conductivity values of heptanenitrile, octanenitrile, nonanenitrile, decanenitrile, and dodecanenitrile at 85 °C is a reference curve at T_r=85

^{o}C, and the plot of dielectric constant and conductivity values at 75^{o}C is a reference curve at T_r=75^{o}C. Figure 2-3 shows this plot for the nitrile solvent family.

The purpose of this plot is three-fold. Firstly, the plot allows for visualization of the data to ensure that they are reasonable. From the plot, as the temperature is increased, for each of the nitrile analog, the dielectric constant decreases while the conductivity increases. This is confirmed with the variable temperature curves for each nitrile analog as in Figure 2-3. At the same time, at each temperature, T_r, as the size of the individual molecule increases, the dielectric constant decreases, and the conductivity decreases. This is shown by each of the reference curves shown in Figure 2-3. Thus, the data for the conductivity in nitrile is reasonable.

The second reason for plotting these data as in Figure 2-3 is to find the mathematical relation for each of the reference curves, T_r. The mathematical description of the curve-fitting will be used to obtain the conductivity values, σ_r. The conductivity values obtained from these curves will be more accurate as the curve fitting is more accurate; i.e. the R^2-value is as close to 1 as possible. Section 2.3 discusses the effect of the curve fitting on the values of the E_a for a few solvent families including nitriles.

The third and final reason to plot conductivity versus dielectric constant data as in Figure 2-3 is as a guide in selecting an appropriate reference temperature, T_r. Certain values of T_r can give a negative value of conductivity if not properly selected. This in turn will affect the value of the E_a calculated. Thus, the T_r is selected such that the dielectric constant values for the T_r curve covers the same range as the dielectric

constant values for the particular nitrile analog. This topic is discussed in detail in Section 2.5 below.

From each of the reference curves, the values of the conductivity, σ_r at each temperature, T are obtained corresponding to the dielectric constant values. Recall that for each solvent species, the dielectric constant value at each temperature from 5 to 85^{o}C is available. Using these dielectric constant values, the reference conductivity, σ_r is calculated using the equation for each reference curve. From equation 2-5, a plot of the natural log of the conductivity at each temperature divided by the reference conductivity ($\ln [\sigma_{hex}(T_2,\varepsilon_2)/\sigma_r(T_r,\varepsilon_2)]$), against the inverse temperature, (1/T), will produce a linear curve fit (refer to Figure 2-4).

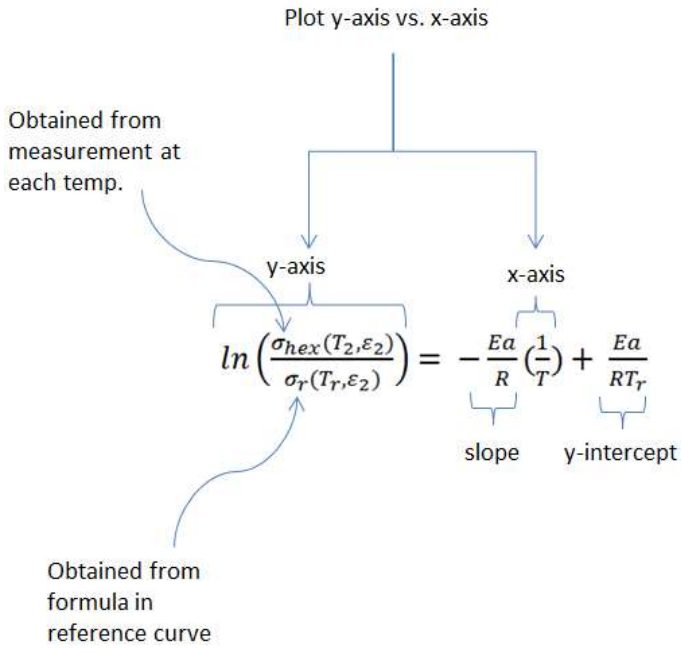

Figure 2-4 Scheme for creating plots for the E_a at each reference temperature. σ_{hex} is the conductivity for each analog (heptanenitrile, octanenitrile, ..., dodecanenitrile), while the σ_r is the conductivity at each reference temperature (T_r=5^{o}C, 15^{o}C, …, 85^{o}C).

Figure 2-5 shows the plot for heptanenitrile for each reference temperature, T_r. The values of the E_a are calculated for each reference temperature using both the slope and the y-intercept. The same procedure is applied to the octanenitrile, nonanenitrile, decanenitrile, and dodecanenitrile. The values of the E_a for all nitrile solvent analogs are tabulated in Table 2-2. The reported E_a for nitrile is the average value of E_a over different family members. The E_a selected for each nitrile analog is taken at a selected reference temperature T_r. Section 2.3 discusses the factors considered in selecting the appropriate T_r for a particular nitrile analog.

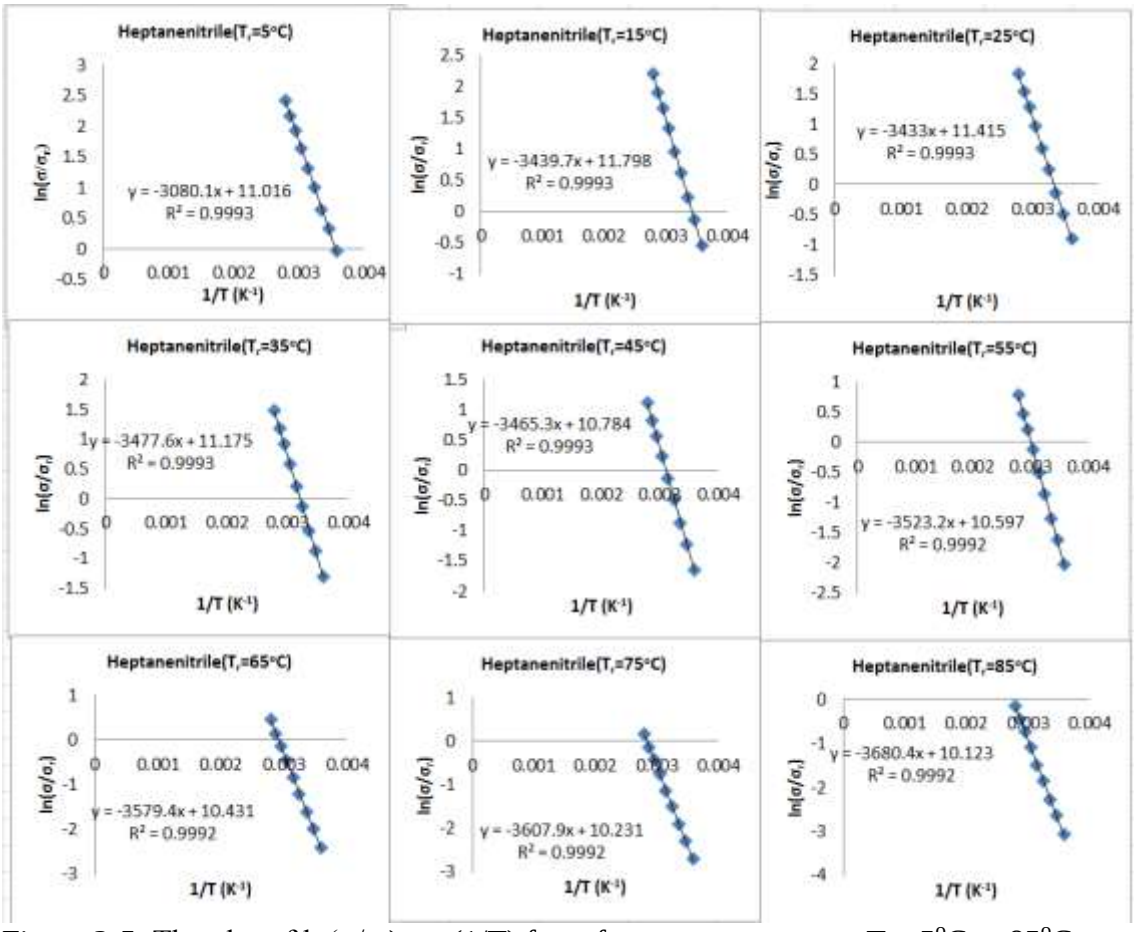

Figure 2-5 The plot of $\ln(\sigma/\sigma_r)$ vs. (1/T) for reference temperature, T_r= 5°C to 85°C.

	Activation Energy, E_a (kJ/mol)				
T_r (°C)	Heptanenitrile	Octanenitrile	Nonanenitrile	Decanenitrile	Dodecanenitrile
5	25.128	27.164	29.185	28.174	60.384
15	24.913	27.137	29.441	28.289	51.655
25	23.763	26.139	28.589	27.364	50.821
35	23.616	25.675	27.563	26.619	54.387
45	22.637	24.614	26.310	25.462	51.420
55	22.625	24.358	25.689	25.023	38.840
65	22.329	23.974	25.161	24.567	35.479
75	21.450	23.144	24.363	23.753	33.940
85	21.212	22.818	23.907	23.363	31.775

Table 2-2 The E_a for the nitrile derivatives at reference temperature, T_r from 5°C to 85°C.

2.3 The Effect of Fitting Parameters on the E_a

In the detailed scaling procedure as described in section 2.2, there are two steps where curve-fitting data with mathematical functions is required. The quality of the curve-fitting can affect the value of the E_a. This section analyzes the first part of the curve fitting step.

The first curve fitting step is applied to the dielectric constant and conductivity data for each reference temperature, T_r (Figure 2-6). This step is essential because in the plot of $\ln[\sigma_{hex}(T,\varepsilon_s)/\sigma_r(T_r,\varepsilon_s)]$ versus 1/T, the $\sigma_r(T_r,\varepsilon_s)$ value at each temperature T is not directly measured. Instead, its value is obtained through the dielectric constant value at the particular temperature of interest (Figure 2-7).

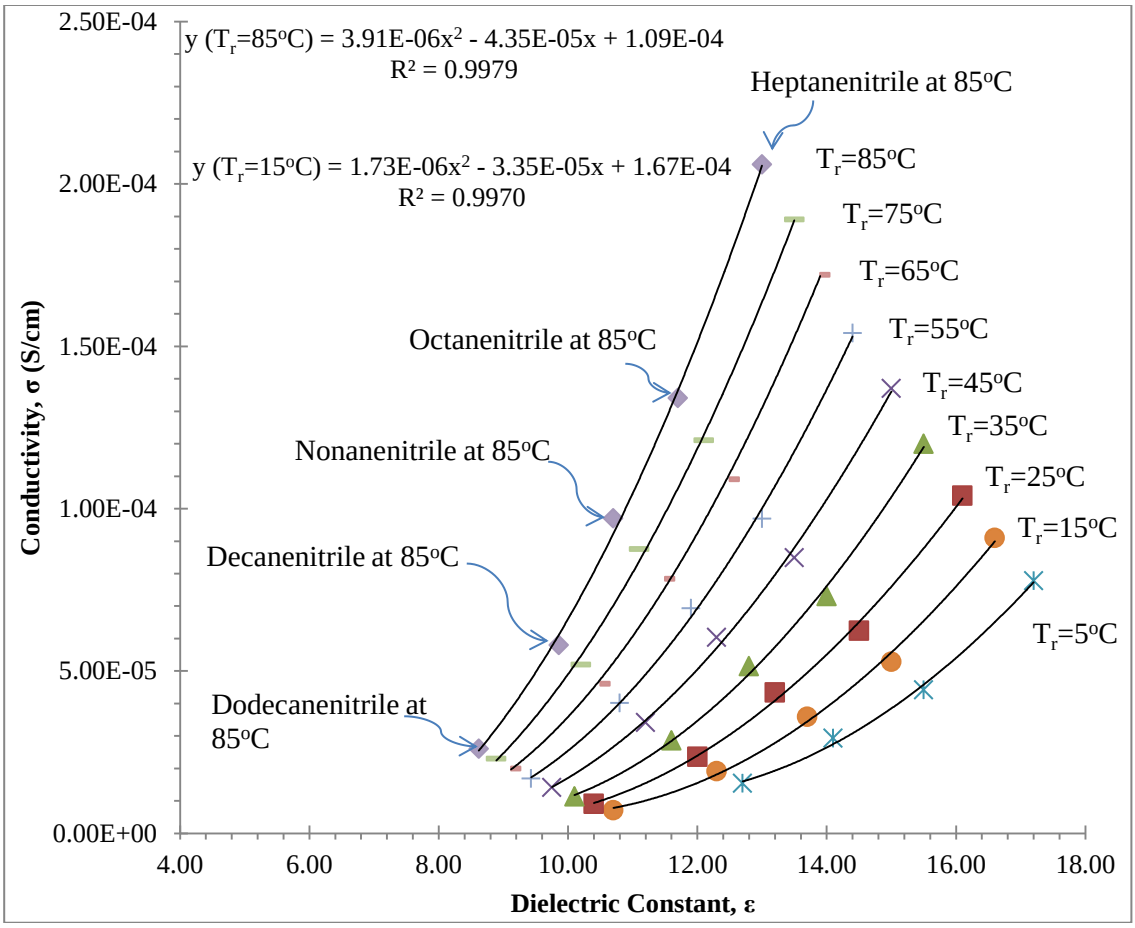

Figure 2-6 Curve fitting for each reference temperature Tr for the nitrile solvent family. Only the mathematical function for T_r = 15°C and T_r=85°C are shown. The fitting functional form used is polynomial of order 2.

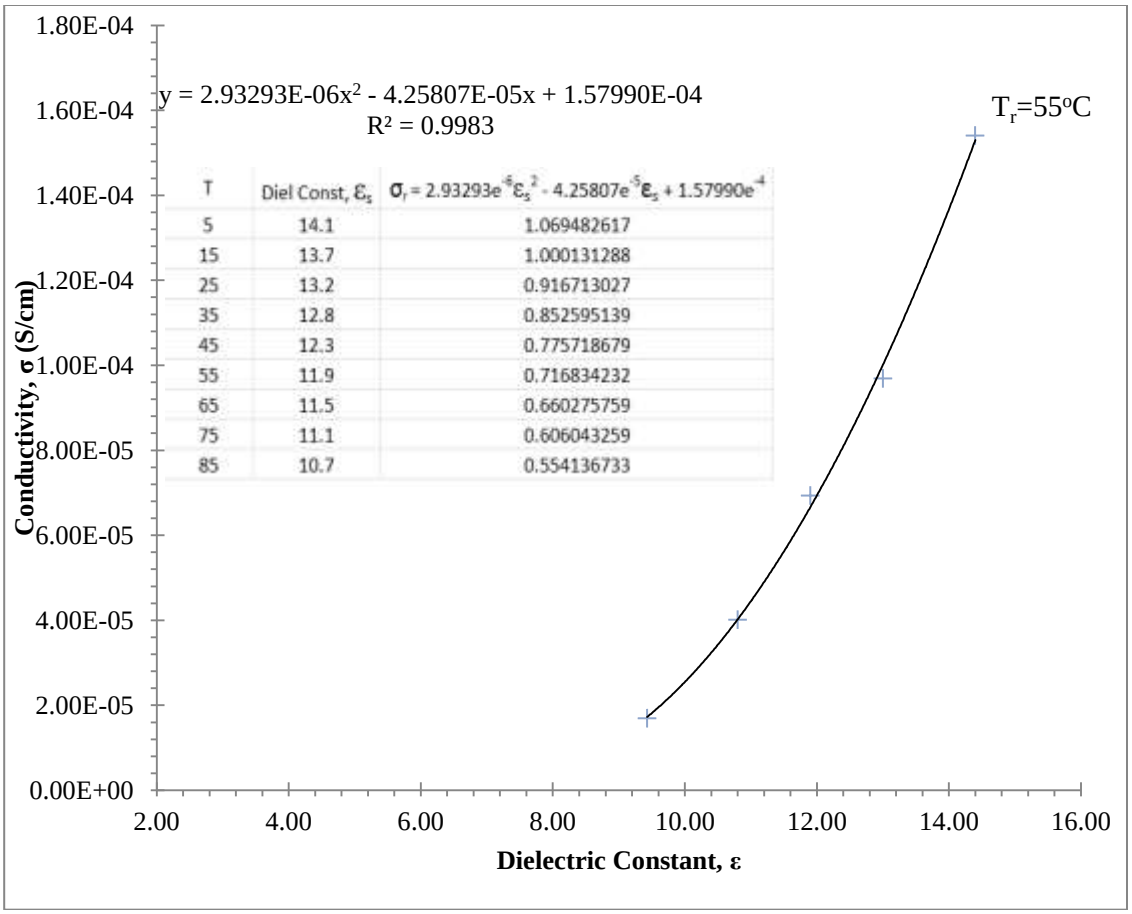

T	Diel Const, ε_s	$\sigma_r = 2.93293e^{-6}\varepsilon_s^2 - 4.25807e^{-5}\varepsilon_s + 1.57990e^{-4}$
5	14.1	1.069482617
15	13.7	1.000131288
25	13.2	0.916713027
35	12.8	0.852595139
45	12.3	0.775718679
55	11.9	0.716834232
65	11.5	0.660275759
75	11.1	0.606043259
85	10.7	0.554136733

Figure 2-7 Using the polynomial curve fitting of order 2 to obtain the conductivity $\sigma_r(T_r,\varepsilon_s)$ for reference temperature T_r=55°C. The dielectric constant at each temperature T is measured. Using the dielectric constant value and the equation for the curve fitting, the $\sigma_r(T_r,\varepsilon_s)$ is obtained for each T.

The quality of the fit is determined by the value of the R^2-value for the fit. In figure 2-7, the polynomial of second order is used for the curve fitting for T_r=55°C. This produces an R^2-value = 0.9983. In theory, one can use very complicated curve fitting functions to get the R^2-value very close to 1 or exactly 1. Figure 2-8 shows an example of using polynomial of fourth order to describe the relationship between dielectric constant and conductivity. As evidenced from the R^2-value, the curve fitting describes the data perfectly. However, such a relation defeats the purpose of the curve fitting step itself, which is to describe the relationship between dielectric constant and conductivity that allows a reasonable interpolation between adjacent data points. What

is required for this step is to get a general relation between the two properties, and thus a second order polynomial is appropriate.

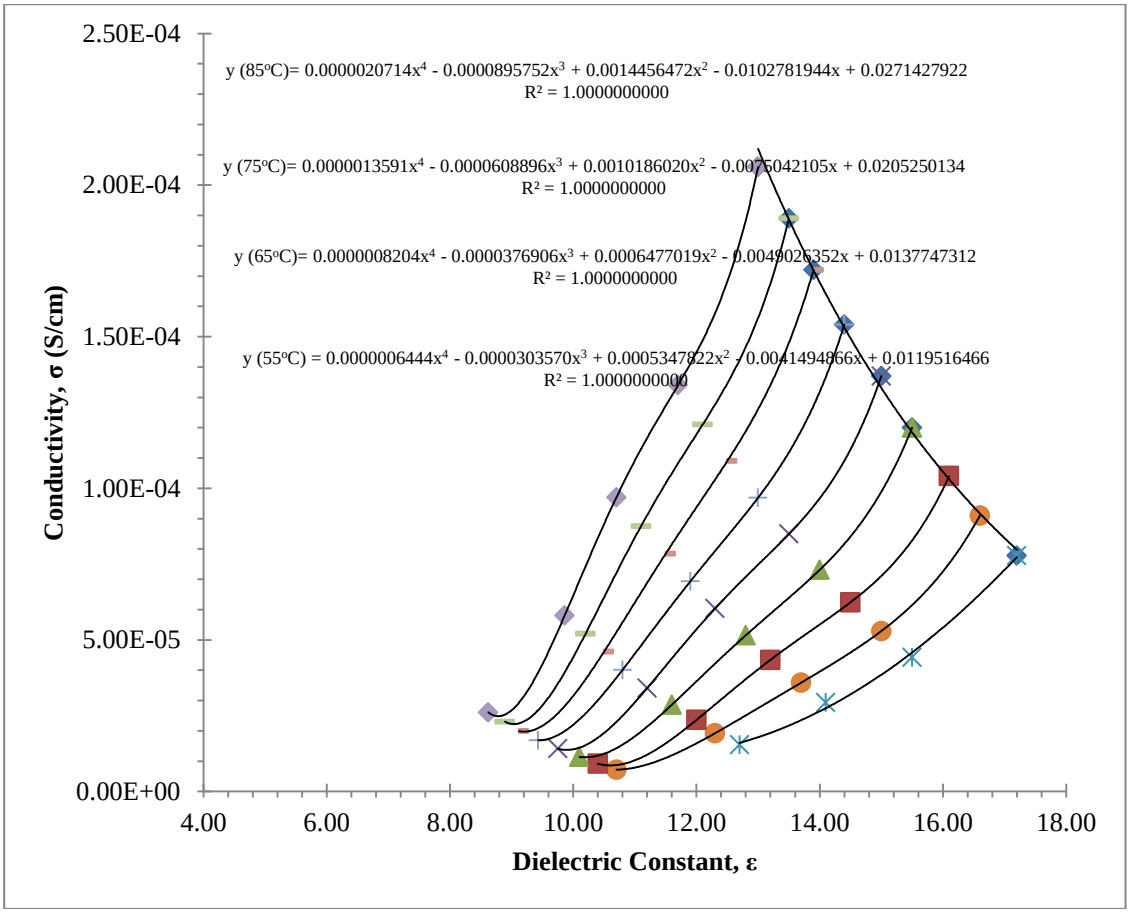

Figure 2-8 An example of curve fitting the nitrile conductivity data with polynomial of the fourth order. While the R^2-values are all equal to 1, the curves fitted do not represent a general relationship between conductivity and dielectric constant.

Two other curve fitting functional forms appropriate for use in this step are exponential, $y = A \exp[Bx]$ and the exponential growth, $y = y_o + A \exp[Bx]$. In these two equations, A, B, and y_o are the variable parameters adjusted so that the curve fitting fits the trend in the data as close as possible. For the polynomial of second order as shown in figure 2-7, the mathematical functional form is $y = Ax^2 + Bx + C$, where A, B, and C are the variable parameters.

Table 2-3 to 2-5 shows the E_a values for the conductivity of 0.0055M TbaTf in nitrile analogs as used in section 2.2. Each table represents the different curve fitting functions. Looking at the R^2-value, for the exponential function, the average R^2-value is 0.9840. This mathematical model is thus less accurate compared to the exponential growth (average R^2-value of 0.9960) and the polynomial of second order models (average R^2-value of 0.9950).

		Activation Energy, E_a (kJ/mol)				
T_r (°C)	R^2-value	Heptane nitrile	Octane nitrile	Nonane nitrile	Decane nitrile	Dodecane nitrile
5	0.996	24.786	24.896	24.375	23.651	23.950
15	0.991	25.635	25.713	25.129	24.307	24.567
25	0.985	25.288	25.384	24.819	24.018	24.291
35	0.986	25.748	25.826	25.221	24.356	24.604
45	0.982	25.546	25.635	25.035	24.173	24.426
55	0.984	26.081	26.149	25.501	24.563	24.788
65	0.982	26.421	26.476	25.796	24.803	25.009
75	0.977	26.457	26.514	25.825	24.814	25.016
85	0.976	26.972	27.009	26.274	25.188	25.364

Table 2-3 The E_a for the conductivity of 0.0055M TbaTf in nitrile analogs. The curve fit employed is the exponential form, y = A exp[Bx].

		Activation Energy, E_a (kJ/mol)				
T_r (°C)	R^2-value	Heptane nitrile	Octane nitrile	Nonane nitrile	Decane nitrile	Dodecane nitrile
5	0.995	25.128	27.164	29.185	32.793	60.384
15	0.998	24.913	27.137	29.441	33.745	51.655
25	0.996	23.763	26.139	28.589	33.039	50.821
35	0.997	23.616	25.675	27.563	30.531	54.387
45	0.996	22.637	24.614	26.310	28.747	51.420
55	0.998	22.625	24.358	25.689	27.423	38.840
65	0.998	22.329	23.974	25.161	26.623	35.479
75	0.997	21.450	23.144	24.363	25.823	33.940
85	0.996	21.212	22.818	23.907	25.147	31.775

Table 2-4 The E_a for the conductivity of 0.0055M TbaTf in nitrile analogs. The curve fit employed is the exponential form, y = yo + A exp[Bx].

		Activation Energy, E_a (kJ/mol)				
T_r (°C)	R^2-value	Heptane nitrile	Octane nitrile	Nonane nitrile	Decane nitrile	Dodecane nitrile
5	0.991	25.419	26.000	22.408	15.749	7.291
15	0.994	24.804	28.202	29.754	28.208	16.255
25	0.995	23.381	26.692	29.154	30.944	30.030
35	0.995	22.827	25.946	28.234	30.033	31.490
45	0.995	21.742	24.587	26.764	28.956	36.440
55	0.997	21.322	24.014	25.986	27.866	34.036
65	0.998	20.856	23.430	25.284	27.064	33.295
75	0.997	20.143	22.565	24.321	26.109	33.168
85	0.996	19.721	22.039	23.678	25.319	31.676

Table 2-5 The E_a for the conductivity of 0.0055M TbaTf in nitrile analogs. The curve fit employed is the polynomial of second order, $y = Ax^2 + Bx + C$.

What is more important however is the effect of these curve fittings on the value of the E_a. Taking the value for the E_a for heptanenitrile at reference temperature T_r=55°C for example, the value is 26.081 kJ/mol, 22.625 kJ/mol, and 21.322kJ/mol for the simple exponential, exponential growth, and polynomial of second order, respectively. A small change in the quality of the curve-fitting from the simple exponential to the exponential growth can move the value of the E_a almost 4 kJ/mol. However, as the quality converges to about 1, the maximum difference in the E_a is only 1.4 kJ/mol. Similar trends are observed for the other nitrile analogs at T_r=55°C (the dodecanenitrile values are not considered because of the obvious erroneous values of the E_a). This shows that the CAF is a robust method with very small deviation in the E_a values as the curve fitting function is varied. While there are other values that show bigger variation in the E_a as different curve fitting functions are used, the overall validity of a specific reference temperature also should be taken into account. This is discussed in section 2.4.

Another effect of the curve fitting function is the spread of the E_a values as the reference temperature, T_r is varied. For the simple exponential function, table 2-3 shows an E_a spread of about 2.113 kJ/mol for octanenitrile. For the exponential growth function however, the spread grows to a maximum value of about 8.598 kJ/mol (the value for dodecanenitrile is again, not considered here). The maximum spread of the E_a for the polynomial of second order curve fit is 6.163 kJ/mol for octanenitrile analog. Overall, for the exponential function, the E_a increases as the reference temperature is increased from 5°C to 85°C. However, for both the exponential growth and the polynomial of second order, the E_a decreases as the reference temperature is increased.

		Activation Energy, E_a (kJ/mol)				
T_r (°C)	R^2-value	Heptane nitrile	Octane nitrile	Nonane nitrile	Decane nitrile	Dodecane nitrile
5	0.990	24.903	24.131	23.998	24.170	20.211
15	0.986	24.796	24.023	23.896	24.081	27.115
25	0.986	24.631	23.861	23.744	23.946	27.322
35	0.986	24.631	23.851	23.731	23.940	26.443
45	0.986	24.609	23.822	23.703	23.920	26.323
55	0.989	25.031	24.195	24.040	24.230	25.240
65	0.990	25.474	24.587	24.392	24.555	25.038
75	0.991	25.904	24.968	24.737	24.873	24.963
85	0.990	26.189	25.214	24.955	25.073	25.263

Table 2-6 The E_a for the diffusion of the nitrile analogs. The curve fit employed is the exponential form, y = A exp[Bx].

		Activation Energy, E_a (kJ/mol)				
T_r (°C)	R^2-value	Heptane nitrile	Octane nitrile	Nonane nitrile	Decane nitrile	Dodecane nitrile
5	0.982	24.973	24.682	24.800	25.503	26.448
15	0.990	24.236	24.463	24.906	26.334	28.716
25	0.991	23.736	23.985	24.452	25.879	28.161
35	0.988	23.559	23.657	24.037	25.226	26.932
45	0.990	23.239	23.343	23.738	24.925	26.576
55	0.987	24.026	23.733	23.888	24.623	25.503
65	0.987	24.706	24.181	24.196	24.714	25.285
75	0.986	25.762	24.885	24.689	24.881	25.033
85	0.985	25.911	25.038	24.840	25.057	25.240

Table 2-7 The E_a for the diffusion of the nitrile analogs. The curve fit employed is the exponential form, y = yo + A exp[Bx].

		Activation Energy, E_a (kJ/mol)				
T_r (°C)	R^2-value	Heptane nitrile	Octane nitrile	Nonane nitrile	Decane nitrile	Dodecane nitrile
5	0.983	25.031	24.255	23.752	22.550	20.211
15	0.989	24.219	24.567	24.973	26.057	27.115
25	0.991	23.677	24.044	24.510	25.769	27.322
35	0.988	23.418	23.685	24.099	25.209	26.443
45	0.990	23.076	23.338	23.776	24.943	26.323
55	0.986	23.525	23.625	23.916	24.704	25.240
65	0.986	23.856	23.932	24.174	24.836	25.038
75	0.984	24.169	24.247	24.459	25.033	24.963
85	0.983	24.080	24.206	24.457	25.144	25.263

Table 2-8 The E_a for the diffusion of the nitrile analogs. The curve fit employed is the exponential form, $y = Ax^2 + Bx + C$.

The diffusion data shows similar R^2-value between the three curve fitting models (averages of 0.9880, 0.9870, 0.9870 for simple exponential, exponential growth, and polynomial of second order model respectively). Furthermore, all three models produce similar E_a values. At T_r=55°C, the maximum deviation in the E_a as the curve fitting model is varied is 1.506 kJ/mol for the heptanenitrile analog. In fact, the variation between the exponential growth and the polynomial of second order models,

the two more accurate models for the conductivity data, is less than 1 kJ/mol for all analogs.

Unlike the conductivity data, the diffusion data shows no general trend as the reference temperature is varied from 5°C to 85°C. The maximum E_a spread for the exponential growth is also very small at 1.286 kJ/mol. The maximum E_a spread for the exponential growth model is 2.672 kJ/mol. The value for the polynomial of second order is 1.955 kJ/mol.

		Activation Energy, E_a (kJ/mol)					
T_r (°C)	R^2-value	2-pentanone	2-hexanone	2-heptanone	2-octanone	2-nonanone	2-decanone
5	0.990	23.425	21.596	19.517	18.586	18.002	18.714
15	0.990	24.003	22.103	19.936	18.830	18.393	18.761
25	0.987	24.588	22.616	20.355	19.195	18.539	18.854
35	0.991	25.743	23.655	21.241	20.000	19.055	19.246
45	0.992	26.825	24.623	22.060	20.738	19.710	19.865
55	0.990	27.305	25.035	22.384	21.014	19.938	19.788
65	0.990	28.805	26.386	23.534	22.057	20.869	20.670

Table 2-9 The E_a for the conductivity of 0.0055M TbaTf in 2-ketone analogs. The curve fit employed is the exponential form, y = A exp[Bx].

		Activation Energy, E_a (kJ/mol)					
T_r (°C)	R^2-value	2-pentanone	2-hexanone	2-heptanone	2-octanone	2-nonanone	2-decanone
5	0.999	22.384	24.945	31.109	42.214	53.413	69.579
15	0.999	22.157	23.956	27.607	54.485	48.893	57.374
25	0.999	21.837	23.290	26.015	36.397	52.017	62.977
35	0.999	22.666	23.193	24.217	28.310	40.111	80.084
45	0.999	23.184	23.255	23.576	26.184	31.574	37.545
55	1.000	22.730	22.667	22.743	24.787	28.648	41.241
65	0.999	23.449	23.062	22.721	24.176	26.880	33.950

Table 2-10 The E_a for the conductivity of 0.0055M TbaTf in 2-ketone analogs. The curve fit employed is the exponential form, y = yo + A exp[Bx].

		Activation Energy, E_a (kJ/mol)					
T_r (°C)	R^2-value	2-pentanone	2-hexanone	2-heptanone	2-octanone	2-nonanone	2-decanone
5	0.997	22.481	26.472	25.744	22.084	17.431	13.364
15	0.998	21.539	25.410	26.438	22.676	20.227	17.171
25	1.000	20.660	24.367	26.545	26.135	23.586	21.610
35	0.998	20.248	23.686	25.700	25.766	21.218	17.360
45	0.998	19.691	22.939	25.111	26.319	23.764	21.274
55	0.999	18.796	21.634	23.722	25.927	26.149	23.746
65	0.999	18.306	20.993	23.040	25.565	26.879	26.442

Table 2-11 The E_a for the conductivity of 0.0055M TbaTf in 2-ketone analogs. The curve fit employed is the polynomial of second order, $y = Ax^2 + Bx + C$.

		Activation Energy, E_a (kJ/mol)					
T_r (°C)	R^2-value	2-pentanone	2-hexanone	2-heptanone	2-octanone	2-nonanone	2-decanone
5	0.997	24.739	22.733	23.025	21.084	19.132	20.584
15	0.996	25.405	23.307	23.544	22.339	19.757	20.535
25	0.991	26.283	24.076	24.238	22.960	20.641	20.579
35	0.993	26.754	24.473	24.599	23.272	21.363	20.857
45	0.986	27.472	25.094	25.158	23.766	21.791	21.238
55	0.976	28.195	25.709	25.701	24.236	22.187	21.836
65	0.972	28.370	25.831	25.810	24.311	22.219	21.854

Table 2-12 The E_a for the diffusion of the 2-ketone analogs. The curve fit employed is the exponential form, $y = A \exp[Bx]$.

		Activation Energy, E_a (kJ/mol)					
T_r (°C)	R^2-value	2-pentanone	2-hexanone	2-heptanone	2-octanone	2-nonanone	2-decanone
5	0.997	23.449	23.543	26.423	27.893	29.879	35.755
15	0.996	23.750	23.475	25.821	26.527	27.056	29.663
25	0.991	25.042	23.882	25.132	24.679	23.622	24.090
35	0.993	24.786	23.819	25.347	25.117	24.311	25.085
45	0.986	25.000	23.983	25.503	25.243	24.399	25.161
55	0.976	24.985	23.950	25.497	25.236	24.386	25.168
65	0.972	23.326	22.689	24.734	24.865	24.460	25.783

Table 2-13 The E_a for the diffusion of the 2-ketone analogs. The curve fit employed is the exponential form, $y = yo + A \exp[Bx]$.

		Activation Energy, E_a (kJ/mol)					
T_r (°C)	R^2-value	2-pentanone	2-hexanone	2-heptanone	2-octanone	2-nonanone	2-decanone
5	0.997	23.429	23.555	26.448	25.901	24.758	27.061
15	0.996	23.701	23.499	25.841	26.468	24.252	25.505
25	0.990	24.659	23.917	25.271	24.640	22.558	22.503
35	0.993	24.413	23.793	25.447	25.127	24.065	23.851
45	0.985	24.449	23.854	25.593	25.327	24.323	24.139
55	0.975	24.155	23.601	25.490	25.373	24.566	25.303
65	0.972	23.001	22.516	24.682	24.884	24.537	25.910

Table 2-14 The E_a for the diffusion of the 2-ketone analogs. The curve fit employed is the exponential form, $y = Ax^2 + Bx + C$.

Similar trends can be seen for the conductivity of 0.0055M TbaTf in 2-ketone solvents (Figure 2-9 to 2-11) and for the diffusion of pure 2-ketone solvents (Figure 2-12 to 2-14). The data for the 2-ketones solvent are also obtained from published literature values[53]. The spread of the E_a across reference temperatures and across solvent family analogs for the conductivity data is bigger, with the difference between the largest E_a and the smallest E_a being as large as 8 kJ/mol. In contrast, the diffusion data have on average a difference of around 2 kJ/mol. The same trend is observed for the acetate solvent family (data not shown)[53].

2.4 Considerations for Choosing Reference Temperature, T_r.

As evident in section 2.3, the value of the E_a can vary as the reference temperature is varied, as the solvent analog is varied, and as the curve fitting model is varied. In theory, erroneous values of E_a can result under certain conditions, for example if the value of $\sigma_r(T_r,\varepsilon_s)$ is negative as shown by Fleshman[35]. Thus there is a need to outline appropriate rules to make sure that the E_a selected is reasonable. This procedure in selecting appropriate reference temperature, T_r, was invented by Fleshman as outlined in the literature[34, 35].

The first consideration for selecting the E_a is that the curve fitting method has to be as close to 1 as possible. As discussed in section 2.3, the simple exponential model produces a regression R^2-value of only 0.9840 as opposed to the higher R^2-value (0.9960 and 0.9950) produced by the exponential growth and polynomial of second order models. Thus, in this case, the E_a from the exponential model is not used. If one of the models produces a significantly higher R^2-value, that model is chosen over the other. If all models produce about the same R^2-value, then the model with the highest R^2-value will be used.

The second consideration in selecting the appropriate E_a is the curve as produced in figure 2-9. In this figure, the range of the dielectric constant for the heptanenitrile is similar to the range of dielectric constant for the 15°C reference curve (the 5°C reference curve has one less data point, and as such is left off). As the reference temperature is increased, the range of the dielectric constant that is similar to the dielectric constant of the heptanenitrile will be less and less. If the range of dielectric constant for a particular solvent analog variable temperature curve, for example dodecanenitrile, is outside the range of the dielectric constant for a particular reference temperature curve, for example the T_r=15°C curve, then to obtain the $\sigma_r(T_r,\varepsilon_s)$, extrapolation instead of interpolation of the data will need to be performed. This can lead to erroneous values of $\sigma_r(T_r,\varepsilon_s)$. As such, only the E_a values for corresponding reference temperatures where their reference temperature curves have the same range of dielectric constant as the particular analog is considered to be valid, and is used for calculating the average E_a values. For example, for heptanenitrile, valid E_a values are

the E_a values calculated using T_r=15°C only. For octanenitrile, T_r=15°C, 25°C, and 35°C can be used. For dodecanenitrile, only the T_r=85°C can be used.

The third consideration in selecting the appropriate E_a is the linearity of the plot $\ln[\sigma_{hex}(T,\varepsilon_s)/\sigma_r(T_r,\varepsilon_s)]$ versus 1/T. As shown in figure 2-5, the R^2-value of the linear plot are all at least 0.9900. This ensures that the relation has at least 0.9900 R^2-value. Figure 2-10 and figure 2-11 show the same plot as figure 2-5 for the decanenitrile analog. In this plot, the E_a's calculated at T_r=15°C and 25°C have R^2-values for the linear regression less than 0.9900. Thus these values are rejected even if the range of the dielectric constant covers the dielectric constant range for decanenitrile.

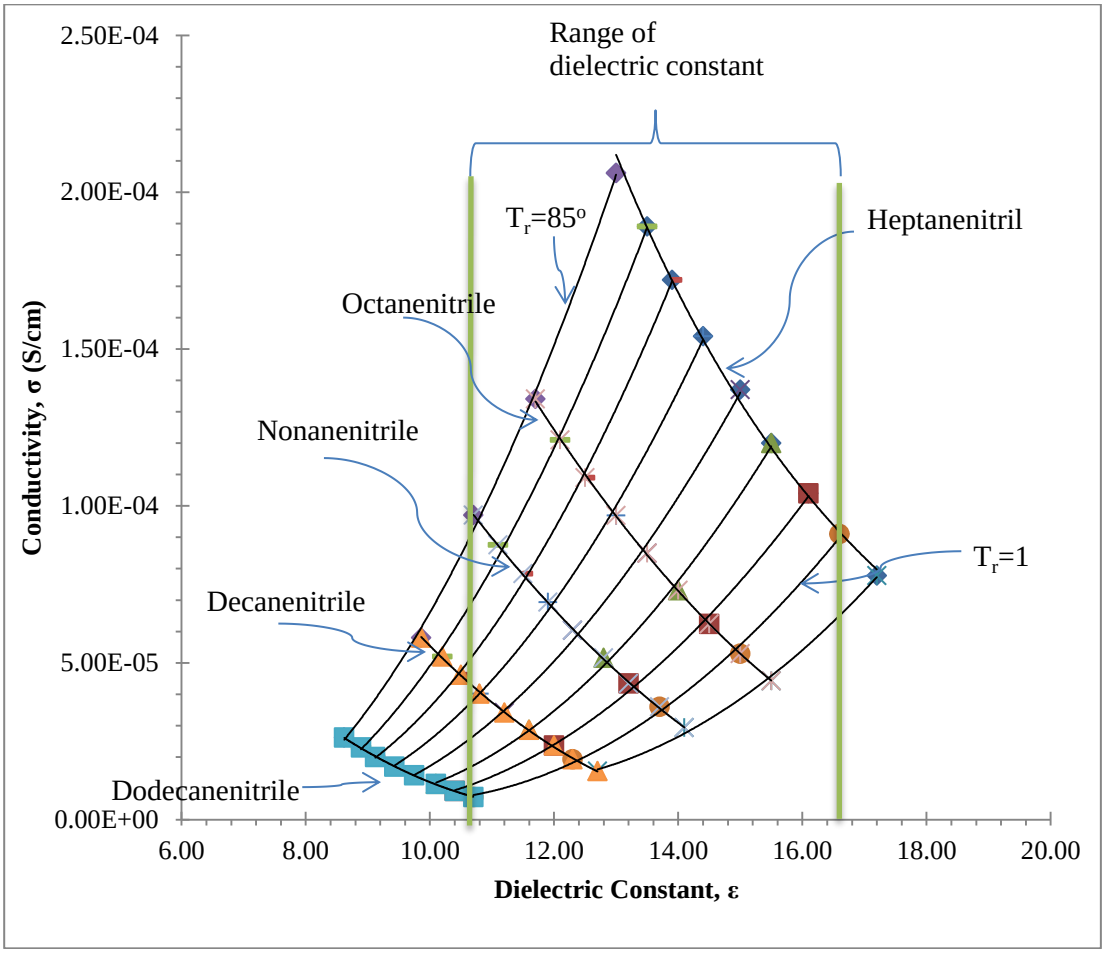

Figure 2-9 The range of the dielectric constant of the reference temperature curve at 15°C overlaps the heptanenitrile, octanenitrile, and nonanenitrile fully, but not decanenitrile and dodecanenitrile.

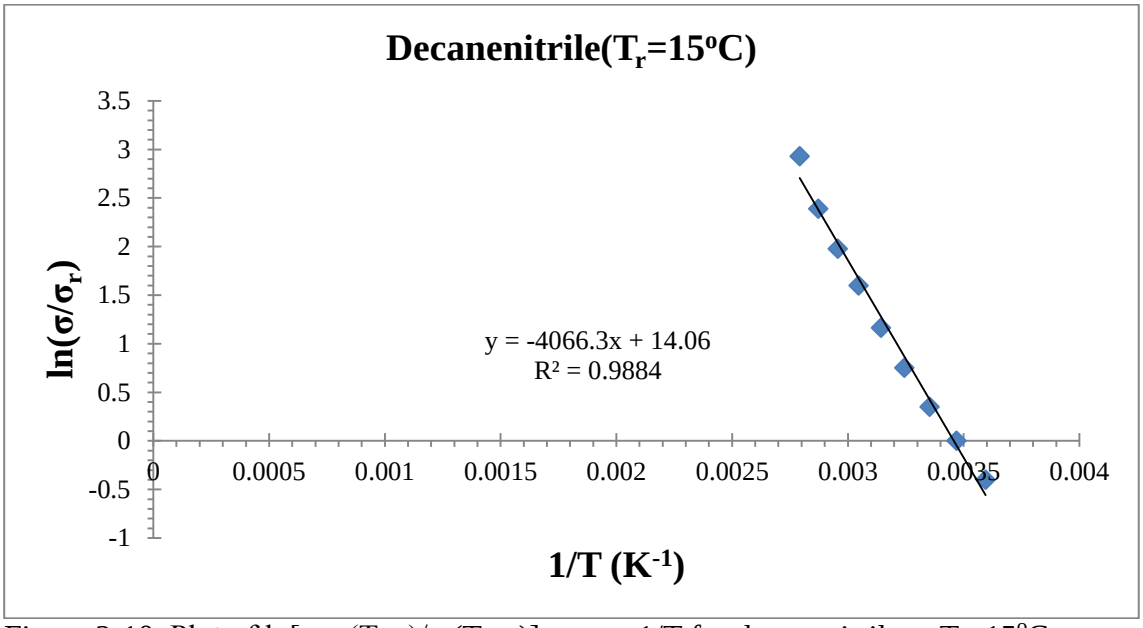

Figure 2-10 Plot of $\ln[\sigma_{hex}(T,\varepsilon_s)/\sigma_r(T_r,\varepsilon_s)]$ versus 1/T for decanenitrile at T_r=15°C.

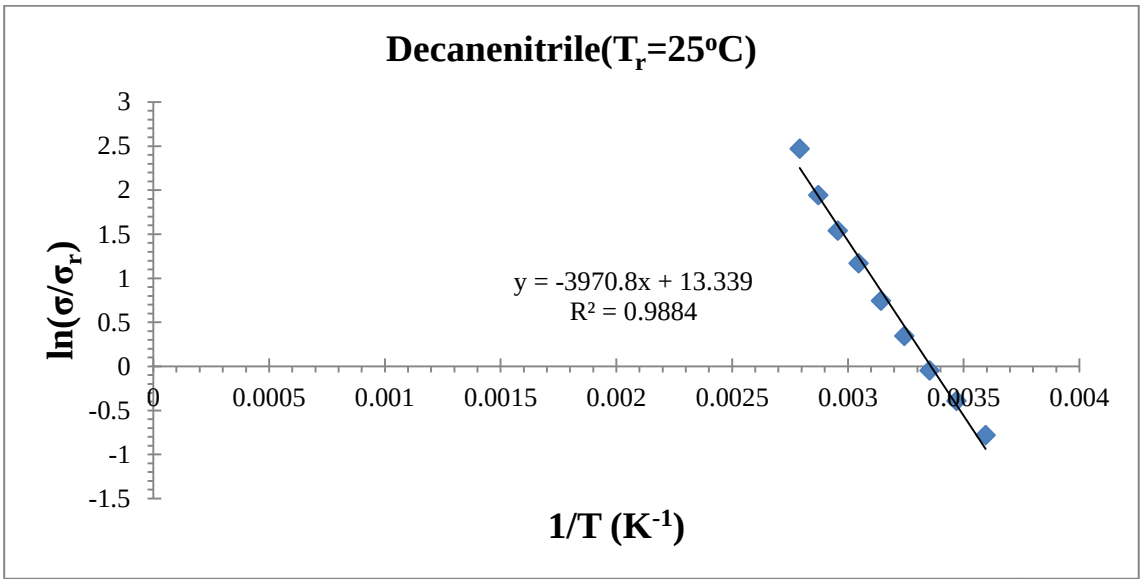

Figure 2-11 Plot of $\ln[\sigma_{hex}(T,\varepsilon_s)/\sigma_r(T_r,\varepsilon_s)]$ versus 1/T for decanenitrile at T_r=25°C.

Using the rules discussed above, only the E_a for T_r=15 °C is considered for heptanenitrile. For octanenitrile, the valid T_rs are 15 °C, 25 °C, and 35 °C, whereas for nonaenitrile, the valid T_rs are 15 °C to 55 °C. The valid T_rs for decanenitrile are 45 °C to

85 ^{o}C. Only T_r=85^{o}C are considered for dodecanenitrile. From these E_a values, the average E_a for the conductivity of 0.0055M TbaTf in the nitrile solvent family is calculated to be 28 ± 2 kJ/mol.

2.5 The Exponential Pre-factor and the Master Curve

As shown by Petrowsky, Frech, and coworkers[34, 35, 40, 49, 53, 66], using the value of the average E_a calculated, the exponential pre-factor, σ_o can be calculated. From equation 1-13:

$$\sigma(T) = \sigma_o(\varepsilon_s(T))\, e^{(-\frac{E_a}{k_B T})} \qquad 1\text{-}13$$

Rearranging equation 1-13, the pre-factor is obtained as:

$$\sigma_o(\varepsilon_s(T)) = \frac{\sigma(T)}{e^{(-\frac{\overline{E_a}}{k_B T})}} \qquad 2\text{-}6$$

Here, $\overline{E_a}$ is the average activation energy calculated. The average E_a value is used since the E_a calculated is the E_a for the nitrile functional group and the concentration of salt used, and thus should be the same for all of the nitrile derivatives. Since the exponential pre-factor depends on the dielectric constant, plotting the exponential pre-factor versus dielectric constant for all the species investigated produces a plot with all the data lying on a single master curve, as shown in figure 2-12. This supports the CAF assumption that each system, in this case the conductivity of 0.0055M TbaTf in nitrile solvent, should have one E_a. If each 0.0055M TbaTf in nitrile solution investigated has different E_a's, the formation of the master curve as in figure 2-12 would not be possible.

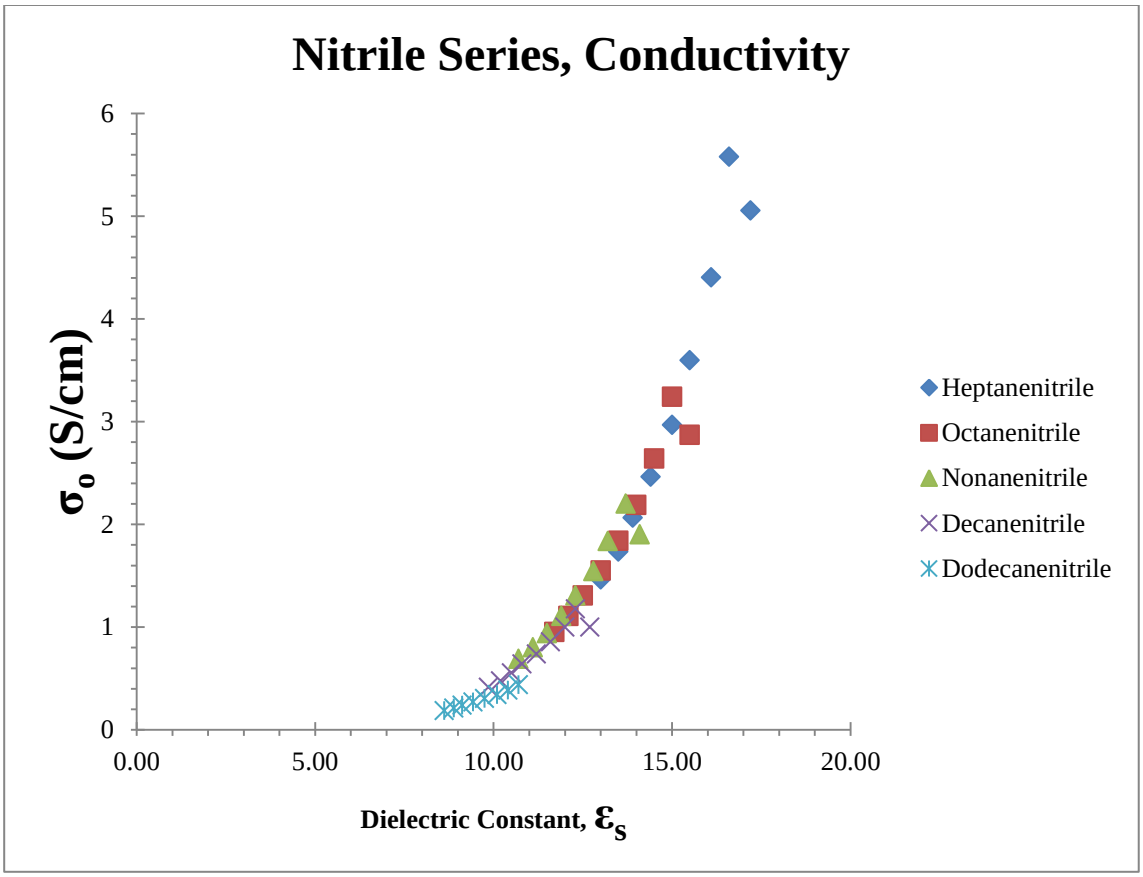

Figure 2-12 The master curve for the conductivity of 0.0055M TbaTf in the nitrile solvent.

Chapter 3 : Synthesis and Application of the Compensated Arrhenius Formulation to Acyclic Carbonates

3.1 Introduction

It has been shown by Petrowsky, Frech and coworkers that the Compensated Arrhenius Formulation (CAF) can be applied to polar aprotic liquids and electrolyte solutions. Among the polar aprotic liquids and electrolytes that have been investigated are nitriles[53], 2-ketones[61], and acetates[51] and their salt solutions.

As mentioned in section 1.9, acyclic carbonates have low dielectric constant values of around 3. This makes acyclic carbonates suitable in testing the applicability of the CAF to very low dielectric constant solvents. Besides testing the CAF's limit, acyclic carbonates are usually used as an additive in liquid electrolytes together with ethylene carbonates[64] in batteries. It is also used as a low polarity solvent in organic chemistry laboratories. Thus understanding electrical properties of acyclic carbonates is important. After several decades of investigation, the factors affecting the values of diffusion and conductivity in these electrolytes are still not well known. Thus it is vital that the properties of acyclic carbonates are elucidated with the CAF.

In addition to its application in battery electrolytes and as organic solvents, another reason to study acyclic carbonates is the interesting results that arose from the studies on acetates and 2-ketones. The energy of activation (E_a) for the propagation of tetrabutylammonium trifluoromethanesulfonate (TbaTf) charged species in the acetate solutions is higher compared to that in 2-ketones. More specifically, the E_a for the conductivity of 0.0055M TbaTf in the acetate solution is roughly 10 kJ/mol higher than in the 2-ketone electrolytes. A similar increase, but on a much smaller scale is also

observed for the E_a for diffusion of liquid 2-ketones (23.9 ± 0.2 kJ/mol) compared to the liquid acetates (25.5 ± 0.3 kJ/mol).

A close look at the molecular structure of the two functional groups will show that the acetate contains one more oxygen atom bonded to the carbon atom of the carbonyl moiety of acetate (figure 3-1). It can be postulated that the increase in the E_a values is related to the increase in the number of oxygen atom around the carbonyl carbon. The increase in the number of the oxygen atoms around the carbonyl carbon increases the number of the electron donor, which can form attractive interaction with the relatively electron deficient carbonyl carbon. This attractive interaction increases as the number of oxygen atom increases. In addition to that, the more electronegative oxygen atom also increases the partial positive charge on the carbonyl carbon. This partial positive charge increases as the number of oxygen atom around the carbonyl carbon increases. The net result is higher attractive interaction between the carbonyl carbon and the oxygen atoms around it as the number of oxygen atom is increased. This attractive interaction impedes the diffusion among the acetate molecules, and increases the E_a for diffusion. In the case of conductivity of charged species like TbaTf, it can be postulated that the increase in the number of electron donor that interacts with the cation increases the E_a. The effect is less when there is only one oxygen atom as in the 2-ketones, resulting in lower E_a values for 2-ketones.

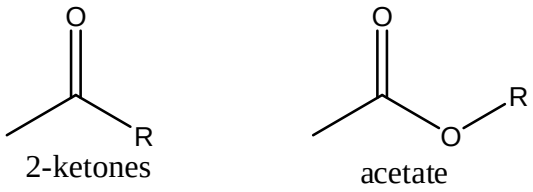

Figure 3-1 Molecular structure of 2-ketones and acetate.

On the other hand, the increase in the E_a could also come from other properties. The addition of the oxygen atom around the carbonyl carbon decreases the dipole moment of the acetates. As a comparison, acetone, the simplest 2-ketone has a measured dipole moment of 2.91 D[68] whereas methyl acetate has a dipole moment of 1.69 D[68]. Ethyl acetate, a common solvent in organic chemistry, has a dipole moment of 1.82 D[68]. On a bulk scale, acetone has a room temperature dielectric constant value of 20.7[68], while methyl acetate and ethyl acetate have room temperature dielectric constant values of 6.70[68] and 6.02[68], respectively. Thus, for some unclear reasons, the addition of another oxygen in the acetates, which decreases the dipole moment and the dielectric constant of acetates, increases the E_a's for both the conductivity and self-diffusion. Due to the importance of E_a, this phenomenon is worth exploring further.

To investigate this phenomenon further, the energy of activation of another similar family of compounds, the acyclic carbonates (figure 3-2) are investigated. Acyclic carbonate contains one extra oxygen atom around the carbonyl carbon. The addition of the third oxygen atom will increase the E_a for the diffusion according the first theory. The acyclic carbonate also has lower dipole moment and dielectric constant compared to 2-ketones and acetates. For example, dimethyl carbonate has a dipole moment of 0.91 D[69] and dielectric constant of around 3.087[69]. If the E_a is

affected by the dipole moment or dielectric constant, the addition of the third oxygen atom should increase the E_a further.

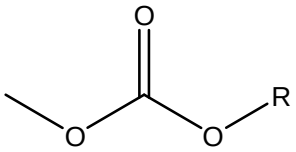

R = alkyl

methyl alkyl carbonate

Figure 3-2 An example of an acyclic carbonate.

3.1.1 Project Goals

The goal of this investigation is to investigate the applicability of the CAF with regards to acyclic carbonates and their electrolyte solutions. Particular attention will be given to the behavior of the dielectric constant values as temperature and molecular volume of the individual acyclic carbonate species are varied. The changes in the dielectric constant values as temperature and molecular volume are varied will be compared to the changes for the nitrile solvent family. A similar analysis will be performed with the self-diffusion coefficient.

If CAF can be applied to the acyclic carbonate and its electrolyte solutions, the E_a values will be elucidated and compared against the E_a values of 2-ketones and acetates, as well as their electrolyte solutions.

This project was collaborative with the group of Professor R. Frech[53] at the University of Oklahoma. Synthesis of the acyclic carbonates was developed and carried out as described here. The dielectric constant and diffusion measurements were performed by Dr. M. Petrowsky.

3.2 Results and Discussions

3.2.1 Synthesis of Acyclic Carbonates

To apply the CAF to acyclic carbonates, methyl hexyl-, methyl octyl-, methyl decyl-, and methyl dodecyl carbonates were needed (figure 3-3). These methyl alkyl tethered acyclic carbonates were not readily available for purchase, and thus had to be synthesized. There are a few routes to synthesize acyclic carbonates as discussed in the literature[70, 71].

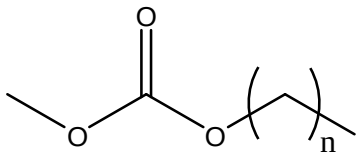

n=5,7,9,11

Figure 3-3 The methyl alkyl species used in the experiment.

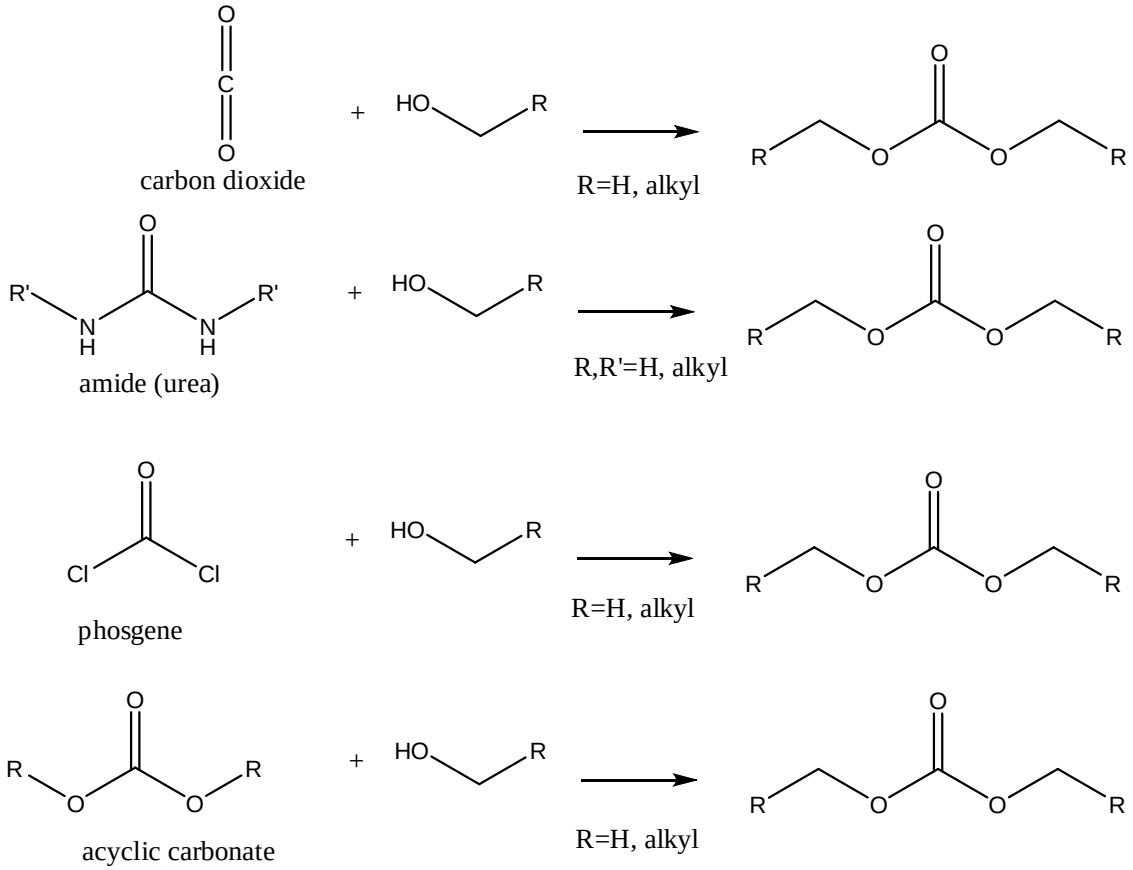

Figure 3-4 Examples of reactions to form acyclic carbonates. Catalysts and side products (if any) are not shown.

In general, alkyl carbonates are synthesized using the reaction of alcohols with a carbonyl containing moiety through a nucleophilic acyl substitution reaction (figure 3-4). In this method, the carbonyl moiety can be carbon dioxide[72], amide (urea)[73], phosgene[70, 71], and other acyclic carbonate[70, 71]. The nucleophiles can be any desired alcohols. However, most of these methods discussed are effective for synthesizing symmetric acyclic carbonates (i.e. dialkyl carbonates). There are only a few methods available for selectively synthesizing the asymmetric acyclic carbonates[74-77] and they are mostly inefficient with yields less than 50%, require difficult separation of the products, or require expensive reagents or catalysts. The most efficient method by Rannard and coworkers[77] requires a special reagent imidazole carboxylic esters. The

challenge in synthesizing asymmetric alkyl carbonates is depicted in figure 3-5. Essentially, the formation of symmetric dialkyl carbonates with the same alkyl chain length is thermodynamically as favorable as formation of asymmetric alkyl carbonates. Thus, in a mixture of 1-alcohols with a carbonyl moiety in the presence of a base, the products formed are mixtures of the symmetric and asymmetric alkyl carbonates that need to be separated if only one of the products is desired. For low molecular weight asymmetric alkyl carbonates, the separation can be performed using methods such as distillation. However, for high molecular weight asymmetric alkyl carbonates where the boiling points might be too high for simple distillation, a synthetic method that produces only the desired asymmetric alkyl carbonates is desirable.

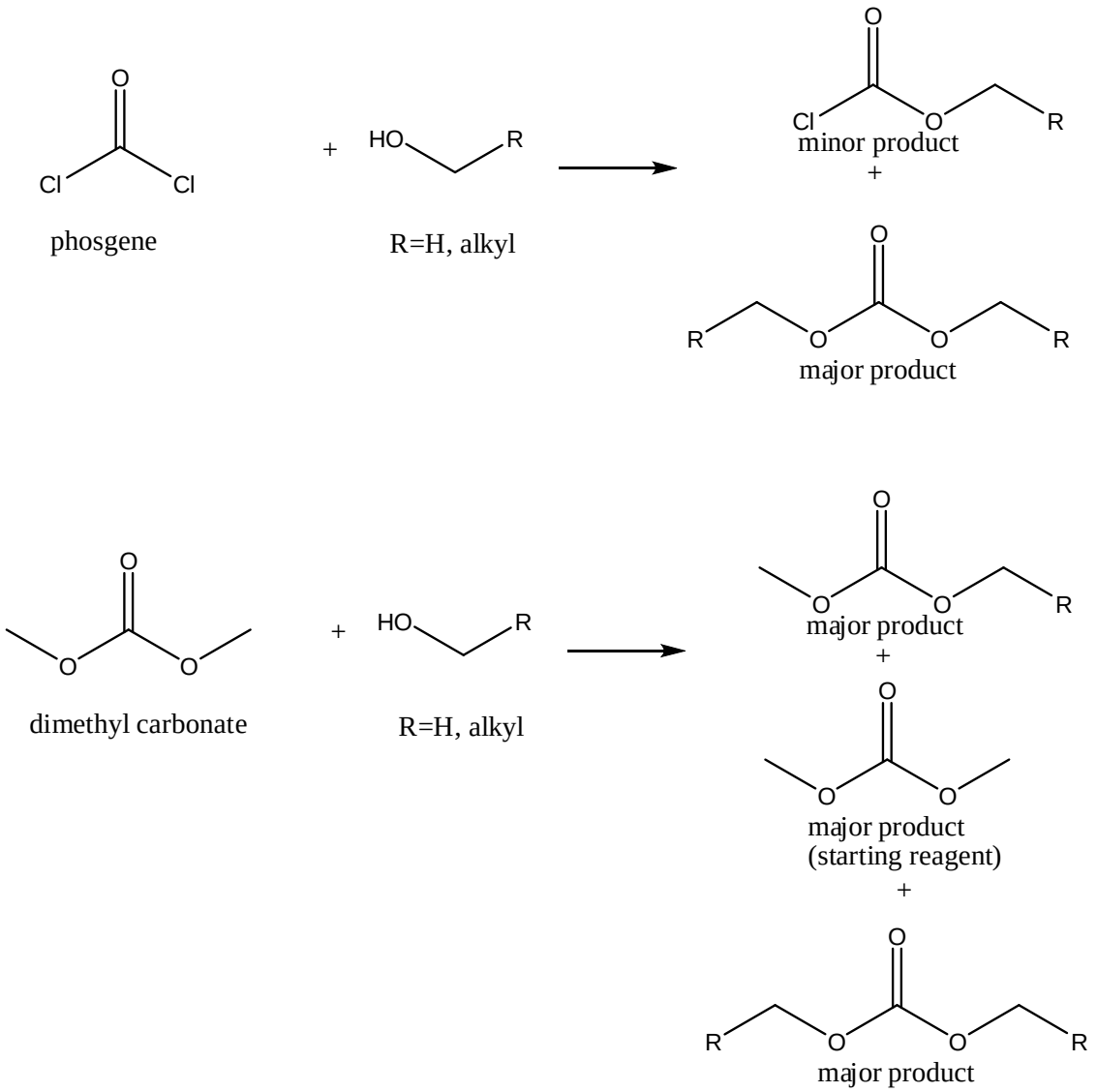

Figure 3-5 The mixture of products in the reactions to form acyclic carbonates are the symmetrical dialkyl carbonates.

To overcome the synthetic challenge, one strategy is to start the reaction with a carbonyl moiety with one poor and one good leaving group. By manipulating the reaction conditions, it is possible to control the reaction so that it will proceed far enough that all of the good leaving group will be substituted by one type of alkoxy group, but is stopped before any of the poor leaving group is substituted. The other

alkoxy group can then be added to form the desired asymmetric alkyl carbonates. However, this strategy can take a long time with multiple purification steps.

Another strategy is to start with a symmetric alkyl carbonate, and perform a trans-esterification reaction on it (figure 3-6). For example, for this particular project, it is possible to start with dimethyl carbonate and replace one methoxy group with the desired alkoxy group. However, the trans-esterification reaction is hard to control. Literature precedence shows that the reaction is not efficient[70, 71].

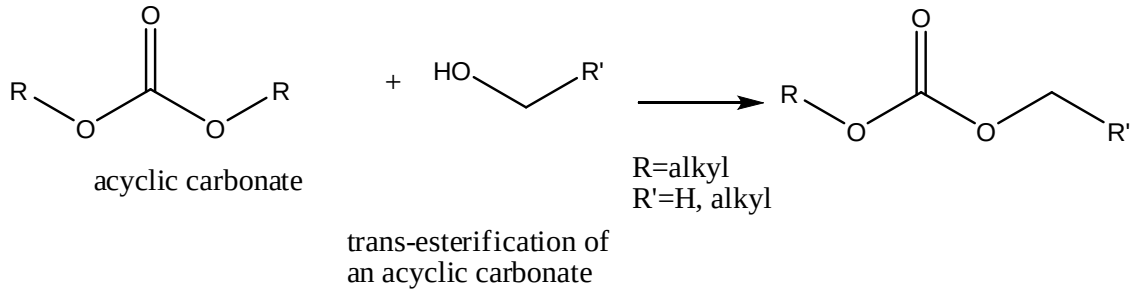

Figure 3-6 Trans-esterification reaction scheme for acyclic carbonates.

This strategy can be simplified if only one of the two substituents on the carbonyl carbon is an alkoxy group, while the other is a good leaving group (figure 3-7). Esters like methyl acetates, or longer chain acetates seems like good candidates for this type of reaction. Using this route, the longer alkoxy group is already attached to the carbonyl moiety. The methoxy group will have to be added in a separate reaction. However, it is well known that methyl anions are strong nucleophiles, and are so much stronger than alkoxide anions. Thus this method is expected to be difficult and might

require extreme conditions.

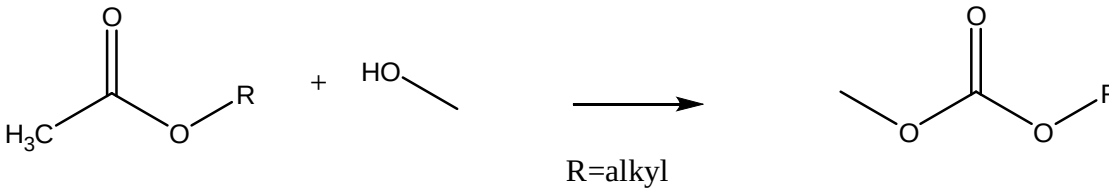

Figure 3-7 Reactions with starting reagent containing alkoxy group. Here, the methyl group on the starting acetate is the leaving group.

Instead of acetates, an analog of methyl acetate, methyl formate can also be used. In a methyl formate, instead of a methyl group, which is a strong nucleophile, the other substituent on the carbonyl carbon can be a good leaving group. Examples of this kind of methyl formate are methyl chloroformate, methyl bromoformate, and methyl iodoformate (figure 3-8). Using this method, the methoxy group is already present on the carbonyl moiety. The longer alkyl chain alkoxy group will have to be added to the carbonyl moiety.

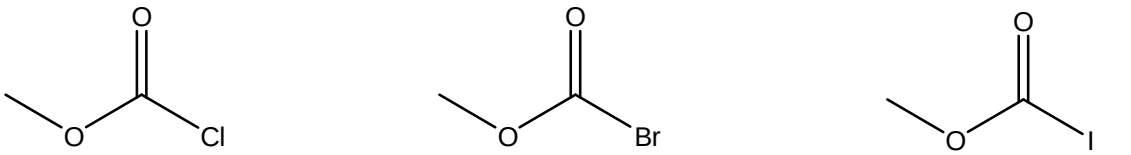

Figure 3-8 The methyl haloformates. The halogens are known to be good leaving group, whereas the methoxy is poor leaving group.

One strategy that can help the reaction is by trapping the leaving group so that it will not react with the product formed, reversing the desired reaction. For example, in the reaction with acetates, if a reagent can be used to trap the carbon anion formed, this can help drive the reaction towards the desired product. However, unless the trapped

leaving group is easy to separate from the methyl alkyl carbonates produced, this strategy is less desirable because of the extra step needed to purify the final product.

In this work, the reaction of methyl chloroformate with a primary alcohol in the presence of a base was chosen to produce the desired methyl alkyl carbonates (figure 3-9). This route is chosen because of the availability of the cheap and less toxic reagent, methyl chloroformate. The longer alkoxy group will come from the 1-alcohol reaction with the methyl chloroformate. However, the longer alkoxide anion can displace both the leaving group and the methoxy group. The challenge is in controlling the reaction conditions such that only the chloride undergoes substitution, instead of both the chloride and the methoxy moieties.

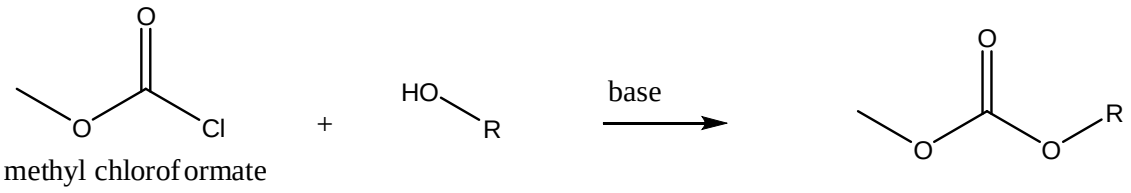

Figure 3-9 Reaction scheme for making the desired methyl hexyl-, methyl octyl-, methyl decyl-, and methyl dodecyl carbonates.

To optimize the reaction conditions, the reactions were run using 1-propanol instead of the longer chain 1-alcohols. The first reaction was run without any base. The idea was that the formation of hydrochloric acid as the side product should the drive the reaction forward at appropriate temperature. In addition to that, the chloride anion is a good leaving group. While the reaction does go forward as expected, the amount of symmetrical product was about 10% (determined using ^{1}H-NMR integration). While this is close to 100% purity, however, the low percent yield necessitated the use of a

base in subsequent reactions. After 108 hours, there remained unreacted 1-propanol in large quantity (determined using ^{1}H-NMR of the hydroxyl hydrogen). Increasing the temperature of the reaction causes the starting reagent to evaporate, and subsequently lowers the percent yield.

The presence of bases during the reaction produces vigorous reactions. All of the bases used produced white precipitates in the reaction flask. This white precipitate was suspected to be the salt of the protonated base with the chloride anion from methyl chloroformate. The use of triethylamine as the base produces a white precipitate that will only dissolve in water, but not the products. Thus the whole reaction flask is filled with white precipitates with little sign of the products. Since the product is immiscible in water, only after the white precipitate is dissolved in water can the product be separated. After various stoichiometry adjustments, the reaction using triethylamine as the base still produced a large amount of symmetrical product. It is suspected that the workup with water may have contributed to the transesterification of the desired product to the undesired symmetrical acyclic carbonates.

Replacing the triethylamine with 1,8-diazabicyclo[5.4.0]undec-7-ene (DBU) produced gooey materials in the flask that are hard to separate. This method was quickly dismissed.

Trial runs with pyridine also produced a white precipitate just like triethylamine. However, unlike the triethylamine base, the white precipitate formed does not stick all over the flask. Instead, it formed a white, soft looking precipitate that stuck together and floated in liquid products. This soft white precipitate is easily removed by filtration. Due to the ease of removal of the white precipitate formed when using

pyridine, and due to the pretty low formation of the unwanted side product, pyridine was retained as the base. Varying the amount of methyl chloroformate up to 5 equivalents relative to the 1-alcohol lead to formation of the desired product with at least 95% purity. Thus, all subsequent reactions to make the acyclic carbonates for this project used 5 equivalents of the methyl chloroformate, 1 equivalent of primary alcohol, and 1 equivalent of pyridine at about 40^{o}C. Attempts to purify the products using an alumina column were unsuccessful. The summary of the optimization is presented in Table 3-1 below. Detailed synthesis and characterization are described in section 3.4 below.

Methyl chloroformate	Primary alcohol	Base	T (^{o}C)	Reaction Time (hours)	% purity	% yield
3 eq.	2 eq.	-	25	24	< 50%	< 30
3 eq.	2 eq.	-	25	60	< 50%	< 30
3 eq.	2 eq.	-	25	108	< 50 %	< 30
2 eq.	1 eq.	-	70	28	< 50 %	low
3 eq.	4 eq.	Triethyl-amine	25	2	low	low
3 eq.	2 eq.	Triethyl-amine	25	24	low	100%
3 eq.	2 eq.	DBU	-78 to 25	12	-	-
3 eq.	2 eq.	pyridine	25	84	high	100
3 eq.	2 eq.	pyridine	50	24	high	100
5 eq.	1 eq.	pyridine	40	12	> 95	100
5 eq.	1 eq.	pyridine	40	24	> 95	100
5 eq.	1 eq.	pyridine	40	96	> 95	100

Table 3-1 Optimization of the reaction condition for the synthesis of asymmetric acyclic carbonates.

3.2.2 Application of the CAF to the Acyclic Carbonates

Due to the low dielectric constant of the acyclic carbonates, the TbaTf salt would not dissolve in the acyclic carbonates. As such, only the diffusion studies of the pure acyclic carbonates were performed. The data are analyzed in section 3.2.2.1 below.

3.2.2.1 Dielectric Constant and Diffusion of Acyclic Carbonates

The dielectric constant and self-diffusion coefficient values of pure acyclic carbonates are tabulated in table 3-2 and plotted in figure 3-10 and figure 3-11. The highest dielectric constant recorded is for the methyl hexyl carbonate at 5^{o}C with a value of 2.781. This value is lower than the reported dielectric constant value for ethyl methyl carbonate of 2.958[64]. It is expected that adding longer alkyl chain on the carbonates decreases the dielectric constant values. Thus the experimental values are reasonable.

As shown in figure 3-10, the dielectric constant decreases as temperature increases from 5 to 85^{o}C for all acyclic carbonate derivatives. From the theory of dielectric constant discussed in Chapter 1, the dielectric constant is inversely related to temperature. Thus as temperature increases, the dielectric constant will decrease. While the dielectric constant decreases as temperature increases, the diffusion coefficient increases with temperature. This is as described by equation 1-12 in chapter 1. As shown in equation 1-12, the diffusion coefficient is dependent on dielectric constant as well as temperature. Although dielectric constant decreases as temperature increases, the direct dependence of diffusion coefficient on temperature in the exponential term causes the overall diffusion coefficient to increase.

	Methyl hexyl carbonate		Methyl octyl carbonate		Methyl decyl carbonate		Methyl dodecyl carbonate	
T (°C)	ε_s	D (m^2/s) ($x10^{-10}$)	ε_s	D (m^2/s) ($x10^{-10}$)	ε_s	D (m^2/s) ($x10^{-10}$)	ε_s	D (m^2/s) ($x10^{-10}$)
5	2.781	4.32	2.709	2.77	2.590	1.64		
15	2.771	5.77	2.699	3.86	2.582	2.27	2.524	1.51
25	2.761	7.29	2.688	4.91	2.573	3.03	2.516	2.10
35	2.750	8.93	2.677	6.23	2.564	3.84	2.507	2.78
45	2.740	10.7	2.666	7.05	2.555	4.82	2.496	3.48
55	2.729	13.1	2.655	9.29	2.545	5.92	2.487	4.34
65	2.718	16.3	2.642	11.6	2.536	6.91	2.478	5.36
75	2.706	19.2	2.630	13.5	2.526	8.89	2.469	6.49
85	2.693	22.9	2.618	16.4	2.517	10.8	2.459	7.90

Table 3-2 The dielectric constant and diffusion coefficient for acyclic carbonate solvents. ε_s = dielectric consant, D = self-diffusion coefficient.

At any particular temperature, the diffusion coefficient is the highest for methyl hexyl carbonate, followed by methyl octyl carbonate, methyl decyl carbonate, and methyl dodecyl carbonate. It is easy to reason that the smaller volume methyl hexyl carbonate diffuses faster because of its small size. On the other hand, according to the CAF, the higher rate of diffusion for methyl hexyl carbonate is really because of its higher dielectric constant.

At any particular temperature, the dielectric constant also decreases as the chain length of the alkyl tether increases from methyl hexyl to methyl dodecylene carbonate. The decrease in dielectric constant at any particular temperature is a result of the decrease in the dipole density of the system.

From the dielectric constant values at 25°C, the smallest change in dielectric constant as the molecular volume is varied is in going from methyl dodecyl carbonate to methyl decyl carbonate. Here, the dielectric constant change is only 0.057. In comparison, for the pure nitrile solvent at 25°C the change in dielectric constant going from dodecanenitrile to decanenitrile is 1.56[53]. The previously studied acetate solvent

family has the lowest dielectric constant change at 20°C of 0.25 going from decyl acetate to octyl acetate[53].

For methyl dodecyl carbonate, the smallest change in dielectric constant is 0.008 as the temperature is increased from 15°C to 25°C. Overall, as the temperature is increased 10°C, the dielectric constant changes about 0.01. Similar change in dielectric constant for the dodecanenitrile is about 0.3, thirty times more than acyclic carbonates.

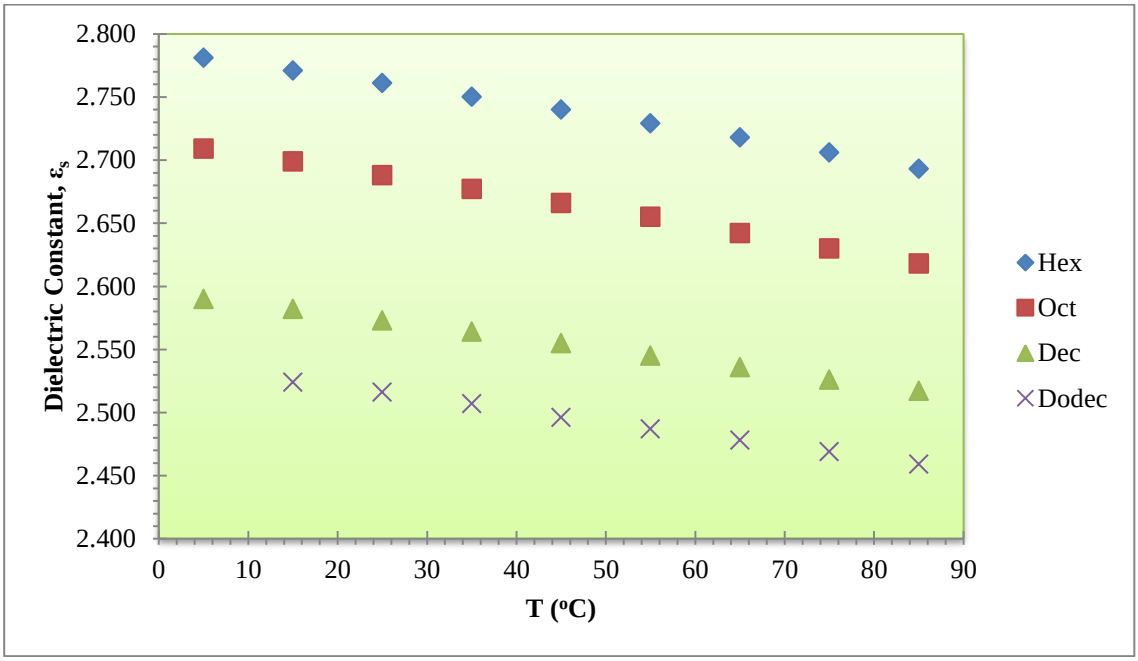

Figure 3-10 Plot of dielectric constant versus temperature for acyclic carbonate. Hex=methyl hexyl carbonate, Oct=methyl octyl carbonate, Dec=methyl decyl carbonate, Dodec=methyl dodecyl carbonate.

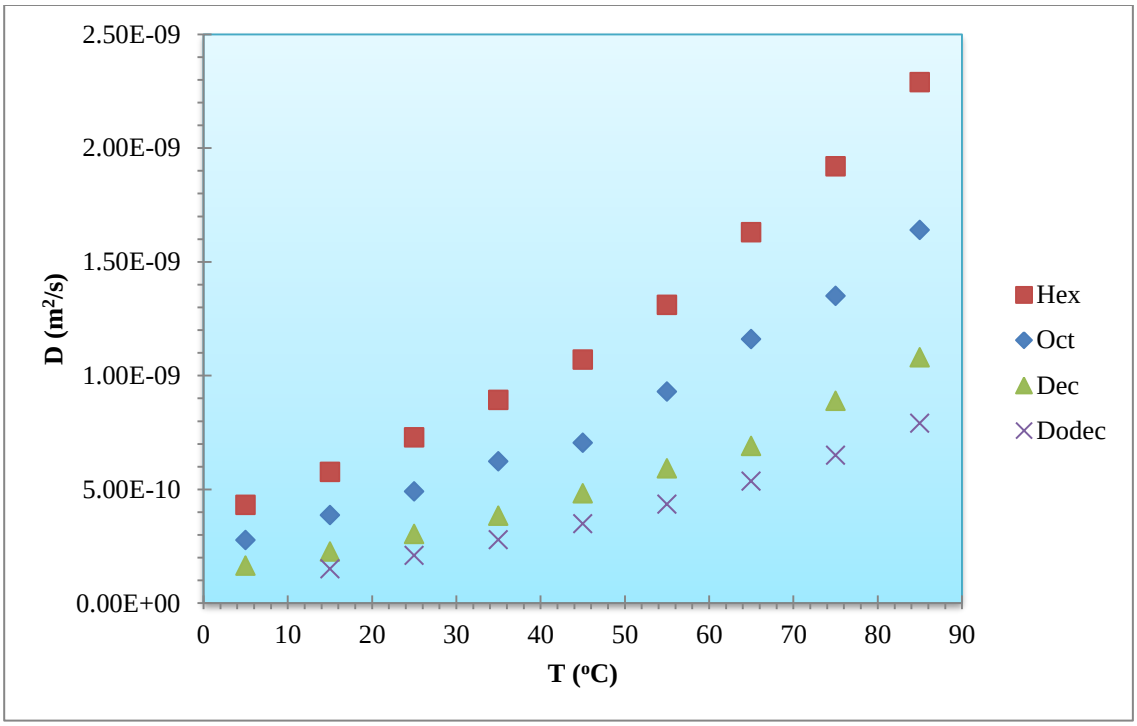

Figure 3-11 Plot of diffusion coefficient versus temperature for acyclic carbonate. Hex=methyl hexyl carbonate, Oct=methyl octyl carbonate, Dec=methyl decyl carbonate, Dodec=methyl dodecyl carbonate.

While the dielectric constant decreases as temperature increases, the reverse is true for the rate of diffusion. As the temperature increases, the rate of diffusion also increases. This can be explained by the temperature term in the Compensated Arrhenius Equation. The dependence of the rate of diffusion on the Boltzmann factor, which itself depends on the temperature, means that as the temperature increases, the value of the Boltzmann factor term increases. Thus, the rate of diffusion increases.

At 25^{o}C when the molecular volume is decreased in going from methyl dodecyl carbonate to methyl decyl carbonate, the change in rate of diffusion is 7.6 x 10^{-11} m^2/s. For comparison, when molecular volume is decreased from dodecanenitrile to decanenitrile, the change in rate of diffusion is 16.7 x 10^{-11} m^2/s. Similar order of magnitude is observed as the temperature is increased from 15^{o}C to 25^{o}C for methyl dodecyl carbonate, where the rate of diffusion changes 5.9 x 10^{-11} m^2/s. As temperature

is increased from 15°C to 25°C for dodecanenitrile, the rate of diffusion changes a total of 7.8 x 10^{-11} m^2/s.

Using the dielectric constant and self-diffusion data for pure acyclic carbonates, the reference temperature curve is plotted (figure 3-12).

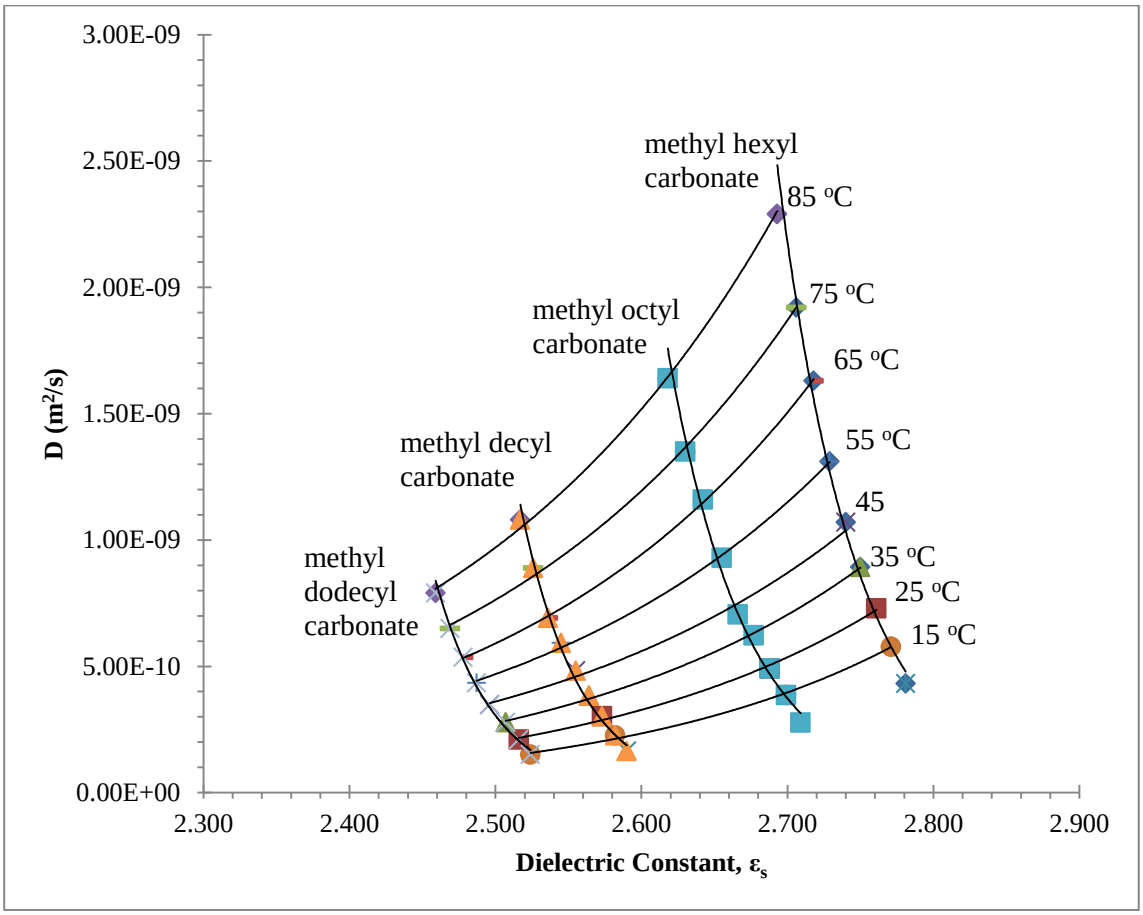

Figure 3-12 Reference curve for acyclic carbonate self-diffusion coefficient (D) and dielectric constant data.

From the reference temperature curve, the simple exponential model is found to produce the best regression value (table 3-3). Thus, the exponential model is used to calculate the value of the $D_r(\varepsilon_s,T_r)$. Table 3-4 shows the values of the E_a for each acyclic carbonate analog for all reference temperature, T_r.

	Fitting Model		
T_r (°C)	y = A*exp[Bx]	y=yo+A*exp[Bx]	$y=Ax^2+Bx+C$
5	0.9827	1.0000	1.0000
15	0.9959	0.9918	0.9849
25	0.9949	0.9906	0.9831
35	0.9981	0.9963	0.9925
45	0.9854	0.9809	0.9650
55	0.9983	0.9967	0.9936
65	0.9995	0.9992	1.0000
75	0.9977	0.9954	0.9923
85	0.9984	0.9975	0.9956
Average	0.9945	0.9935	0.9897

Table 3-3 The R^2-values for different mathematical model to fit the reference temperature curve.

	Activation Energy, E_a (kJ/mol)			
T_r (°C)	Methyl hexyl carbonate	Methyl octyl carbonate	Methyl decyl carbonate	Methyl dodecyl carbonate
15	24.91	27.14	29.44	33.75
25	23.76	26.14	28.59	33.04
35	23.62	25.67	27.56	30.53
45	22.64	24.61	26.31	28.75
55	22.62	24.36	25.69	27.42
65	22.33	23.97	25.16	26.62
75	21.45	23.14	24.36	25.82
85	21.21	22.82	23.91	25.15

Table 3-4 The E_a values for the diffusion of pure acyclic carbonate at reference temperature 5°C to 85°C.

Using the reference temperature plot, the T_r=15°C includes the largest dielectric constant range that coincides with the dielectric constant range of the methyl hexyl carbonate (the T_r=5°C is not considered because data is not available for the methyl dodecyl carbonate at 5°C). For the methyl octyl carbonate and methyl decyl carbonate, all reference temperature curves include the dielectric constant ranges of the two analogs. Thus all the E_a at all T_r should be able to be used to calculate the average E_a

for these two analogs. For the methyl dodecyl carbonate, the T_r=85^{o}C includes the most dielectric constant values that coincide with the dielectric constant value of this analog.

Checking the regression values of the plots of $\ln[D(T,\varepsilon_s)/D_r(T_r,\varepsilon_s)]$ versus 1/T, the $D_r(T_r,\varepsilon_s)$, all of the R^2-values for the T_r's mentioned above are at least equal to 0.9900 (figure 3-13), and thus the E_a values at these T_r's can be used to calculate the average E_a. From the E_a values at these T_r's, the average E_a for the diffusion of pure acyclic carbonate is calculated to be 22.5 ± 0.4 kJ/mol.

By dividing the diffusion coefficient values by the Boltzmann terms, the exponential pre-factor can be obtained. Plotting the exponential pre-factor versus the dielectric constant produces a master curve as shown in figure 3-14 below. The ability to plot the master curve shows that the CAF can be applied to the diffusion of pure acyclic carbonate, with a single E_a value for the acyclic carbonate solvent family.

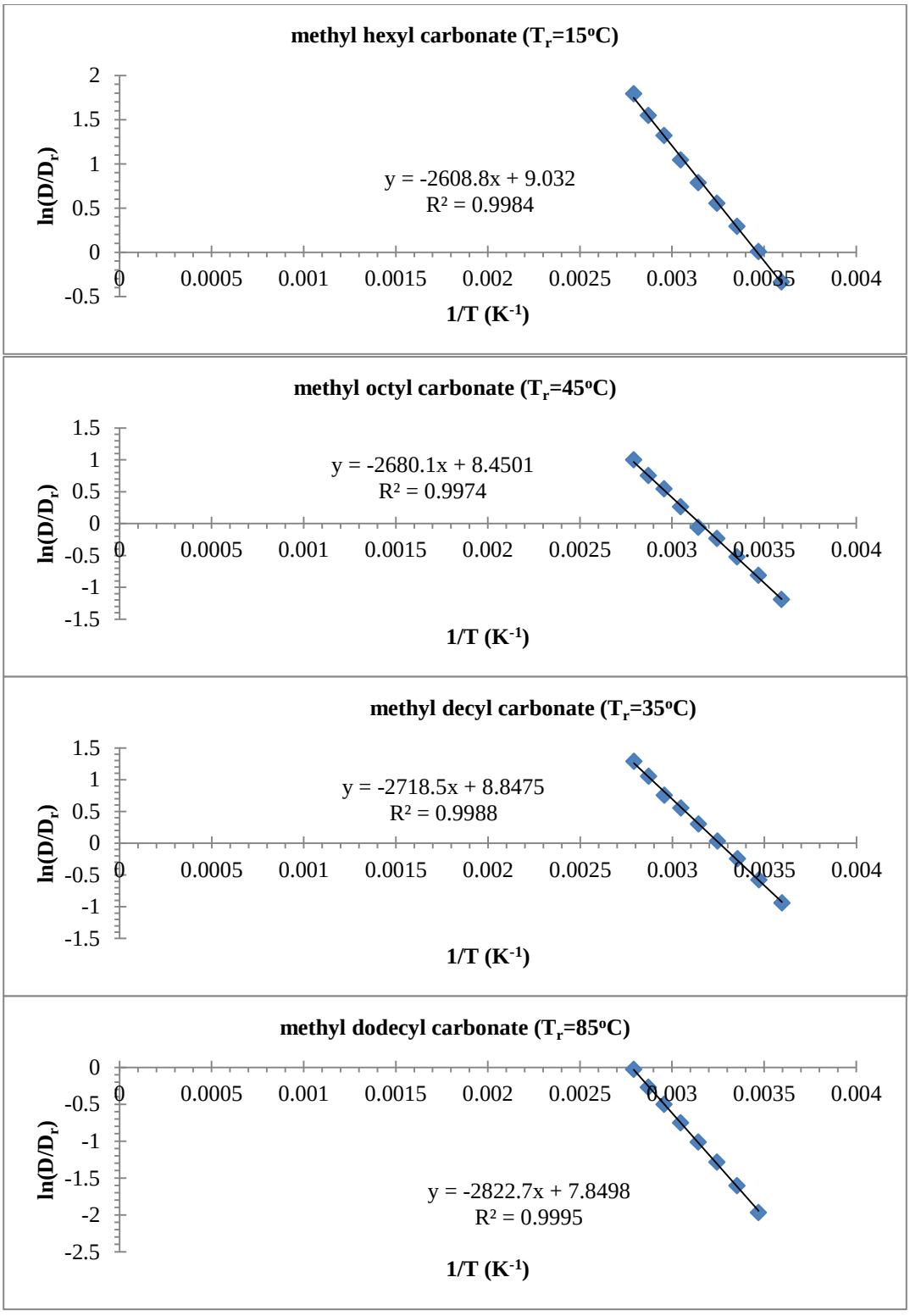

Figure 3-13 Plot of ln (D/D_r) vs (1/T) for selected acyclic carbonate analogs.

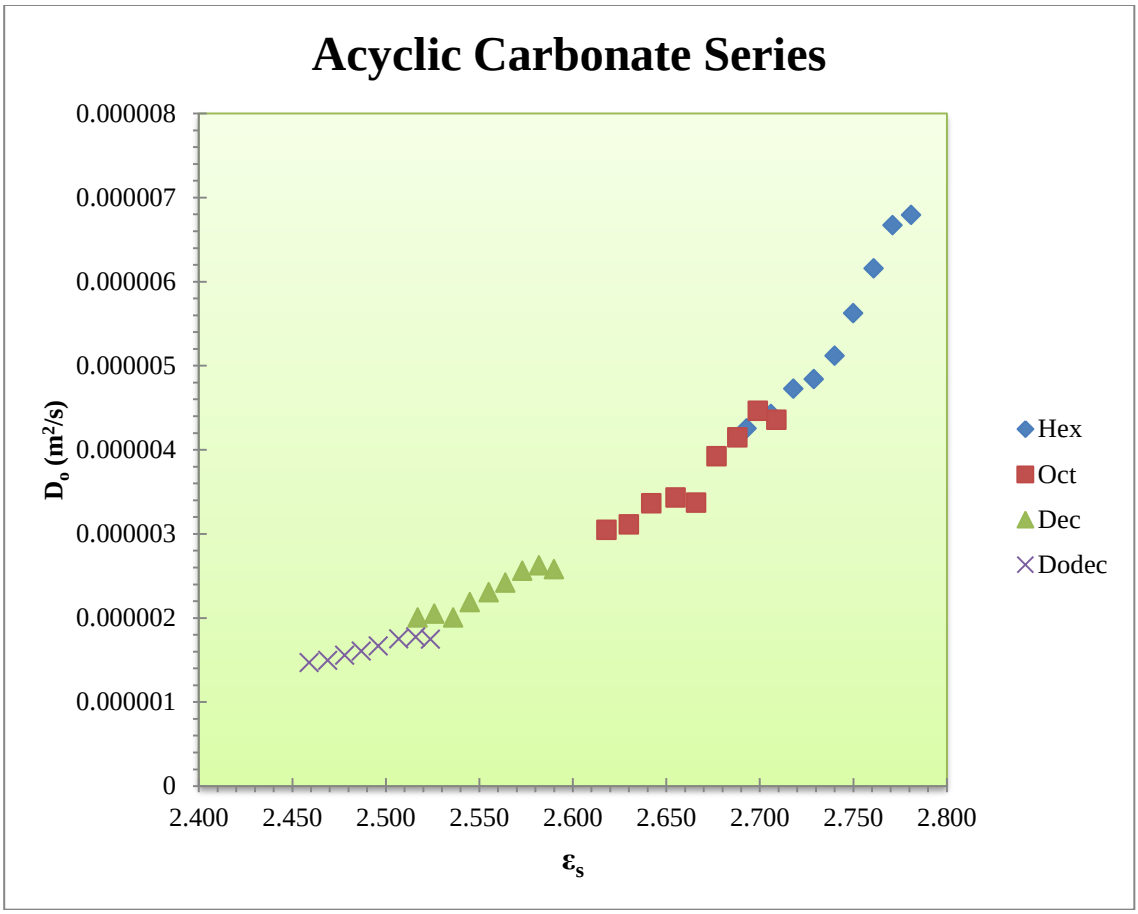

Figure 3-14 The master curve for acyclic carbonate series.

3.3 Conclusion

From the CAF analysis, the family of methyl alkyl carbonates can be analyzed using the CAF. The low dielectric constant value as low as 2.459 and self-diffusion coefficient value as low as 1.51 x 10^{-10} m^2/s do not seem to affect the ability to perform the CAF scaling procedure.

Unfortunately, the low dielectric constant values of the acyclic carbonate derivatives prevented the TbaTf salt from dissolving in the acyclic carbonate solvent. Thus the applicability of the CAF to conductivity in acyclic carbonate cannot be determined.

The calculated E_a value for methyl alkyl carbonates is 22.5 ± 0.4 kJ/mol. This value is lower than the value of the E_a for the diffusion of 2-ketones (23.9 ± 0.2 kJ/mol) and acetates (25.5 ± 0.3 kJ/mol). Thus the proposed idea that the E_a is related to the number of oxygen atoms around the carbonyl carbon is not true. Similarly, the idea that the E_a is inversely proportional to the dipole moment of the species is also not true.

However, one interesting note about the E_a for the self-diffusion of acyclic carbonate is that the value seems to be similar to other higher dielectric constant solvents. These other higher dielectric constant solvents also have higher molecular dipole moment values. It is possible that the E_a for self-diffusion is not affected by the dipole moment values or dielectric constant values, and that the values for all solvents lie between 20 kJ/mol to 25 kJ/mol. Since the nature of the E_a is not known, the trend in the E_a for self-diffusion is interesting and might provide a clue to its physical nature.

3.4 Detailed Synthesis, Sample Preparations, and Measurements

3.4.1 Detail Synthesis

The acyclic carbonates used in this work were synthesized in house. The ^{1}H NMR spectra were obtained using a Varian Mercury-300 NMR spectrometer. The IR spectra were obtained using Shimadzu IRAffinity-1 using dry KBr method.

All chemicals for the synthesis work are obtained from Sigma-Aldrich or TCI America and are used as is. The synthesis of the methyl alkyl carbonates resulted from the following typical procedure: A 3-neck flask was charged with 5.00 equivalent of methyl chloroformate and fitted with a thermometer, pressure-equalizing funnel, and a reflux condenser with drying tube. The methyl chloroformate was cooled to around 5^{o}C using a water-ice bath, and with stirring (magnetic), 1.00 equivalent of the desired

primary alcohol was added to the mixture dropwise to keep the temperature below 10°C, followed by 1.00 equivalent of dry pyridine. The mixture was allowed to warm to room temperature and was then heated to 40 to 60°C. At this point, the solid pyridinium hydrochloride that formed in the flask had dissolved. The disappearance of primary alcohol was monitored using NMR spectroscopy. After the primary alcohol was consumed (typically in 24 to 60 hours), the mixture was cooled to room temperature, and the pyridinium hydrochloride that precipitated was removed by filtration through Celite on a fritted funnel. The filtrate was washed with distilled water until the pH was neutral. The resulting acyclic carbonate was dried over anhydrous magnesium sulfate overnight. IR spectroscopy showed no detectable amount of water or residual primary alcohol was present in the sample. All the samples were greater than 97% purity by ^{1}H-NMR. Spot checks of methyl hexyl carbonate and methyl octyl carbonate using GC-MS (CI-methane, (M+1 = 161 and 189 respectively) showed purities of >97 and >99%.

^{1}H NMR (300MHz, $CDCl_3$):

Methyl hexyl carbonate[78]: 83% yield; ^{1}H NMR (300 MHz, $CDCl_3$): δ 0.81 (t, 3H, *J* = 6.5 Hz); 1.27 (m, 6H); 1.1-1.4 (m, 6H); 1.5-1.7 (m, 2H); 3.70 (s, 3H); 4.06 (t, 2H, *J* = 6.5 Hz)

Methyl octyl carbonate[79]: 86% yield; ^{1}H NMR (300 MHz, $CDCl_3$): δ 0.88 (t, 3H, *J* = 6.5 Hz); 1.1-1.5 (m, 10H); 1.6-1.8 (m, 2H); 3.77 (s, 3H); 4.13 (t, 2H, *J* = 6.5 Hz). Lit.: δ 0.86-0.90 (t, 3H); 1.27 (m, 10H); 1.62-1.70 (m, 2H); 3.78 (s, 3H); 4.11-4.16 (t, 2H)

Methyl decyl carbonate: 87% yield; ^{1}H NMR (300MHz, $CDCl_3$): δ 0.88 (t, 3H, *J* = 6.5 Hz); 1.1-1.5 (m, 14H); 1.6-1.8 (m, 2H); 3.77 (s, 3H); 4.13 (t, 2H, *J* = 6.5 Hz). Lit.: δ 0.86-0.90 (t, 3H); 1.27 (m, 14H); 1.62-1.70 (m, 2H); 3.78 (s, 3H); 4.11-4.16 (t, 2H)

Methyl dodecyl carbonate[80]: 86% yield; ^{1}H NMR (300 MHz, $CDCl_3$): δ 0.86 (t, 3H, *J* = 6.5 Hz); 1.1-1.4 (m, 18H); 1.5-1.7 (m, 2H); 3.75 (s, 3H); 4.11 (t, 2H, *J* = 6.5 Hz)

Chapter 4 : Synthesis and Application of the Compensated Arrhenius Formulation (CAF) to Cyclic Carbonates

4.1 Introduction

The acyclic carbonates have very low dielectric constant values such that ionic species like tetrabutyl ammonium trifluoromethansulfonate (TbaTf) could not dissolve in them. A solvent family very closely related to acyclic carbonates that has a very high dielectric constant is cyclic carbonates (figure 4-1). As mentioned in section 1.9, cyclic carbonates have high dielectric constants with propylene carbonate having a room temperature dielectric constant of 64.9[64]. If successful, cyclic carbonate will be the highest dielectric constant compound analyzed by the CAF.

Cyclic carbonates like propylene carbonate and ethylene carbonate have been used in batteries or in electrolyte studies[64]. Unlike acyclic carbonates, which are usually used as additives in batteries, cyclic carbonates are usually the main solvent used as battery electrolytes. To improve batteries, it is thus imperative that the transport properties of cyclic carbonates are well understood.

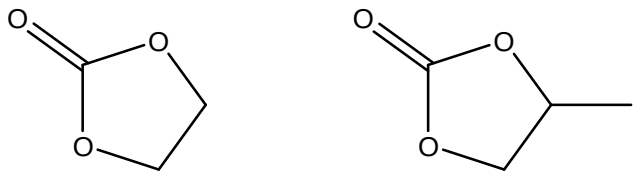

Ethylene carbonate Propylene carbonate

Figure 4-1 Two cyclic carbonate compounds typically used in batteries, ethylene carbonate and propylene carbonate.

It has been shown through the Compensated Arrhenius Formulation (CAF) by Petrowsky, Frech and coworkers[49, 52] that rate of diffusion and ionic conductivity are

dependent on the dielectric constant. However, it has also been shown by Petrowsky[40] that propylene carbonate, which has a dielectric constant value of 64[81], has a lower conductivity value compared to solvent with lower dielectric constant values like acetonitrile (dielectric constant ~38[81]) and acetone (~21[81]) (figure 4-2). A similar discrepancy is also observed for dimethyl sulfoxide (~46[81]). It is suspected that the reason for these discrepancies is the higher values of the E_a for cyclic carbonates and dimethyl sulfoxides.

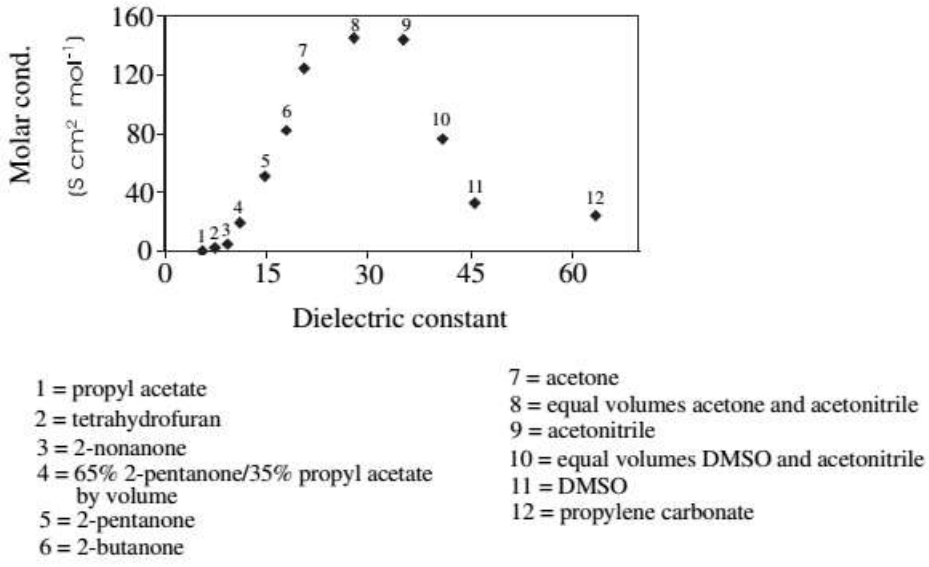

Figure 4-2 Plot of molar conductivity versus dielectric constant for 0.0055M TbaTf solutions at 25°C. Adapted from Petrowsky[40].

4.1.1 Project Goals

In this project, the aim is to investigate the applicability of the CAF to cyclic carbonates and their electrolyte solutions. Unlike acyclic carbonates, the dielectric constant for cyclic carbonates and their alkyl derivatives is expected to be high. It is expected that the CAF will be applicable to cyclic carbonates.

If the CAF is applicable to cyclic electrolytes, the energy of activation values (E_a's) of cyclic carbonates and their electrolyte solutions will be elucidated. The E_a's obtained will be compared against other solvent families. The E_a for conductivity is of high interest because it can help answer analyze the trend as shown in figure 4-2. The E_a for self-diffusion is expected to be between 20kJ/mol to 25kJ/mol, just like the E_a for self-diffusion for acyclic carbonates and other solvents previously investigated.

This project was collaborative with the group of Professor R. Frech[54] at the University of Oklahoma. Synthesis of the cyclic carbonates was developed and carried out as described here. The dielectric constant, conductivity, and self-diffusion measurements were performed as described here. The density measurements were performed by Dr. M. Petrowsky.

4.2 Results and Discussions

4.2.1 Synthetic Development

4.2.1.1 Synthesis of Cyclic Carbonates

To apply the CAF to cyclic carbonates, alkyl chain tethered cyclic carbonates are needed. These are not readily available for purchase. Thus, the cyclic carbonates have to be synthesized. There are a few routes that have been developed to synthesize cyclic carbonates[70, 79, 82, 83]. All methods essentially employ cyclo-addition reaction of nucleophilic oxygen from a hydroxyl, an epoxide, or a 1,2-diol moiety to an electrophilic carbon species in a carbonyl moiety. The electrophilic carbon species used include carbon dioxide, diethyl- or dimethyl carbonates, and phosgene. The reaction involving phosgene with a diol is less desirable because of the toxicity of phosgene.

The reaction involving carbon dioxide with a diol, an epoxide, or an acetal, while very environment friendly and is used in the industry, is less desirable in a laboratory setting since it is hard to control the pressure. Furthermore, it requires a transition metal catalyst to work well. A method involving diethyl- or dimethylcarbonate with a diol seems to be the easiest, with formation of methanol or ethanol as side products would seem to be mild and easy to separate the products.

Another possible method is to replace phosgene with a milder reagent. Methyl chloroformate is a cheap and easy to handle reagent. It is less toxic compared to phosgene. In this experiment, the modified phosgene route was chosen, in part because of the availability of the reagent methyl chloroformate in the lab. Another reason this route was chosen is because of the experience gained in handling methyl chloroformate, a result of an earlier synthetic development work on acyclic carbonates[53]. For example, one problem learned about such reactions involving methyl chloroformate is the formation of side products hydrochloric acid and methanol. Based on the previous work, it was found that the easiest and best way to remove these side products is by evaporating them off under the rotovap. Besides the experience in handling methyl chloroformate, the method was also chosen because it requires no expensive transition metal catalyst, while the diols, except for 1,2-undecanediol, are all commercially available. Synthesis of 1,2-diols is described in the next section below.

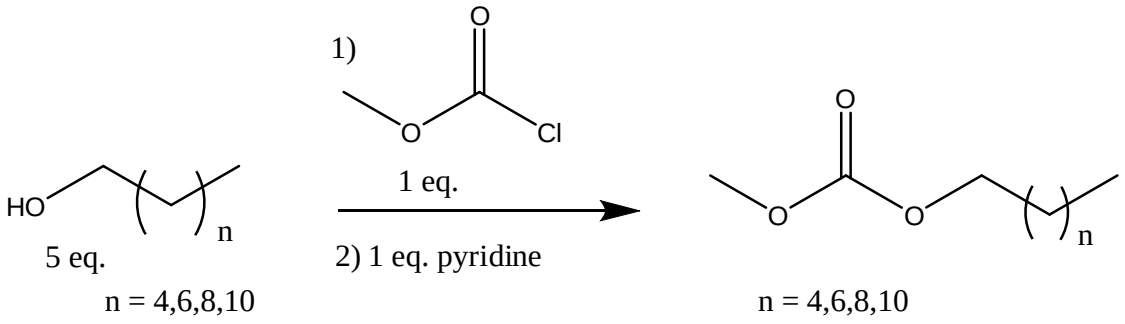

Figure 4-3 The formation of acyclic carbonates from previous work (see chapter 3).

In the development of the acyclic carbonate (Figure 4-3), the electrophile methyl chloroformate was reacted with a primary alcohol using pyridine to accelerate the reaction. The exact role of pyridine is unknown. It could have reacted as a base, pulling the proton from 1-alcohol (Figure 4-4), although this is unlikely because of the pK_a difference between a primary alcohol (~15-16) and a protonated pyridine (~5). It could also have reacted as a nucleophile, attacking the electrophilic carbon on methyl chloroformate to facilitate the reaction (Figure 4-5).

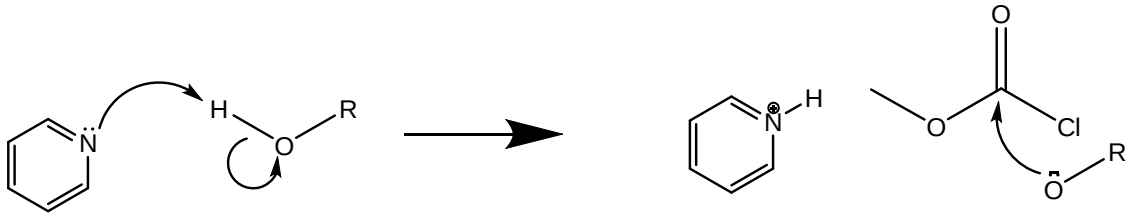

Figure 4-4 Pyridine acts as a base that deprotonates the hydroxyl hydrogen.

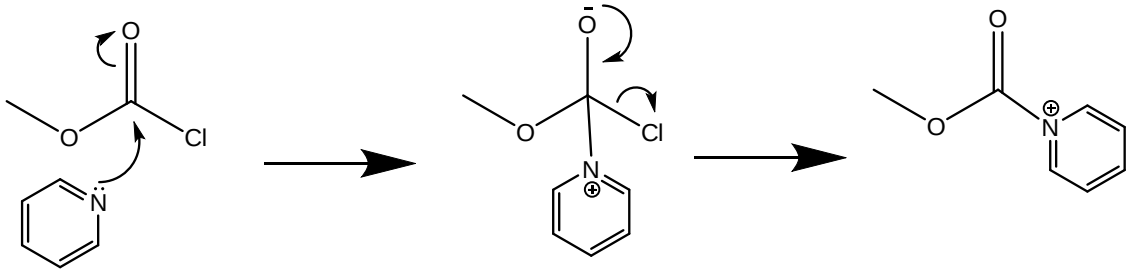

Figure 4-5 Pyridine acts as a nucleophile that attacks the carbonyl carbon and forms the carbonyl-pyridinium complex.

Besides helping to accelerate the reaction, the addition of pyridine also produces an easy to remove pyridinium hydrochloride salt from the reaction of the pyridine and the byproduct hydrochloric acid. Thus, pyridine was considered the best base/additive over other possible bases/additives like alkali metal hydroxides (sodium hydroxide, potassium hydroxide), metal hydrides (sodium hydride), or sodium amide. Nitrogen based base like triethylamine and DBU were tested in the development of acyclic carbonate synthesis and were found to produce unwanted side products (DBU) or vigorous reactions that were hard to control (triethylamine).

In the present work, the reaction of a 1,2-diol with methyl chloroformate was first performed with the presence of pyridine or triethylamine as a base (Figure 4-6). However, with the base in the solution, the reaction produced a dark brown solution after prolonged heating. This dark brown solution did not show any defining peak in the proton NMR and carbon NMR. The IR spectrum obtained also did not show any peak that can help to determine the species present in the resulting solution. Attempts to purify the resulting solution with a column consisting of different compositions of neutral, basic and acidic alumina were fruitless.

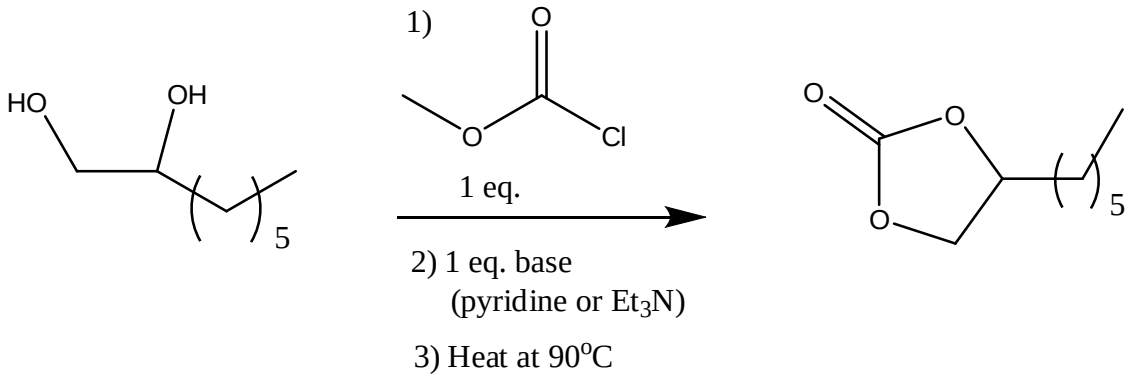

Figure 4-6 The first reaction to synthesize cyclic carbonate.

Because of the formation of the unwanted dark brown solution, another route without the addition of pyridine was chosen (Figure 4-7). The reaction, as expected, takes a long time to complete (determined based on the presence of 1,2-diol). The problem of long reaction time however is not the biggest problem. The amount of the products formed even after two weeks of reaction time depends on the amount of methyl chloroformate used. Varying the amount of methyl chloroformate used in the reaction shows that at least six equivalent is needed for the 1,2-diol to be fully consumed. It is possible that this could be because of the methyl chloroformate evaporating. However, varying the temperature of the reaction does not change the amount of the 1,2-diol consumed. This eliminates methyl chloroformate evaporation as the reason for the 1,2-diol not being fully consumed in the reaction.

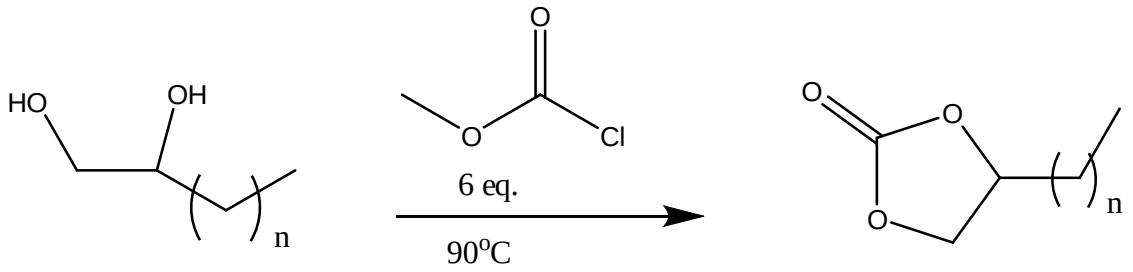

n = 6,8,9,10 n = 6,8,9,10

Figure 4-7 The final synthetic scheme for the synthesis of cyclic carbonates from the respective 1,2-diols.

After successful consumption of the starting 1,2-diol reagent, optimizing the products formed is the next goal. There seems to be two products formed in the reaction. One is the desired cyclic carbonate. The other product is the undesirable bis-carbonate side product (Figure 4-8). The formation of the side product was shown by a

group of small peaks in the proton NMR around 3.9 ppm. This peak is also observed in the product NMR of the acyclic carbonate previously synthesized as mentioned above.

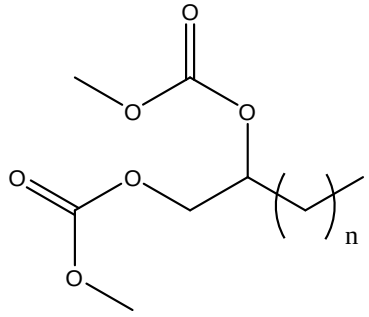

Figure 4-8 The bis-carbonate side products formed.

By using eight equivalents of methyl chloroformate, the bis-carbonate side product formed is only 5%, while about 20% of the bis-carbonate side product is formed when only six equivalents of methyl chloroformate used. Thus it seems that using eight equivalents of methyl chloroformate is the optimum reaction condition. However, another option is to try to eliminate the bis-carbonate side product using a column packed with alumina. A few combinations of neutral, acidic, and basic alumina were tested. The best combination of alumina was determined to be 50/50 acidic/neutral alumina layered combination. It is not known whether the alumina actually catalyzed the complete conversion of the bis-carbonate side products to the cyclic carbonate product, or if the bis-carbonate side products stuck to the alumina and were thus eliminated from the cyclic carbonate product. The column purified cyclic carbonate product seems to vary from 93 to 100% purity. The optimization results are shown in Table 4-1 and Table 4-2.

The best reaction condition was determined to be using six equivalents of methyl chloroformate at around 90^{o}C, followed by purification with column using 50/50

acidic/neutral alumina. The reactions, however, take between one to two weeks to complete. After about two weeks of heating at about 90^{o}C, the resulting solution was a clear, slightly yellow solution.

Methyl chloro-formate	Base	T (^{o}C)	Reaction Time (hours)	% Unreacted Diol	% Bis-carbonate	Product	% yield
1.1 eq	-	65	24 hrs	75%	-	Clear liquid	25%
1.1 eq	-	100	48 hrs	75%	-	Dark brown	10%
1.1 eq	trace Et_3N	100	2 hrs	75%	-	Dark brown	20%
2 eq	1 eq pyridine	60	48 hrs	80%	-	Clear liquid	20%
2 eq	1 eq pyridine	60	96 hrs	80%	-	Dark brown	20%
2 eq	1 eq pyridine	90	120 hrs	70%	5%	Dark brown	25%
4 eq	-	60	24 hrs	20%	-	Clear liquid	40%
4 eq	-	60	96 hrs	15%	-	Clear liquid	40%
1.1 eq	trace Et_3N	100	2 hrs	75%	-	Dark brown	20%
6 eq	-	90	168 hrs	trace	20%	Clear liquid	80%
6 eq	-	90	336 hrs	trace	20%	Clear liquid	80%
8 eq	-	100	168 hrs	trace	5%	Clear liquid	95%
8 eq	-	120	336 hrs	trace	5%	Dark brown	95%

Table 4-1 Optimization of the reaction condition for the synthesis of cyclic carbonates.

In this experiment, four cyclic carbonate analogs were synthesized and used. The octyl-, decyl-, undecyl-, and dodecyl-carbonate were synthesized by reacting the appropriate 1,2-diol with methyl chloroformate. The resulting cyclic carbonates used were of at least 93% purity. Detailed synthesis of the cyclic carbonates, the 1,2-undecanediol, as well as the preparation of the salt solutions of lithium trifluoromethane sulfonate (LiTf) in cyclic carbonates and tetrabuylammonium trifluoromethane sulfonate (TbaTf) in cyclic carbonates are described in section 4.4 below.

Methyl chloro-formate	% Unreacted Diol	% Bis-carbonate Product	Product	% yield unpurified	% yield purified	Alumina Type
1.1 eq	75%	-	Dark brown	20%	25%	acidic/ neutral
6 eq	trace	20%	Clear liquid	80%	80%	neutral
6 eq	trace	20%	Clear liquid	80%	93-100%	acidic/ neutral
6 eq	trace	20%	Clear liquid	80%	80%	basic/ neutral
8 eq	trace	5%	Clear liquid	95%	95%	neutral
8 eq	trace	5%	Clear liquid	95%	95-100%	Acidic /neutral
8 eq	trace	5%	Clear liquid	95%	95%	basic/ neutral

Table 4-2 Alumina screening for purification with column.

4.2.1.2 Synthesis of 1,2-diols

Since the 1,2-undecanediol is not commercially available, it had to be synthesized. There a few methods developed to synthesize 1,2-diols[84]. The Sharpless Dihydroxylation and Upjohn Dihydroxylation reactions (and their modifications) both involve osmium tetraoxide reaction with an olefin and are well developed. However, due to the very toxic nature of the osmium compounds, this method was avoided.

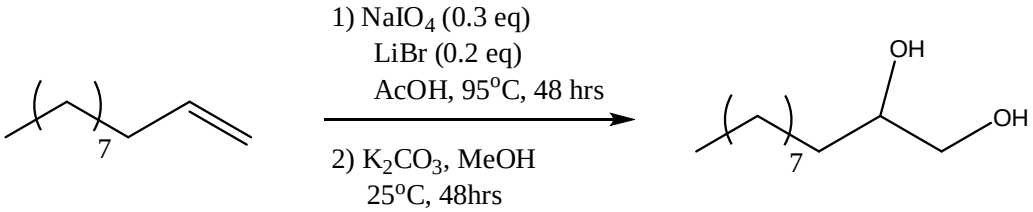

Figure 4-9 Synthetic scheme for the synthesis of 1,2-undecane diol.

The oxidation of olefin with potassium permanganate is also well established. However, due to the low solubility of potassium permanganate in non-aqueous media,

the reaction with 1-undecane only produces trace amount of the diol product. Furthermore, this reaction requires careful control of the temperature or the olefin produced will be cleaved into a ketone and an aldehyde before it can be isolated.

Another general method is addition of two acetyl groups to the olefin double bond, which was discovered separately by Prevost[85] and Woodward[86]. The modification of this method by Sudalai and coworkers was chosen[87] for this work (Figure 4-9). In the method, electrophilic bromine will first coordinate to the olefin forming a bromonium species. Attack by an acetate molecule on the carbon alpha to the bromine atom will then form the bromoacetoxy-olefin complex. At this point, the other oxygen from the same acetate group in the bromoacetoxy-olefin complex will attack the carbon bearing the bromine, forming acetoxynium species. Attack by another acetate molecule on the 1- or 2-position carbon will form the intermediate 1,2-diacetoxy alkane. The acetoxy groups were hydrolyzed to the final 1,2-diol products, which was then purified before use in undecylene carbonate synthesis.

4.2.2 Dielectric Constant and Self-Diffusion of Pure Cyclic Carbonates

Table 4-3 shows the dielectric constant and self-diffusion coefficient values of pure octylene carbonate, decylene carbonate, undercylene carbonate, and dodecylene carbonate.

	Octylene carbonate		Decylene carbonate		Undecylene carbonate		Dodecylene carbonate	
T (°C)	ε_s	D (m^2/s) ($x10^{-10}$)	ε_s	D (m^2/s) ($x10^{-10}$)	ε_s	D (m^2/s) ($x10^{-10}$)	ε_s	D (m^2/s) ($x10^{-10}$)
5	34.2	0.537	28.9	0.284	24.4	0.236	21.6	0.168
15	32.8	0.867	27.7	0.493	23.5	0.412	20.8	0.299
25	31.5	1.30	26.6	0.781	22.5	0.653	20.0	0.497
35	30.1	1.85	25.5	1.16	21.6	0.975	19.2	0.766
45	28.7	2.44	24.3	1.59	20.6	1.34	18.4	1.09
55	27.4	3.20	23.2	2.15	19.6	1.84	17.6	1.50
65	26.2	4.09	22.2	2.83	18.8	2.42	16.8	2.04
75	25.0	5.09	21.2	3.53	18.0	3.04	16.1	2.61
85	24.0	6.29	20.3	4.47	17.3	3.93	15.6	3.34

Table 4-3 The dielectric constant and self-diffusion coefficient data for cyclic carbonates investigated. ε_s = dielectric constant, D = self-diffusion coefficient.

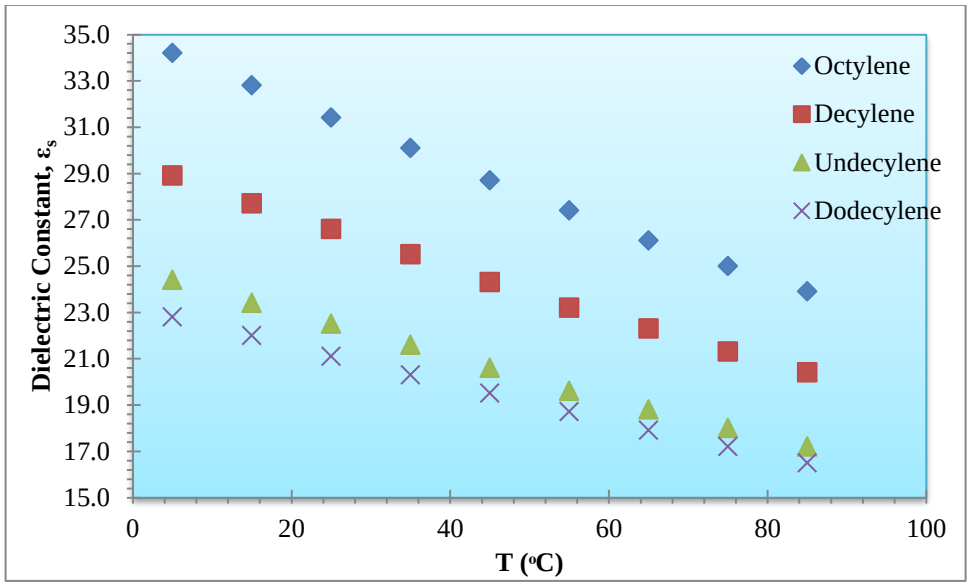

Figure 4-10 Plot of dielectric constant versus temperature for pure cyclic carbonates.

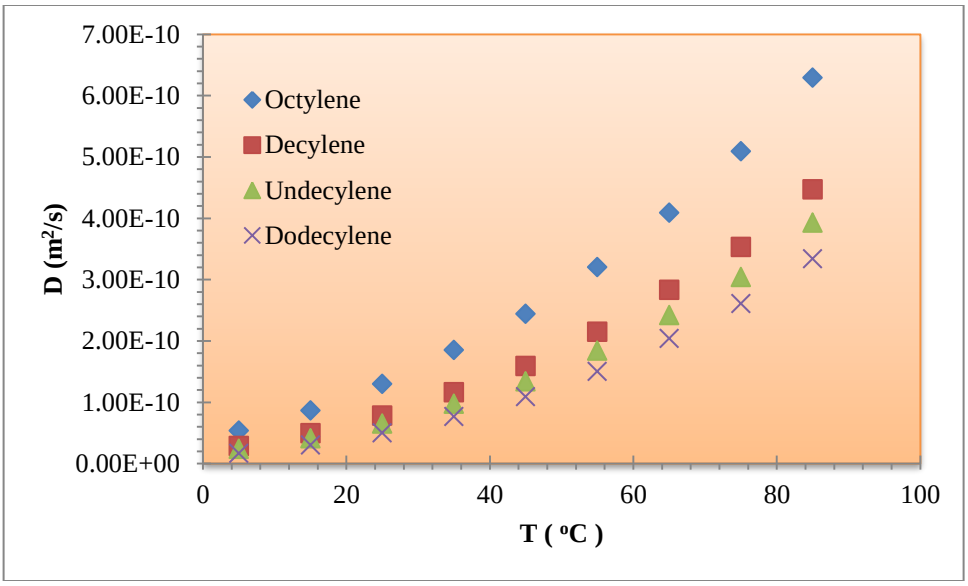

Figure 4-11 Plot of self-diffusion of cyclic carbonates under varying temperature.

The dielectric constant and self-diffusion values of pure cyclic carbonates are plotted in Figure 4-10 and Figure 4-11. As shown in Figure 4-10 above, the dielectric constant decreases as temperature increases from 5 to 85^{o}C for all cyclic carbonate derivatives. From the theory of dielectric constant discussed in Chapter 1, the dielectric constant is inversely related to the temperature. Thus as temperature increases, the dielectric constant will decrease.

While the dielectric constant decreases as temperature increases, the diffusion coefficient increases exponentially with temperature. This is as described by equation 1-12. As shown in equation 1-12, the diffusion coefficient is dependent on dielectric constant as well as temperature. Although dielectric constant decreases as temperature increases, the direct dependence of diffusion coefficient to temperature in the Boltzmann term causes overall diffusion coefficient to increase.

At any particular temperature, the diffusion coefficient is the highest for octylene carbonate, followed by decylene carbonate, undecylene carbonate, and

dodecylene carbonate. It is easy to reason that the smaller volume octylene carbonate diffuse faster because of its small size. On the other hand, according to CAF, the higher rate of diffusion for octylene carbonate is really because of its higher dielectric constant or lower energy of activation compared to those of the other cyclic carbonates investigated.

At any particular temperature, the dielectric constant also decreases as the chain length of the alkyl tether increases from octylene to dodecylene carbonate. The decrease in dielectric constant at any particular temperature is a result of the increase in the volume of the system.

To validate the results, the dielectric constant values are compared to the calculated values using modified Onsager equation

$$\varepsilon_S \approx \frac{N\mu^2(\varepsilon_\infty+2)^2}{18\,k\,T\,\varepsilon_o} \qquad (4\text{-}1)$$

Here ε_s is the static dielectric constant, N is the number density of molecular dipoles, k is the Boltzmann constant, T is the temperature in kelvin, ε_o is the vacuum permittivity constant, ε_∞ is the real component of dielectric constant at infinite frequency and is approximated by the square of the refractive index of the compound ($\varepsilon_\infty \approx \eta^2$), and μ is the dipole moment. N is calculated by dividing the mass density by the molecular weight of the cyclic carbonate species, and multiplied by the Avogadro constant. The mass density is given in Table 4-4 below. η is taken from the value for propylene carbonate (1.42)[88]. μ is taken from the literature values for propylene carbonate (4.94D)[89]. The result is shown in Table 4-5 below for undecylene carbonate.

	Density (g/cm^3) of Pure Cyclic Carbonate			
T (°C)	Octylene	Decylene	Undecylene	Dodecylene
5	1.03009	1.00248	0.98884	0.97656
15	1.02195	0.99465	0.98115	0.96883
25	1.01378	0.98685	0.97348	0.96128
35	1.00564	0.97907	0.96588	0.95398
45	0.99751	0.97133	0.95832	0.94677
55	0.98938	0.96357	0.95075	0.93949
65	0.98124	0.95581	0.94317	0.93207
75	0.97312	0.94807	0.93562	0.92463
85	0.96498	0.94033	0.92808	0.91719

Table 4-4 Density of pure cyclic carbonates used in the calculation of the dipole density.

From Table 4-5, the biggest deviation from calculated value is 26%. Thus the experimental values are reasonable.

	Dielectric Constant, ε_s					
	Octylene			Decylene		
T (^{0}C)	Exp	Calc	% error	Exp	Calc	% error
5	34.2	25.75	24.7	28.9	21.55	25.4
15	32.8	24.66	24.8	27.7	20.64	25.5
25	31.4	23.64	24.7	26.6	19.79	25.6
35	30.1	22.69	24.6	25.5	18.99	25.5
45	28.7	21.80	24.0	24.3	18.25	24.9
55	27.4	20.96	23.5	23.2	17.55	24.4
65	26.1	20.17	22.7	22.3	16.90	24.2
75	25	19.43	22.3	21.3	16.28	23.6
85	23.9	18.73	21.6	20.4	15.70	23.0
	Dielectric Constant, ε_s					
	Undecylene			Dodecylene		
T (^{0}C)	Exp	Calc	% error	Exp	Calc	% error
5	24.4	19.86	18.6	22.8	18.41	19.3
15	23.4	19.02	18.7	22	17.63	19.9
25	22.5	18.24	18.9	21.1	16.91	19.9
35	21.6	17.51	18.9	20.3	16.23	20.0
45	20.6	16.83	18.3	19.5	15.60	20.0
55	19.6	16.19	17.4	18.7	15.01	19.7
65	18.8	15.58	17.1	17.9	14.45	19.3
75	18	15.01	16.6	17.2	13.93	19.0
85	17.2	14.48	15.8	16.5	13.43	18.6

Table 4-5 The calculated vs. experimental dielectric constant for pure cyclic carbonates (Exp=experimental, Calc=calculated).

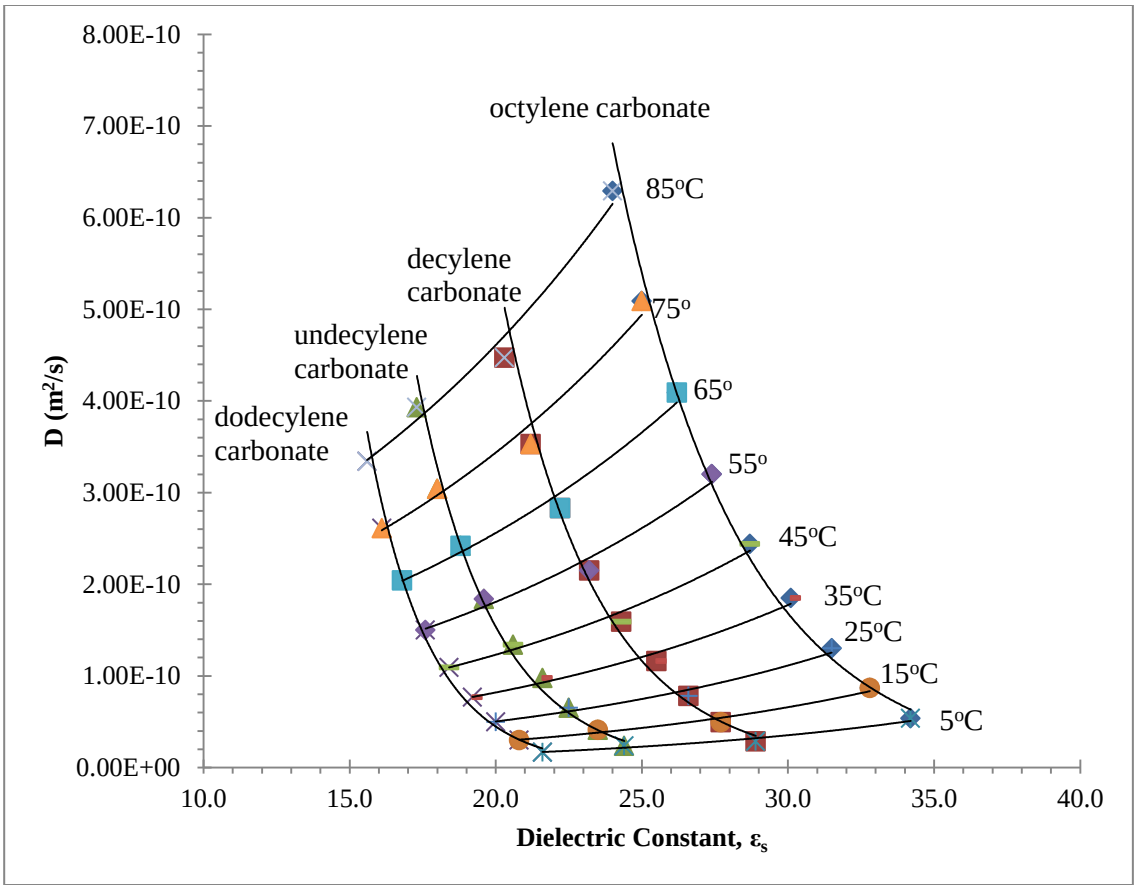

Figure 4-12 The reference curve for the self-diffusion coefficient (D) and dielectric constant of cyclic carbonates.

Using the dielectric constant and self-diffusion coefficient data, the reference curve is plotted (figure 4-12). From the reference curve, the exponential growth function is found to give the best fit (table 4-6) with R^2-value of 0.9996 and thus it is used to calculate the values of the $D_r(\varepsilon_s,T_r)$. Table 4-7 lists the values of the E_a for each cyclic carbonate analog for all reference temperature T_r.

	Fitting model		
T_r (°C)	y=A*exp(Bx)	y=yo+A*exp(Bx)	$y=A*x^2+B*x+C$
5	0.9587	0.9610	0.9332
15	0.9659	0.9605	0.9404
25	0.9684	0.9654	0.9486
35	0.9693	0.9691	0.9539
45	0.9729	0.9752	0.9629
55	0.9707	0.9662	0.9545
65	0.9745	0.9783	0.9684
75	0.9703	0.9817	0.9708
85	0.9718	0.9693	0.9600
Average	0.9692	0.9696	0.9547

Table 4-6 The R^2-values for different mathematical model to fit the reference temperature curve.

	Activation Energy, E_a (kJ/mol)			
T_r (°C)	Octylene carbonate	Decylene carbonate	Undecylene carbonate	Dodecylene carbonate
5	35.27	33.56	31.59	32.30
15	35.37	34.20	32.24	32.83
25	35.42	34.34	32.35	32.92
35	35.91	34.69	32.55	33.05
45	36.36	35.14	32.91	33.35
55	36.58	35.55	33.32	33.72
65	37.33	36.05	33.59	33.91
75	39.68	37.46	34.25	34.24
85	38.78	37.39	34.64	34.75

Table 4-7 The E_a values for the diffusion of pure cyclic carbonate at reference temperature 5°C to 85°C.

Using the reference temperature plot, the T_r=5°C includes the largest dielectric constant range that coincides with the dielectric constant range of the octylene carbonate. For the decylene carbonate , the reference curves at temperatures from 5°C to 35°C covers the same range of dielectric constant values as the decylene carbonate. For undecylene carbonate, the reference curves from 55°C to 85°C have the same dielectric constant range. Only the T_r=85°C is considered sufficient for the dodecylene

carbonate. All of the linear plots of ln (D/D_r) vs (1/T) have regression values of at least 0.9900 (plots not shown).

From the dielectric constant and diffusion coefficient of the pure cyclic carbonates, the CAF is applied to the data to obtain the average energy of activation E_a of the diffusion process. The calculated E_a for cyclic carbonates is found to be 34.3 $\pm$ 0.6 kJ/mol.

By dividing the diffusion coefficient values by the Boltzmann terms, the exponential pre-factor can be calculated. Plotting the exponential pre-factor against the dielectric constant, a master curve can be plotted as shown in figure 4-13 below. As discussed in section 2.5, the ability to form a master curve shows that the CAF is applicable to the diffusion of cyclic carbonate.

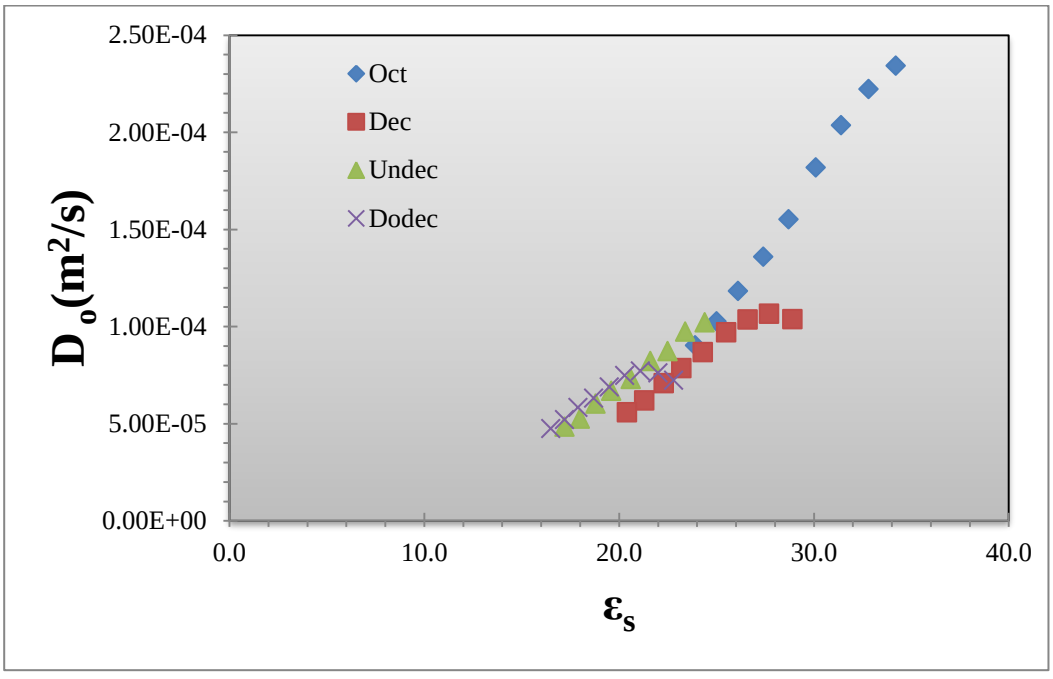

Figure 4-13 Master curve from Pure Cyclic Carbonate Diffusion Data.

The values of the E_a for the diffusion of pure cyclic carbonates are a little high compared to other aprotic solvents (table 4-8).

Solvent Family	E_a (kJ/mol)
Acetates	25.5 $\pm$ 0.3
2-ketones	23.9 $\pm$ 0.2
Nitriles	24.1 $\pm$ 0.1
Acyclic carbonates	22.5 $\pm$ 0.4
Thiols	25.2 $\pm$ 0.3
Cyclic carbonates	34.3 $\pm$ 0.6

Table 4-8 Comparison of activation energy for various aprotic solvents.

The E_a data are gathered from Chapter 3 and from previous work by Petrowsky, Frech and co-workers[53]. From the table, it is apparent that cyclic carbonates have a distinctly higher energy of activation compared to other aprotic solvents. The difference with the next highest E_a from acetates is almost 9 kJ/mol. From their previous work[50], Petrowsky, Frech and coworkers have shown that the polar protic solvent primary alcohols show an E_a value of 37 $\pm$ 1 kJ/mol. Polar protic solvents like primary alcohols are known to have strong intermolecular association because of hydrogen bonding. Intermolecular association is usually described by the Kirkwood g-factor[90].

The Kirkwood g-factor value is usually close to 1 for non-interacting molecules. For primary alcohols, Kirkwood and coworker have observed the value to be 2.68 at 25^{o}C[91]. A couple of studies on propylene carbonate and ethylene carbonate have shown that the g-factor for these compounds is close to 1[88, 92]. This shows that there is no specific intermolecular association between cyclic carbonates. However, the E_a of cyclic carbonates is still closer to the E_a of primary alcohols, which have specific

molecular interactions through hydrogen bonding. This suggests some sort of intermolecular interaction, although the specific of this interaction is still not known.

4.2.3 Dielectric Constant and Conductivity of LiTf and TbaTf in Cyclic Carbonates

Table 4-9 and 4-10 show the values of the dielectric constant and ionic conductivity of 0.3 molal lithium triflate (LiTf) and 0.3 molal tetrabutyl ammonium triflate (TbaTf) in cyclic carbonates.

	Octylene carbonate		Decylene carbonate		Undecylene carbonate		Dodecylene carbonate	
T_r (^oC)	ε_s	σ (S/cm)	ε_s	σ (S/cm)	ε_s	σ (S/cm)	ε_s	σ (S/cm)
5	35.1	0.000084	29.0	0.000041	23.7	0.000020	21.6	0.000016
15	33.9	0.000121	28.4	0.000056	23.2	0.000031	21.2	0.000026
25	32.6	0.000175	27.3	0.000085	22.7	0.000048	20.6	0.000041
35	31.4	0.000243	26.3	0.000122	22.3	0.000071	20.1	0.000060
45	30.2	0.000329	25.4	0.000172	21.9	0.000103	19.6	0.000089
55	29.2	0.000431	24.4	0.000231	21.2	0.000141	19.0	0.000123
65	28.0	0.000542	23.5	0.000300	20.3	0.000183	18.5	0.000164
75	27.1	0.000664	22.8	0.000375	19.6	0.000230	18.0	0.000210
85	26.3	0.000796	22.0	0.000458	19.0	0.000283	17.5	0.000261

Table 4-9 Dielectric constant and conductivity values for 0.3 molal LiTf in cyclic carbonates. ε_s = dielectric constant, σ = conductivity.

	Octylene carbonate		Decylene carbonate		Undecylene carbonate		Dodecylene carbonate	
T_r (^oC)	ε_s	σ (S/cm)	ε_s	σ (S/cm)	ε_s	σ (S/cm)	ε_s	σ (S/cm)
5	31.1	0.000353	25.8	0.000169	24.5	0.000128	20.8	0.000080
15	30.1	0.000516	25.2	0.000261	23.8	0.000199	20.3	0.000129
25	29.3	0.000724	24.6	0.000380	23.1	0.000295	19.7	0.000197
35	28.3	0.000990	24.0	0.000545	22.5	0.000433	19.2	0.000296
45	27.3	0.001330	23.3	0.000765	21.7	0.000626	18.7	0.000432
55	26.2	0.001730	22.7	0.001030	21.1	0.000859	18.2	0.000602
65	25.2	0.002170	22.0	0.001340	20.6	0.001120	17.8	0.000798
75	24.1	0.002630	21.5	0.001680	20.1	0.001430	17.4	0.001020
85	23.1	0.003140	21.2	0.002050	19.5	0.001760	17.0	0.001270

Table 4-10 Dielectric constant and conductivity values for 0.3 molal TbaTf in cyclic carbonates. ε_s = dielectric constant, σ = conductivity.

Figure 4-14 shows the plot of dielectric constant for 0.30 molal LiTf in cyclic carbonate solutions. Figure 4-15 shows the plot of dielectric constant for 0.30 molal TbaTf in cyclic carbonate solutions. The dielectric constant values are the highest for octylene carbonate solutions at each temperature for both ionic species. This is expected since octylene carbonate is the smallest member of the group. The dielectric constant decreases as the molecular volume (chain length) is increased.

Comparing the two solutions, the dielectric constant is higher for LiTf solution. In fact, the TbaTf solutions have lower dielectric constant than the pure cyclic carbonate solutions. This is certainly unexpected since typically it is observed that electrolyte solutions have higher dielectric constant than the pure solvents.

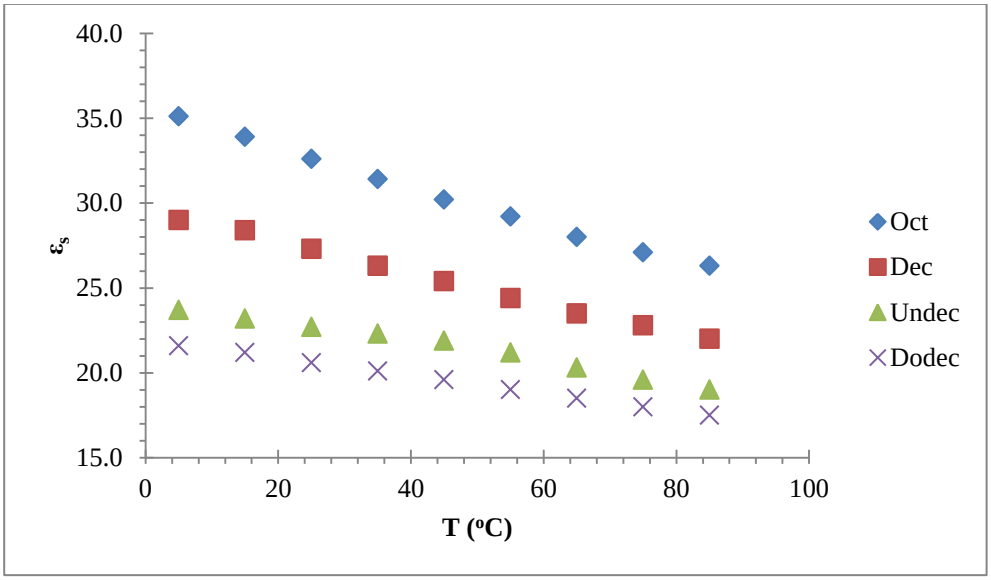

Figure 4-14 Plot of dielectric constant versus temperature for 0.3 molal LiTf-cyclic carbonates solution.

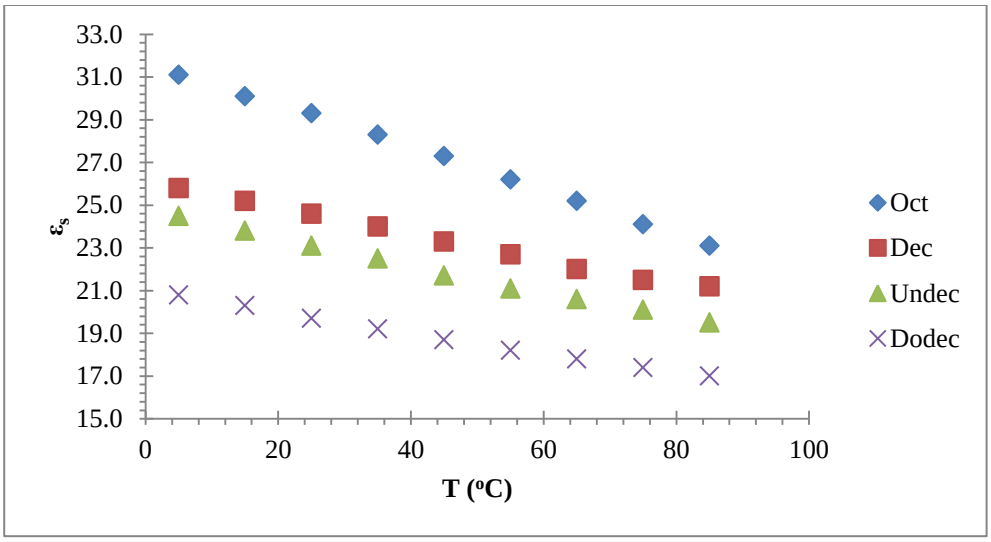

Figure 4-15 Plot of dielectric constant versus temperature for 0.3 molal TbaTf-cyclic carbonates solution.

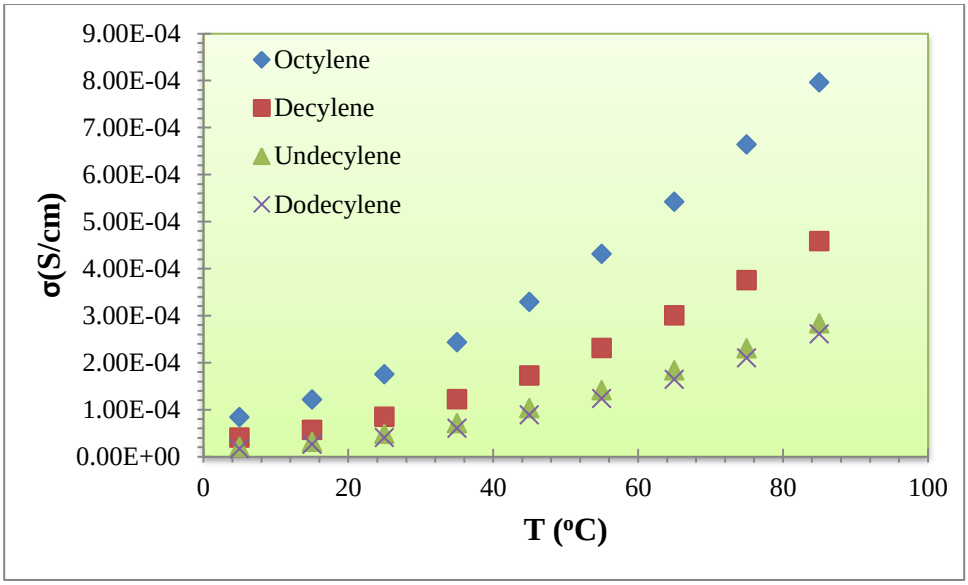

Figure 4-16 Plot of conductivity versus temperature for 0.3 molal LiTf-cyclic carbonates solution.

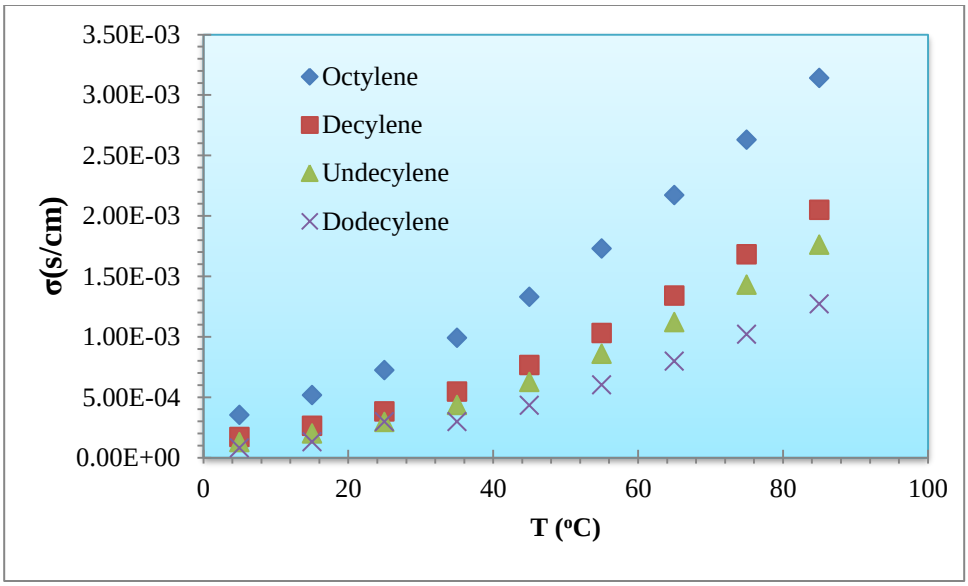

Figure 4-17 Plot of conductivity versus temperature for 0.3 molal TbaTf-cyclic carbonates solution.

Figure 4-16 shows the conductivity values for 0.30 molal LiTf in cyclic carbonate solutions. The conductivity values are the highest for octylene carbonate at each temperature. This is also as expected since octylene carbonate is the smallest member of the group. The dielectric constant decreases as the molecular volume (chain length) is increased. Since conductivity is proportional to the dielectric constant, the conductivity also decreases as dielectric constant decreases.

Figure 4-17 shows the conductivity values for 0.30 molal TbaTf in cyclic carbonate solutions. The trend is the same as for lithium triflate solutions. Comparing the salt solutions, the conductivity is higher for TbaTf solutions. Since there is evidence that ionic association does not occur for TbaTf ions, the Tba cations and Tf anions exist as free ions. This allows for higher number of charge carriers, resulting in higher conductivity values compared to conductivity values for lithium triflate solutions.

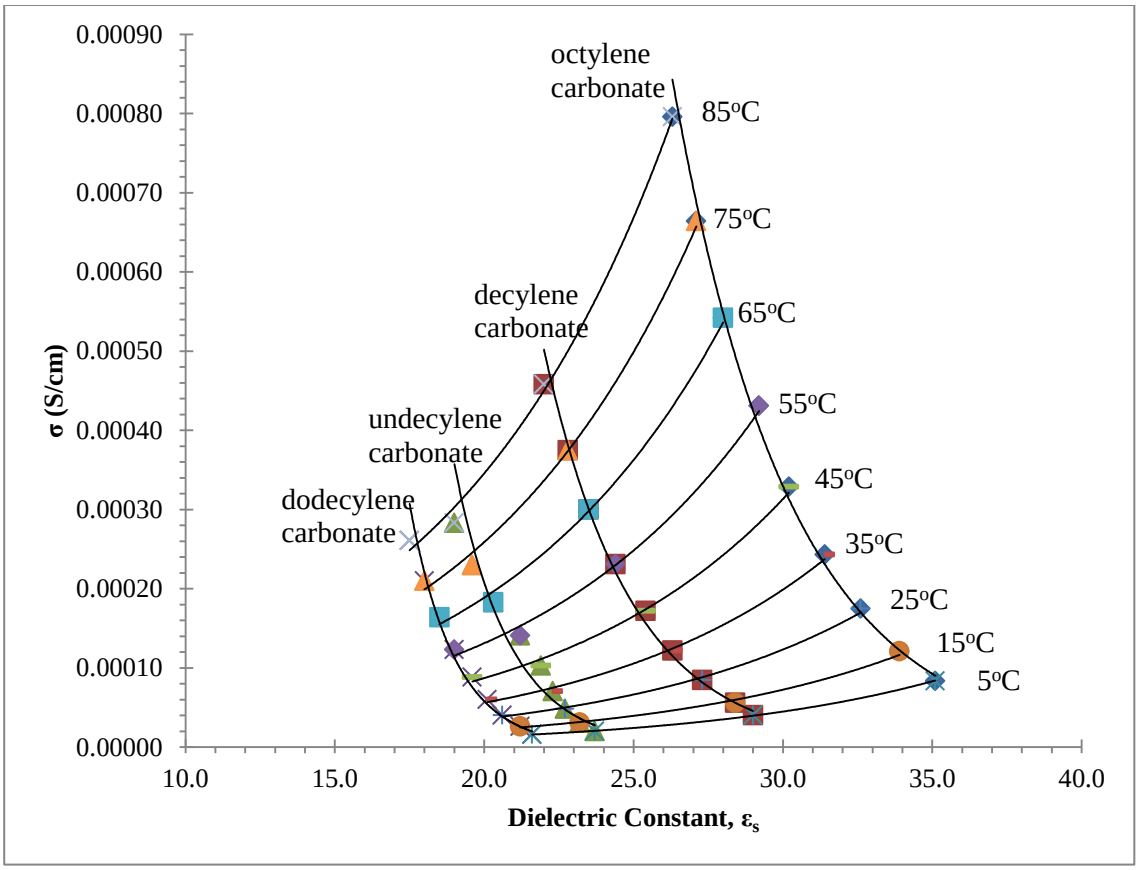

Figure 4-18 The reference curve of conductivity versus dielectric constant for 0.3 molal LiTf in cyclic carbonates. σ = conductivity.

Using the data from ionic conductivity and dielectric constant, the reference curves are plotted (figure 4-18 and 4-19). From the reference curves, it was found that the best fit for 0.3 molal LiTf in cyclic carbonate solutions is the polynomial of second order model, while the best fit for the 0.3 molal TbaTf in cyclic carbonate solutions is the exponential growth fit.

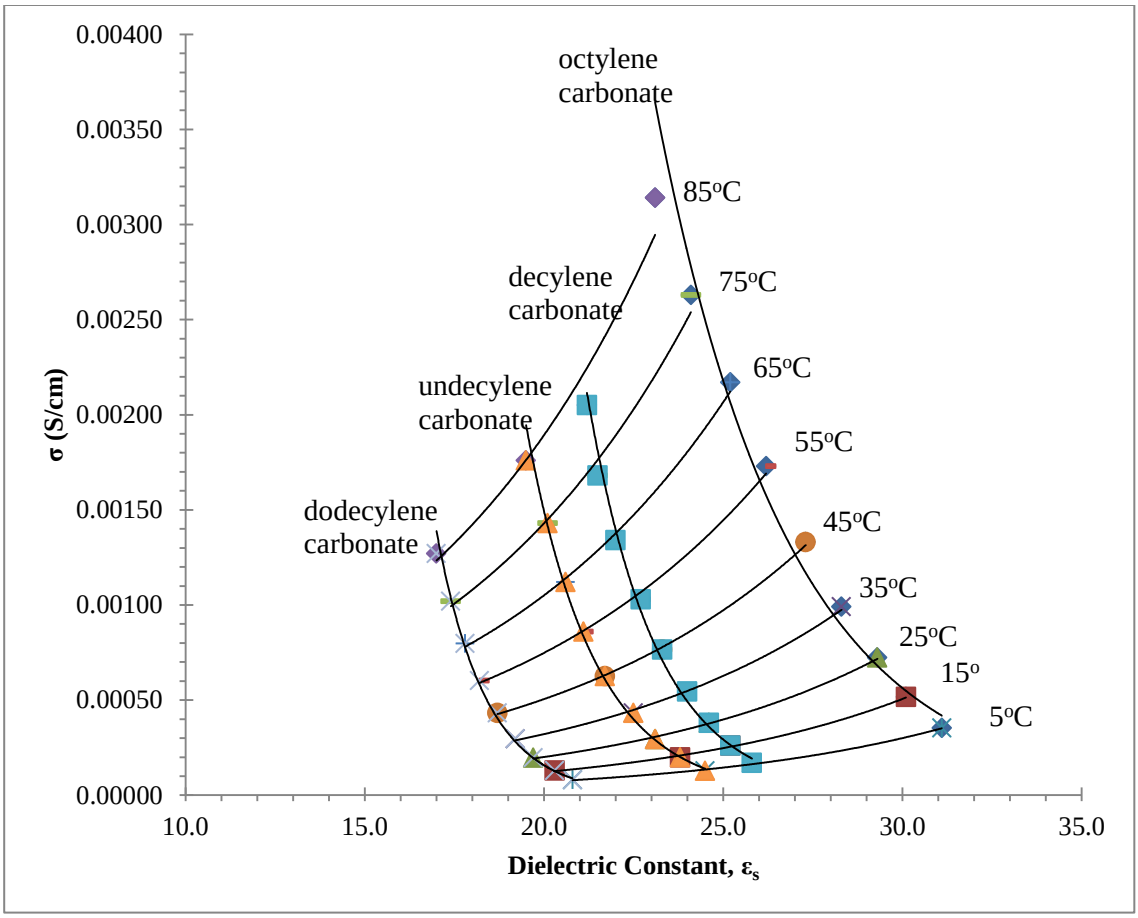

Figure 4-19 The reference curve of conductivity versus dielectric constant for 0.3 molal TbaTf in cyclic carbonates. σ = conductivity.

	Fitting model		
T_r (°C)	y=A*exp(Bx)	y=yo+A*exp(Bx)	$y=A*x^2+B*x+C$
5	0.9995	0.9994	1.0000
15	0.9956	1.0000	0.9974
25	0.9970	0.9997	0.9991
35	0.9973	0.9978	1.0000
45	0.9956	0.9948	0.9989
55	0.9950	0.9917	0.9964
65	0.9958	0.9923	0.9962
75	0.9959	0.9927	0.9962
85	0.9950	0.9900	0.9933
Average	0.9963	0.9954	0.9975

Table 4-11 R^2-values for 0.3 molal LiTf in cyclic carbonate solution.

	Fitting model		
T_r (°C)	y=A*exp(Bx)	y=yo+A*exp(Bx)	$y=A*x^2+B*x+C$
5	0.9970	0.9950	0.9963
15	0.9976	0.9977	0.9974
25	0.9984	0.9961	0.9990
35	0.9982	0.9971	0.9998
45	0.9990	0.9963	0.9992
55	0.9956	0.9977	0.9961
65	0.9959	0.9981	0.9987
75	0.9872	0.9968	0.9917
85	0.9489	0.9959	0.9433
Average	0.9909	0.9967	0.9913

Table 4-12 R^2-values for 0.3 molal TbaTf in cyclic carbonate solution.

Table 4-13 shows the E_a for 0.3 molal LiTf in cyclic carbonate solutions for all cyclic carbonate analogs. From the reference curve plot, the valid reference temperature for octylene carbonate is 5°C. The valid reference curves for decylene carbonate are 5°C to 85°C. The valid reference curves for undecylene carbonate are 35°C to 85°C. The valid reference curve for dodecylene carbonate is 85°C. Looking at the linear regression values for the plot of $\ln(\sigma/\sigma_r)$ vs (1/T) at these reference temperatures shows that all of them are at least 0.9900. A comparison between the CAF plot and a simple Arrhenius plot is shown in figure 4-20. The average E_a for the conductivity of 0.3 molal LiTf in cyclic carbonate solutions is calculated to be 35.2 ± 0.9 kJ/mol.

	Activation Energy, E_a (kJ/mol)			
T_r (°C)	Octylene carbonate	Decylene carbonate	Undecylene carbonate	Dodecylene carbonate
5	35.12	35.37	30.93	29.37
15	36.29	35.02	28.30	26.41
25	35.74	35.71	30.17	28.20
35	35.35	36.12	31.60	29.79
45	35.07	36.27	32.41	30.82
55	34.41	36.00	33.28	32.36

65	34.04	35.92	33.89	33.45
75	33.80	35.76	34.06	33.91
85	33.36	35.47	34.42	34.84

Table 4-13 The energy of activation, E_a for 0.3 molal LiTf in cyclic carbonate solutions.

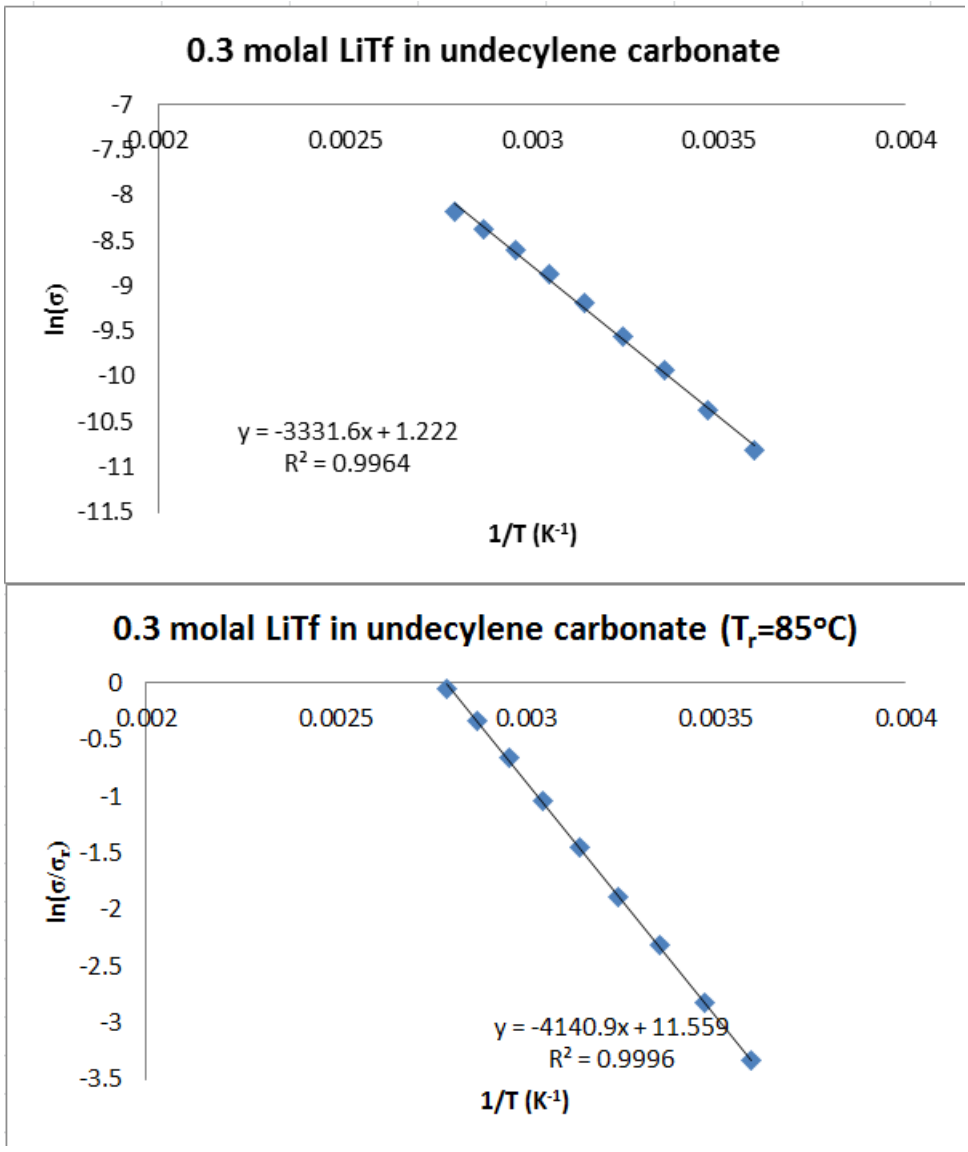

Figure 4-20 Simple Arrhenius (top) and Compensated Arrhenius (bottom) plot of conductivity against inverse temperature. The simple Arrhenius plot contains a more curved data compared to the Compensated Arrhenius plot.

Table 4-14 shows the E_a for 0.3 molal TbaTf in cyclic carbonate solutions for all cyclic carbonate analogs. From the reference curve plot, the valid reference

temperature for octylene carbonate is 5°C. The valid reference curves for decylene carbonate are 5°C to 85°C. The valid reference curves for undecylene carbonate are 55°C to 85°C. The valid reference curve for dodecylene carbonate is 85°C. Looking at the linear regression values for the plot of $\ln(\sigma/\sigma_r)$ vs (1/T) at these reference temperatures shows that all of them are at least 0.9900. The average E_a calculated for the conductivity of 0.3 molal TbaTf in cyclic carbonate solutions is calculated to be 34 ± 2 kJ/mol.

	Activation Energy, E_a (kJ/mol)			
T_r (°C)	Octylene carbonate	Decylene carbonate	Undecylene carbonate	Dodecylene carbonate
5	34.87	33.38	35.03	34.78
15	34.77	33.17	34.76	34.39
25	34.54	32.83	34.32	33.81
35	34.74	32.69	34.08	33.36
45	34.50	32.59	34.04	33.40
55	35.72	32.91	34.19	33.09
65	36.50	33.37	34.67	33.43
75	39.63	34.64	35.66	33.50
85	47.94	37.94	37.96	33.34

Table 4-14 The energy of activation, E_a for 0.3 molal TbaTf in cyclic carbonate solutions.

The values for the E_a of the ionic conductivity in 0.3 molal LiTf-cyclic carbonate solution, and in 0.3 molal TbaTf-cyclic carbonate solution are different from the trends observed previously by Petrowsky, Frech and coworkers[51, 52, 61] for other solvent families. It has been shown that for the conductivity of LiTf in primary alcohol solutions, the E_a is lower (25.8 $\pm$ 0.9 kJ/mol) than the E_a for the pure primary alcohol diffusion (36 $\pm$ 1 kJ/mol). This trend is in reverse to what is seen in this work, where the E_a goes higher, albeit a tiny increase, (34.3 $\pm$ 0.6 to 35.2 $\pm$ 0.9 kJ/mol) for LiTf solutions. In section 4.2.2, it was suggested that the activation energy for pure cyclic

carbonates is very high because of some non-specific interaction that involves the dipole moment of the cyclic carbonate molecules. The result for the LiTf ionic conductivity value partly supports the idea. In the primary alcohol solution it is well known that hydrogen bonding exists[93]. The reason that the E_a is lower for the conductivity could have been because the hydrogen bonding network is broken by Li-cation coordination to the 1-alcohol oxygen. As such, the E_a for the ionic conductivity is lower than the E_a for pure 1-alcohol diffusion. In the case of cyclic carbonate, there is no specific interaction like in 1-alcohol. Thus, there is almost no change in the value of E_a for Li-cation conductivity.

For the conductivity of TbaTf in primary alcohol solutions, the E_a goes higher (43.3 $\pm$ 0.8 kJ/mol). This trend is also different from the trend seen in this work. In this work, the E_a for 0.3 molal TbaTf in cyclic carbonate solutions essentially remains the same (34 $\pm$ 2 kJ/mol). In another study by Petrowsky, Frech and coworkers[62], the E_a for the conductivity of 0.0055M TbaTf in acyclic acetates shows that the E_a for the conductivity goes really high from 25.5 $\pm$ 0.3 kJ/mol for pure acyclic acetate to 36.5 $\pm$ 0.8 kJ/mol for TbaTf solutions. Yet in another study involving ketones[61], the E_a for the conductivity of 0.0055M TbaTf in acyclic ketones is only around 24.1 $\pm$ 0.8 kJ/mol, which is essentially the same as the E_a for the pure acyclic ketones (23.9 $\pm$ 0.8 kJ/mol). The three solvent families are very similar structurally, in that all three contains a carbonyl group. Of the three species, cyclic carbonates have the highest dielectric constant values (~64 for propylene carbonate at room temperature), followed by acyclic ketones (~22 for acetone), and finally acyclic acetates (~7 for methyl acetates). For

unknown reasons, low dielectric solvents and solvents with hydrogen bonding networks increase the E_a for TbaTf ionic conductivity.

A master curve can be generated in each case, showing that CAF is applicable to analyze charge transport in cyclic carbonates (Figure 4-21 and 4-22).

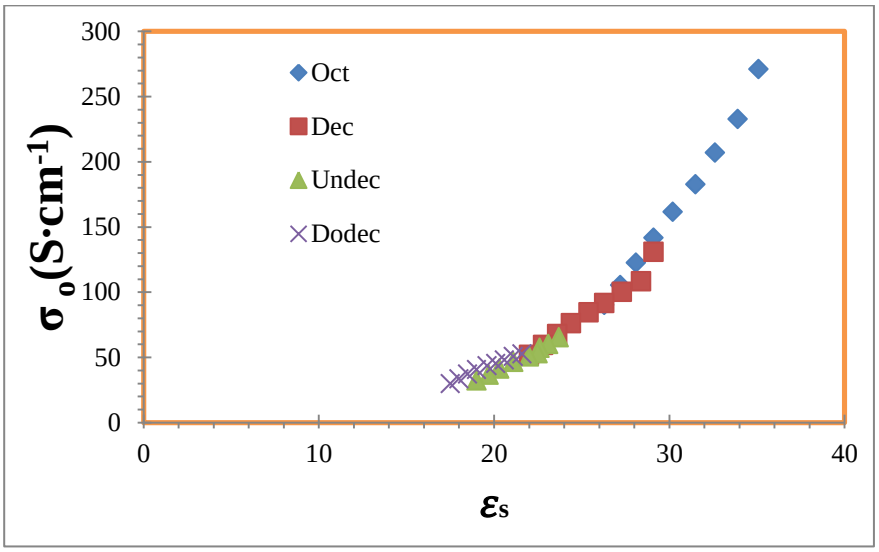

Figure 4-21 Master curve from LiTf Conductivity Data.

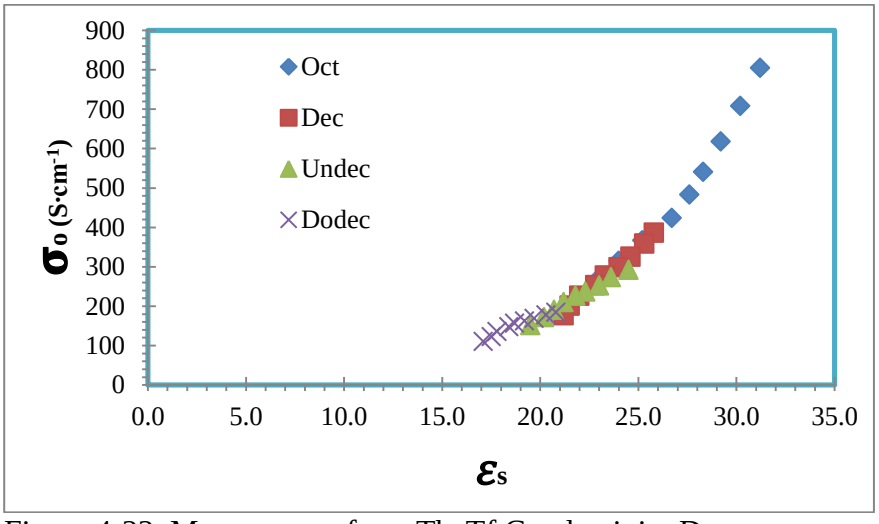

Figure 4-22 Master curve from TbaTf Conductivity Data.

4.3 Conclusions

Using dielectric constant values and the diffusion coefficient values of pure cyclic carbonates, it is shown in this work that cyclic carbonates can be analyzed using the CAF method. Similar analysis using ionic conductivity values of LiTf in cyclic carbonate solutions, and separately TbaTf in cyclic carbonate solutions shows that ion transport in cyclic carbonates can also be analyzed using the CAF.

The calculated E_a value for self-diffusion is higher than the other aprotic solvents investigated previously. Aside from 1-alcohols, which is a family of polar protic solvents and thus have hydrogen bonding to account for, cyclic carbonates are the first polar aprotic solvents analyzed with the CAF that have activation energy this high. This breaks the trends observed with the other polar aprotic solvents where the E_a's for self-diffusion lie between 20 kJ/mol and 25 kJ/mol.

The calculated E_a for the conductivity of 0.3 molal TbaTf in cyclic carbonates solution is higher compared to 2-ketones (24.1 ± 0.8 kJ/mol)[61] and nitriles (28 ± 2kJ/mol as shown in Chapter 2). This explains the lower conductivity value for 0.0055M TbaTf in propylene carbonate compared to acetone and acetonitrile as shown in figure 4-2. From the figure, it is expected that the lower conductivity value for DMSO is also because of the higher E_a in the DMSO electrolyte solution.

4.4 Detail Synthesis, Sample Preparations, and Measurements

4.4.1 Detail Synthesis

The cyclic carbonates used in this work were synthesized in house. The ^{1}H NMR spectra were obtained using a Varian Mercury-300 NMR spectrometer. The IR spectra were obtained using Shimadzu IRAffinity-1 using dry KBr.

All chemicals for the synthesis work were obtained from Sigma-Aldrich or TCI America and are used as is. The synthesis of the octylene, decylene, and dodecylene carbonates resulted from the following procedure: A round bottom flask was charged with 1 equivalent of the desired 1,2-diols. 6 equivalents of methyl chloroformate were added to the flask. A reflux condenser was attached to the flask. The mixture was then heated with stirring (magnetic) to approximately 60 ^{0} C until the formation of the cyclic carbonate was completed (1 to 2 weeks). The reaction was monitored using NMR spectroscopy. After the reaction was completed, the reaction flask was cooled to room temperature. The excess methyl chloroformate was taken off under vacuum with a rotator evaporator. The final liquid product was then filtered through a column packed with 50% acid alumina (bottom layer) and 50% of neutral alumina (top layer) and eluted with diethyl ether. The ^{1}H NMR spectra showed purity of the products of at least 93%. IR spectra showed comparable peaks to commercial propylene carbonate spectrum; only trace hydroxyl peak was visible.

The synthesis of undecylene carbonate was as follows: First, the 1,2-undecane diol was synthesized using the procedures described by Sudalai and coworkers[87]. In short, 56.25 g of 1-undecene (365 mmol), 23.42 g of sodium periodate (110 mmol, ~30 mol %), 6.333 g of lithium bromide (73 mmol, ~20 mol %), and 240 mL (4,000 mmol) of glacial acetic acid were added to a 1,000 mL round bottom flask. A reflux condenser was attached to the flask. The flask was heated to 95 ^{0} C with stirring (magnetic) for 5 days. After 5 days, the flask was allowed to cool to room temperature. The 1,2-dicarboxylated undecane product was extracted with ethyl acetate three times. The organic layer was then washed with sodium thiosulfate solution, water, and aqueous

sodium bicarbonate, and dried overnight with sodium sulfate. The next day, the solution was filtered through celite. Ethyl acetate was evaporated under vacuum. 75.587 g of potassium carbonate (1.5 equivalents) and 100 mL methanol were added to the product. The solution was heated for 24 hours with stirring (magnetic). The final product was extracted with dichloromethane solution, and run through a neutral alumina packed column using dichloromethane as eluent. The solvent was removed under reduced pressure. The yield was 60%. The 1,2-undecane diol was not purified further.

The resulting diol was charged into a 500 mL round bottom flask. Eight equivalents of methyl chloroformate were then added to the diol. A reflux condenser was attached to the flask. The mixture was then heated with stirring (magnetic) to approximately 60°C until the formation of the cyclic carbonate was completed (1 to 2 weeks). The reaction was monitored using NMR spectroscopy. After the reaction was completed, the reaction flask was cooled to room temperature. The excess methyl chloroformate was taken off under vacuum using a rotator evaporator. The final product was distilled under high vacuum (1 mmHg, 140°C). The final yield was 33%. ^{1}H NMR spectrum showed >97% purity. The IR spectrum showed comparable peaks to commercial propylene carbonate spectrum; only trace hydroxyl peak was visible.

^{1}H NMR (300MHz, $CDCl_3$):

1,2-undecane diol[94]: 1H NMR (300 MHz, $CDCl_3$): δ 0.87 (t, 3H, *J* = 6.7); 1.14-1.55 (m, 14H); 2.94 (s, 2H); 3.41 (t, 1H, *J* = 9.4 Hz); 3.59-3.73 (m, 2H)

Octylene carbonate[78]: 72% yield; ^{1}H NMR (300 MHz, $CDCl_3$): δ 0.88 (t, 3H, *J* = 6.7 Hz); 1.15-1.54 (m, 8H); 1.60-1.86 (m, 2H); 4.06 (t, 1H, *J* = 7.6 Hz); 4.52 (t, 1H, *J* = 8.2 Hz); 4.64-4.74 (m, 1H)

Decylene carbonate[79]: 78% yield; ^{1}H NMR (300 MHz, $CDCl_3$): δ 0.87 (t, 3H, J = 6.5 Hz); 1.15-1.54 (m, 12H); 1.60-1.86 (m, 2H); 4.06 (t, 1H, J = 7.6 Hz); 4.51 (t, 1H, J = 7.9 Hz); 4.64-4.74 (m, 1H)

Undecylene carbonate: ^{1}H NMR (300MHz, $CDCl_3$): δ 0.87 (t, 3H, J = 6.5 Hz); 1.15-1.54 (m, 14H); 1.60-1.86 (m, 2H); 4.05 (t, 1H, J = 7.6 Hz); 4.51 (t, 1H, J = 8.2 Hz); 4.64-4.74 (m, 1H); IR: $\nu_{C\text{-}H}$: 2928,2857; $\nu_{C=O}$: 1807; $\nu_{C\text{-}O}$: 1169,1065 cm^{-1}.

Dodecylene carbonate[80]: 68% yield; ^{1}H NMR (300 MHz, $CDCl_3$): δ 0.86 (t, 3H, J = 6.7 Hz); 1.15-1.54 (m, 16H); 1.60-1.86 (m, 2H); 4.05 (t, 1H, J = 7.6 Hz); 4.51 (t, 1H, J = 8.2 Hz); 4.64-4.74 (m, 1H)

4.4.2 Sample Preparations

All glassware and components were cleaned with soap and water before being rinsed with distilled water. They were dried overnight in an oven before use. All cyclic carbonates synthesized were stored in a dry glove box with water level less than 10 ppm under a nitrogen atmosphere. TbaTf and LiTf salts were obtained from Sigma-Aldrich and were used as is. All solutions were made in the same dry glove box. The 0.30 molal TbaTf-cyclic carbonate solutions are prepared by weighing the appropriate amount of cyclic carbonates into a glass jar, on a balance inside the dry glove box. The needed amount of TbaTf/LiTf was then added to the jar. A stir bar was inserted into the jar, and the jar was capped. The solutions were stirred overnight inside the glove box.

To prepare the sample for impedance analyzer, inside the glove box, the sample is inserted into an Agilent 16452A liquid holder using a clean dry syringe or pipette.

To prepare the sample for NMR PFG measurements, inside the glove box, the solution of interest was inserted into a 5 mm-outer diameter NMR tube. The amount

inserted was such that the height of the solution in the NMR tube was about 8 to 9 mm. The NMR tube was capped, and a small piece of parafilm was used to wrap the cap twice.

4.4.3 Measurements

There were four types of data collected. The dielectric constant and the conductivity data were collected using an impedance analyzer. The diffusion coefficient values are collected using the nuclear magnetic resonance (NMR) pulsed-field gradient (PFG) method. Density measurements were made using an Anton-Paar DMA 4500M density meter, fitted with an internal temperature control unit.

For the dielectric constant and conductivity measurements, an HP 4192 impedance analyzer with a Huber ministat 125 bath were used. The ministat was used to control the temperature. The impedance analyzer was first calibrated to eliminate any impedance from the instruments. This is done by measuring the impedance value of the instrument at 10 MHz while the whole circuit including the liquid sample holder is connected to the impedance analyzer. The instrument impedance value is stored and subtracted automatically by the impedance analyzer when actual data collection is performed. The measurements are made by inserting the liquid sample holder into an oil bath that has its temperature regulated by the ministat mentioned above. The impedance analyzer is set to sweep the circuit at frequencies from 1 kHz to 13 MHz. The impedance analyzer averages the conductance (G), capacitance (C), and the phase angle (θ). The conductivity, σ was calculated using the equation $\sigma = L \times G \times A^{-1}$ with L equals to the electrode gap of the liquid sample holder, G is the average conductance of the solution, and A is the surface area of the electrode. The static dielectric constant, ε_s

was calculated using the equation $\varepsilon_s = \alpha \; x \; C \; x \; C_o^{-1}$ where α is the stray capacitance variable calculated automatically by the impedance analyzer, *C* is the average capacitance of the solution, and C_o is the atmospheric capacitance.

The NMR PFG sample measurements were made using a Varian NMR-400 system fitted with Auto-X-Dual broadband probe. The temperature was controlled using a FTS XR401 air-jet regulator. Each sample was allowed to equilibrate at the desired temperature for 10 minutes. The probe was then adjusted to the specific frequency needed. This frequency depends on the nuclei of interest and on the instrument. The value was provided by the NMR administrator. The best signal was arrived at by determining the pulse at 90 degree period. The frequency determined was set, and an array was setup. The gradient strength, relaxation delay, and cycle delay was adjusted as desired. The measurement was started and collected using Varian VNMR software. The signal produced at each gradient strength was integrated to produce the relative intensity values. The natural log of the resulting intensity values was plotted against the gradient strength to give a slope. This slope provides a means to get the value of the diffusion coefficient, *D* through the equation

$$\ln(I) = -(\gamma^2\delta^2(\Delta-(\gamma/3)D)\, g^2$$

Here, *I* is the intensity of the signal determined from NMR, γ is the gyromagnetic ratio, δ is the time of the pulsed gradient, Δ is the relaxation delay, and *g* is the gradient strength. The slope then equals the terms "$-(\gamma^2\delta^2(\Delta-(\gamma/3)D)$" and the diffusion coefficient *D* is solved from the slope.

The density measurement was performed by adding about ~1mL of the sample into the sample holder. The temperature was adjusted to the appropriate value, and the

sample was equilibrated at the desired temperature for 10 minutes before measurement was made. The after approximately 1 minute, the instrument displays the density value.

Chapter 5 : Synthesis and Application of Compensated Arrhenius Formulation (CAF) to Oligomers of Poly(ethylene Oxide)

5.1 Introduction

For years, scientists have been trying to understand transport properties in polymers. While significant advancements have been made that allow for crude approximations, the gold mine of the knowledge, the structure and transport property relationship in polymers, is still not understood. The lack of understanding of the relationship linking the structure to transport properties of polymers has impeded further advancement in battery technologies and advanced polymeric materials. For these technologies to advance further, the transport properties of polymers, and of species in polymers need to be better understood.

It has been shown that viscosity plays an important role in the properties of polymers, including transport properties[65]. It is also thought that the transport of small molecules in polymers, for example ions, is also controlled by the viscosities of polymers[95, 96]. However, while it is well known that viscosity is related to the velocity gradient in bulk polymers, this knowledge provides no relationship what-so-ever to the molecular structure of the polymers. Thus, the structural factors that control transport in these polymers are still not known.

As discussed in chapter 1, viscosity has also been used to understand transport properties in liquids. However, because of the lack of insight into the relation between viscosity and molecular structure, the effort has been fruitless. The Compensated Arrhenius Formulation, as developed by Petrowsky, Frech and coworkers, appears to

provide a better route to relate transport properties to molecular structure[34, 49, 51-54, 61, 62, 66, 67].

Since the introduction of the CAF method, Petrowsky, Frech and coworkers have shown the CAF's applicability to many polar liquid electrolytes[34, 51, 52, 54, 61, 62, 66, 67]. The CAF has been used to uncover important mass transport properties in these liquids such as self-diffusion and ionic conductivity. However, all studies involving the CAF so far were application to non-polymeric species that are liquids. Since polymers behave like regular liquids, albeit with complex properties, as long as their temperatures are above their glass transition temperatures, it is possible that the CAF can also be applied to study transport properties in polymers. In essence, applying the CAF will allow the calculation of the energy of activation, E_a.

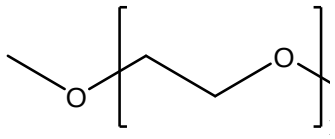

Figure 5-1 Poly(ethylene oxide).

Polyethylene oxide (PEO) (Figure 5-1) is the most widely studied polymer for application as solid battery electrolyte[64, 97, 98]. Copious amounts of data have been collected for PEO[99-106]. However, to this day, there is no conclusion as to how a polymer should be modified so that it will provide the properties needed for battery electrolyte applications.

Oligomers are shorter chain polymers. Oligomers should, in theory, have properties similar to the parent polymers. In certain cases, it is easier to work with oligomers because of the ability to control the exact number of repeat units in oligomers.

5.1.1 Project Goals

This project was collaborative with the group of Professor R. Frech at the University of Oklahoma. Synthesis of the glyme derivatives was developed and carried out as described here. The dielectric constant, conductivity, and self-diffusion measurements were performed by Dr. M. Petrowsky.

In this project, the goal is to determine the applicability of the CAF to polymers by applying the CAF to poly(ethylene oxide). However, as shown in chapter 2, to apply the CAF, the dielectric constant of the liquids needs to be altered by varying the temperature or by varying the molecular volume of the polymer molecules. The molecular volume is varied by tethering alkyl chains to the polymer molecules. The change in dielectric constant as the ratio of the polymer repeat units to the alkyl chain length is increased, is expected to be small. While it has been shown with the acyclic carbonate that the CAF is applicable even when the dielectric constant values change less than 0.01, the difference in dielectric constant as one polymer repeat unit is added to a thousand polymer repeat unit might be too small for the measurement to be of any use for the CAF analysis.

Additionally, it is expected that high molecular weight poly(ethylene oxide) will be solids at room temperature. Because of this, to apply the CAF for poly(ethylene oxide), the temperature range will have to be altered. Lack of an appropriate apparatus to alter the temperature range, coupled with lack of experience in dealing with the CAF at higher temperature, makes the measurements on poly(ethylene oxide) impossible at present. Furthermore, it is difficult to control the number of repeat units of polymer

molecules in an exact way as there is no known method to determine the molecular weight of a single polymer molecule.

To overcome these difficulty, instead of applying the CAF to poly(ethylene oxide), the CAF is applied to the oligomers of poly(ethylene oxide). Three oligomers of poly(ethylene oxide), monoglyme, diglyme, and triglyme are used in this study. The values of the dielectric constant and self-diffusion coefficient of the pure oligomers will be measured as well as the conductivity of their electrolyte solutions. From these data, the energy of activation, E_a for self-diffusion of pure oligomers and the E_a of the ionic conductivity in these oligomers will be calculated. The effect of repeat units in each molecule on the behavior of dielectric constant, self-diffusion, ionic conductivity, and E_a's will be investigated, and attempts to relate these properties to the parent poly(ethylene oxide) will be made.

5.2 Results and Discussion

5.2.1 Synthesis of Poly(ethylene oxide) Oligomers

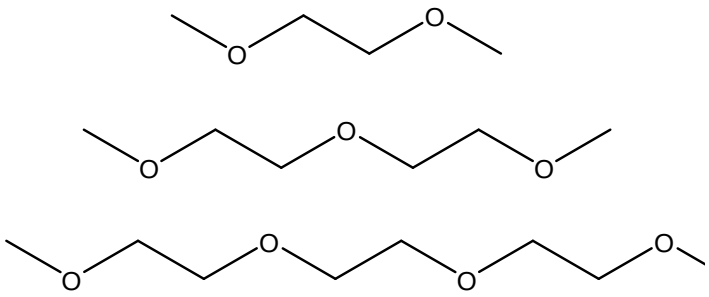

Figure 5-2 From top to bottom: monoglyme, diglyme, triglyme.

In this experiment, three different oligomers of PEO are used, the monoglyme, the diglyme, and the triglyme (Figure 5-2). Each of these oligomers is modified to create four analogs of each, the hexyl-, octyl-, nonyl-, and decyl-oligomers (Figure 5-3).

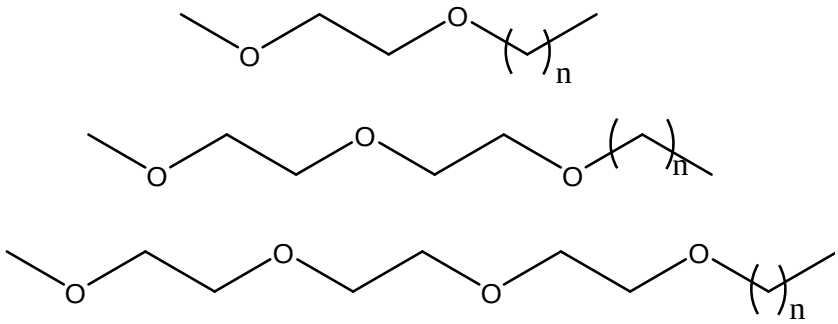

where n=5,7,8,9

Figure 5-3 From top to bottom: monoglyme-, diglyme-, and triglyme-derivatives.

Poly(ethylene oxide) is usually synthesized using a ring opening reaction of epoxide[107, 108] (figure 5-4). To apply this method to the alkyl monoglyme desired for this project, methanol can be employed as the nucleophile, while the hexyl-, octyl-, nonyl-, and decylbromide can be employed as the capping group (figure 5-5).

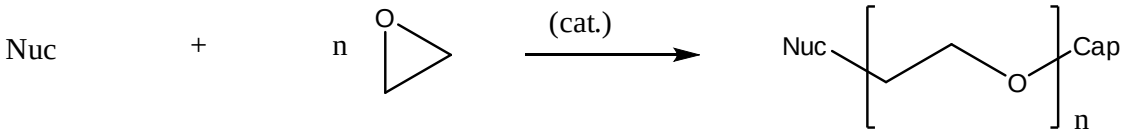

Nuc = nucleophile
Cap = capping group

Figure 5-4 Reaction scheme for ring opening polymerization of poly(ethylene oxide).

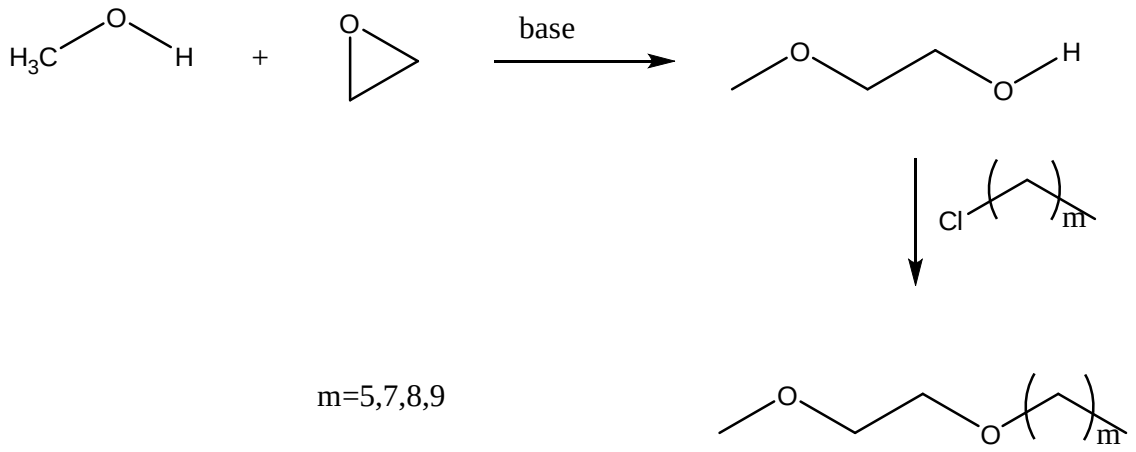

Figure 5-5 Applying the ring opening reaction of epoxide to the synthesis of alkyl monoglyme.

However, the reaction sequence requires at least two steps. Furthermore, the reaction to obtain the intermediate product for diglyme and triglyme synthesis will have to be controlled such that only the two and three repeat unit intermediate are produced. Since for the project only the mono-, di-, and tri-repeat units are desired, it only makes sense to start the reaction with the commercially available mono-, di-, and triethylene glycol monomethyl ether (figure 5-6), essentially only performing the second part of the reaction sequence as in figure 5-5.

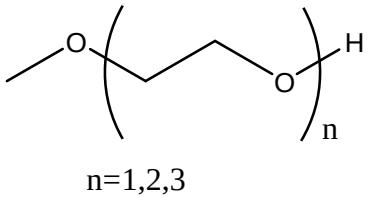

Figure 5-6 Commercially available ethylene glycol monomethyl ether derivatives.

Thus, the pertinent reaction is the substitution reaction of the alkoxy group (from the hydroxyl derivative) with an alkyl halide to obtain the desired alkylated mono-, di-, and triglyme analogs. The remaining challenge is to attach the two moieties

together to form the desired products in such a way that the desired products are easily separable from the unwanted side products of the reaction. One method to attach the two moieties together is to perform the second order nucleophilic substitution reaction (S_N2)[109] (figure 5-7). In this reaction, the hydroxyl group on the ethylene glycol monomethyl ether unit is first transformed into a sodium alkoxide group. The alkoxide group is then reacted with an alkyl halide group to form the desired alkylated glyme products.

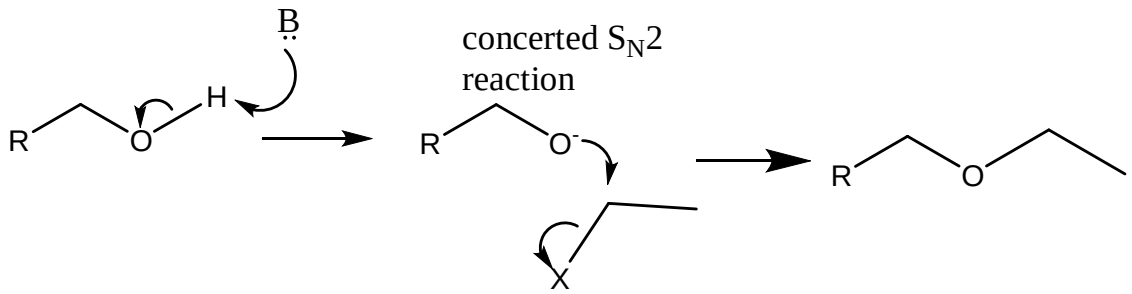

R = any atom

B = base

X = leaving group

Figure 5-7 An example of the S_N2 reaction.

The method to form the alkoxide species is very important. Typical methods of using a base to form the alkoxide may cause two unwanted side products in the reaction, the protonated base as well as the halide species. On the other hand, it is well known that a single electron transfer from an alkali metal group such as lithium metal or sodium metal to a hydrogen atom on a hydroxy group can produce a metal alkoxide species, as well as liberate hydrogen gas (figure 5-8). This will eliminate one unwanted side product from the reaction, and leave only the metal halide species to be separated from the product.

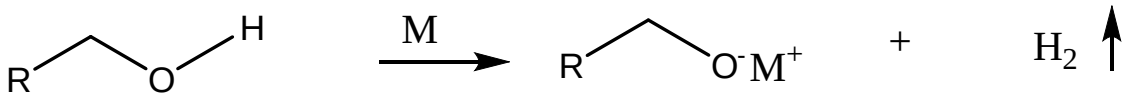

M = alkali metal (Li, Na, K)

R = any atom

Figure 5-8 Reaction of a hydroxyl group with alkali metal to produce an alkoxide metal species as well as liberate hydrogen gas.

A representative reaction scheme for the synthesis of monoglyme derivatives is shown below (figure 5-9). The metal halide side product is expected to be water soluble, while the resultant alkylated product was expected not to be very soluble in water, and thus the metal halide side product can be washed off with water.

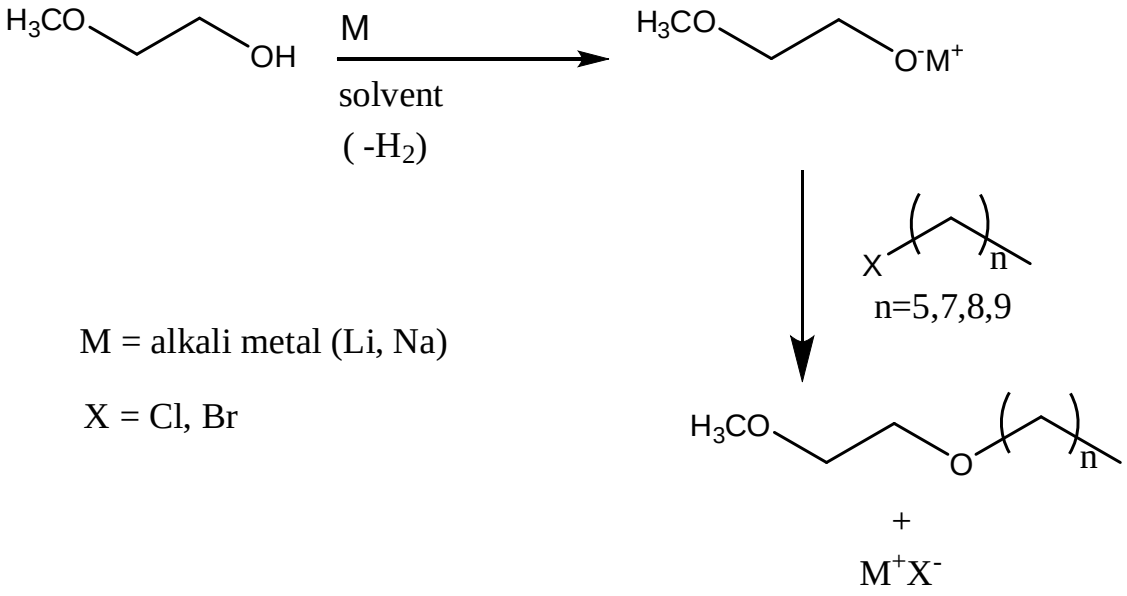

Figure 5-9 The reaction scheme for making alkyl glyme series.

The synthesis was started by optimizing the reaction to form the alkoxide intermediate. The first alkali metal used was lithium metal. However, the reaction with lithium metal was slow because lithium metal is less reactive compared to other alkali

metals like sodium or potassium. Because of this, the lithium metal would not dissolve completely, even after 7 days of reaction, with or without solvent. Adding 2 equivalent of the glycol used did not help the lithium metal to dissolve.

Switching the lithium with sodium makes the reaction a little faster. The reaction without solvent would stop before all of the sodium metal would dissolve. Adding approximately 150 mL of solvent allows all the sodium metal to dissolve after 7 days. To accelerate the reaction, 5 equivalent of the glycol was used. The sodium dissolved after a maximum of 72 hours. A summary of the optimum condition for the reaction to form the alkoxide intermediate is presented in table 5-1.

Alkaline metal	**Glycol**	**Solvent**	**Reaction time (hours)**	**Description**
1 eq Li	1 eq	-	> 168	Not all lithium dissolved
1 eq Li	2 eq	-	> 168	Not all lithium dissolved
1.2 eq Li	2 eq	150 mL diethyl ether	> 168	Not all lithium dissolved
1.2 eq Li	2 eq	150 mL diethyl ether	> 168	Not all lithium dissolved
1.2 eq Na	2 eq	-	> 72	Not all sodium dissolved
1.2 eq Na	2 eq	150 mL acetonitrile	> 72	All sodium dissolved, solution turns to yellow
1.2 eq Na	2 eq	150 mL diethyl ether	> 72	All sodium dissolved
1.5 eq Na	5 eq	150 mL diethyl ether	< 72	All sodium dissolved
2.0 eq Na	5 eq	150 mL diethyl ether	< 72	All sodium dissolved

Table 5-1 Optimum conditions for the reaction to form the intermediate alkoxide.

After the reaction to form the intermediate alkoxide species was optimized, the next step was the substitution reaction with the alkyl halide. It is well known that the S_N2 reaction competes with the second order elimination reaction (E2)[109] (figure 5-10).

In the elimination reaction, instead of substituting the halide, the alkoxide will react as a base, abstracting a nearby proton from the alkyl halide to form terminal alkenes and primary alcohols. Among the reaction conditions that favor the E2 reaction are elevated temperatures, bulky nucleophiles/bases, and poor leaving groups.

Since the alkoxide is a desired feature of the product, and is not bulky, its use should favor the S_N2 reaction. The reaction S_N2 reaction can be exothermic. The chloride functional group on an alkyl chloride is a good leaving group. However, it can be a slower leaving group compared to a bromide or an iodide functional group. Because of its availability and lower costs, the alkyl bromide was used in the reaction.

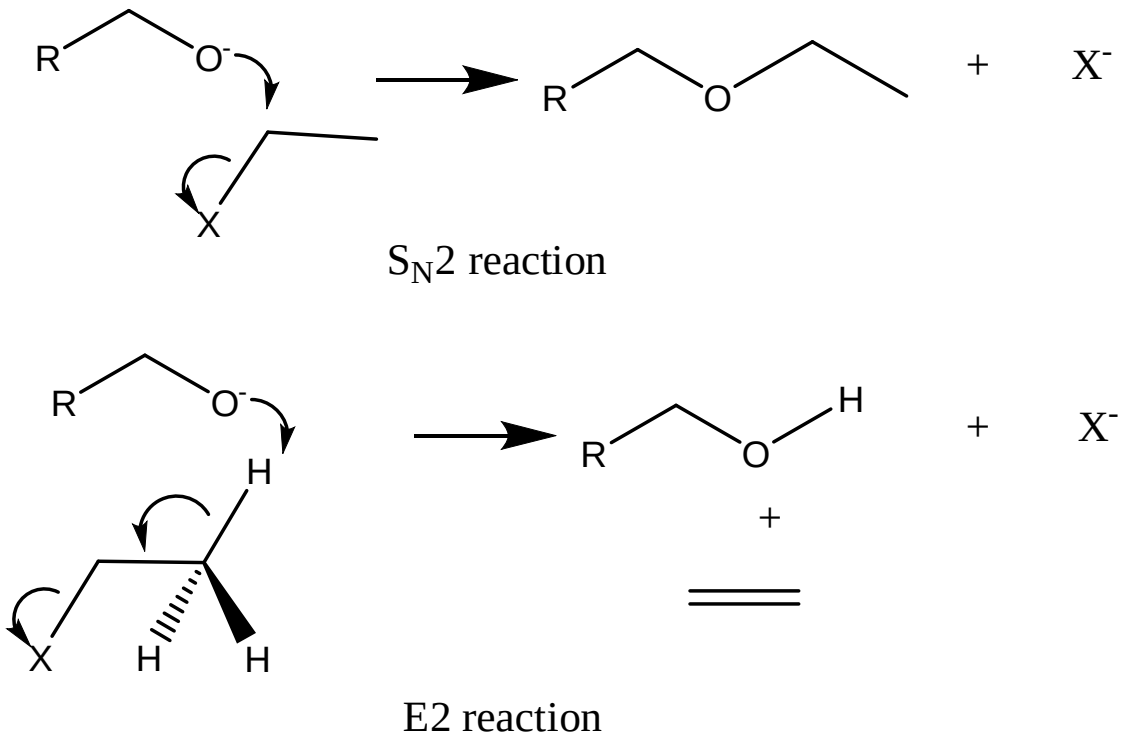

Figure 5-10 The scheme for S_N2 and E2 reaction.

Using 1 to 1.2 equivalent of the alkoxide relative to the alkyl bromide produces the desired product with noticeable amount of alkyl bromide as shown by ^{1}H-NMR spectroscopy. The remaining unreacted alkyl bromide is hard to separate from the

desired product because of its similar polarity as well as similar boiling point to the product formed. On the other hand, while the E2 product was not wanted, removing this product was easier than the unreacted alkyl bormide starting reagent. In order to ensure that all of the alkyl bromide is reacted, the amount of alkoxide was increased to 1.5 to 2.0 equivalent. On top of that, the reaction flask is heated for up to 80^{o}C for 24 hours. With this amount of alkoxide to alkyl bormide ratio used, there is no unreacted alkyl bromide left as confirmed by ^{1}H-NMR spectroscopy. A summary of the optimum conditions is presented in table 5-2. The unwanted alkene side product was removed under reduced pressure. A more detailed description of the synthesis work, as well as solution preparation is presented in section 5.4 below.

Alkoxide	Alkyl halide	Reaction time (hours)	Unreacted alkyl halide
1.2 eq	1 eq alkyl bromide	24	significant
1.5 eq	1 eq alkyl bromide	24	none
2.0 eq	1 eq alkyl bromide	24	none

Table 5-2 The optimum conditions for the synthesis of the glyme series.

5.2.2 Dielectric Constant and Diffusion of Pure Oligoethers

Table 5-3 shows the data for the pure monoglyme, diglyme, and triglyme family. Figure 5-11 shows the plot of dielectric constant versus temperature for these glyme families.

	Hexyl monoglyme		Octyl monoglyme		Nonyl monoglyme		Decyl monoglyme	
T_r (^oC)	ε_s	D (m^2/s) ($x10^{-10}$)	ε_s	D (m^2/s) ($x10^{-10}$)	ε_s	D (m^2/s) ($x10^{-10}$)	ε_s	D (m^2/s) ($x10^{-10}$)
5	4.40	5.83	3.96	3.78	3.83	2.97	3.65	2.43
15	4.28	7.32	3.87	5.02	3.74	3.87	3.57	3.21
25	4.17	9.18	3.77	6.36	3.66	4.91	3.50	4.13
35	4.05	10.9	3.69	7.86	3.58	6.02	3.43	5.16
45	3.92	13.1	3.59	9.46	3.49	7.36	3.35	6.22
55	3.80	15.8	3.50	11.5	3.40	8.75	3.27	7.53
65	3.70	18.7	3.41	13.9	3.33	1.05	3.20	9.04
75	3.59	22.2	3.34	16.3	3.25	12.2	3.14	10.6
85	3.50	26.1	3.25	19.7	3.18	14.7	3.07	12.6
	Hexyl diglyme		Octyl diglyme		Nonyl diglyme		Decyl diglyme	
T_r (^oC)	ε_s	D (m^2/s) ($x10^{-10}$)	ε_s	D (m^2/s) ($x10^{-10}$)	ε_s	D (m^2/s) ($x10^{-10}$)	ε_s	D (m^2/s) ($x10^{-10}$)
5	4.94	2.77	4.54	1.92	4.32	1.56	4.14	1.36
15	4.82	3.76	4.44	2.69	4.23	2.11	4.06	1.87
25	4.70	4.81	4.34	3.52	4.14	2.80	3.98	2.48
35	4.57	6.05	4.23	4.47	4.04	3.61	3.88	3.20
45	4.43	7.28	4.11	5.50	3.94	4.43	3.79	3.90
55	4.30	8.85	4.00	6.73	3.84	5.43	3.69	4.86
65	4.18	10.7	3.90	8.22	3.74	6.61	3.61	5.92
75	4.06	12.7	3.80	9.67	3.66	7.75	3.53	7.01
85	3.94	15.3	3.70	11.8	3.57	9.56	3.45	8.44
	Hexyl triglyme		Octyl triglyme		Nonyl triglyme		Decyl triglyme	
T_r (^oC)	ε_s	D (m^2/s) ($x10^{-10}$)	ε_s	D (m^2/s) ($x10^{-10}$)	ε_s	D (m^2/s) ($x10^{-10}$)	ε_s	D (m^2/s) ($x10^{-10}$)
5	5.35	1.77	4.94	1.19	4.78	0.977	4.59	0.883
15	5.23	2.44	4.83	1.70	4.68	1.43	4.49	1.30
25	5.09	3.16	4.71	2.29	4.58	1.94	4.40	1.77
35	4.95	4.02	4.59	2.99	4.46	2.58	4.29	2.34
45	4.79	4.88	4.46	3.71	4.34	3.24	4.18	2.95
55	4.65	5.93	4.33	4.48	4.22	4.06	4.07	3.70
65	4.50	7.31	4.22	5.64	4.11	4.97	3.97	4.58
75	4.38	8.42	4.10	6.65	4.01	5.89	3.87	5.42
85	4.25	9.99	4.00	7.90	3.91	7.12	3.78	6.52

Table 5-3 Dielectric constant and self-diffusion coefficient for monoglyme analogs, diglyme analogs, and triglyme analogs. ε_s = dielectric constant, D = self-diffusion coefficient.

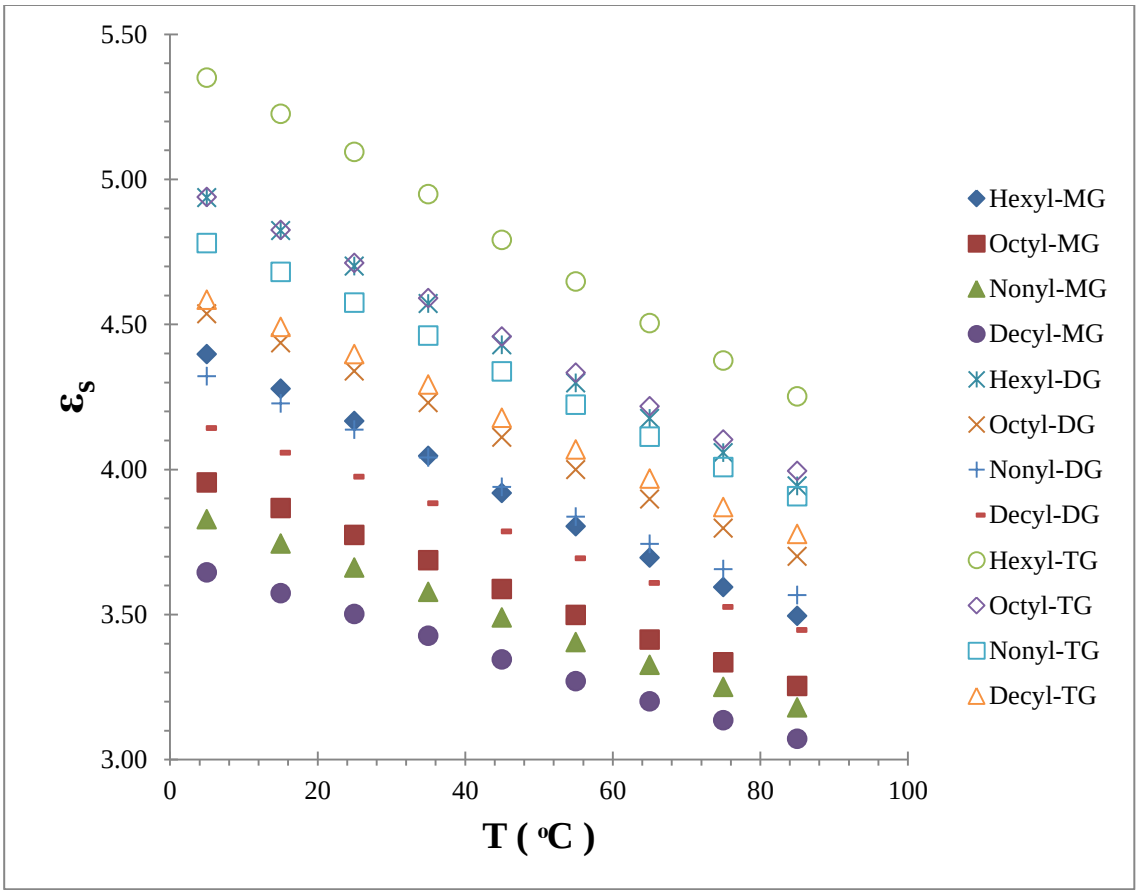

Figure 5-11 Plot of dielectric constant for all the glyme series versus temperature (MG=monoglyme, DG=diglyme, TG=triglyme).

As discussed in chapter 1, the dielectric constant is affected by variations in molecular volume and in temperature. The increase in molecular volume in turn increases the bulk volume. The increase in bulk volume lowers the value of the dipole density and subsequently lowers the value of dielectric constant. Thus, the higher the molecular volume, the lower dielectric constant becomes. Since dielectric constant is also affected by temperature, the higher the temperature, the lower the value of dielectric constant measured. The dielectric constant values of these glyme derivatives range from 3.07 (decyl monoglyme, 85°C) to 5.35 (hexyl triglyme, 5°C). These values

are reasonable since the room temperature dielectric constant of monoglyme with only two methyl groups attached is ~7.20[110].

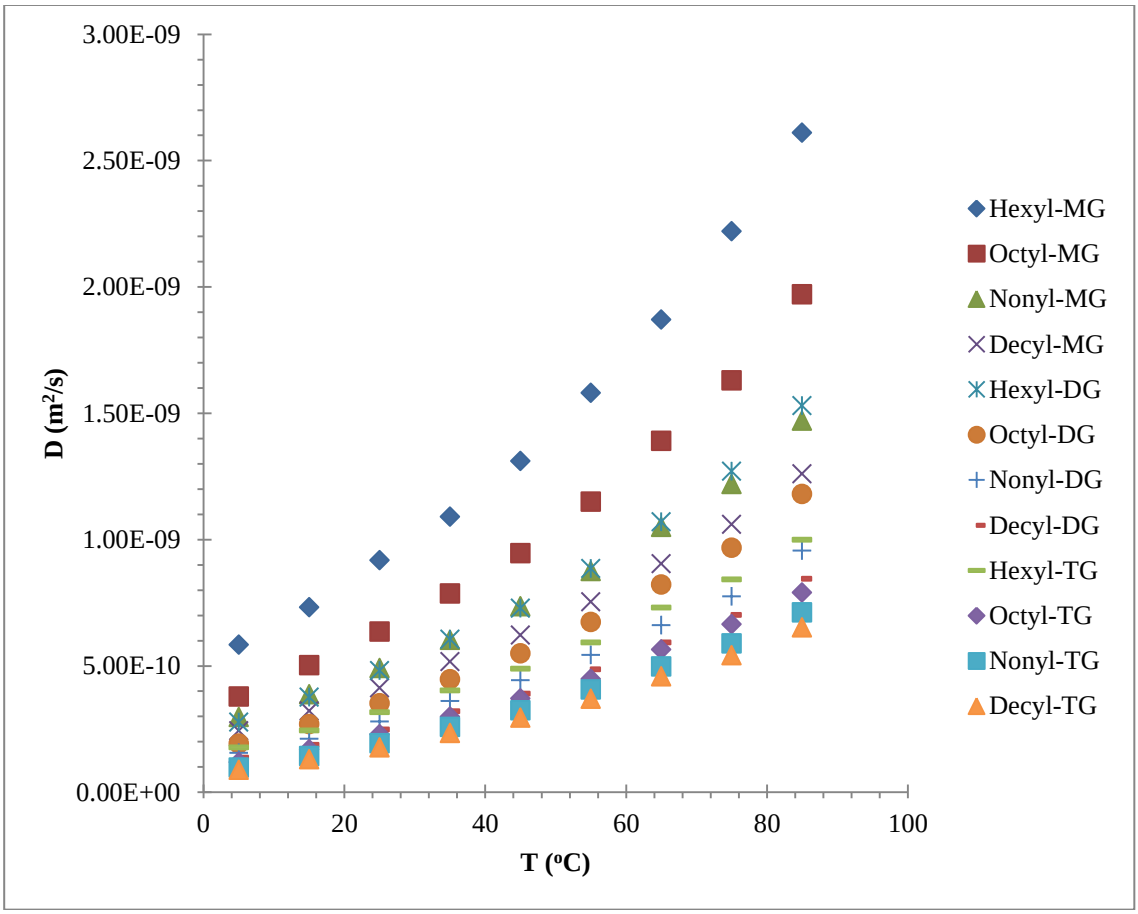

Figure 5-12 Plot of self-diffusion coefficient, D versus temperature, T for all analogs of monoglyme, diglyme, triglyme (MG=monoglyme, DG=diglyme, TG=triglyme).

Figure 5-12 shows the self-diffusion coefficient versus temperature for all glyme species. The diffusion coefficients for all the glyme series increase as the temperature is increased. The dependence of diffusion coefficient on temperature is in the Boltzmann term and in the dielectric constant in the pre-factor. While the decrease in dielectric constant as the temperature is increased should bring the diffusion coefficient values down, the increase in temperature lowers the Boltzmann term even more, causing the net diffusion coefficient to increase.

Across different glyme repeat units, at each temperature point, the dielectric constant increases going from hexyl monoglyme to hexyl diglyme to hexyl triglyme (Figure 5-13). A similar trend is exhibited by the other three alkyl derivatives. Going into the project, the effect of increasing the number of repeat units on the values of dielectric constant was not known. But it can be rationalized that since the dielectric constant is dependent on the dipole moment, the various orientations of the triglyme and diglyme functional units create higher dipole moments compared to monoglyme repeat units. The increase in dipole moment must have been bigger than the increase in volume as the number of repeat units is increased.

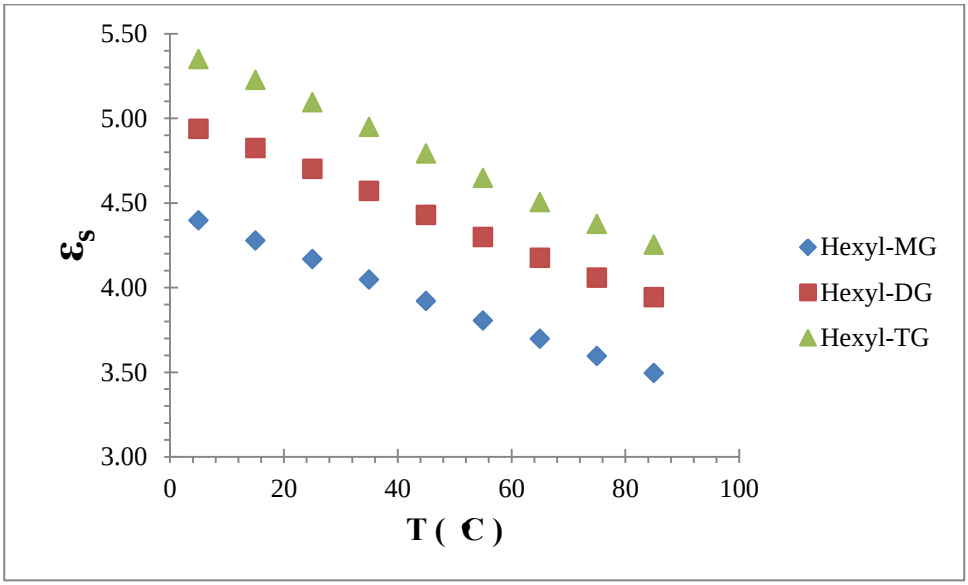

Figure 5-13 Dielectric constant versus temperature for hexyl glyme series (MG=monoglyme, DG=diglyme, TG=triglyme).

Across different repeat units, increasing the number of repeat units from one to two to three decreases the diffusion coefficient (figure 5-14). It is convenient to rationalize that the bigger size of triglyme and diglyme as the reason why their diffusion coefficient values are smaller compared to that of monoglyme. However, recall that from equation 2-6 the diffusion coefficient is dependent on the dielectric constant and

the activation energy. Thus, since the dielectric constants of the triglyme and diglyme series are higher than the monoglyme series, the lower diffusion coefficient values have to be because of higher activation energy for the triglyme and diglyme species.

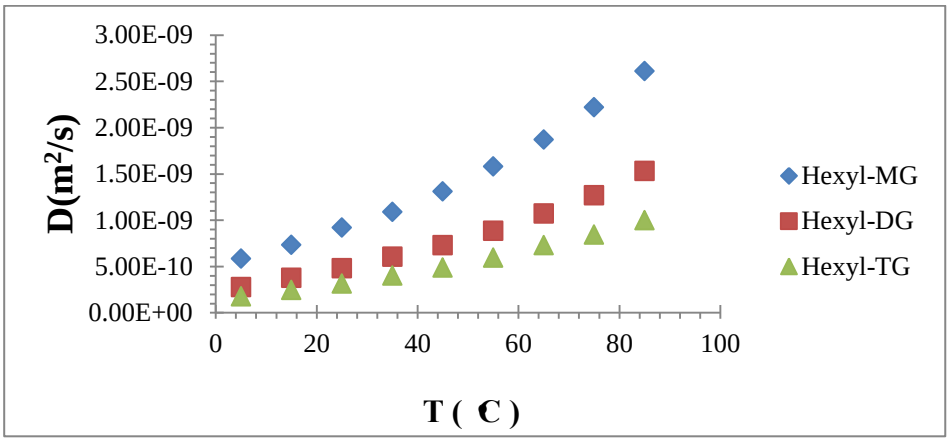

Figure 5-14 Diffusion coefficient versus temperature for hexyl glyme series (MG=monoglyme, DG=diglyme, TG=triglyme).

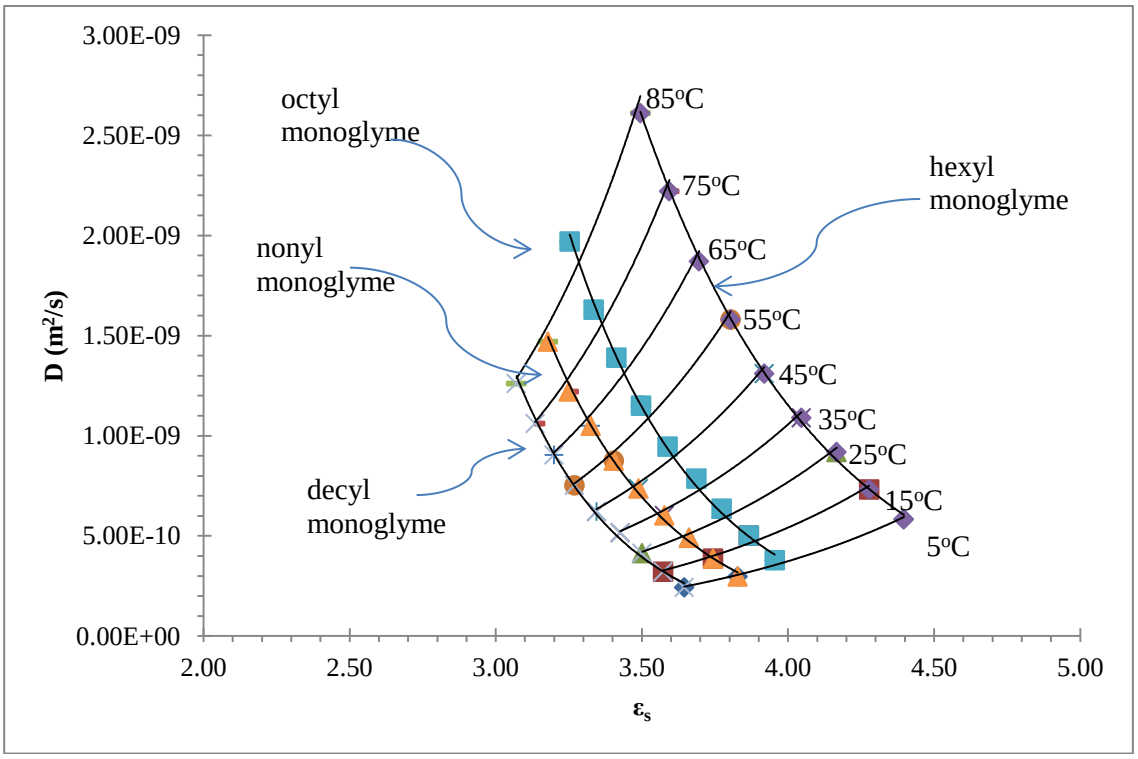

Figure 5-15 Reference curve for pure monoglyme self-diffusion coefficient data and dielectric constant data.

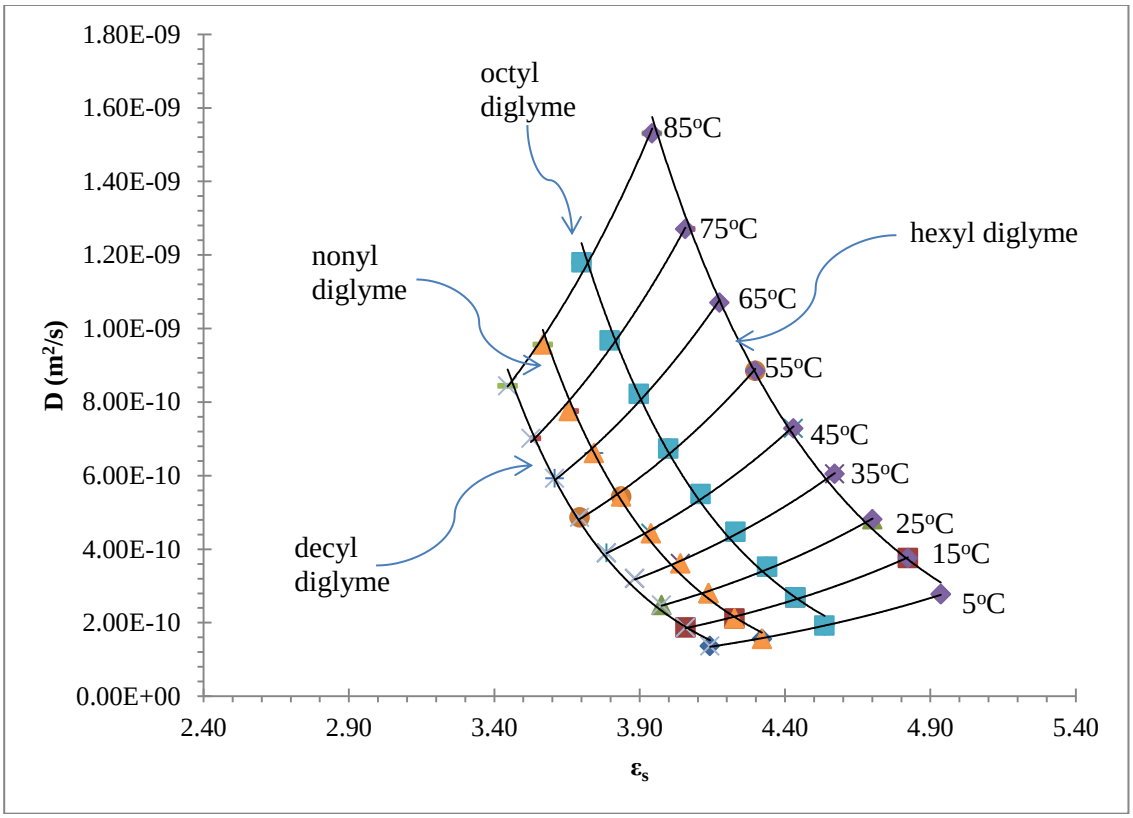

Figure 5-16 Reference curves for pure diglyme from self-duffusion coefficient and dielectric constant data.

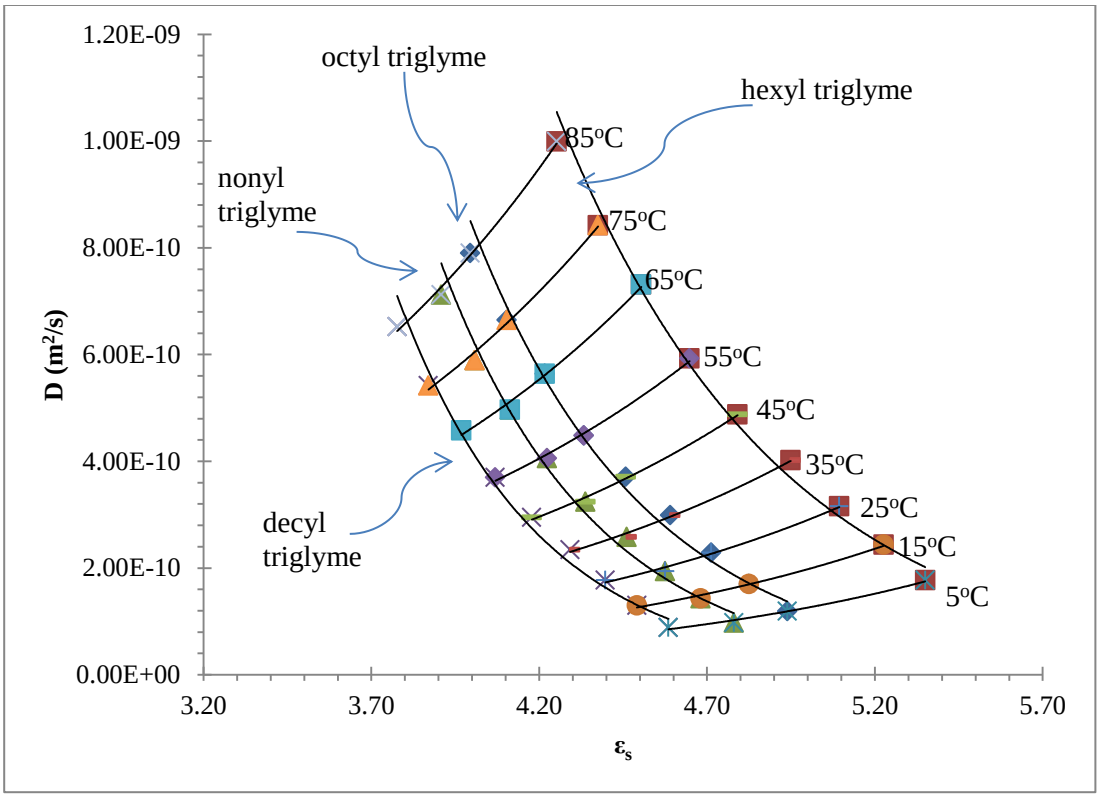

Figure 5-17 Reference curves for pure triglyme from self-duffusion coefficient and dielectric constant data.

Using the dielectric constant and self-diffusion coefficient data, the reference curves for each of the monoglyme, diglyme, and triglyme is plotted (figure 5-15 to figure 5-17). From the reference curve, the simple exponential function is found to give the best fit (table 5-4 to table 5-6) with R^2-values of 0.9568 for the monoglyme series, 0.9936 for the diglyme series, and 0.9912 for the triglyme series. Thus the simple exponential function is used to calculate the values of the $D_r(\varepsilon_s,T_r)$. Table 5-7, table 5-8 and table 5-9 list the values of the E_a for each of the glyme analogs for all reference temperatures T_r.

	Fitting Model		
T_r (°C)	y=A*exp(B*x)	y=yo+A*exp(B*x)	$y=Ax^2+Bx+C$
5	0.9846	0.9789	0.9835
15	0.9709	0.9409	0.9693
25	0.9669	0.9088	0.9619
35	0.9571	0.8664	0.9464
45	0.9608	0.8866	0.9546
55	0.9529	0.7878	0.9375
65	0.9413	0.7017	0.9237
75	0.9484	0.6626	0.9285
85	0.9273	0.5427	0.9099
Average	0.9567	0.8085	0.9461

Table 5-4 R^2-values for various fitting model applied to pure monoglyme reference curves.

	Fitting Model		
T_r (°C)	y=A*exp(B*x)	y=yo+A*exp(B*x)	$y=Ax^2+Bx+C$
5	0.9991	0.9988	0.9994
15	0.9950	0.9907	0.9917
25	0.9957	0.9923	0.9932
35	0.9965	0.9934	0.9941
45	0.9927	0.9879	0.9895
55	0.9920	0.9837	0.9864
65	0.9906	0.9798	0.9842
75	0.9892	0.9554	0.9799
85	0.9914	0.9826	0.9875
Average	0.9936	0.9850	0.9895

Table 5-5 R^2-values for various fitting model applied to pure diglyme reference curves.

	Fitting Model		
T_r (°C)	y=A*exp(B*x)	y=yo+A*exp(B*x)	$y=Ax^2+Bx+C$
5	0.9897	0.9867	0.9896
15	0.9892	0.9527	0.9879
25	0.9897	0.9441	0.9841
35	0.9928	0.9628	0.9881
45	0.9929	0.9622	0.9885
55	0.9932	0.9979	0.9987
65	0.9894	0.9455	0.9867
75	0.9899	0.9327	0.9830
85	0.9938	0.9596	0.9913
Average	0.9912	0.9605	0.9886

Table 5-6 R^2-values for various fitting model applied to pure triglyme reference curves.

	Activation Energy, E_a (kJ/mol)			
T_r (°C)	Hexyl monoglyme	Octyl monoglyme	Nonyl monoglyme	Decyl monoglyme
5	26.04	25.11	23.92	23.60
15	26.02	25.09	23.87	23.55
25	26.34	25.34	24.09	23.75
35	26.50	25.47	24.19	23.83
45	27.27	26.09	24.75	24.34
55	28.19	26.82	25.41	24.94
65	28.82	27.31	25.85	25.33
75	30.27	28.47	26.92	26.30
85	30.91	28.95	27.35	26.68

Table 5-7 The E_a values for the diffusion of pure monoglyme family at reference temperature 5°C to 85°C.

	Activation Energy, E_a (kJ/mol)			
T_r (°C)	Hexyl diglyme	Octyl diglyme	Nonyl diglyme	Decyl diglyme
5	26.84	26.38	25.63	25.35
15	26.99	26.50	25.73	25.44
25	26.98	26.48	25.70	25.41
35	27.14	26.62	25.81	25.51
45	27.56	26.98	26.13	25.81
55	27.88	27.26	26.37	26.03
65	28.41	27.71	26.77	26.41
75	29.35	28.52	27.51	27.10
85	29.85	28.94	27.87	27.45

Table 5-8 The E_a values for the diffusion of pure diglyme family at reference temperature 5°C to 85°C.

	Activation Energy, E_a (kJ/mol)			
T_r (°C)	Hexyl triglyme	Octyl triglyme	Nonyl triglyme	Decyl triglyme
5	28.83	28.86	29.05	28.65
15	28.13	28.24	28.46	28.09
25	27.74	27.89	28.13	27.77
35	27.54	27.71	27.97	27.61
45	27.51	27.69	27.95	27.59
55	27.50	27.68	27.95	27.59
65	28.20	28.30	28.53	28.13
75	28.14	28.26	28.50	28.10
85	28.40	28.48	28.71	28.29

Table 5-9 The E_a values for the diffusion of pure triglyme family at reference temperature 5°C to 85°C.

Inspecting the reference temperature plot for monoglyme, the T_r=5°C and T_r=15°C include the largest dielectric constant range that coincide with the dielectric constant range of the hexyl monoglyme. For the octyl monoglyme , the reference curves at temperature of 35°C, 45°C and 55°C cover the most similar range of dielectric constant values. For nonyl monoglyme, the reference curves from 45°C to 65°C have the most similar dielectric constant range. The T_r=65°C and T_r=75°C have the most similar dielectric constant range for decyl monoglyme. All of the linear plots of ln (D/D_r) vs (1/T) have regression values of at least 0.9900 (plots not shown). From the E_a at these temperatures, the average E_a for the monoglyme series was found to be 25.8 $\pm$ 0.6 kJ/mol.

For the diglyme series, looking closely at the reference temperature plot for shows that the T_r=5°C to T_r=35°C include the largest dielectric constant range that coincide with the dielectric constant range of the hexyl diglyme. For the octyl diglyme , the reference curves at temperature of 35°C and 45°C cover the most similar range of dielectric constant values. For nonyl diglyme, the reference curves from 55°C to 75°C have the most similar dielectric constant range. The T_r=55°C and T_r=65°C have the

most similar dielectric constant range for decyl diglyme. All of the linear plots of ln (D/D_r) vs (1/T) have regression values of at least 0.9900 (plots not shown). From the E_a at these temperatures, the average E_a for the diglyme series was found to be 26.8 $\pm$ 0.4 kJ/mol.

For the triglyme series, looking closely at the reference temperature plot for shows that the T_r=5^{o}C to T_r=35^{o}C include the largest dielectric constant range that coincide with the dielectric constant range of the hexyl triglyme. For the octyl triglyme , the reference curves at temperature of 35^{o}C and 45^{o}C cover the most similar range of dielectric constant values. For nonyl triglyme, the reference curves from 45^{o}C to 55^{o}C have the most similar dielectric constant range. The T_r=55^{o}C and T_r=65^{o}C have the most similar dielectric constant range for decyl triglyme. All of the linear plots of ln (D/D_r) vs (1/T) have regression values of at least 0.9900 (plots not shown). From the E_a at these temperatures, the average E_a for the triglyme series was found to be 27.9 $\pm$ 0.4 kJ/mol.

Applying the CAF analysis to the dielectric constant values and the pure monoglyme, diglyme, and triglyme derivatives allows the determination of the activation energy. Table 5-10 lists the activation energy for each of the pure glyme family. The activation energy increases as the number of repeat unit is increased. In a polymer, the diffusion is expected to decrease as the number of repeat unit goes from a monomer to a dimer to a trimer and so on. On the other hand, as shown above, the value of dielectric constant also increases as the number of repeat unit is increased. Thus it is expected that the activation energy also increases such that the diffusion coefficient decreases.

Glyme Family	E_a (diffusion) (kJ/mol)
Monoglyme	25.8 ± 0.6
Diglyme	26.8 ± 0.4
Triglyme	27.9 ± 0.4

Table 5-10 The activation energy for pure glyme family.

Figure 5-18 to 5-20 below show the master curves generated for each of the glyme family. The master curve plots confirm that the CAF method can be applied to the glyme oligomers.

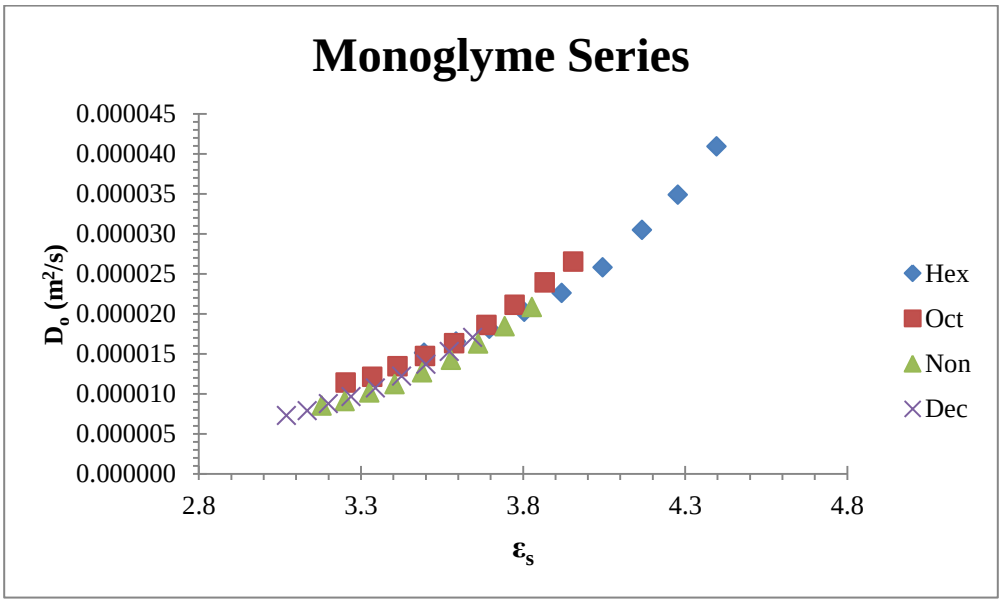

Figure 5-18 Master curve for the pure monoglyme.

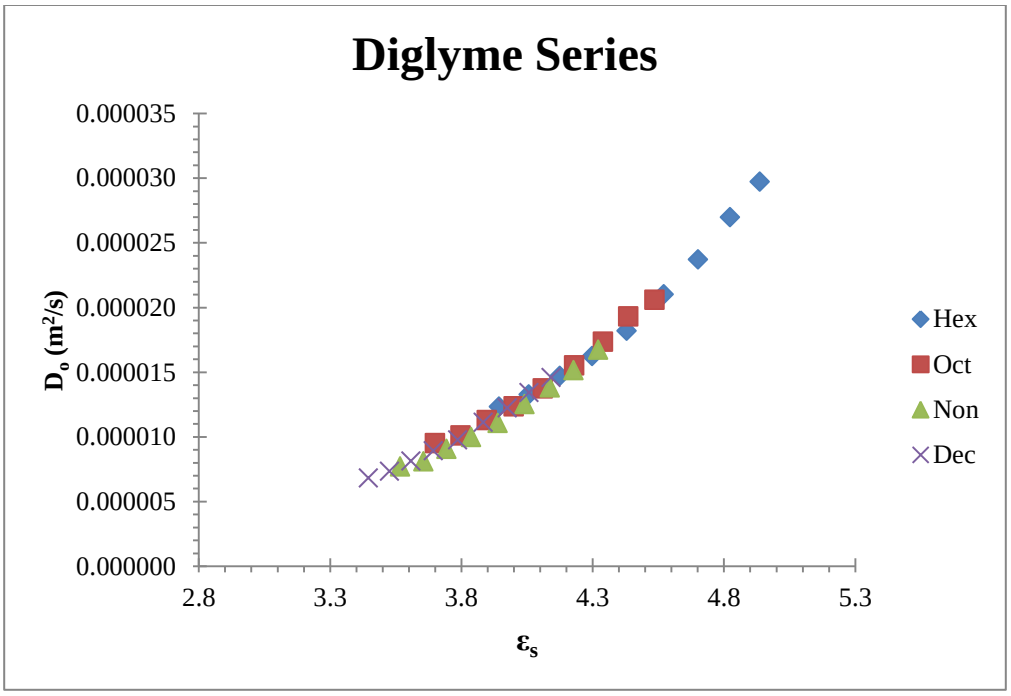

Figure 5-19 Master curve for the diglyme series.

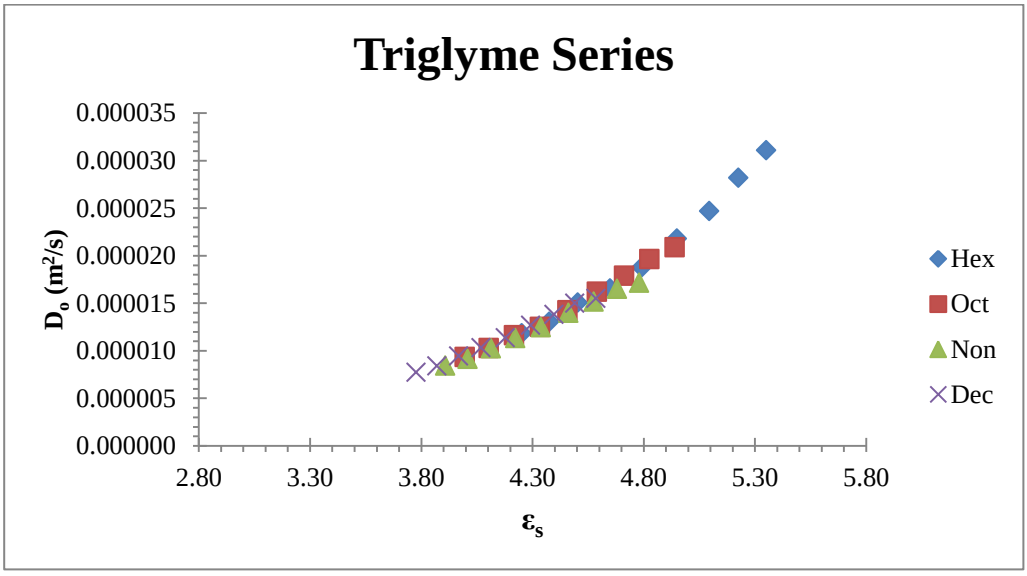

Figure 5-20 Master curve for the triglyme series.

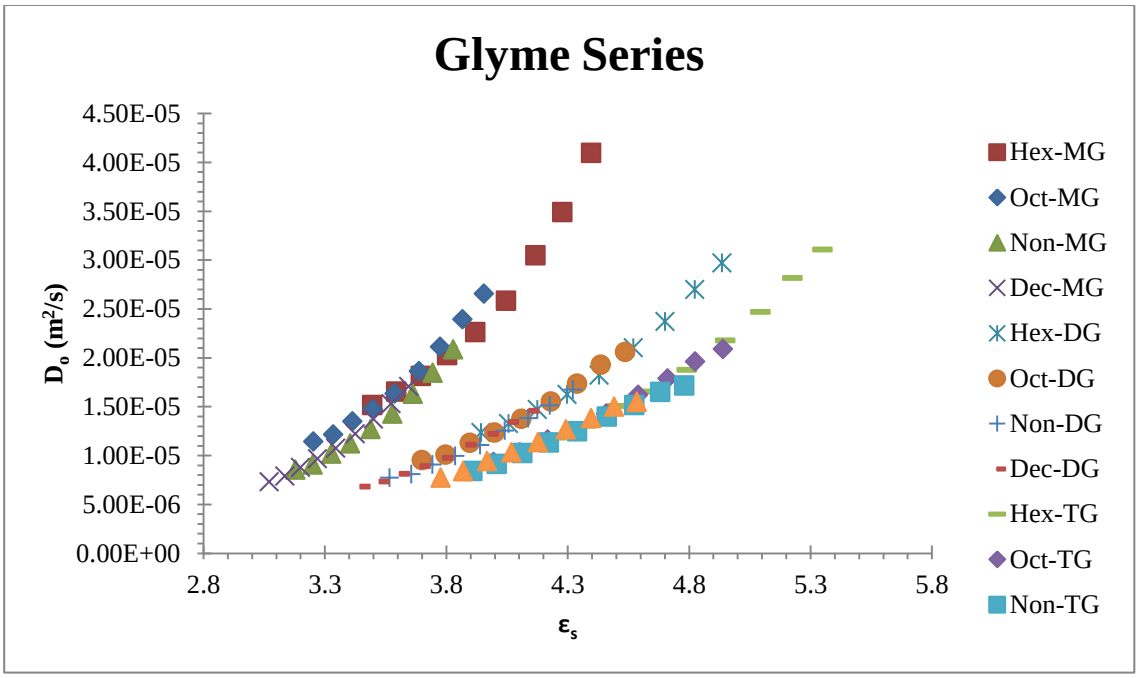

Figure 5-21 Combine master curve for all glyme series. MG=monoglyme, DG=diglyme, TG= triglyme.

Figure 5-21 shows the combine master curve for all three glyme families all on one plot. As discussed in section 2.5, the formation of a master curve supports the idea that each system should contain one E_a. Thus, the master curves for monoglyme, diglyme, and triglyme families do not lie on a single curve as expected. The position of the master curve follows the trend of the E_a for each system, where the master curve for the diglyme system lies in between the master curves for the monoglyme and the triglyme systems. From the plot of the master curve, it appears that the exponential pre-factor for self-diffusion is converging to a value of ~ 5 x 10^{-6} m^2/s.

5.2.3 Dielectric Constant and Conductivity of 0.1 molal LiTf in Glyme Derivatives

Table 5-11 lists the dielectric constant and ionic conductivity values for all the glyme species investigated. Figure 5-22 shows the plot of the values of dielectric constant versus temperature for 0.1 molal LiTf in glyme solutions. The temperature

range is from 5°C to 85°C. Overall, the value of dielectric constant of the salt solution increases compared to the dielectric constant of the pure glyme derivatives.

The behavior of the dielectric constant of the 0.1 molal LiTf in these glyme family is similar to the behavior of the pure solution. For a particular repeat unit, the dielectric constant decreases as the length of the alkyl chain increases. As the temperature increases, the dielectric constant values decrease.

Across different repeat unit, similar to the pure glyme series, the dielectric constant increases as the number of oligomer repeat unit increases. The dielectric constant of the hexyl monoglyme, hexyl diglyme and hexyl triglyme is shown in Figure 5-23. Similar behavior is exhibited by the octyl, nonyl, and decyl derivatives.

	Hexyl monoglyme		Octyl monoglyme		Nonyl monoglyme		Decyl monoglyme	
T_r (°C)	ε_s	σ (S/cm)	ε_s	σ (S/cm)	ε_s	σ (S/cm)	ε_s	σ (S/cm)
5	4.92	8.50×10^{-8}	4.38	1.86×10^{-8}	4.17	1.08×10^{-8}	4.01	6.04×10^{-9}
15	4.76	9.00×10^{-8}	4.25	2.09×10^{-8}	4.06	1.23×10^{-8}	3.91	7.09×10^{-9}
25	4.60	9.51×10^{-8}	4.14	2.32×10^{-8}	3.95	1.40×10^{-8}	3.81	8.25×10^{-9}
35	4.45	1.01×10^{-7}	4.01	2.60×10^{-8}	3.84	1.60×10^{-8}	3.71	9.64×10^{-9}
45	4.29	1.08×10^{-7}	3.90	2.91×10^{-8}	3.73	1.83×10^{-8}	3.61	1.13×10^{-8}
55	4.14	1.13×10^{-7}	3.79	3.30×10^{-8}	3.63	2.08×10^{-8}	3.52	1.31×10^{-8}
65	4.00	1.19×10^{-7}	3.69	3.79×10^{-8}	3.53	2.34×10^{-8}	3.44	1.50×10^{-8}
75	3.87	1.25×10^{-7}	3.60	4.34×10^{-8}	3.45	2.62×10^{-8}	3.36	1.71×10^{-8}
85	3.75	1.30×10^{-7}	3.51	4.83×10^{-8}	3.36	2.91×10^{-8}	3.28	1.92×10^{-8}
	Hexyl diglyme		Octyl diglyme		Nonyl diglyme		Decyl diglyme	
T_r (°C)	ε_s	σ (S/cm)	ε_s	σ (S/cm)	ε_s	σ (S/cm)	ε_s	σ (S/cm)
5	6.09	6.40×10^{-7}	5.47	2.27×10^{-7}	5.10	1.12×10^{-7}	4.84	5.99×10^{-8}
15	5.89	6.92×10^{-7}	5.27	2.56×10^{-7}	4.95	1.26×10^{-7}	4.69	6.89×10^{-8}
25	5.67	7.36×10^{-7}	5.10	2.79×10^{-7}	4.79	1.40×10^{-7}	4.55	7.77×10^{-8}
35	5.44	7.74×10^{-7}	4.92	3.06×10^{-7}	4.64	1.54×10^{-7}	4.40	8.74×10^{-8}
45	5.21	8.04×10^{-7}	4.73	3.35×10^{-7}	4.47	1.68×10^{-7}	4.25	9.70×10^{-8}
55	5.00	8.27×10^{-7}	4.56	3.54×10^{-7}	4.32	1.81×10^{-7}	4.11	1.08×10^{-7}
65	4.82	8.43×10^{-7}	4.40	3.68×10^{-7}	4.18	1.94×10^{-7}	3.98	1.18×10^{-7}
75	4.64	8.57×10^{-7}	4.26	3.80×10^{-7}	4.05	2.06×10^{-7}	3.86	1.27×10^{-7}
85	4.48	8.71×10^{-7}	4.12	3.89×10^{-7}	3.93	2.16×10^{-7}	3.76	1.36×10^{-7}
	Hexyl triglyme		Octyl triglyme		Nonyl triglyme		Decyl triglyme	
T_r (°C)	ε_s	σ (S/cm)	ε_s	σ (S/cm)	ε_s	σ (S/cm)	ε_s	σ (S/cm)
5	6.94	1.79×10^{-6}	6.31	6.47×10^{-7}	6.09	4.22×10^{-7}	5.73	2.75×10^{-7}
15	6.72	2.03×10^{-6}	6.12	7.67×10^{-7}	5.92	5.08×10^{-7}	5.58	3.34×10^{-7}
25	6.49	2.28×10^{-6}	5.93	8.97×10^{-7}	5.74	6.02×10^{-7}	5.41	4.01×10^{-7}
35	6.25	2.53×10^{-6}	5.73	1.03×10^{-6}	5.54	7.11×10^{-7}	5.24	4.73×10^{-7}
45	5.99	2.76×10^{-6}	5.51	1.17×10^{-6}	5.35	8.18×10^{-7}	5.05	5.52×10^{-7}
55	5.74	2.95×10^{-6}	5.29	1.30×10^{-6}	5.14	9.33×10^{-7}	4.87	6.27×10^{-7}
65	5.52	3.09×10^{-6}	5.11	1.41×10^{-6}	4.97	1.03×10^{-6}	4.70	6.93×10^{-7}
75	5.30	3.21×10^{-6}	4.94	1.50×10^{-6}	4.80	1.12×10^{-6}	4.55	7.55×10^{-7}
85	5.11	3.30×10^{-6}	4.78	1.58×10^{-6}	4.64	1.19×10^{-7}	4.40	8.07×10^{-7}

Table 5-11 Dielectric constant and ionic conductivity for 0.1 molal LiTf in monoglyme family, diglyme family, and triglyme family. ε_s = dielectric constant, σ = ionic conductivity.

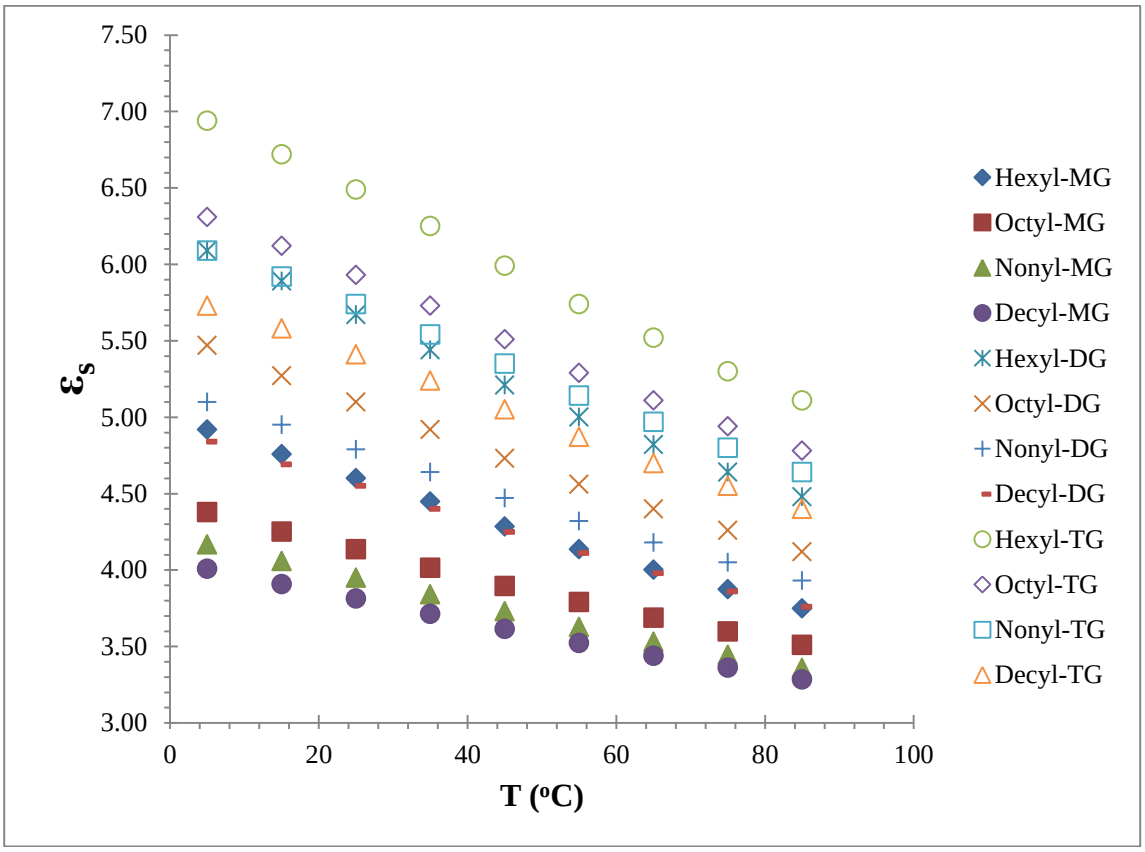

Figure 5-22 Dielectric constant of 0.1 molal LiTf solution in the gylme series versus temperature (MG=monoglyme, DG=diglyme, TG=triglyme).

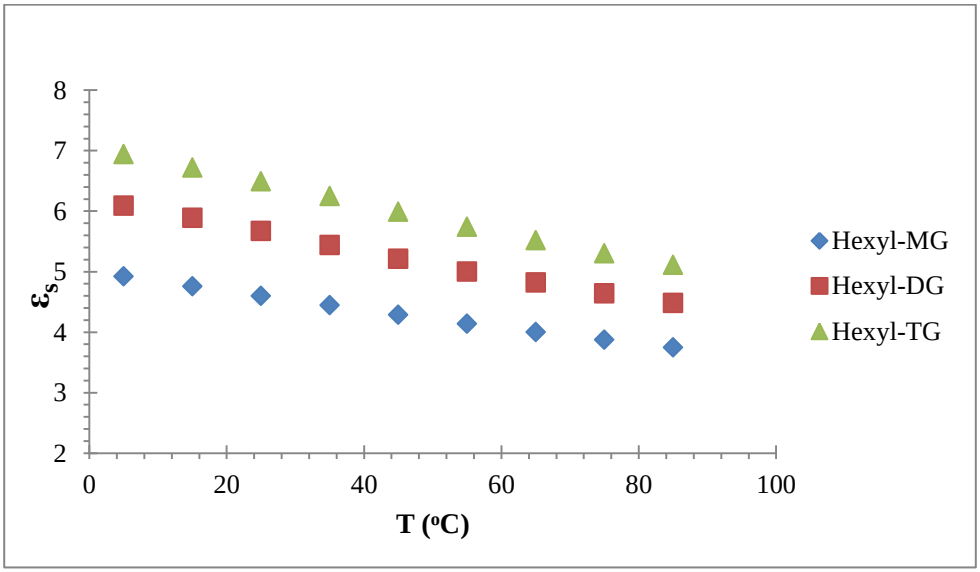

Figure 5-23 Dielectric constant versus temperature for hexyl monoglyme, hexyl diglyme, hexyl triglyme.

Figure 5-24 shows the plot of conductivity values versus temperature for 0.1 molal LiTf in glyme solutions. While the dielectric constant values for the salt solution shows similar behavior as the pure glyme solvents across different alkyl chain length and different oligomer repeat unit, the conductivity values are not all similar. For a particular repeat unit, the conductivity values decrease as the alkyl chain length is increased from hexyl to decyl for all members of the monoglyme, diglyme, and triglyme families. This decrease follows the trend in dielectric constant values.

However, for different repeat units, the conductivity values do reveal one different trend. It was shown in the previous section that the diffusion of the pure triglyme is lower than the diffusion of the pure diglyme, which in turn is lower than the diffusion of the pure monoglyme. For the conductivity however, the value is highest for the longest repeat unit triglyme, followed by diglyme, and finally monoglyme. An example of this trend is shown in figure 5-25 for the conductivity in hexyl monoglyme, hexyl diglyme, and hexyl triglyme. This is a reverse of the trend seen in the self-diffusion of pure glyme solutions.

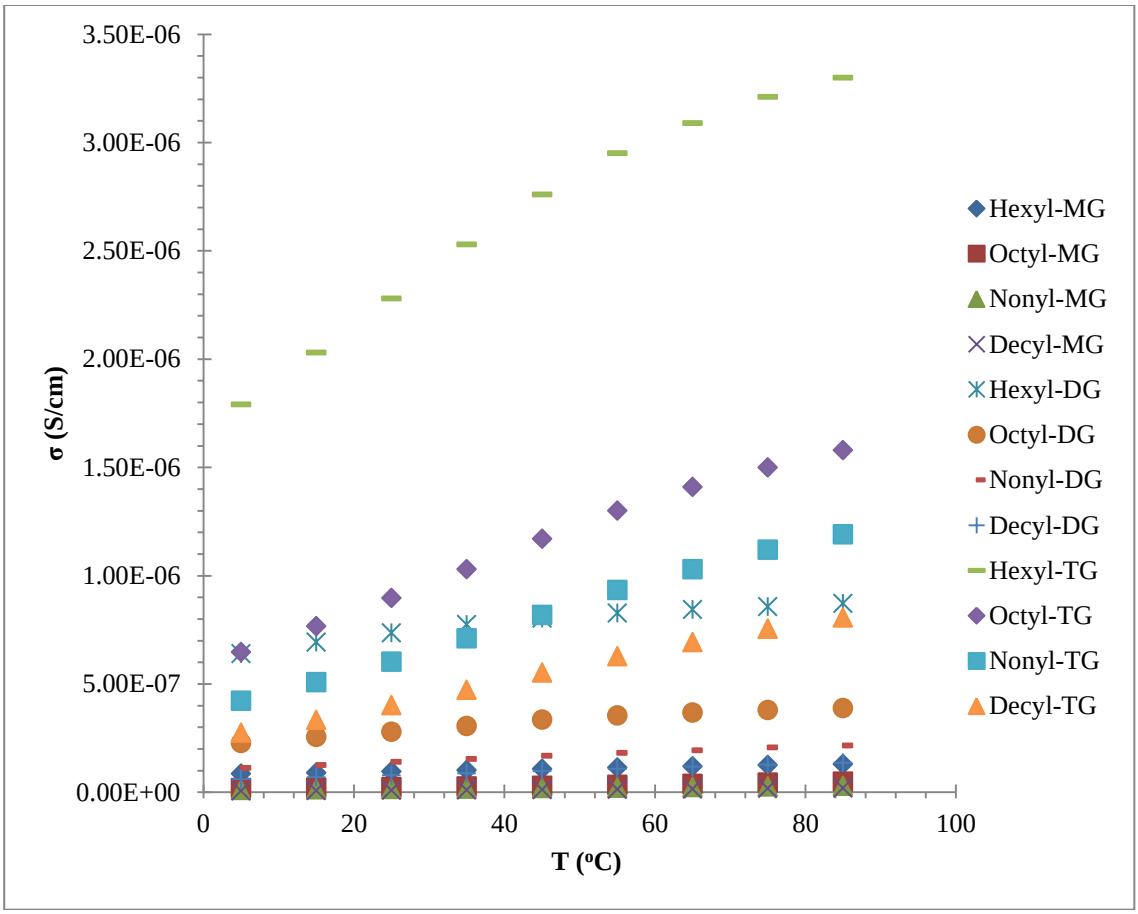

Figure 5-24 Ionic conductivity of 0.1 molal LiTf solution in the gylme series versus temperature (MG=monoglyme, DG=diglyme, TG=triglyme).

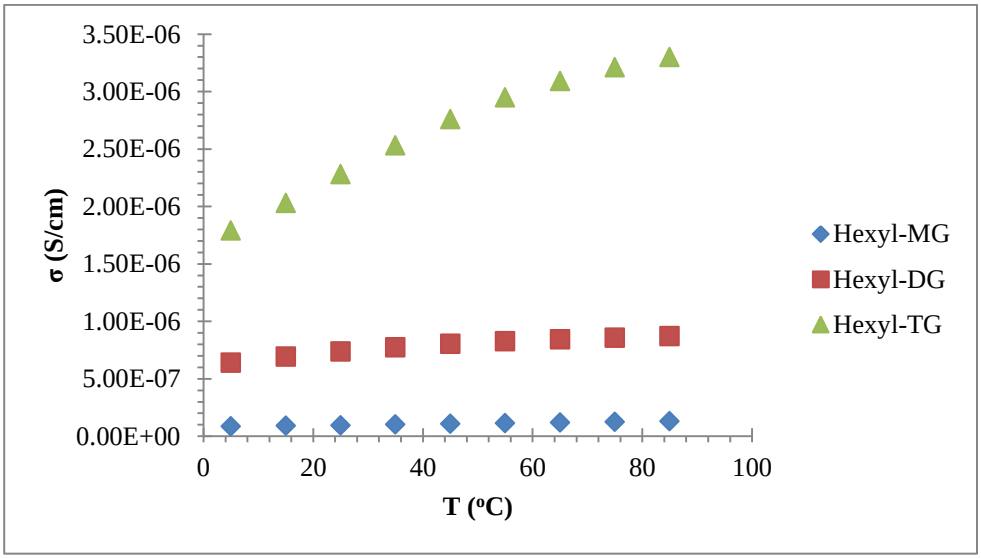

Figure 5-25 Ionic conductivity versus temperature for hexyl monoglyme, hexyl diglyme, hexyl triglyme.

Using the dielectric constant and ionic conductivity data, the reference curves for each of the monoglyme family, diglyme family, and triglyme family are generated (figures 5-26 to figure 5-28).

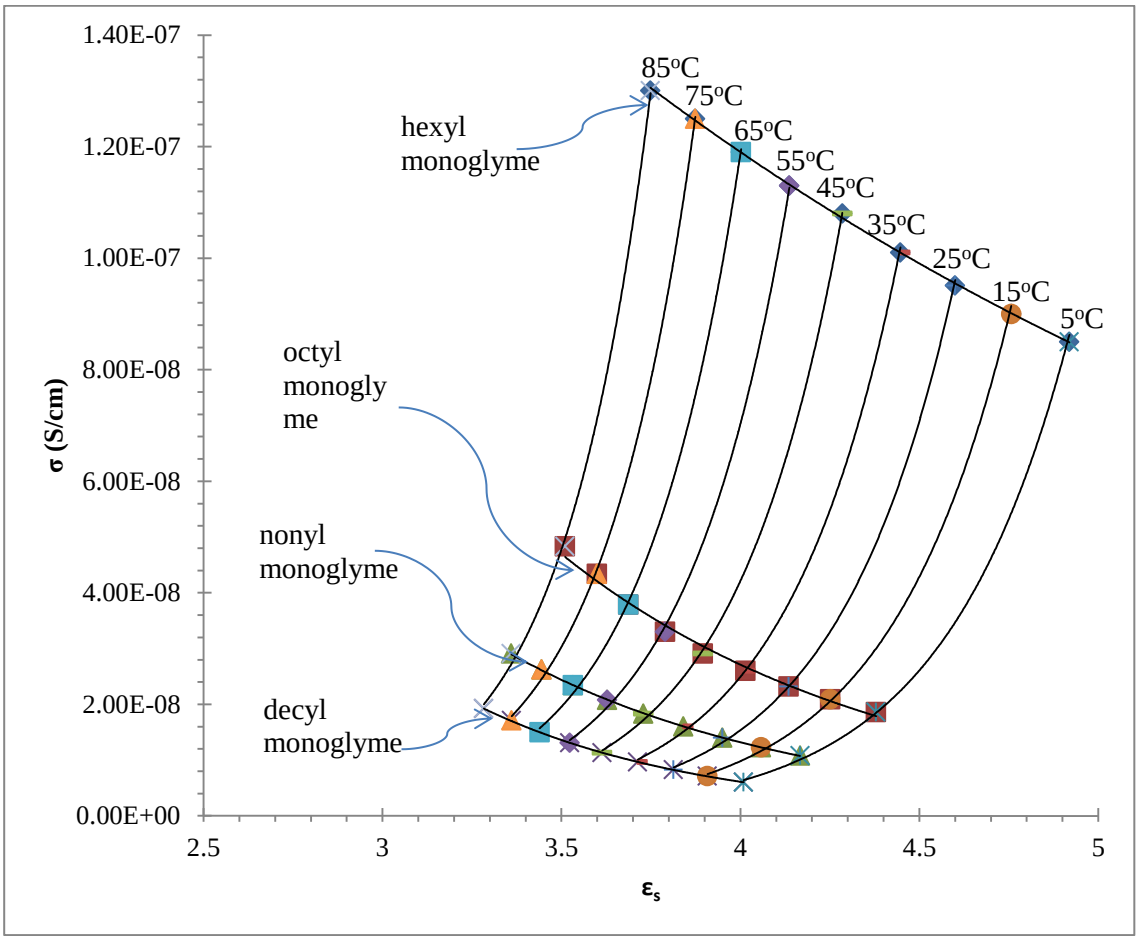

Figure 5-26 Reference curve for 0.1 molal LiTf in monoglyme solvents.

-

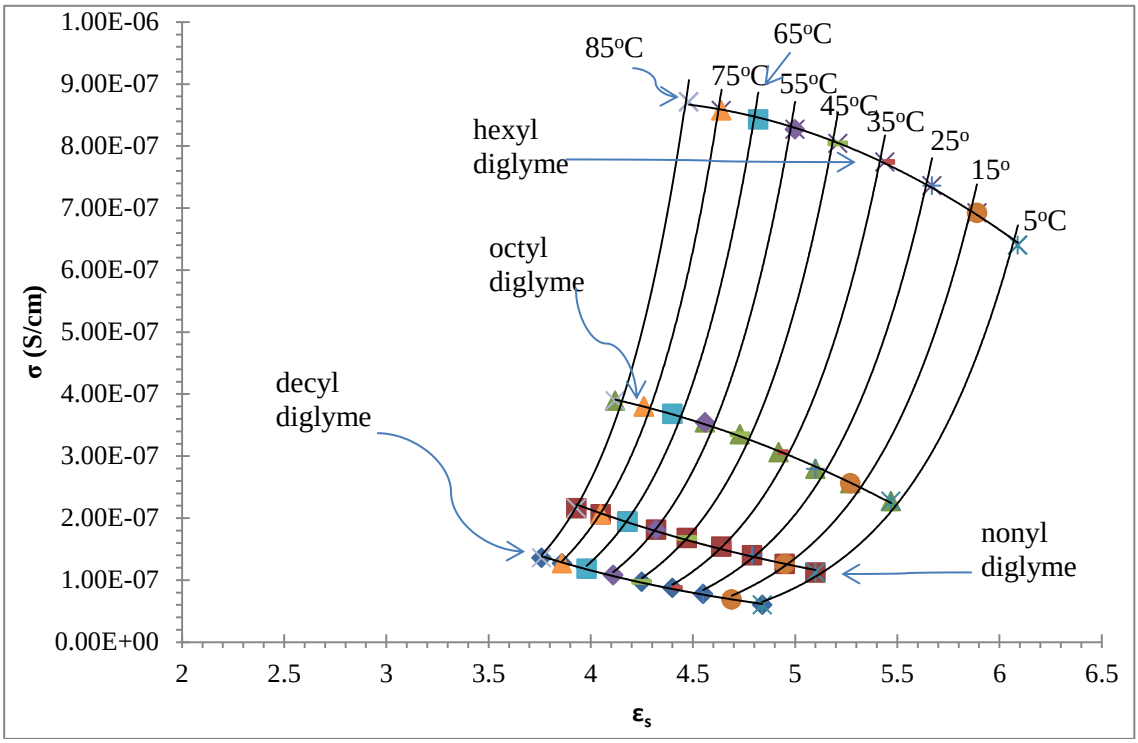

Figure 5-27 Reference curve for 0.1 molal LiTf in diglyme solvents.

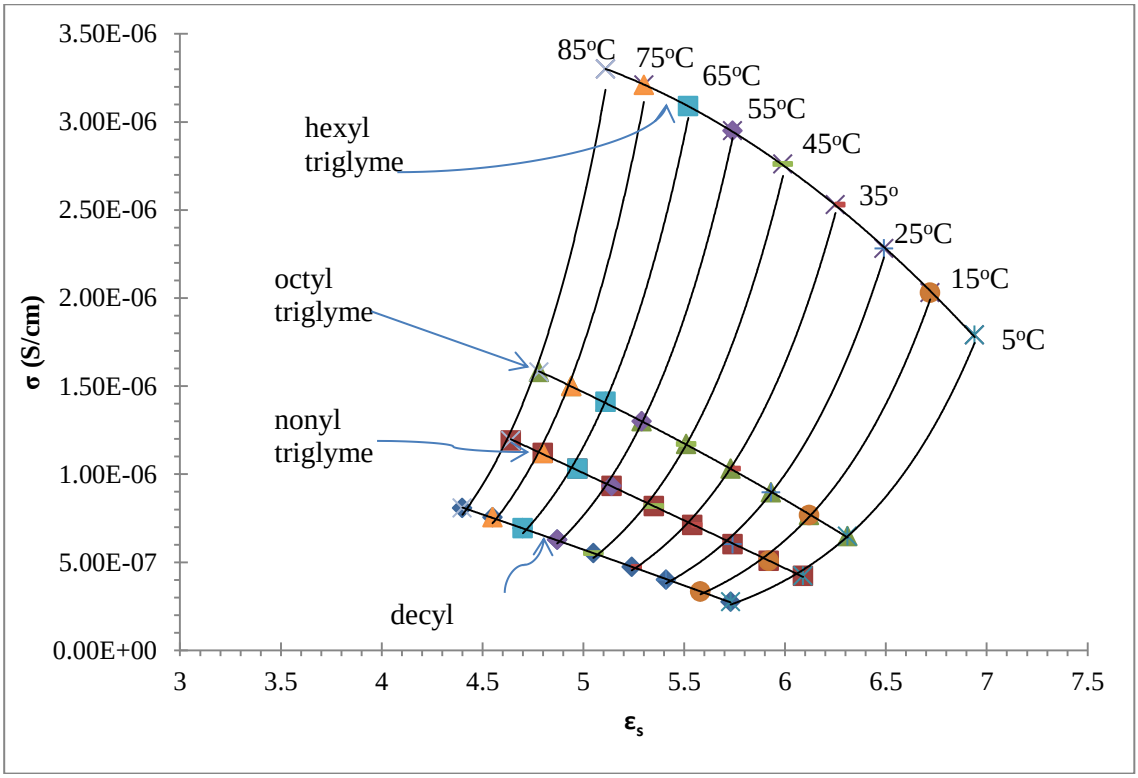

Figure 5-28 Reference curve for 0.1 molal LiTf in triglyme solvents.

Based on these reference temperature curves, the fitting parameters are determined. For the monoglyme series, the simple exponential produces the best R^2-value. For the diglyme and triglyme series, the polynomial of second order has the highest R^2-values (table 5-12 to 5-14). However, for both series, a closer look at the plot of $\ln(\sigma/\sigma_r)$ versus (1/T) shows that the using the polynomial of second order curve fitting produces non-linear plots and linear plots with R^2-values that are less than 0.9900 (figures 5-29 and 5-30). Thus the next best model, the exponential growth model is used instead for triglyme series. For diglyme series, the exponential model also produces plots with R^2-values less than 0.9900 (plots not shown). Thus the simple exponential model is used instead.

	Fitting Model		
T_r (°C)	y=A*exp(B*x)	y=yo+A*exp(B*x)	$y=Ax^2+Bx+C$
5	0.9998	0.9996	0.9967
15	0.9998	0.9998	0.9975
25	0.9998	0.9996	0.9968
35	0.9997	0.9995	0.9969
45	0.9995	0.9991	0.9958
55	0.9993	0.9987	0.9948
65	0.9994	0.9988	0.9955
75	0.9993	0.9985	0.9948
85	0.9988	0.9979	0.9931
Average	0.9995	0.9991	0.9958

Table 5-12 R^2-values of the reference curves for 0.1 molal LiTf in monoglyme solutions.

	Fitting Model		
T_r (°C)	y=A*exp(B*x)	y=yo+A*exp(B*x)	$y=Ax^2+Bx+C$
5	0.9982	0.9999	0.9983
15	0.9951	0.9992	1.0000
25	0.9959	0.9996	0.9999
35	0.9954	0.9987	0.9999
45	0.9932	0.9979	0.9995
55	0.9937	0.9973	0.9992
65	0.9933	0.9967	0.9988
75	0.9957	0.9978	0.9995
85	0.9952	0.9978	0.9994
Average	0.9951	0.9983	0.9994

Table 5-13 R^2-values of the reference curves for 0.1 molal LiTf in diglyme solutions.

	Fitting Model		
T_r (°C)	y=A*exp(B*x)	y=yo+A*exp(B*x)	$y=Ax^2+Bx+C$
5	0.9986	0.9979	0.9999
15	0.9984	0.9971	0.9996
25	0.9980	0.9968	0.9995
35	0.9989	0.9987	0.9999
45	0.9975	0.9966	0.9993
55	0.9985	0.9977	0.9995
65	0.9979	0.9978	0.9997
75	0.9973	0.9996	0.9998
85	0.9961	0.9999	0.9996
Average	0.9979	0.9980	0.9997

Table 5-14 R^2-values of the reference curves for 0.1 molal LiTf in triglyme solutions.

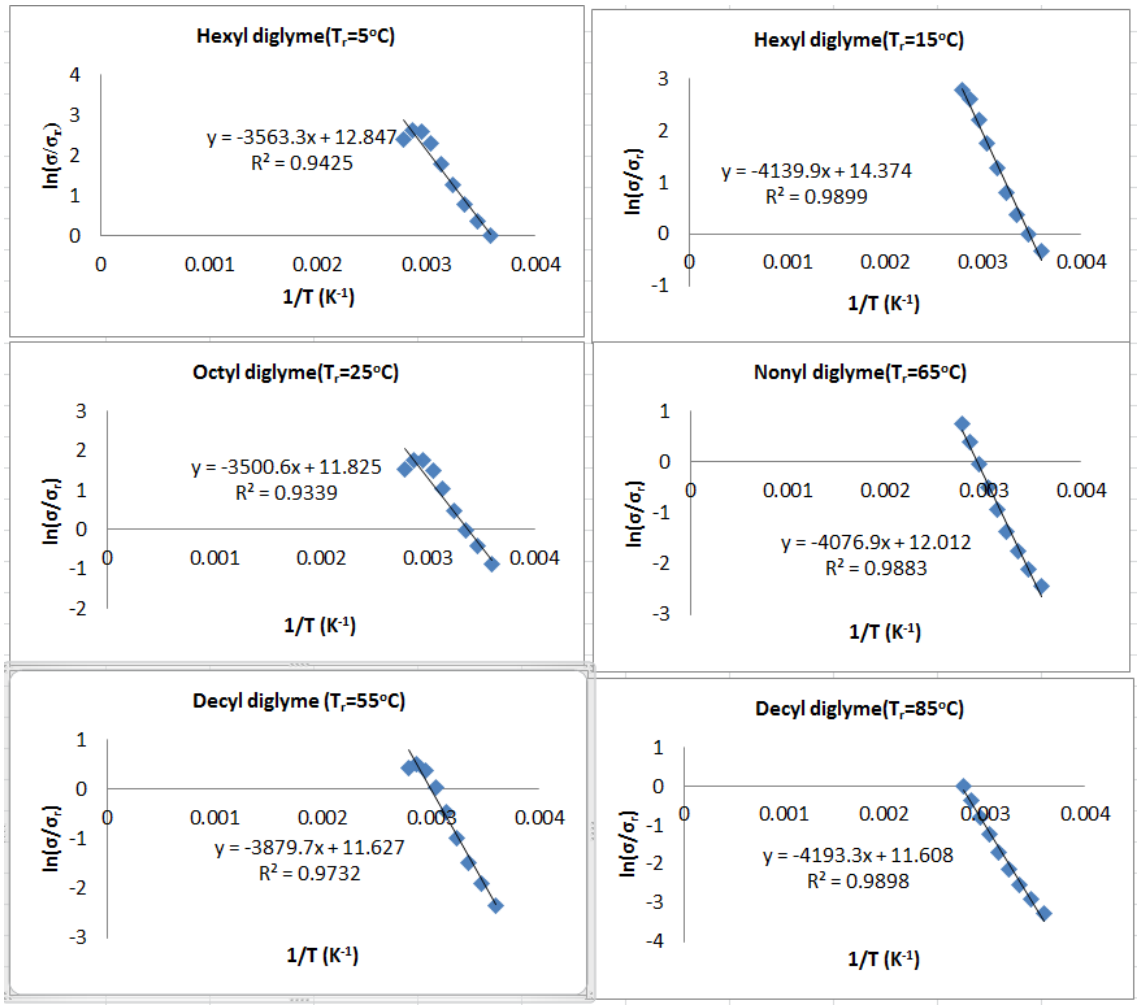

Figure 5-29 Erroneous $\ln(\sigma/\sigma_r)$ vs (1/T) for 0.1 molal LiTf in diglyme electrolytes using second order polynomial curve fitting. Plots shown for selected T_r's.

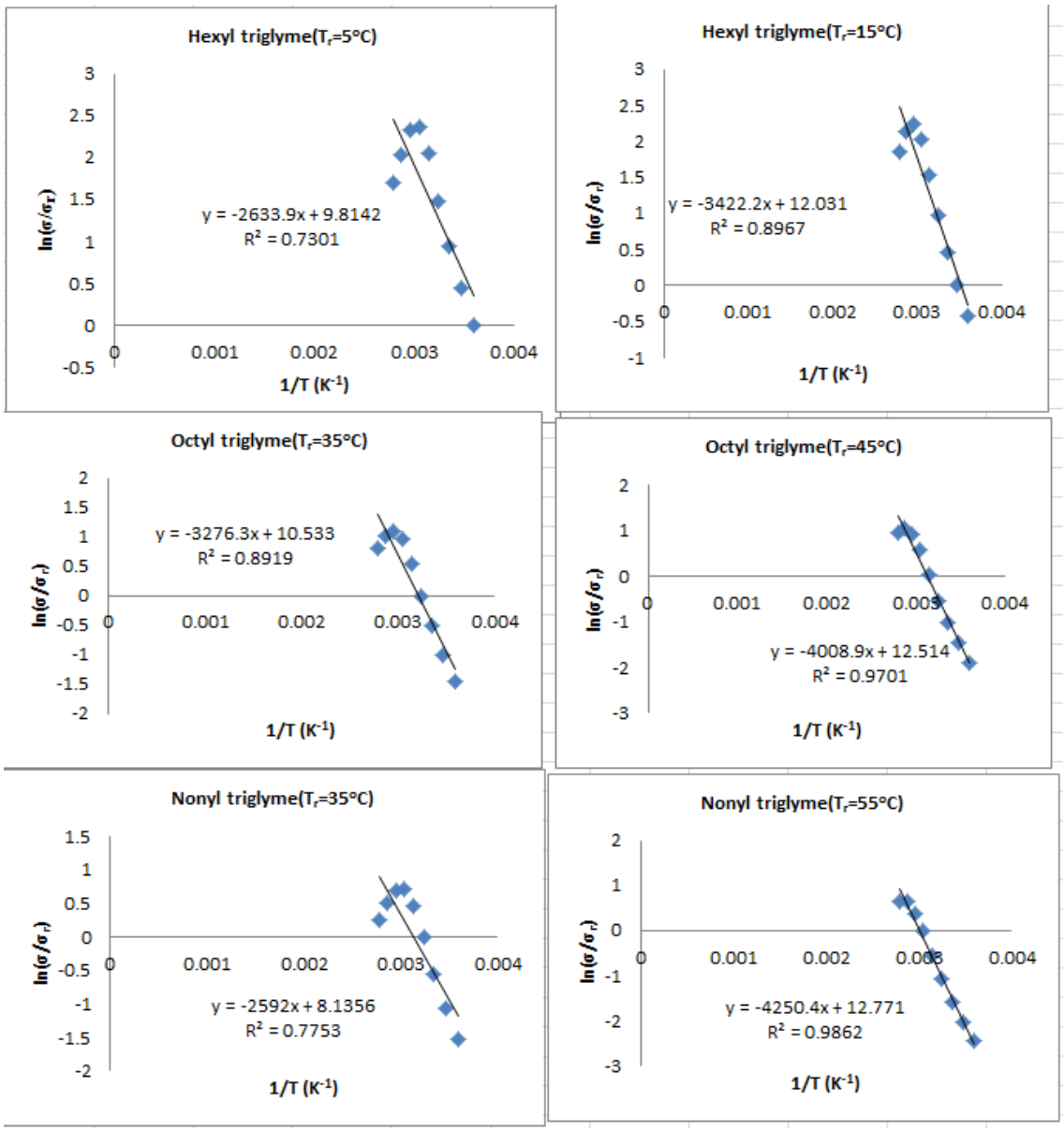

Figure 5-30 Erroneous $\ln(\sigma/\sigma_r)$ versus (1/T) for 0.1 molal LiTf in triglyme electrolytes using second order polynomial curve fitting. Plots shown for selected T_r's.

Tables 5-15 to 5-17 tabulate the E_a values for these glymes and their alkyl derivatives. For the monoglyme series, the appropriate reference temperatures for hexyl monoglyme are 5°C, 15°C, 25°C, and 35°C. For octyl monoglyme, T_r=35°C, 45°C, and 55°C match the best dielectric constant range. For nonyl monoglyme, T_r=45°C, 55°C,

65°C, and 75°C are the most valid. For decyl monoglyme, T_r= 55°C, 65°C, 75°C, and 85°C are valid reference temperatures.

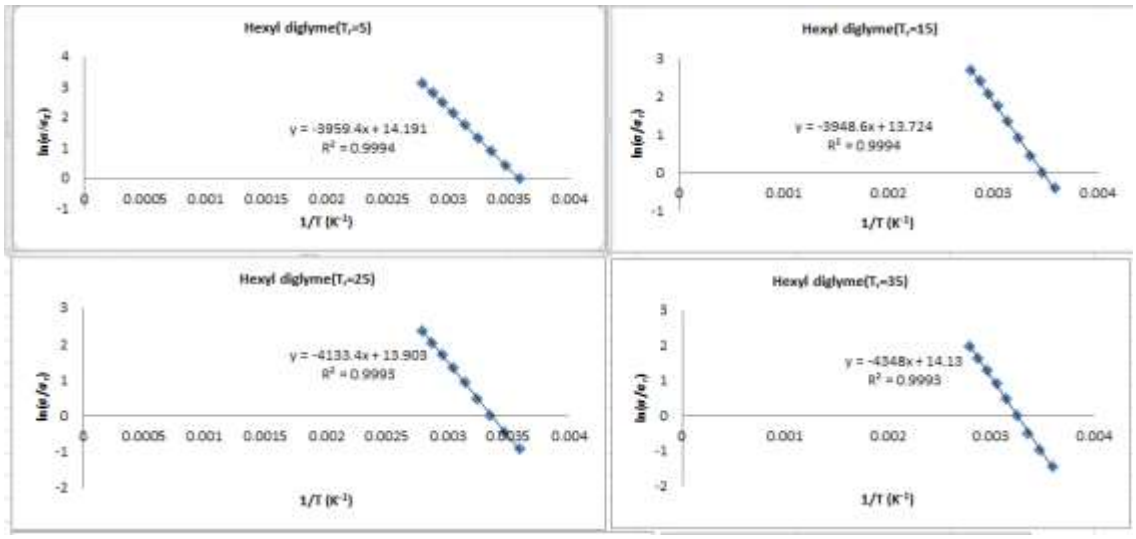

Figure 5-31 Plots of $\ln(\sigma/\sigma_r)$ vs (1/T) using simple exponential curve fitting model for 0.1 molal LiTf in hexyl diglyme electrolyte for selected T_r's.

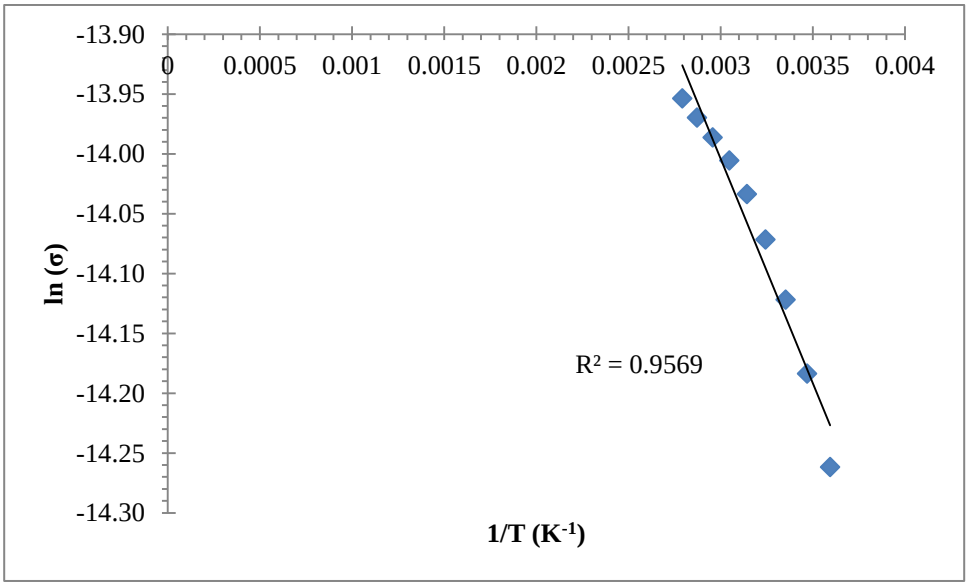

Figure 5-32 A plot of ln(σ) versus (1/T) for 0.1 molal LiTf in hexyl diglyme electrolyte. The simple Arrhenius plot produces non-linear curve. Because of this, a single E_a cannot be obtained since at different temperature, the slope is different.

For the diglyme series, the valid reference temperatures for hexyl diglyme are 5°C, 15°C, 25°C and 35°C. For octyl diglyme, the valid reference temperatures are

T_r=25°C, 35°C, 45°C, and 55°C. For nonyl diglyme, the valid reference temperatures are T_r=45°C, 55°C, 65°C, and 75°C. For decyl diglyme, T_r=55°C, 65°C, 75°C, and 85°C have the most similar dielectric constant range. Figure 5-31 shows the plot of $\ln(\sigma/\sigma_r)$ versus (1/T) for the hexyl monoglyme. All of the R^2-values for the reference temperature selected are at least 0.9993 or better. Figure 5-32 shows the simple Arrhenius plot for hexyl diglyme. As mentioned in chapter 2, simple Arrhenius plot produces non-linear curve when plotting $\ln(\sigma)$ versus (1/T). Thus, the slope is not a single value. Instead, the slope depends on the temperature at which the slope is measured. Since for simple Arrhenius plot, the E_a is equals to the *slope* x k_B (where k_B is the Boltzmann constant), the E_a is also not a single value.

For the triglyme series, the reference temperatures appropriate for hexyl triglyme are 5°C and 15°C reference temperatures. For octyl triglyme, 35°C and 45°C are the most appropriate reference temperatures. For nonyl triglyme, valid reference temperatures are from 35°C to 65°C. For decyl triglyme, T_r=65°C is the most appropriate.

	Activation Energy, E_a (kJ/mol)			
T_r (°C)	Hexyl monoglyme	Octyl monoglyme	Nonyl monoglyme	Decyl monoglyme
5	38.73	35.34	34.13	33.26
15	39.86	36.19	34.92	33.98
25	41.47	37.41	36.08	35.02
35	42.68	38.30	36.91	35.77
45	44.94	39.98	38.50	37.20
55	46.84	41.38	39.81	38.38
65	48.30	42.44	40.80	39.25
75	50.71	44.21	42.47	40.75
85	53.66	46.39	44.53	42.59

Table 5-15 The E_a values for 0.1 molal LiTf in monoglyme solutions at various reference temperature.

	Activation Energy, E_a (kJ/mol)			
T_r (°C)	Hexyl diglyme	Octyl diglyme	Nonyl diglyme	Decyl diglyme
5	32.87	30.36	28.33	28.23
15	32.85	30.31	28.25	28.15
25	34.41	31.62	29.40	29.24
35	36.17	33.10	30.69	30.46
45	37.48	34.17	31.60	31.31
55	39.31	35.70	32.94	32.57
65	40.32	36.52	33.63	33.21
75	42.70	38.50	35.36	34.85
85	44.73	40.19	36.83	36.23

Table 5-16 The E_a values for 0.1 molal LiTf in diglyme solutions at various reference temperature.

	Activation Energy, E_a (kJ/mol)			
T_r (°C)	Hexyl triglyme	Octyl triglyme	Nonyl triglyme	Decyl triglyme
5	34.71	29.44	28.17	24.39
15	36.93	32.45	31.42	27.89
25	38.35	33.35	32.14	28.24
35	40.18	35.24	34.06	30.15
45	42.88	37.50	36.14	31.86
55	43.66	39.39	38.57	35.29
65	47.13	41.93	40.73	36.68
75	53.22	46.81	45.13	40.09
85	57.66	50.79	49.00	43.68

Table 5-17 The E_a values for 0.1 molal LiTf in triglyme solutions at various reference temperature.

Applying the CAF analysis to the dielectric constant and ionic conductivity data reveals the following activation energy trend (Table 5-18):

Glyme Series	**Activation Energy (Ionic Conductivity) kJ/mol**
Monoglyme	40 $\pm$ 2
Diglyme	34 $\pm$ 1
Triglyme	37 $\pm$ 2

Table 5-18 Activation energy for ionic conductivity.

The result shows the significance of dielectric constant in the pre-factor. The simple Arrhenius equation applied to ion transport phenomena previously assumed that the pre-factor is dependent on the viscosity of the solution. In this case, since a polymer has higher viscosity compared to a single repeat unit monomer, it is reasonable to expect that triglyme, which has more repeat units than monoglyme, to have a higher viscosity. By the reasoning provided using the simple Arrhenius equation ionic conductivity should be lower in the triglyme solution. But it is shown here that the ionic conductivity is actually highest in the 0.1 molal LiTf in triglyme series.

Formation of master curves that lie on one line for all three of the 0.1 molal LiTf in glyme oligomers shows that the CAF can be applied to oligomers (figures 5-33 to 5-35).

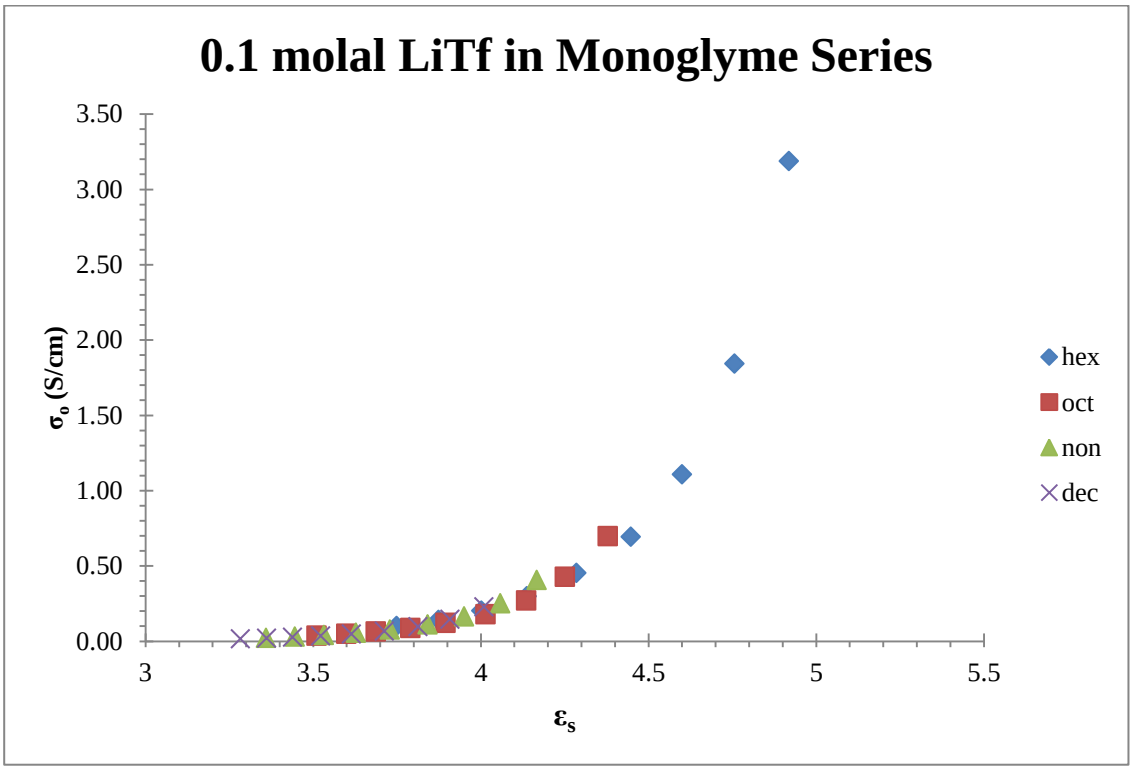

Figure 5-33 Master curve for the 0.1 molal LiTf in monoglyme series.

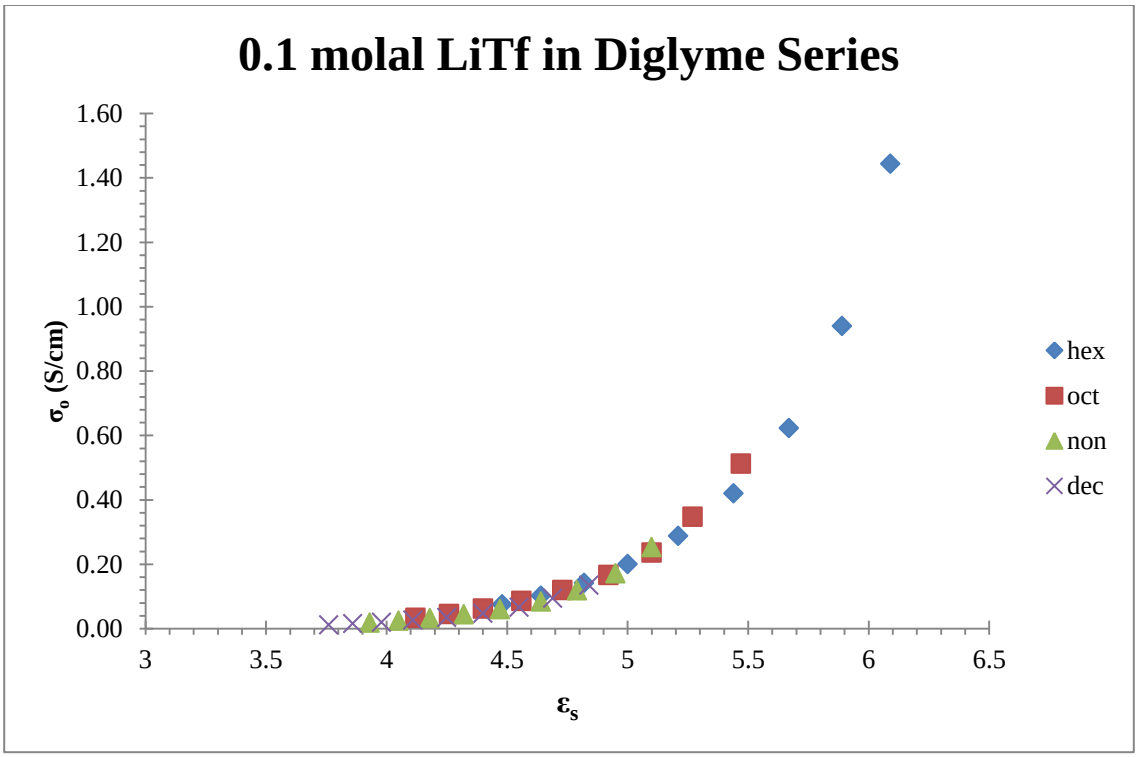

Figure 5-34 Master curve for the 0.1 molal LiTf in diglyme series.

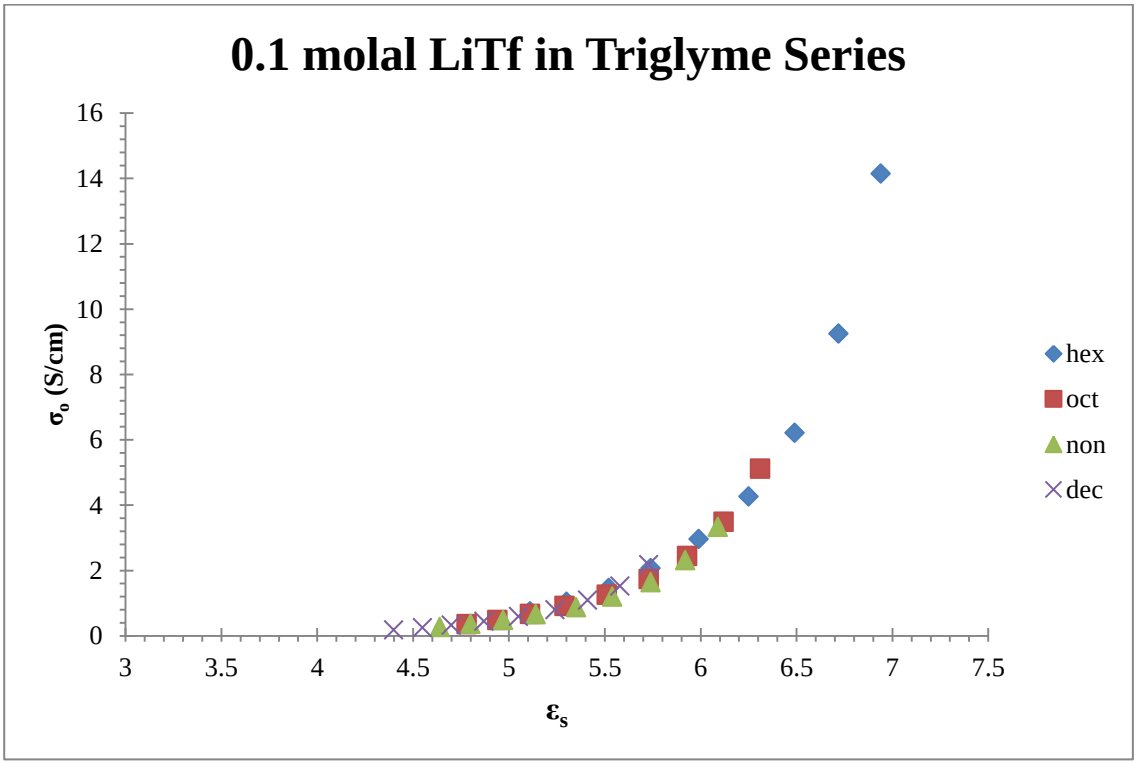

Figure 5-35 Master curve for the 0.1 molal LiTf in triglyme series.

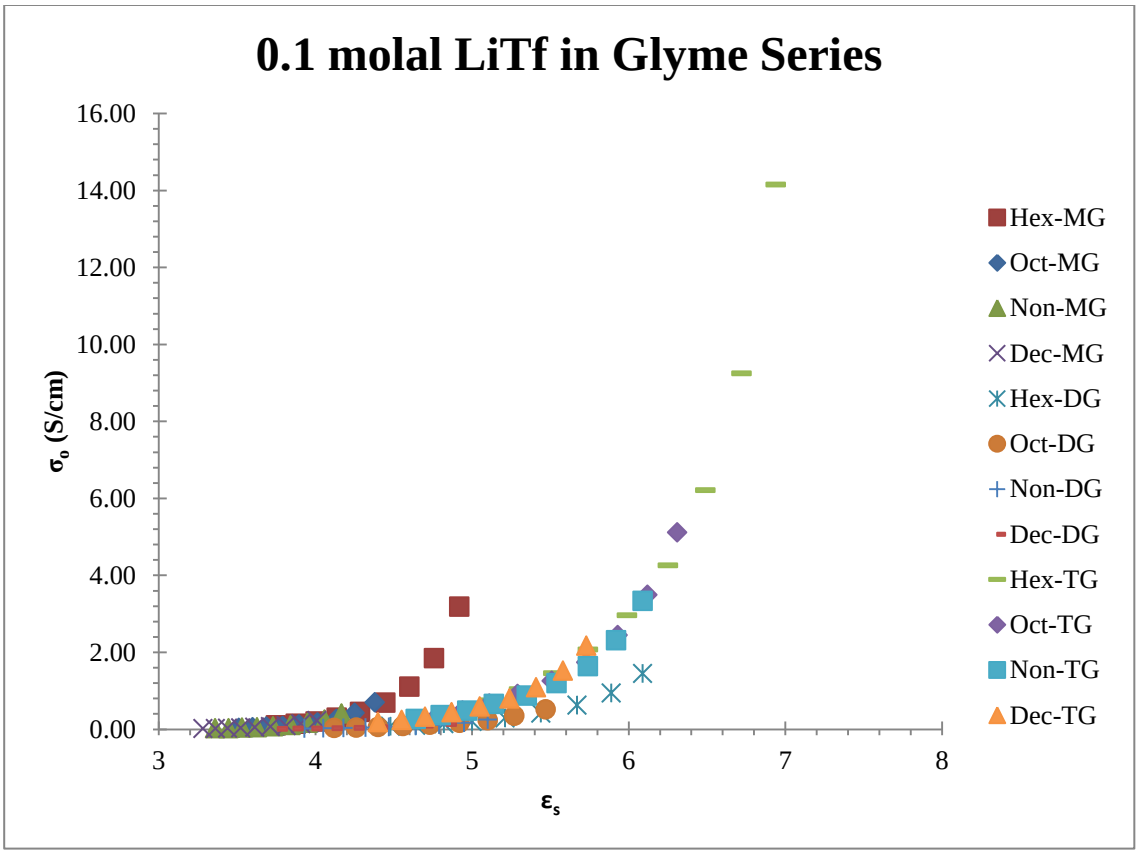

Figure 5-36 Master curve for 0.1 molal LiTf in glyme series. (MG=monoglyme, DG=diglyme, TG=triglyme).

Figure 5-36 shows the master curve for the conductivity of 0.1 molal LiTf in all of the glyme series on one plot. Similar to the master curves for the pure glyme series, the master curve for each distinct system does not lie on top of each other, but forms a separate curve. However, unlike the master curve for the pure glyme series, the master curve for the 0.1 molal LiTf in the glyme series does not follow the trend of going from triglyme to diglyme to monoglyme. Instead, it goes from monoglyme, to triglyme, to diglyme. This trend is similar to the trend in the value of the average E_a for each system.

5.3 Conclusions

The results of the CAF analysis suggest that the CAF can be applied to pure oligomers and oligomer-salt solutions under conditions that allow the oligomers to

behave as liquids. From subsequent analysis using the CAF, a few properties are elucidated from the oligomers of ethylene oxide.

It should be noted that several of the points made in the following discussions are highly speculative as they arise from trends based on three data points. This leads to the more general conclusion that synthesis and measurements on the tetra- and possibly pentaglyme series are needed to strengthen, or disconfirm any speculations made here.

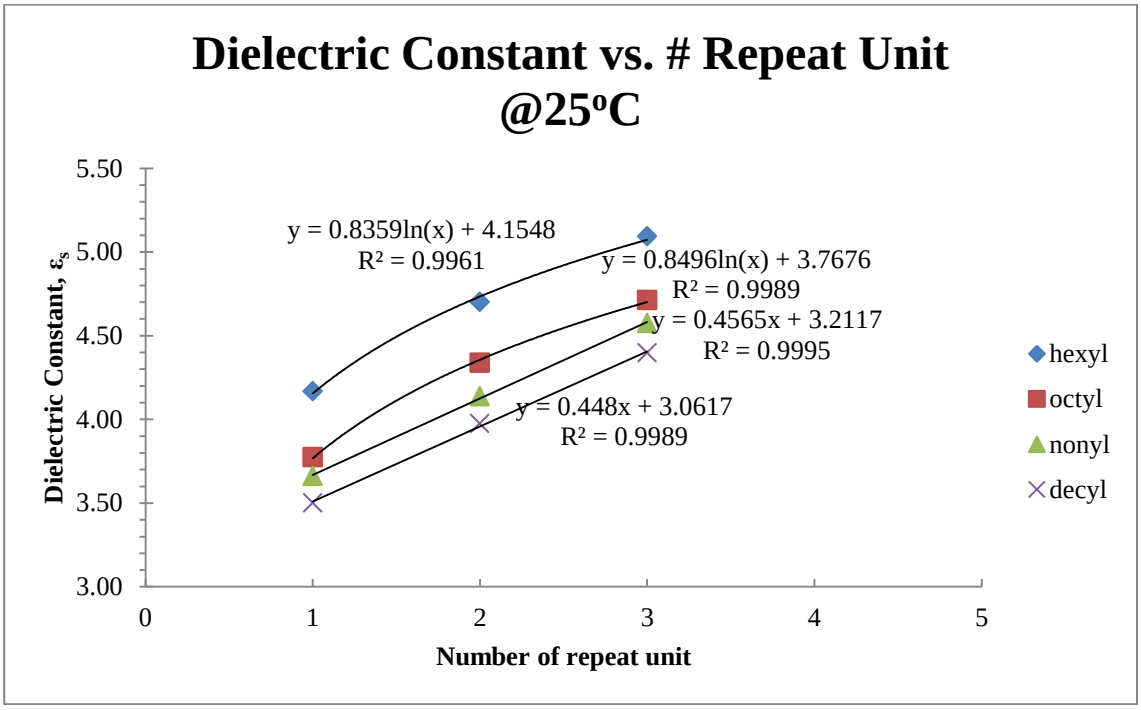

Figure 5-37 Plot of dielectric constant versus oligomer repeat units for pure glyme oligomers at 25°C.

Figure 5-37 shows the plot of dielectric constant against the polymer repeat units for pure glyme family investigated. The plot suggests that the dielectric constant of all glyme analogs will converge to a value except for the nonyl- and the decyl glyme analogs. It is expected that as the number of repeat units is increased, the effect of the tethered alkyl chain is diminished and the dielectric constant converges to a single value. This is evidenced from the curve fitting of the hexyl- and octyl analogs versus

the nonyl and decyl analogs. As the ratio of repeat unit to alkyl chain length increases (hexyl analog has higher repeat unit to alkyl chain length ratio than the decyl analog), the logarithmic model fits the data better. The logarithmic model suggests that the dielectric constant will converge to a single value, presumably near that for liquid PEO.

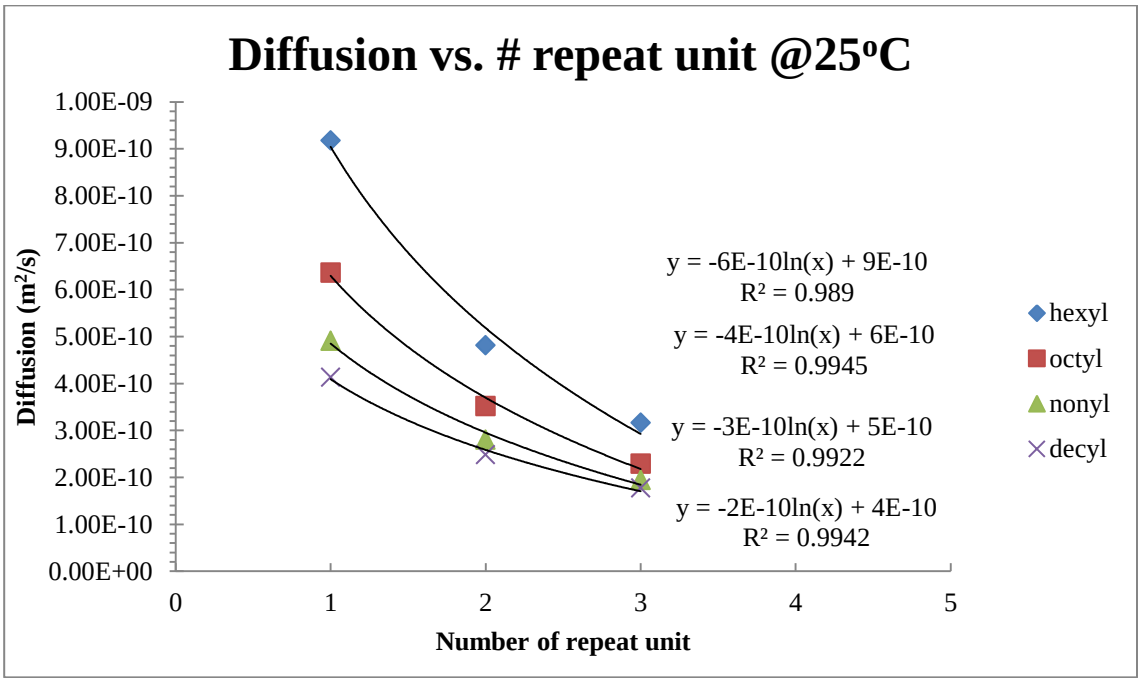

Figure 5-38 Plot of diffusion versus number of oligomer repeat units for pure glyme oligomers at 25°C.

Figure 5-38 shows the plot of self-diffusion coefficient against the number of oligomer repeat unit for pure glyme series. The self-diffusion appears to converge to a single value, as expected as the number of the polymer repeat unit is increased. This is evidenced from the physical state of a poly(ethylene oxide) at room temperature, which is in solid form, whereas the oligomers are in liquid form.

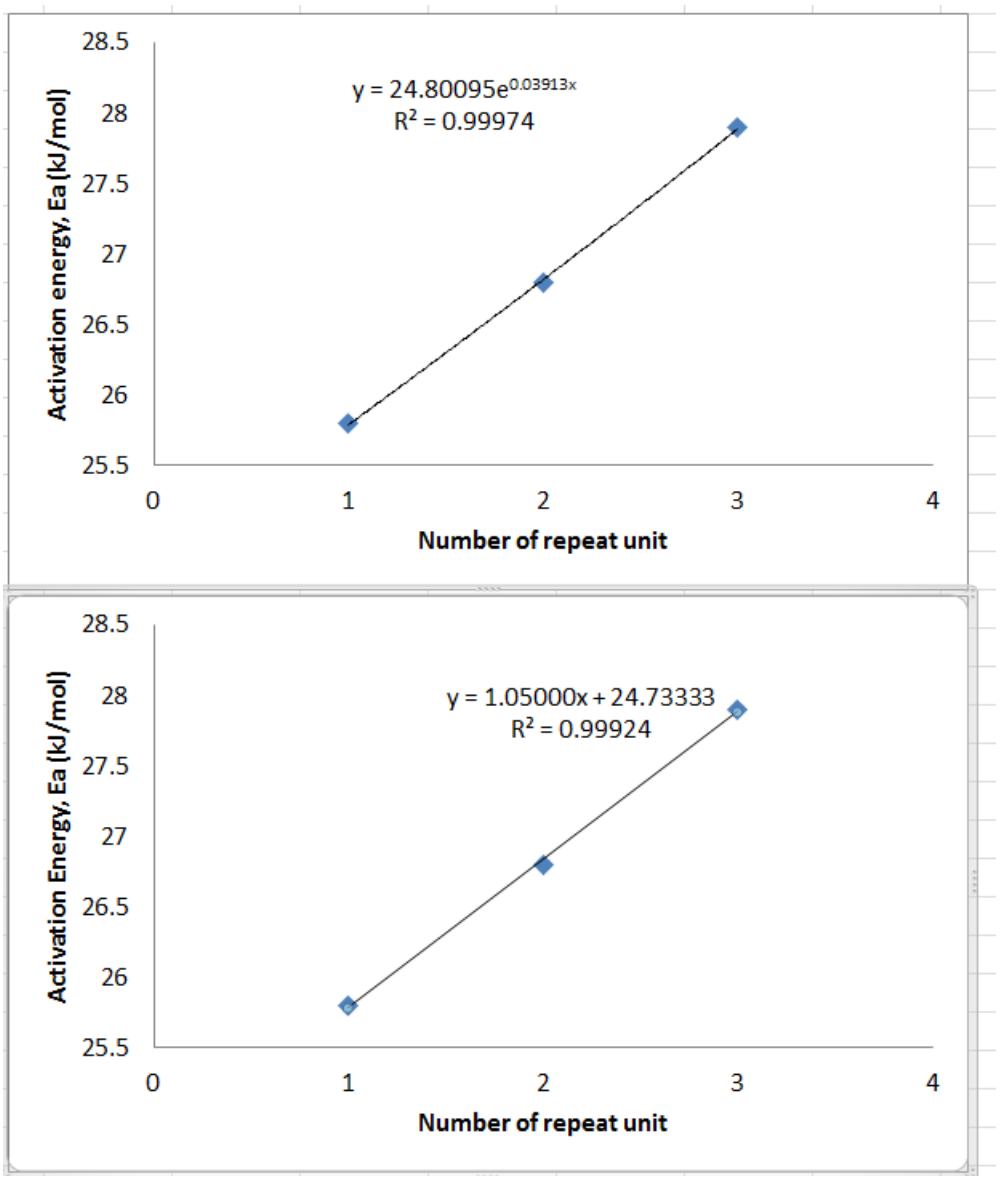

Figure 5-39 Plot of E_a versus oligomer repeat units for pure glyme series at 25°C.

Figure 5-39 shows the plot of the activation energy against the number of oligomer repeat unit for pure glyme series at 25°C. The E_a appears to increase infinitely instead of converging to a single value. Since the nature of the E_a is not well understood, it is possible that the E_a will keep increasing as the number of polymer repeat units is increased.

The dielectric constant of the solutions of 0.1 molal lithium triflate in glyme oligomers follows a similar trend as shown by the pure oligomer solutions. The dielectric constant increases as the number of repeat units increases. It is thus expected that the dielectric constant of the polymer electrolyte to be higher than the dielectric constant of its oligomer electrolytes and reaches a maximum for a particular salt concentration. This is evidenced from figure 5-40 below.

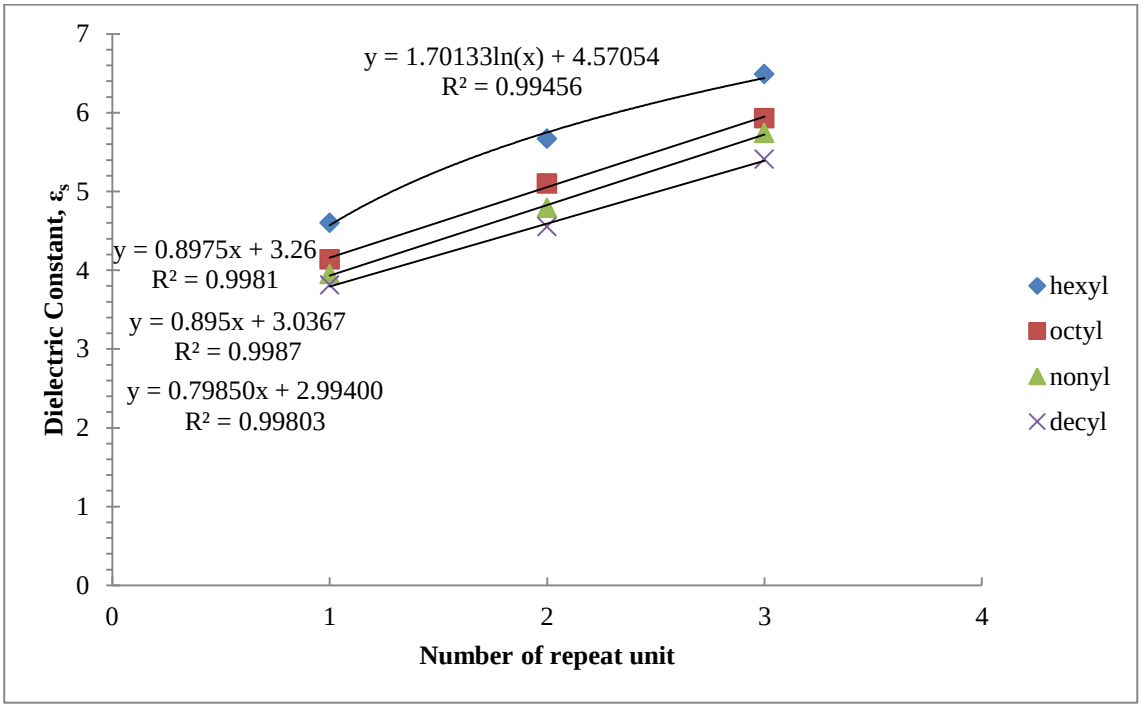

Figure 5-40 Plot of dielectric constant versus number of repeat unit for 0.1 molal LiTf in glyme oligomers at 25°C.

Figure 5-40 shows the plot of dielectric constant against the number of oligomer repeat units for electrolyte solutions of 0.1 molal LiTf in the oligomers at 25°C. As the number of repeat unit is increased, the dielectric constants for the glyme-salt solutions appear to increase infinitely except for the hexyl glyme analog. Thus, it is concluded that the glyme-salt solutions show similar trend to the pure glyme solution, where the

dielectric constant converges as the number of repeat unit to alkyl chain length increases as expected.

The conductivity values of the lithium triflate in the oligomer solutions also show similar trend to that of the dielectric constant; the highest conductivity is attained with the triglyme oligomer over the diglyme oligomer. The lowest conductivity value is obtained with the monoglyme oligomers. The result in conductivity values for the oligomers electrolyte solutions showcases the importance of the CAF. Without the CAF, it is hard to interpret the results. The simple Arrhenius explanation that the exponential pre-factor is inversely dependent on the viscosity of the electrolyte would have predicted that the highest conductivity is attained with the monoglyme oligomers. Thus it is expected that the triglyme, which should have the highest viscosity to have the lowest conductivity. Instead, the triglyme electrolyte has the highest conductivity value.

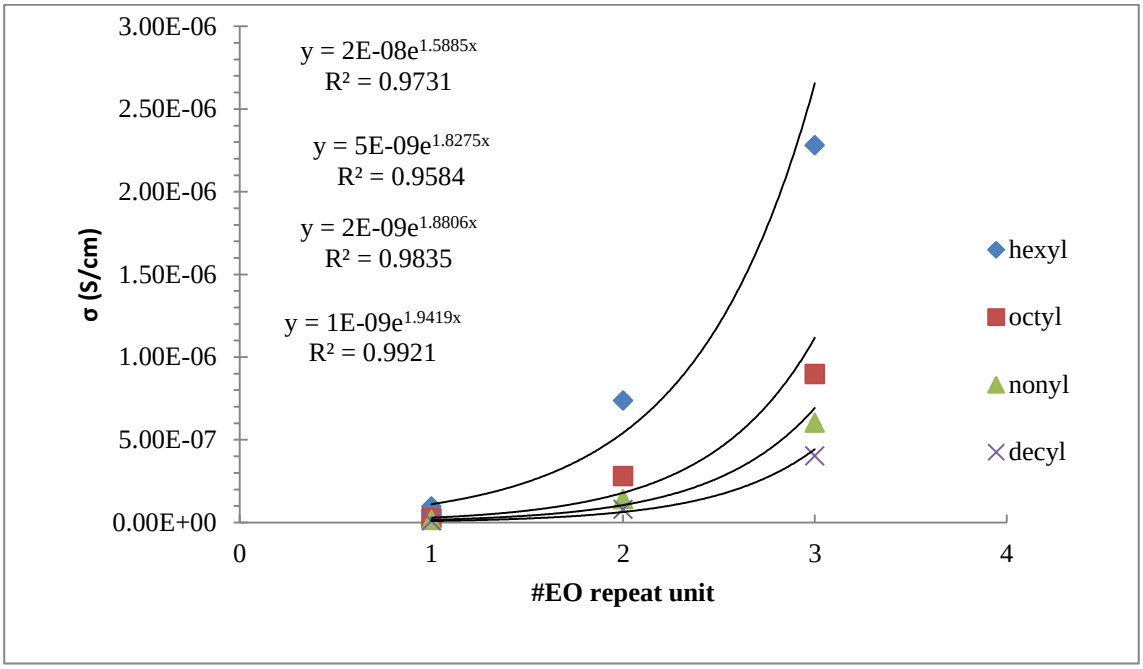

Figure 5-41 Plot of ionic conductivity versus oligomer repeat units for 0.1 molal LiTf in glyme oligomers at 25°C.

Figure 5-41 shows the plot of ionic conductivity against the number of oligomer repeat unit at 25°C. Unlike the self-diffusion, the conductivity appears to increase infinitely as the number of repeat unit is increased. This is impossible since it is known that poly(ethylene oxide) has a certain conductivity values at a particular temperature.

While the conductivity and the dielectric constant show a particular trend with increasing or decreasing the number of repeat units, the energy of activation, E_a for the ionic conductivity of lithium triflate in the glyme series does not show a particular trend. In particular, the E_a for the diglyme oligomer is very low compared to the E_a for the monoglyme and triglyme oligomers. Because of this, the trend seen in the conductivity values has to be because of the dielectric constant values. Thus for conductivity, the dielectric constant plays a more important role than the E_a. To increase the conductivity in polymer electrolytes, higher dielectric constant polymer hosts are desirable.

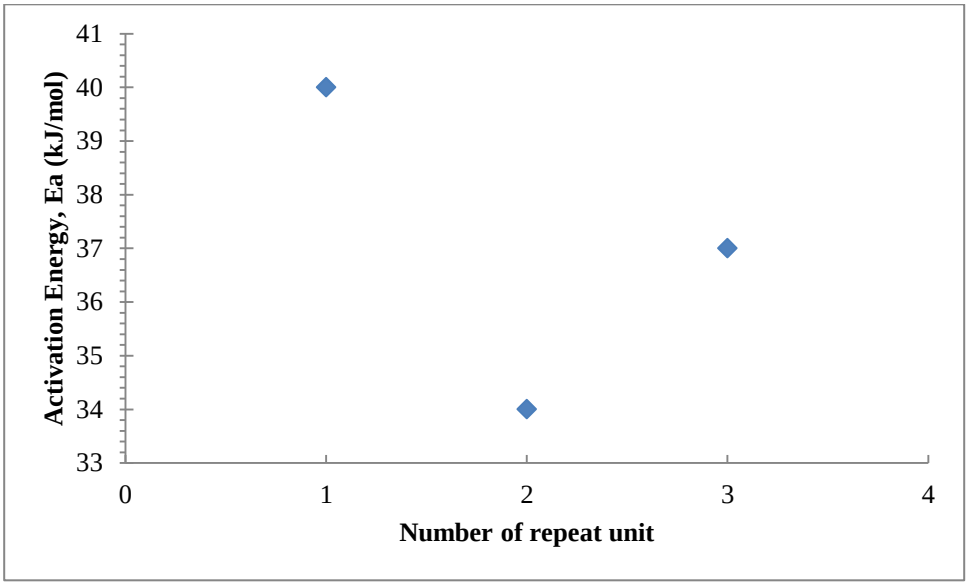

Figure 5-42 Plot of activation energy versus oligomer repeat unit for 0.1 molal LiTf in glymes at 25°C.

Figure 5-42 shows the plot of the activation energy for ionic conductivity versus the number of repeat unit for the 0.1 molal LiTf in glyme solutions at 25^{o}C. The E_a for ionic conductivity unfortunately shows no trend what so ever for the glyme series investigated in the series.

From the application of the CAF to oligomers of poly(ethylene oxide), it appears that it is possible to apply the CAF to obtain the transport properties of polymers for self-diffusion. However, similar analysis for ionic conductivity is inconclusive and requires further studies, including the higher glyme series.

5.4 Detailed Synthesis of Glyme Series

The glyme series used in this work were synthesized in house. The ^{1}H NMR spectra were obtained using a Varian Mercury-300 NMR spectrometer. The GC chromatogram and mass spectra were obtained using a coupled Agilent Technologies 7890A Gas Chromatograph and an Agilent Technologies 5975C inert XL EI Mass Spectrometer (Agilent 19091S-433 HP-5MS Column, He carrier gas).

Typical alkyl glyme synthesis resulted from the following procedure: Into a 250 mL round bottom flask was charged 5.0 equivalents of ethylene glycol monomethyl ether. A stir bar was inserted into the round bottom flask. 150 mL of dry diethyl ether was added to the round bottom flask. Chunks of sodium metal were taken out of the paraffin storage, immersed in methanol, and cut into small pieces onto a dry paper towel sitting on top of a balance. After 1.5 equivalents of sodium metal were obtained, the sodium metals were quickly added into the round bottom flask. The round bottom flask was fitted with an adapter attached to a drying tube through a 30 cm tygon tube. The sodium was let to react with the ethylene glycol monomethyl ether until all of the

sodium metal disappears. This process can take as long as 72 hours. After all of the sodium metal disappears, 1.0 equivalent of bromohexane was added to the flask dropwise, with stirring, using a pressure equalizing funnel. A condenser was fitted to the round bottom flask. The reaction mixture was heated to 80^{o}C for 48 hours.

After 48 hours, the round bottom flask was cooled to room temperature. The solution in the round bottom flask was poured into a separatory funnel. 100 mL of hexane and 100 mL of distilled water were added to the separatory funnel to extract the product into the organic phase. The water layer was removed. The hexane layer was washed 5 more times with 100 mL distilled water each. The hexane layer was then dried for 24 hours over anhydrous magnesium sulfate powder. After 24 hours, the magnesium sulfate powder was removed by vacuum filtration. The solvent was removed under reduced pressure at room temperature. The final product was filtered through a column consists of neutral alumina. NMR and GC analysis were done on the products.

The procedure yielded 87% of the desired product. Spot checks with GC-MS showed at least 98% purity. Similar procedures were performed to synthesize the octyl, nonyl, and decyl monoglyme. The desired bromo alkane is used to synthesize the desired alkyl monoglyme. To synthesize the diglyme and the triglyme derivatives, the ethylene glycol monomethyl ether is replaced with diethyl glycol monomethyl ether and triethylene glycol monomethyl ether respectively.

^{1}H NMR (300MHz, $CDCl_3$):

Hexylmonoglyme: ^{1}H NMR (300 MHz, $CDCl_3$): δ 0.87 (t, 3H, J = 6.6 Hz); 1.16-1.38 (m, 6H); 1.60 (p, 2H, J_1 = 7.2 Hz, J_2 = 6.9 Hz); 3.38 (s, 3H); 3.45 (t, 2H, J = 6.8 Hz); 3.51-3.59 (m, 4H); GC-purity check: >98% purity

Octylmonoglyme: ^{1}H NMR (300 MHz, $CDCl_3$): δ 0.87 (t, 3H, J = 6.8 Hz); 1.14-1.38 (m, 10H); 1.58 (p, 2H, J_1 = 7.2 Hz, J_2 = 6.9 Hz); 3.37 (s, 3H); 3.44 (t, 2H, J = 6.8 Hz); 3.50-3.59 (m, 4H); GC-purity check: >97% purity

Nonylmonoglyme: ^{1}H NMR (300 MHz, $CDCl_3$): δ 0.86 (t, 3H, J = 6.8 Hz); 1.14-1.38 (m, 12H); 1.58 (p, 2H, J_1 = 7.2 Hz, J_2 = 6.9 Hz); 3.37 (s, 3H); 3.44 (t, 2H, J = 6.8 Hz); 3.50-3.58 (m, 4H); GC-purity check: >96%

Decylmonoglyme: ^{1}H NMR (300 MHz, $CDCl_3$): δ 0.86 (t, 3H, J = 6.5 Hz); 1.14-1.37 (m, 14H); 1.58 (p, 2H, J_1 = 7.1 Hz, J_2 = 6.8 Hz); 3.38 (s, 3H); 3.44 (t, 2H, J = 7.1 Hz); 3.50-3.59 (m, 4H)

Hexyldiglyme: ^{1}H NMR (300 MHz, $CDCl_3$): δ 0.85 (t, 3H, J = 6.8 Hz); 1.18-1.36 (m, 6H); 1.55 (p, 2H, J_1 = 7.1 Hz, J_2 = 7.1 Hz); 3.36 (s, 3H); 3.42 (t, 2H, J = 6.8 Hz); 3.50-3.58 (m, 4H); 3.59-3.65 (m, 4H); GC-purity check: >97%

Octyldiglyme: ^{1}H NMR (300 MHz, $CDCl_3$): δ 0.85 (t, 3H, J = 6.8 Hz); 1.15-1.36 (m, 10H); 1.56 (p, 2H, J_1 = 6.8 Hz, J_2 = 7.1 Hz); 3.36 (s, 3H); 3.43 (t, 2H, J = 7.1 Hz); 3.51-3.59 (m, 4H); 3.60-3.66 (m, 4H); GC-purity check: >96%

Nonyldiglyme: ^{1}H NMR (300 MHz, $CDCl_3$): δ 0.86 (t, 3H, J = 6.8 Hz); 1.16-1.37 (m, 12H); 1.56 (p, 2H, J_1 = 6.8 Hz, J_2 = 6.6 Hz); 3.37 (s, 3H); 3.44 (t, 2H, J = 6.6 Hz); 3.52-3.60 (m, 4H); 3.61-3.67 (m, 4H); GC-purity check: >94%

Decyldiglyme: ^{1}H NMR (300 MHz, $CDCl_3$): δ 0.86 (t, 3H, J = 6.8 Hz); 1.14-1.37 (m, 14H); 1.56 (p, 2H, J_1 = 6.8 Hz, J_2 = 6.6 Hz); 3.37 (s, 3H); 3.44 (t, 2H, J = 6.6 Hz); 3.52-3.60 (m, 4H); 3.61-3.67 (m, 4H); GC-purity check: >93%

Hexyltriglyme: ^{1}H NMR (300 MHz, $CDCl_3$): δ 0.85 (t, 3H, J = 7.0 Hz); 1.21-1.36 (m, 6H); 1.54 (p, 2H, J_1 = 7.0 Hz, J_2 = 7.0 Hz); 3.35 (s, 3H); 3.42 (t, 2H, J = 7.0 Hz); 3.50-3.57 (m, 4H); 3.59-3.65 (m, 8H)

Octyltriglyme: ^{1}H NMR (300 MHz, $CDCl_3$): δ 0.85 (t, 3H, J = 7.0 Hz); 1.20-1.36 (m, 10H); 1.54 (p, 2H, J_1 = 7.0 Hz, J_2 = 7.0 Hz); 3.35 (s, 3H); 3.42 (t, 2H, J = 7.0 Hz); 3.50-3.58 (m, 4H); 3.59-3.66 (m, 8H); GC-purity check: >97%

Nonyltriglyme: ^{1}H NMR (300 MHz, $CDCl_3$): δ 0.85 (t, 3H, J = 6.8 Hz); 1.20-1.36 (m, 12H); 1.55 (p, 2H, J_1 = 7.0 Hz, J_2 = 7.0 Hz); 3.36 (s, 3H); 3.42 (t, 2H, J = 6.8 Hz); 3.50-3.58 (m, 4H); 3.60-3.66 (m, 8H); GC-purity check: >93%

Decyltriglyme: ^{1}H NMR (300 MHz, $CDCl_3$): δ 0.85 (t, 3H, J = 6.7 Hz); 1.18-1.36 (m, 14H); 1.55 (p, 2H, J_1 = 7.0 Hz, J_2 = 7.0 Hz); 3.36 (s, 3H); 3.42 (t, 2H, J = 6.8 Hz); 3.50-3.58 (m, 4H); 3.59-3.66 (m, 8H); GC-purity check: >90%

For comparison, these compounds ^{1}H NMR data are found in the literature:

Monoglyme[111]: ^{1}H NMR (400MHz, $CDCl_3$): δ 3.40 (s, 6H); 3.55 (s, 4H)

Diglyme[112]: ^{1}H NMR (400 MHz, THF-d_8): δ 3.28 (s, 6H, CH_3); 3.44-3.53 (^{2}J(H,H) = -6.07 Hz/ -4.10 Hz, ^{3}J(H,H) = 12.3 Hz/12.3 Hz, 4H/4H, CH_2)

Butyldiglyme[113]: ^{1}H NMR (CCl_4): δ 0.7-1.1 (m, 3H); 1.15-1.65(m, 4H); 3.30 (s, 3H); 3.3-3.7(m, 10H)

2-(hexyloxy)ethanol[114]: ^{1}H NMR (90 MHz, $CDCl_3$): δ 0.90 (t, 3H, *CH_3*); 1.16-1.49 (m, 6H, *CH_2*); 1.59 (m, 2H, *CH_2*); 2.51 (s, 1H, *OH*); 3.48 (t, 2H, *CH_2*); 3.52 (m, 2H, *CH_2*); 3.72 (m, 2H, *CH_2*)

2-(2-hexyloxyethoxy)ethanol[115]: ^{1}H NMR (90 MHz, $CDCl_3$): δ 0.89 (t, 3H, *CH_3*); 1.30 (m, 6H, *CH_2*); 1.59 (m, 2H, *CH_2*); 2.79 (s, 1H, *OH*); 3.47 (t, 2H, *CH_2*); 3.44-3.83 (m, 8H, *CH_2*)

Chapter 6: Conclusion

6.1 Overall conclusion

Three different organic liquid families were synthesized and their electrolyte systems were prepared. Their transport behaviors were analyzed using the Compensated Arrhenius Formulation (CAF) to determine the range of applicability of the CAF and to help understand transport properties in these liquids and electrolytes.

From the results, the CAF was found to be applicable to very low dielectric constant liquids as well as very high dielectric constant liquids. From the core postulates of the CAF, the change in the values of the dielectric constant of a medium plays an important role in the success of the CAF. As the polarity of a liquid is lowered, the change in the dielectric constant might not be as significant as needed for the CAF to be applicable. However, the results with the acyclic carbonates suggest that the CAF can work with very low polarity solvents.

As expected, the CAF is also applicable to high dielectric constant solvents. However, high dielectric constant solvents appear to have very high energy of activation for both self-diffusion and ionic conductivity. Thus, although high dielectric constant is desirable to increase the exponential pre-factor, it has an unknown impact of increasing the value of the energy of activation.

It appears that the CAF can be used to predict the self-diffusion parameters in polymers. However, the analysis on ionic conductivity is inconclusive. The energy of activation in polymers appears to increase infinitely as the number of polymer repeat units is increased. However the dielectric constant appears to converge to a single value as expected. This is true for both the diffusion as well as ionic conductivity cases. The

exponential pre-factor for self-diffusion in pure poly(ethylene oxide) appears to converge to a single value. However, the exponential pre-factor for ionic conductivity appears to converge to a negative value, which is erroneous.

The energy of activation, E_a is a mystery. The results offer a few hints about manipulating the E_a. One, the E_a for self-diffusion is affected by the dielectric constant of the liquid as evidenced by the higher self-diffusion E_a for cyclic carbonates. It appears that the E_a increases after a certain value of dielectric constant is reached. To lower the E_a, the dielectric constant needs to be below a certain threshold. The second hint is the E_a for self-diffusion of polymers is additive. Thus the E_a in a solvent can be manipulated by either adding functional groups or increasing the dielectric constant. The dielectric constant can be manipulated by controlling the factors as discussed in chapter 1 like dipole moment of the repeat unit or the dipole density of the repeat unit.

The E_a for ionic conductivity in the glyme oligomers shows peculiar trend where the E_a for one repeat unit monoglyme oligomer is higher than the E_a for the two repeat units diglyme oligomer and three repeat units triglyme oligomer. The reason for this weird trend is not known. However, this does suggest that there is a possibility that the conformations in polymers can affect the E_a for charge transport in polymers.

6.2 Future Directions

While significant knowledge about the CAF and transport properties has been gained, there is a lot more research that needs to be performed in order to gain a complete understanding of transport phenomena in organic liquids and in general.

In this work, the CAF is shown to be applicable to low polarity solvents such as acyclic carbonates and high polarity solvents such as cyclic carbonates. The effect on

even higher polarity solvents like oxazolidinone and sydnone is not known and should be investigated. Similarly, while the CAF has been shown to be applicable to oligomers and postulated above to be applicable to polymers in 'solid' form, this is speculative and would need to be confirmed experimentally.

From the work on acyclic carbonates, the E_a's for self-diffusion are similar for low dielectric constant liquids. This is evidenced by the E_a's for acyclic carbonates, nitriles, acetates, and 2-ketones which hover around 20 to 25 kJ/mol. It has been postulated that the E_a is the results of dipole-dipole interaction among the liquids[57]. However, from the values of the E_a's for these solvents and the dipole moments of solvent molecules, this relation appears to be complicated and should be tackled to increase the understanding of the E_a's.

References

1. J. G. M. Albright, R., *J Phys Chem-Us*, 1965, **69**, 3120-3126.
2. R. Mills, *J Phys Chem-Us*, 1965, **69**, 3116-3119.
3. A. Fick, *Pogg. Annual Physical Chemistry*, 1855, **170**, 59-86.
4. K. M. Laidler, J.; Sanctuary, B.;, *Physical Chemistry Ch. 19: Transport Properties*, Houghton Mifflin Company, USA, 2003.
5. G. K. Batchelor, *Journal of Fluid Mechanics*, 1976, **74**, 1-29.
6. J. L. Aguirre and T. J. Murphy, *Physics of Fluids*, 1971, **14**, 2050-2052.
7. O. Borodin and G. D. Smith, *Journal of Solution Chemistry*, 2007, **36**, 803-813.
8. Z. Li, G. D. Smith and D. Bedrov, *The journal of physical chemistry. B*, 2012, **116**, 12801-12809.
9. G. D. Smith, O. Borodin, S. Russo, R. Rees and A. Hollenkamp, *Physical chemistry chemical physics : PCCP*, 2009, **11**, 9884-9897.
10. M. Petrowsky and R. Frech, *The Journal of Physical Chemistry B*, 2008, **112**, 8285-8290.
11. F. J. Gutter and G. Kegeles, *Journal of the American Chemical Society*, 1953, **75**, 3893-3896.
12. A. R. Gordon, *Journal of the American Chemical Society*, 1950, **72**, 4840-4840.
13. G. S. Hartley and J. Crank, *Transactions of the Faraday Society*, 1949, **45**, 801-818.
14. P. C. Carman and L. H. Stein, *Transactions of the Faraday Society*, 1956, **52**, 619-627.

15. C. L. Sandquist and P. A. Lyons, *Journal of the American Chemical Society*, 1954, **76**, 4641-4645.

16. G. K. Batchelor, *Journal of Fluid Mechanics*, 1979, **95**, 369-400.

17. G. K. Batchelor and C. S. Wen, *Journal of Fluid Mechanics*, 1982, **124**, 495-528.

18. G. K. Batchelor, *Journal of Fluid Mechanics*, 1983, **131**, 155-175.

19. T. J. Murphy and J. L. Aguirre, *The Journal of Chemical Physics*, 1972, **57**, 2098-2104.

20. T. J. Murphy, *The Journal of Chemical Physics*, 1972, **56**, 3487-3489.

21. J. L. Aguirre and T. J. Murphy, *The Journal of Chemical Physics*, 1973, **59**, 1833-1840.

22. J. L. Anderson and C. C. Reed, *The Journal of Chemical Physics*, 1976, **64**, 3240-3250.

23. C. Y. Mou and S. A. Adelman, *The Journal of Chemical Physics*, 1978, **69**, 3135-3145.

24. K. J. Gaylor, I. K. Snook, W. van Megen and R. O. Watts, *Chemical Physics*, 1979, **43**, 233-239.

25. B. D. Fair and A. M. Jamieson, *Journal of Colloid and Interface Science*, 1980, **73**, 130-135.

26. S. Glasstone, K. Laidler and H. Eyring, *The Theory of Rate Processes*, McGraw-Hill, New York, 1941.

27. R. Furth, *Proc. Cambridge Phil. Soc.*, 1941, **37**, 281.

28. K. Wirtz, *Z. Phys.*, 1948, **124**, 482.

29. D. E. O'Reilly and G. E. Schacher, *J. Chem. Phys.*, 1963, **39**, 1968.

30. D. E. O'Reilly, *Chem. Phys.*, 1971, **55**, 2876-2881.

31. D. E. O'Reilly, *Chem. Phys.*, 1972, **56**, 2490-2495.

32. D. E. O'Reilly, *Chem. Phys.*, 1973, **58**, 1272-1277.

33. D. E. O'Reilly, *J Phys Chem-Us*, 1974, **78**, 2275-2279.

34. A. Fleshman, M. Petrowsky, J. Jernigen, R. S. P. Bokalawela, M. Johnson and R. Frech, *Electrochim. Acta*, 2011, **57**, 147.

35. Fleshman, A. Mass and Charge Transport in Alcohol and Ketone Solvents and Electrolyte Solutions. Ph.D. Dissertation, University of Oklahoma, Norman, OK, 2012.

36. P. W. Bridgman, *The Physics of High Pressure*, 1949.

37. A. Jobling and A. S. C. Lawrence, *Proc. R. Soc. A*, 1951, **206**, 257.

38. S. B. Baumann, D. R. Wozny, S. K. Kelly and F. M. Meno, *Biomedical Engineering, IEEE Transactions on*, 1997, **44**, 220-223.

39. A. M. Brown, A. G. Hope, J. J. Lambert and J. A. Peters, *The Journal of Physiology*, 1998, **507**, 653-665.

40. Petrowsky, M. Ion Transport in Liquid Electrolytes. Ph.D. Dissertation, University of Oklahoma, Norman, OK, 2008.

41. O. Borodin and G. D. Smith, *The Journal of Physical Chemistry B*, 2000, **104**, 8017-8022.

42. O. Borodin, G. D. Smith and P. Fan, *The Journal of Physical Chemistry B*, 2006, **110**, 22773-22779.

43. O. Borodin and G. D. Smith, *The Journal of Physical Chemistry B*, 2006, **110**, 4971-4977.

44. J. Bockris and A. Reddy, in *Modern Electrochemistry*, Plenum Press, New York City, 2nd Ed. edn., 1998, vol. 1.

45. M. L. Williams, R. F. Landel and J. D. Ferry, *Journal of the American Chemical Society*, 1955, **77**, 3701-3707.

46. G. S. Fulcher, *J. Am. Ceram. Soc.*, 1925, **8**, 339.

47. G. Tamman and W. Hesse, *Z. Anorg. Allg. Chem.*, 1926, **156**, 245.

48. H. Vogel, *Phys. Z.*, 1921, **22**, 645.

49. M. Petrowsky and R. Frech, *The Journal of Physical Chemistry B*, 2009, **113**, 5996-6000.

50. M. Petrowsky and R. Frech, *The Journal of Physical Chemistry B*, 2010, **114**, 8600-8605.

51. D. N. Bopege, M. Petrowsky, A. M. Fleshman, R. Frech and M. B. Johnson, *The Journal of Physical Chemistry B*, 2011, **116**, 71-76.

52. M. Petrowsky, A. Fleshman, D. N. Bopege and R. Frech, *The Journal of Physical Chemistry B*, 2012, **116**, 9303-9309.

53. M. Petrowsky, A. Fleshman, M. Ismail, D. T. Glatzhofer, D. N. Bopege and R. Frech, *The Journal of Physical Chemistry B*, 2012, **116**, 10098-10105.

54. M. Petrowsky, M. Ismail, D. T. Glatzhofer and R. Frech, *The Journal of Physical Chemistry B*, 2013.

55. C. P. Smyth, *Dielectric behavior and structure: dielectric constant and loss, dipole moment, and molecular structure*, 1955.

56. S. O. M. E. J. Murphy, *Bell System Tech. Journal*, 1937, **16**, 493-499.

57. W. Kauzmann, *Reviews of Modern Physics*, 1942, **14**, 12-44.

58. M. Petrowsky and R. Frech, *The Journal of Physical Chemistry B*, 2009, **113**, 16118-16123.

59. W. S. Price, *Concepts Magn. Reson.*, 1997, **9**, 299.

60. W. S. Price, *Concepts Magn. Reson.*, 1998, **10**, 197.

61. D. N. Bopege, M. Petrowsky, R. Frech and M. B. Johnson, *J. Solution Chem.*, 2013, **42**, 584-591.

62. D. Bopege, M. Petrowsky, A. Fleshman, R. Frech and M. Johnson, *J. Phys. Chem. B*, 2012, **116**, 71-76.

63. R. Weast, *CRC Handbook of Chemistry and Physics*, 1974.

64. K. Xu, *Chemical Reviews*, 2004, **104**, 4303-4418.

65. M. Rubinstein and R. H. Colby, *Polymer Physics*, Oxford University Press, Oxford New York, 2003.

66. M. Petrowsky, A. Fleshman and R. Frech, *The Journal of Physical Chemistry B*, 2012, **116**, 5760-5765.

67. A. M. Fleshman, M. Petrowsky and R. Frech, *The Journal of Physical Chemistry B*, 2013.

68. J. A. Riddick, W. B. Bunger and T. K. Sakano, *Organic Solvents. Physical Properties and Methods of Purification*, 1986.

69. P. Tundo and M. Selva, *Acc. Chem. Res.*, 2002, **35**, 706.

70. A.-A. G. Shaikh and S. Sivaram, *Chemical Reviews*, 1996, **96**, 951-976.

71. H.-J. Buysch, in *Ullmann's Encyclopedia of Industrial Chemistry*, Wiley-VCH Verlag GmbH & Co. KGaA, 2000.

72. T. Sakakura and K. Kohno, *Chem. Commun.*, 2009, 1312.

73. M. Wang, N. Zhao, W. Wei and Y. Sun, *Ind. Eng. Chem. Res.*, 2005, **44**, 7596.

74. Z. Shen, X. Jiang and W. Zhao, *Catalysis Letters*, 2003, **91**, 63-67.

75. B. Xu, R. J. Madix and C. M. Friend, *Journal of the American Chemical Society*, 2011, **133**, 20378-20383.

76. X. Zhou, H. P. Zhang, G. Y. Wang, Z. G. Yao, Y. R. Tang and S. S. Zheng, *Journal of Molecular Catalysis A: Chemical*, 2013, **366**, 43-47.

77. S. P. Rannard and N. J. Davis, *Organic Letters*, 1999, **1**, 933-936.

78. C. Qi, J. Ye, W. Zeng and H. Jiang, *Advanced Synthesis & Catalysis*, 2010, **352**, 1925-1933.

79. J. Meléndez, M. North and R. Pasquale, *European Journal of Inorganic Chemistry*, 2007, **2007**, 3323-3326.

80. S. G. Davies, A. M. Fletcher, W. Kurosawa, J. A. Lee, G. Poce, P. M. Roberts, J. E. Thomson and D. M. Williamson, *The Journal of Organic Chemistry*, 2010, **75**, 7745-7756.

81. D. R. Lide, *CRC Handbook of Chemistry and Physics*, 2009.

82. B. Schäffner, F. Schäffner, S. P. Verevkin and A. Börner, *Chemical Reviews*, 2010, **110**, 4554-4581.

83. M. North, R. Pasquale and C. Young, *Green Chemistry*, 2010, **12**, 1514-1539.

84. H. C. Kolb, M. S. VanNieuwenhze and K. B. Sharpless, *Chemical Reviews*, 1994, **94**, 2483-2547.

85. Z. Wang, in *Comprehensive Organic Name Reactions and Reagents*, John Wiley & Sons, Inc., 2010.

86. R. B. Woodward and F. V. Brutcher, *Journal of the American Chemical Society*, 1958, **80**, 209-211.

87. L. Emmanuvel, T. M. A. Shaikh and A. Sudalai, *Organic Letters*, 2005, **7**, 5071-5074.

88. L. Simeral and R. L. Amey, *J. Phys. Chem.*, 1970, **74**, 1443.

89. R. Kempa and W. H. Lee, *J. Chem. Soc.*, 1958, 1936.

90. G. Oster and J. G. Kirkwood, *The Journal of Chemical Physics*, 1943, **11**, 175.

91. T. Vasiltsova and A. Heintz, *The Journal of Chemical Physics*, 2007, **127**, 114501.

92. R. Payne and I. E. Theodorou, *J. Phys. Chem.*, 1972, **76**, 2892.

93. M. Naoki and T. Seki, *Fluid Phase Equilibria*, 2009, **281**, 172-185.

94. K. Orito, Y. Seki, H. Suginome and T. Iwadare, *Bulletin of the Chemical Society of Japan*, 1989, **62**, 2013-2017.

95. J. J. Fontanella, M. C. Wintersgill, M. K. Smith, J. Semancik and C. G. Andeen, *Journal of Applied Physics*, 1986, **60**, 2665-2671.

96. J. J. Fontanella, M. C. Wintersgill and J. J. Immel, *The Journal of Chemical Physics*, 1999, **110**, 5392-5402.

97. G. E. Blomgren, *J. Power Sources*, 2003, **119/121**, 326.

98. G. E. Blomgren, *J. Power Sources*, 1999, **82**, 112.

99. M. Armand, *Solid State Ionics*, 1994, **69**, 309.

100. M. Ratner, *Polymer Electrolyte Reviews*, 1987.

101. M. A. Ratner and D. F. Shriver, *Chem. Rev.*, 1988, **88**, 109.

102. P. G. Bruce, *Solid State Electrochemistry*, 1995.

103. F. B. Dias, L. Plomp and J. B. J. Veldhuis, *J. Power Sources*, 2000, **88**, 169.

104. J. Y. Song, Y. Y. Wang and C. C. Wan, *J. Power Sources*, 1999, **77**, 183.

105. S. Megahed and B. Scrosati, *J. Power Sources*, 1994, **51**, 79.

106. J. M. Tarascon and M. Armand, *Nature*, 2001, **414**, 359.

107. M. Yokoyama, T. Okano, Y. Sakurai, A. Kikuchi, N. Ohsako, Y. Nagasaki and K. Kataoka, *Bioconjugate Chemistry*, 1992, **3**, 275-276.

108. M. S. Thompson, T. P. Vadala, M. L. Vadala, Y. Lin and J. S. Riffle, *Polymer*, 2008, **49**, 345-373.

109. F. A. Carey and R. J. Sundberg, *Advanced Organic Chemistry, Part A: Structure and Mechanisms*, Springer Science + Business Media, LLC, New York, 2008.

110. J. L. M. Abboud and R. Notario, *Pure Appl. Chem.*, 1999, **71**, 645-718.

111. I. C. Jones, G. J. Sharman and J. Pidgeon, *Magnetic Resonance in Chemistry*, 2005, **43**, 497-509.

112. R. I. Yousef, B. Walfort, T. Rüffer, C. Wagner, H. Schmidt, R. Herzog and D. Steinborn, *Journal of Organometallic Chemistry*, 2005, **690**, 1178-1191.

113. W. Kirmse and U. Jansen, *Chemische Berichte*, 1985, **118**, 2607-2625.

114. *Spectral Database for Organic Compounds (SDBS);* proton NMR spectrum; SDBS No.: 6857. CAS RN 112-22-4. http:// sdbs.db.aist.go.jp/sdbs/ (accessed December 5th 2013).

115. *Spectral Database for Organic Compounds (SDBS);* proton NMR spectrum; SDBS No.: 10102. CAS RN: 112-59-4. http:// sdbs.db.aist.go.jp/sdbs/ (accessed December 5th 2013).